The University of Alabama in Huntsville

Final Report

MICROGRAVITY LIQUID PROPELLANT MANAGEMENT

NASA Contract: NAS8-36955/

Delivery Order No. 37

Prepared by

R. J. Hung

The University of Alabama in Huntsville

Huntsville, Alabama 35899

October 1990

Abstract

The requirement to settle or to position liquid fluid over the outlet end of a spacecraft propellant tank prior to main engine restart poses a microgravity fluid behavior problem. Resettlement or reorientation of liquid propellant can be accomplished by providing optimal acceleration to the spacecraft such that the propellant is reoriented over the tank outlet without any vapor entrainment, any excessive geysering, or any other undesirable fluid motion for the space fluid management under microgravity environment. The purpose of the present study is to investigate most efficient technique for propellant resettling through the minimization of propellant usage and weight penalties. Both full-scale and sub-scale liquid propellant tank of Space Transfer Vehicle have been used to simulate flow profiles for liquid hydrogen reorientation over the tank outlet. In sub-scale simulation, both constant and impulsive resettling acceleration have been used to simulate the liquid flow reorientation. Comparison between the constant reverse gravity acceleration and impulsive reverse gravity acceleration to be used for activation of propellant resettlement, it shows that impulsive reverse gravity thrust is superior to constant reverse gravity thrust for liquid reorientation in a reduced gravity environment.

(I) Statement of Problems

Behavior of liquid propellant becomes fairly uncertain when the gravity environment reduces to the order of 10^{-6} g_0 level. The requirement to settle or to position liquid fuel over the outlet end of the spacecraft propellant tank prior to main engine restart poses a microgravity fluid behavior problem. Retromaneuvers of spacecraft, such as Orbital Maneuvering Vehicle (OMV) and Space Transfer Vehicle (STV)[1] taking a flight from high earth orbit to low earth orbit, require settling or reorientation of propellant prior to main engine firing. Cryogenic liquid propellant is required to position over the tank outlet by using small auxillary thrusters which provide a thrust parallel to the tank's major axis in the direction of flight. During the reorientation process, the liquid flows in an annular sheet along the tank wall, with the gas or ullage bubble "rising" centrally into the liquid. This motion would also clear the tank vent of liquid so that venting of vapor is possible.

An efficient propellant settling technique should minimize propellant usage and weight penalties. This can be accomplished by providing optimal acceleration to the spacecraft such that the propellant is reoriented over the tank outlet without any vapor entrainment, any excessive geysering, or any other undesirable fluid motion.

Time-dependent dynamical behaviors of fluids in a microgravity environment have been investigated by numerically computing full set of Navier-Stokes equation[2-15].

(II) Problems Attempted

Liquid propellant (hydrogen) tank is 168 inch in diameter, has a square root of 2 domes and a 48 inch long barrel section. Figure 1 shows the size and dimension of hydrogen tank. A settling acceleration, ranging from 1.5×10^{-3} to 3.0×10^{-3} g_0, has been assumed to be produced by idle-mode thrust from the main engine. Settling of propellant prior to main engine start is defined to be required at two tanks with fill percentages of 30% and 70%.

To provide conservative settling conditions, the liquid is assumed to be initially oriented at the top of the tank. If the spacecraft has been coasting for a long time, aligned with its direction of motion, the most significant force, drag would be axial.

Axisymmetric representation of the tank, with a cylindrical coordinate system is assumed. The settling acceleration is assumed to be parallel to by the axial direction, and the liquid is initially oriented symmetrically at the top of the tank.

Numerical simulations have been carried out for both full-scale and sub-scale of liquid hydrogen propellant tanks for the Space Transfer Vehicle (STV).

(III) Full-Scale Simulation for Liquid Reorientation and Resettlement

The following four cases have been accomplished for the cases of full-scale STV propellant tank liquid fluid reorientation: (A) Liquid filled level of 30% and settling acceleration of 1.5×10^{-3} g_0; (B) Liquid filled level of 30% and settling acceleration of 3.0×10^{-3} g_0; (C) Liquid filled level of 70% and settling acceleration of $1.5 \times$

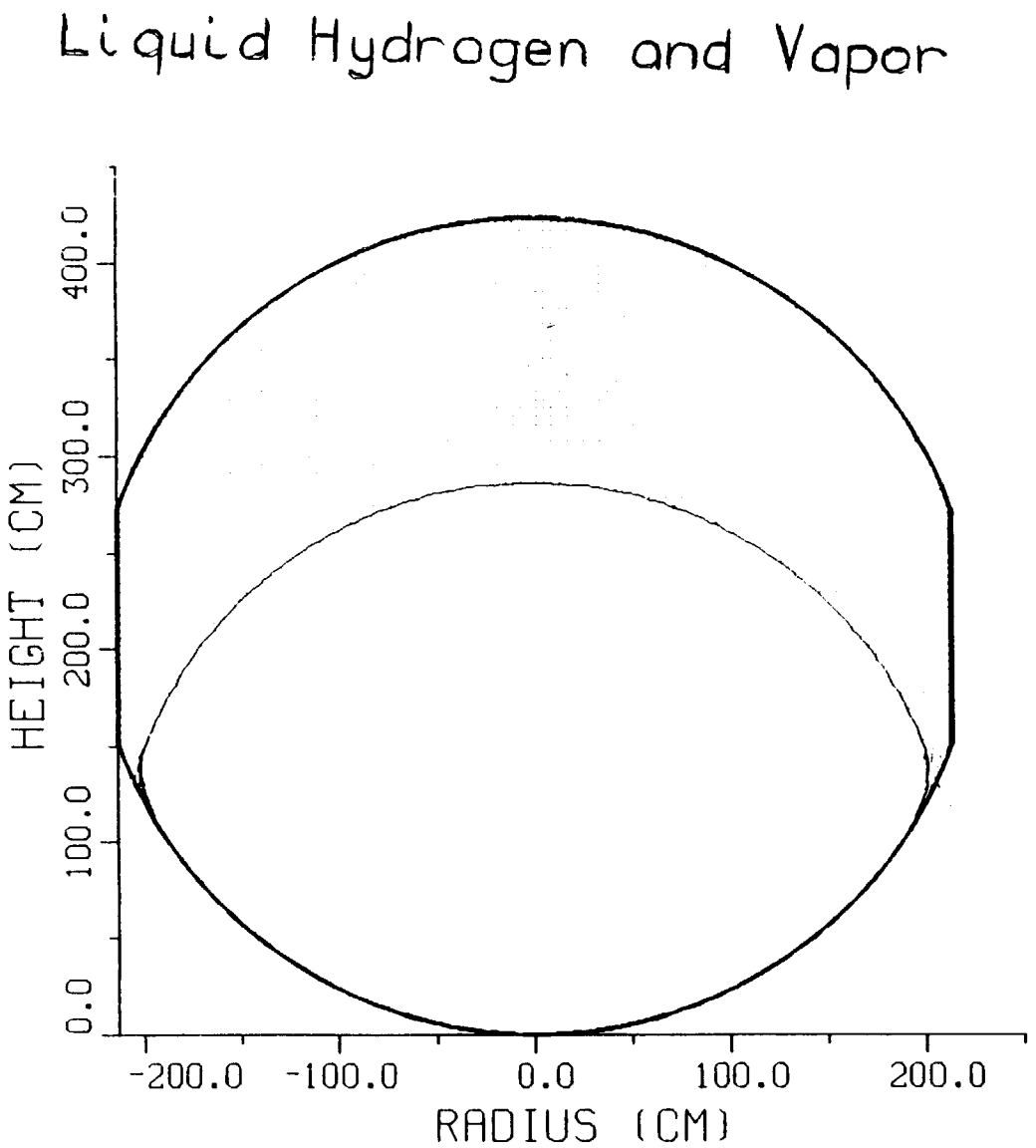

Figure 1 Size and Diameter of Space Transfer Vehicle

10^{-3} g_0; and (D) Liquid filled level of 70% and settling acceleration of 3.0×10^{-3} g_0.

Figures 2 to 11 show the time evolution of liquid hydrogen reorientation for liquid filled level of 30% and settling acceleration of 1.5×10^{-3} g_0. Figure 12 to 21 illustrate the time evolution of liquid hydrogen reorientation for liquid filled level of 30% and resettling accleration of 3.0×10^{-3} g_0. Figure 22 to 31 show the time evolution of liquid hydrogen reorientation of liquid hydrogen for liquid filled level of 70% and resettling acceleration of 1.5×10^{-3} g_0. Figure 32 to 41 illustrate the time evolution of liquid hydrogen for liquid filled level of 70% and resettling of 3.0×10^{-3} g_0.

(A) Full-Scale Simulation

Liquid Filled: 30%

Settling Acceleration: 1.5×10^{-3} g_0

Liquid Hydrogen and Vapor

Liquid Filled=30% t= 0.00s

$g = -1.50 \times 10^{-3} g_0$

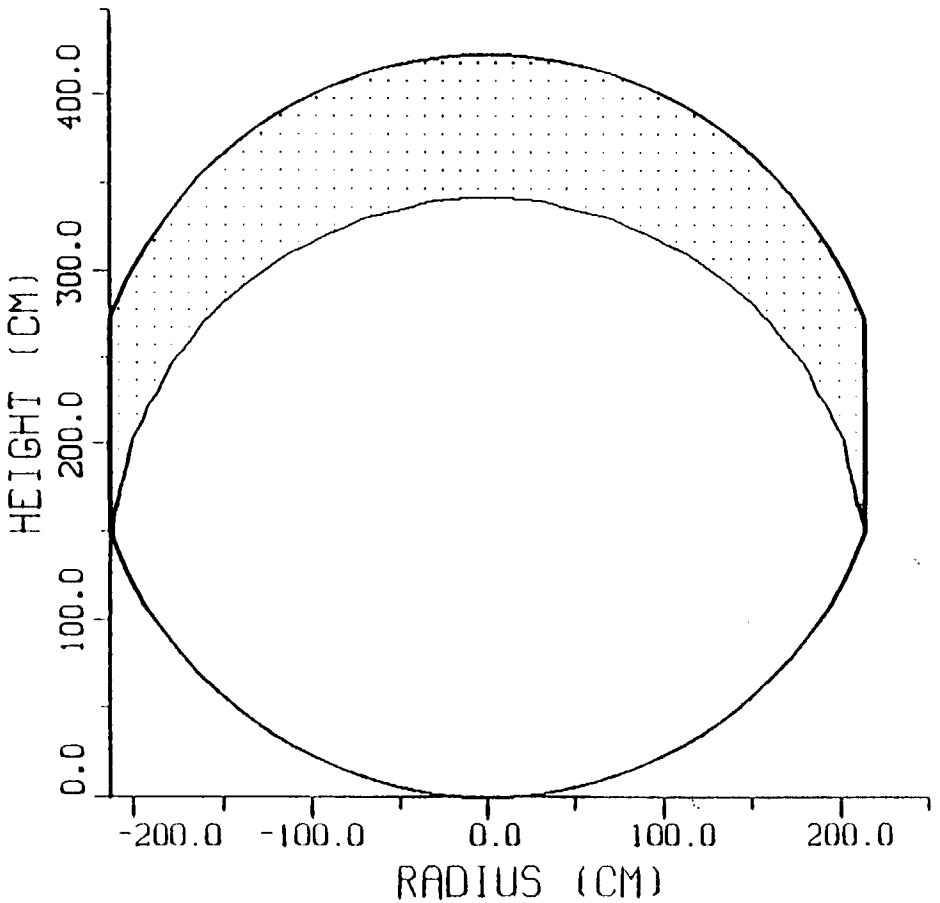

Figure 2

Liquid Hydrogen and Vapor

Liquid Filled=30% $t = 2.81 \times 10^{1}$ s

$g = -1.50 \times 10^{-3} g_o$

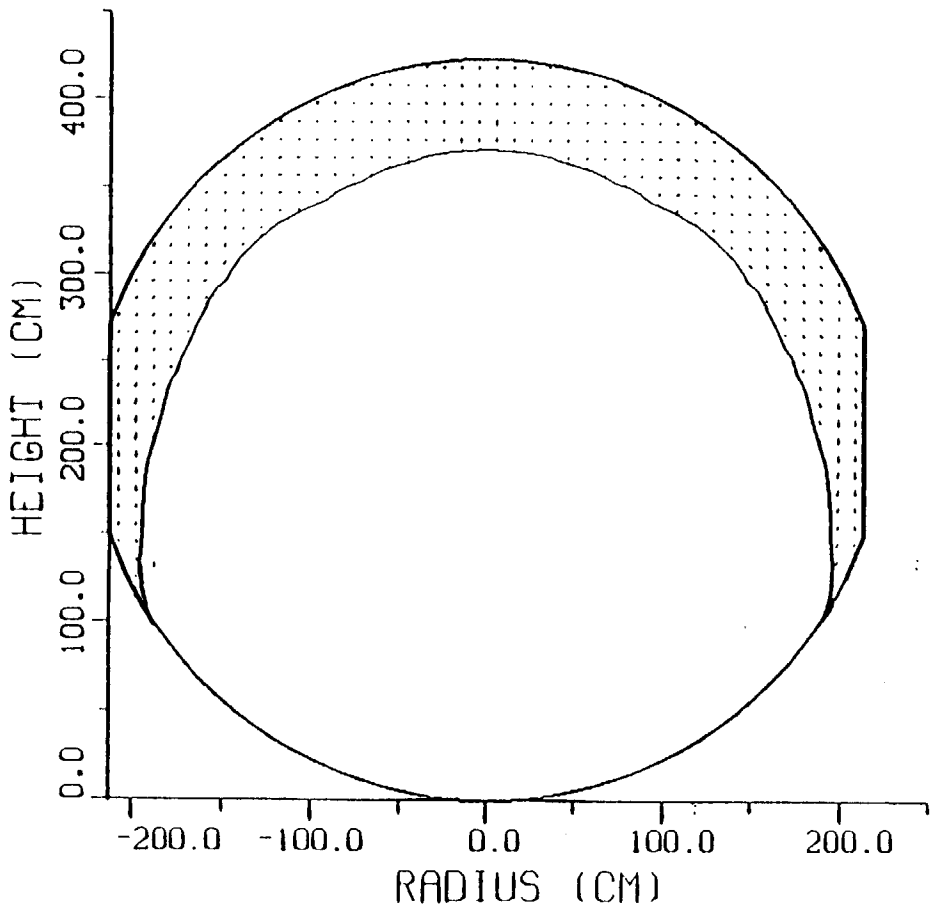

Figure 3

Liquid Hydrogen and Vapor

Liquid Filled=30% $t = 5.61 \times 10^{1}$ s

$g = -1.50 \times 10^{-3} g_0$

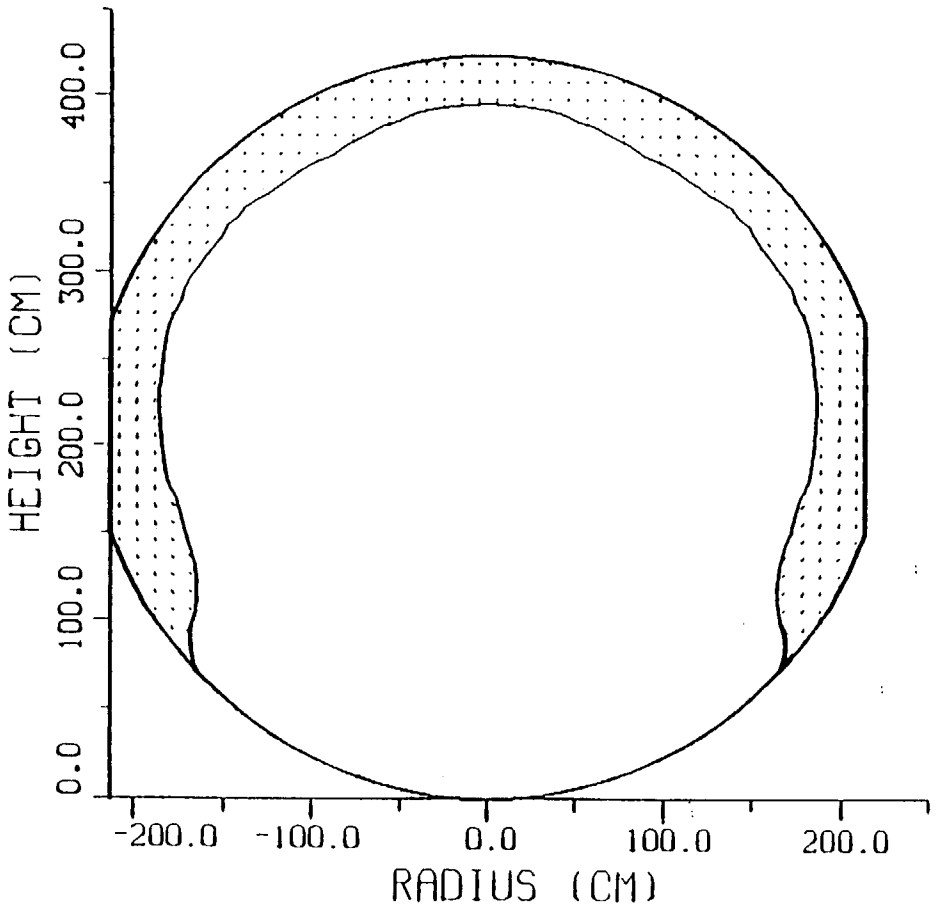

Figure 4

Liquid Hydrogen and Vapor

Liquid Filled=30% $t = 8.82 \times 10^{1}$ s

$g = -1.50 \times 10^{-3} g_o$

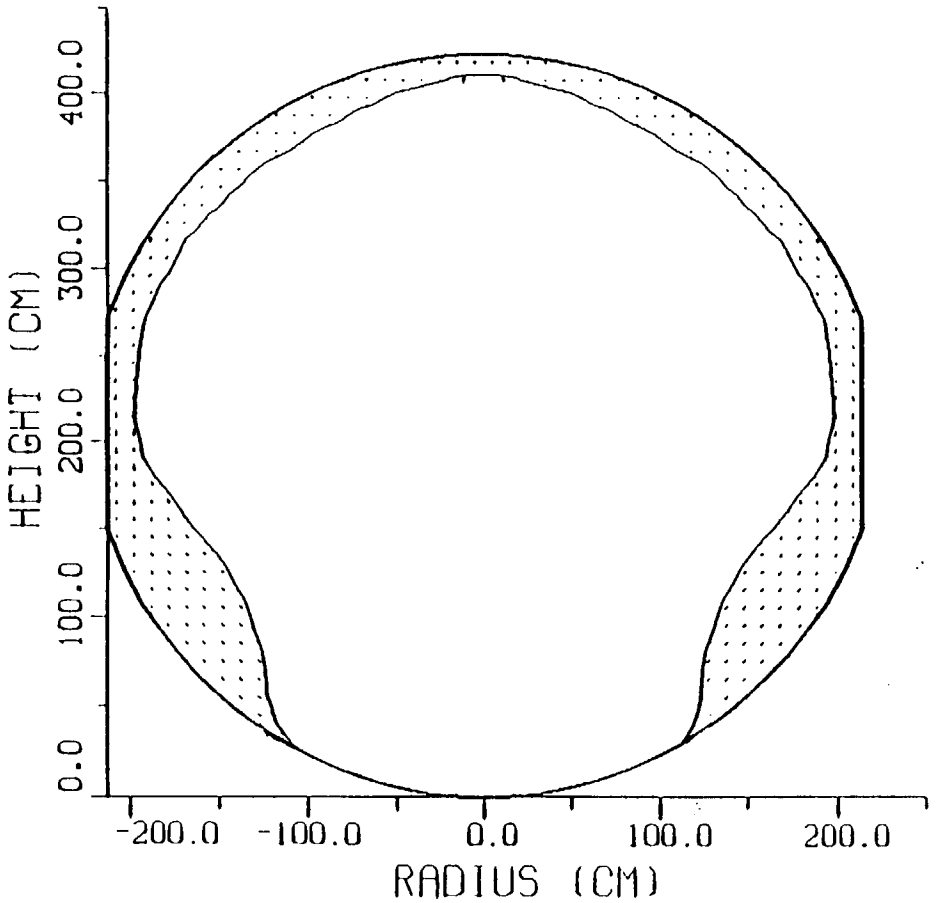

Figure 5

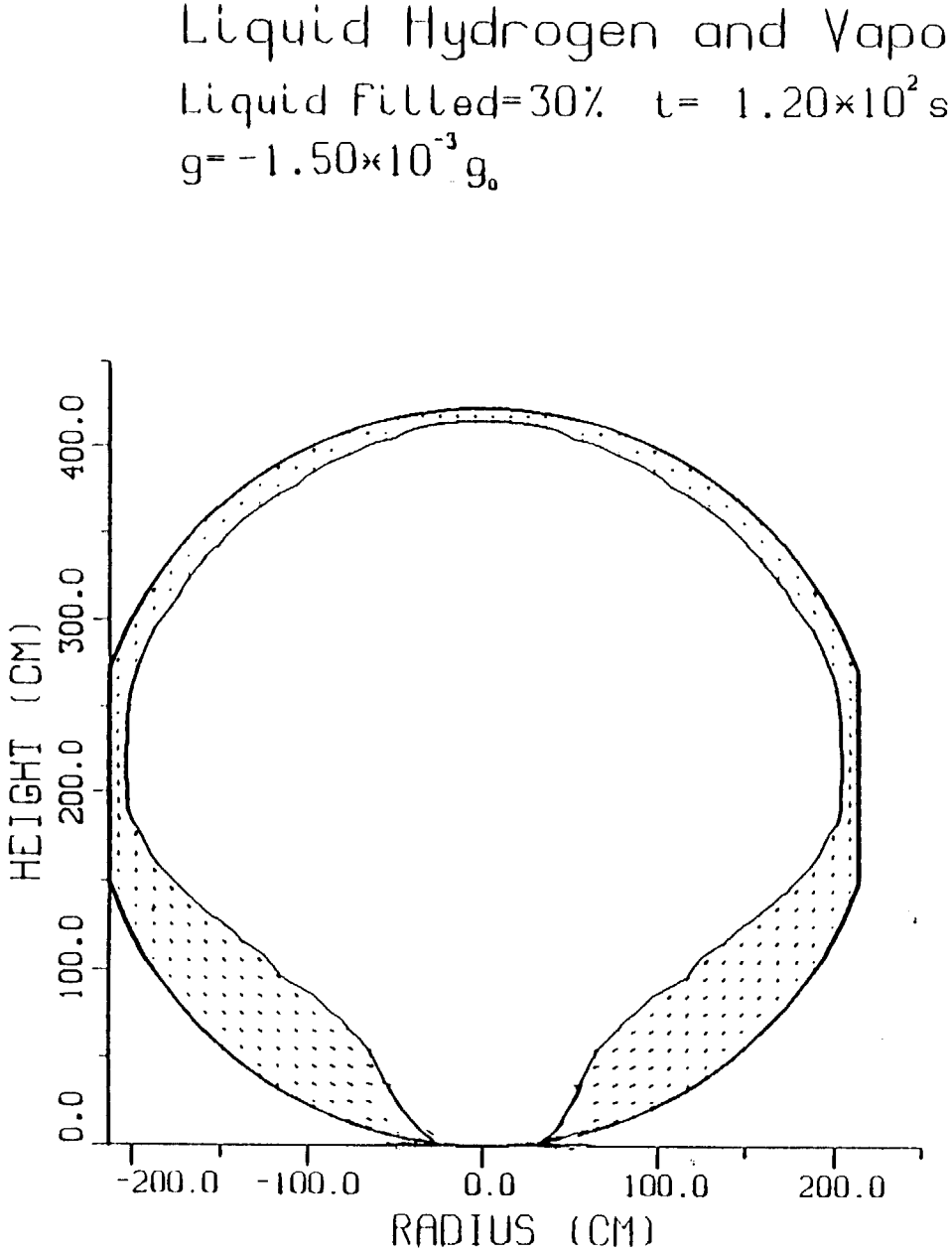
Liquid Hydrogen and Vapor
Liquid Filled=30% t= 1.20×10^2 s
g= -1.50×10^-3 g0
HEIGHT (CM)
0.0
100.0
200.0
300.0
400.0
-200.0
-100.0
0.0
100.0
200.0
RADIUS (CM)

Figure 6

Liquid Hydrogen and Vapor

Liquid Filled=30% $t = 1.24 \times 10^{2}$ s

$g = -1.50 \times 10^{-3} g_o$

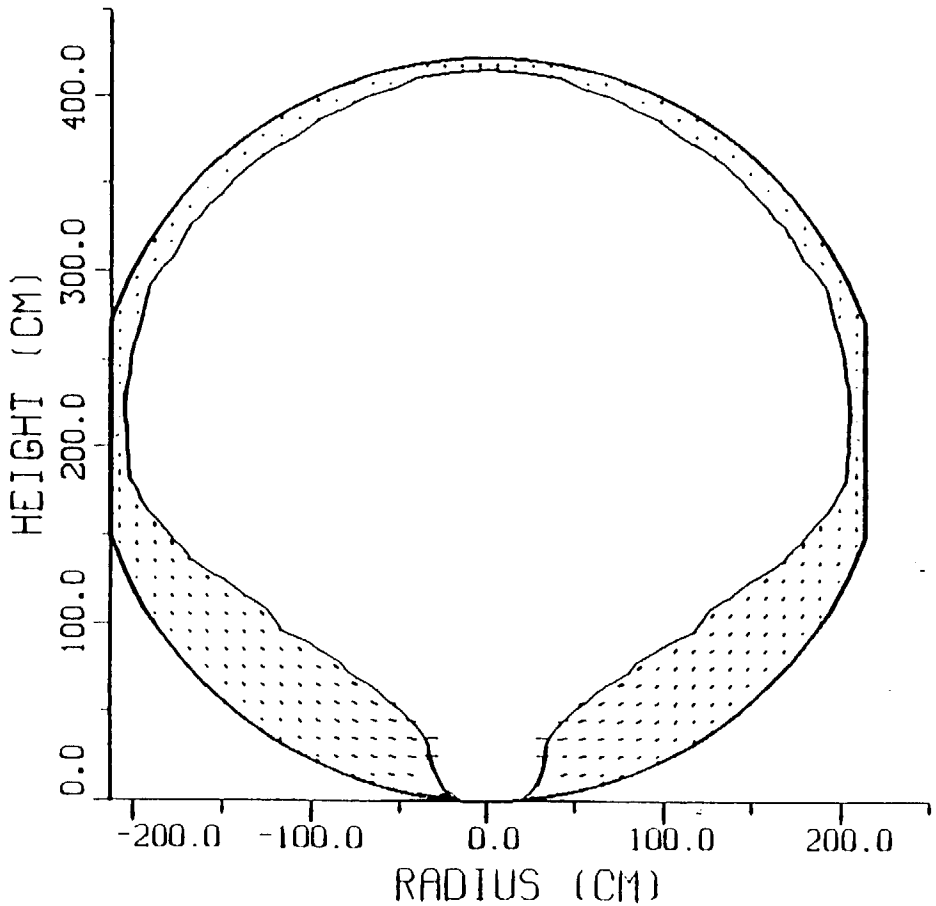

Figure 7

Liquid Hydrogen and Vapor

Liquid Filled=30% $t = 1.28 \times 10^{2}$ s

$g = -1.50 \times 10^{-3} g_o$

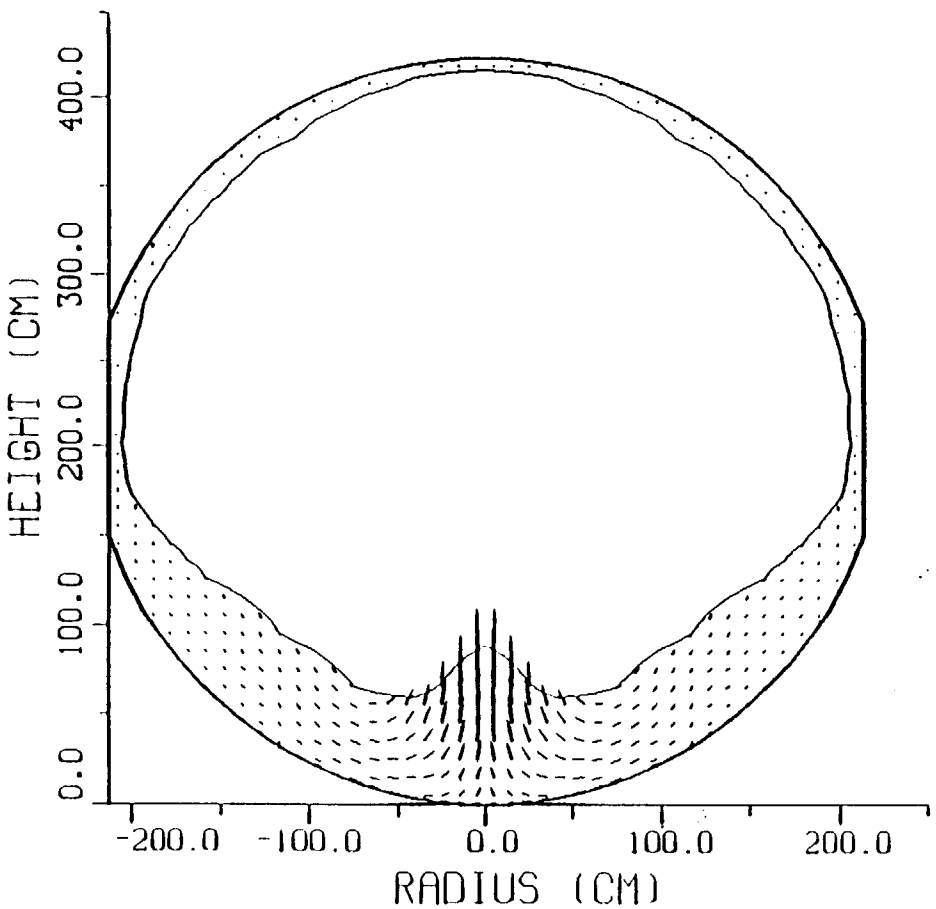

Figure 8

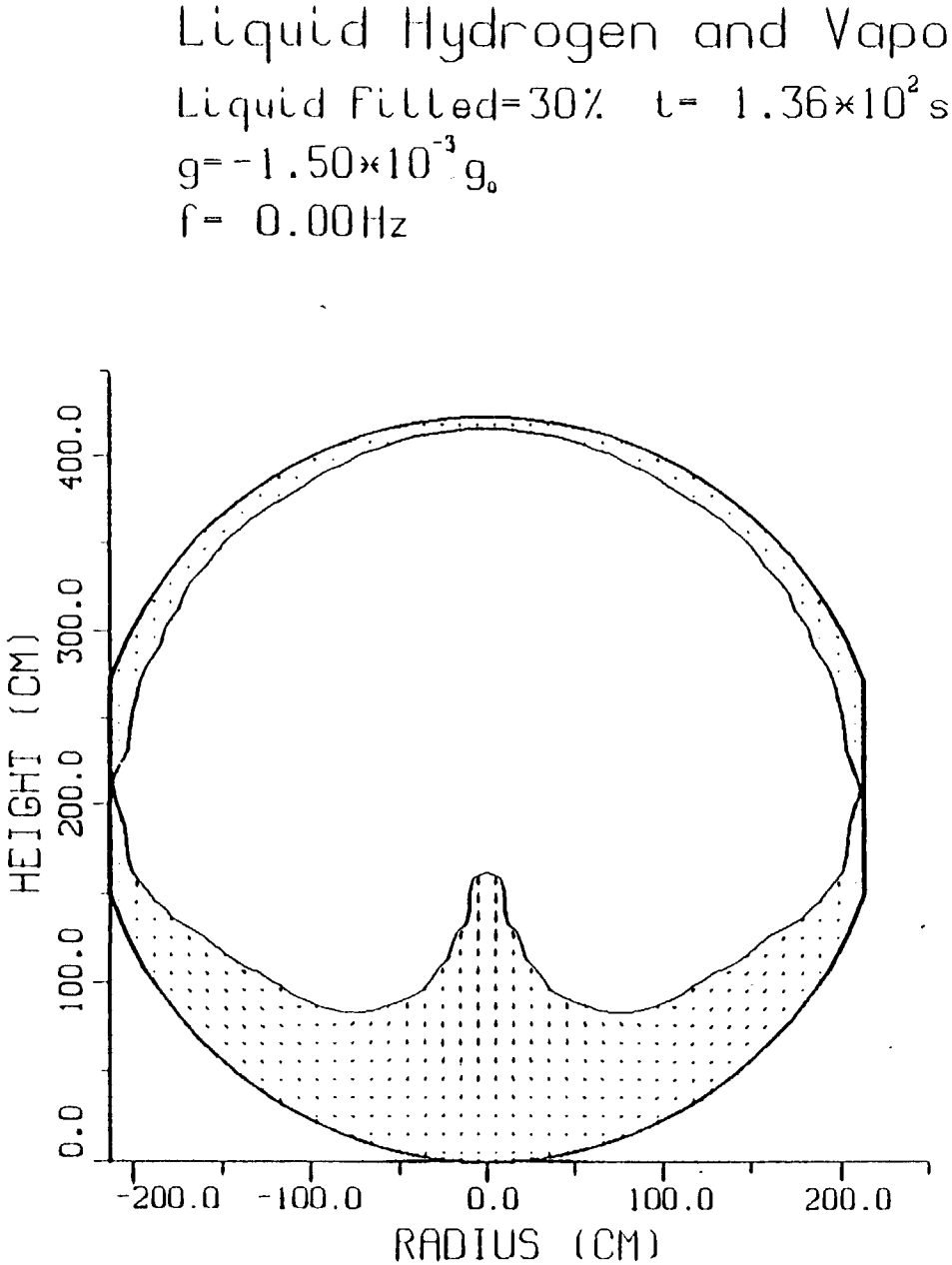
Liquid Hydrogen and Vapor
Liquid Filled=30% t= 1.36×10^2 s
g=-1.50×10^-3 g0
f= 0.00Hz
HEIGHT (CM)
0.0
100.0
200.0
300.0
400.0
-200.0
-100.0
0.0
100.0
200.0
RADIUS (CM)

Figure 9

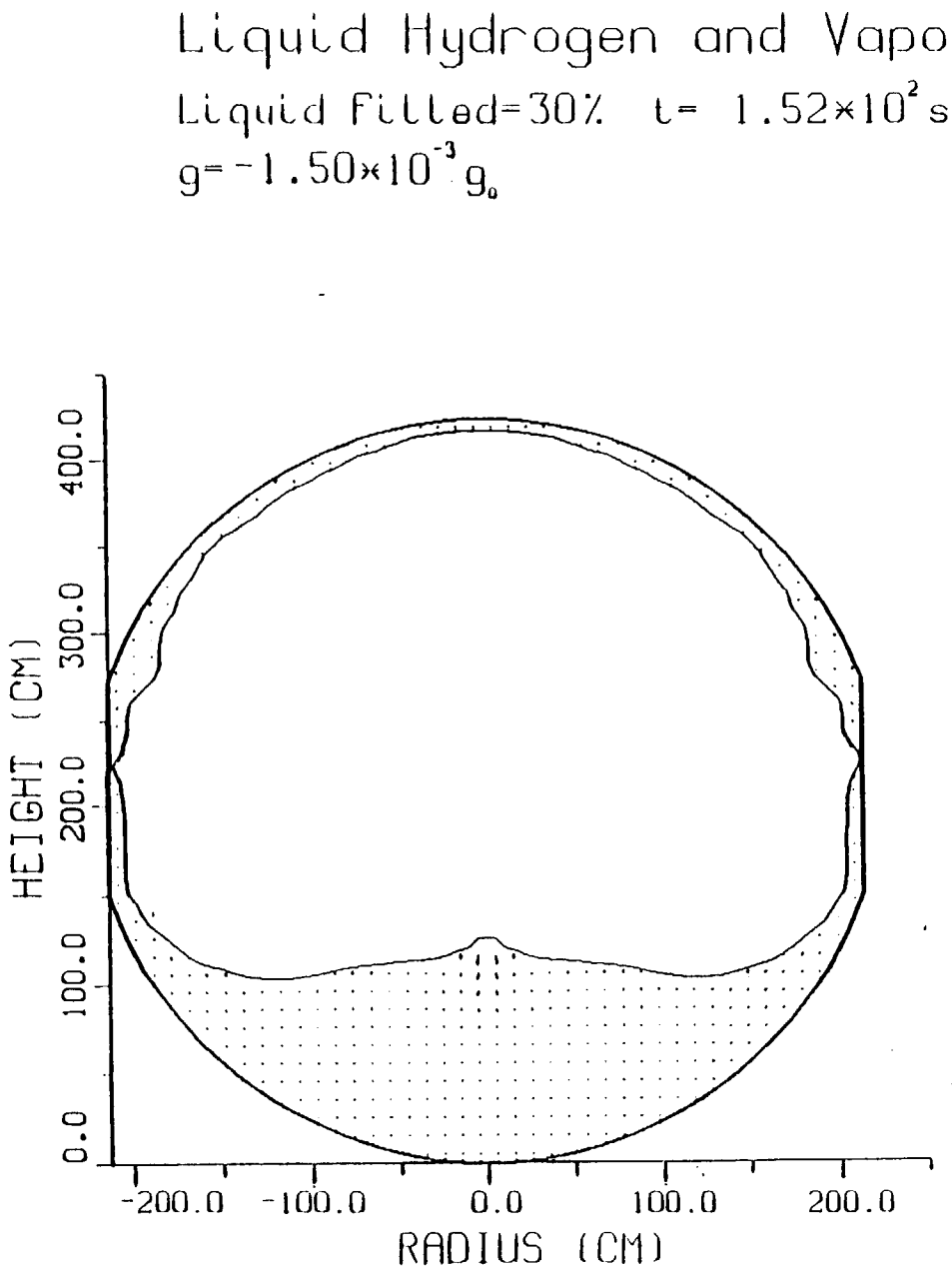
Liquid Hydrogen and Vapor
Liquid Filled=30% t= 1.52×10^2 s
g=-1.50×10^-3 g0
HEIGHT (CM)
0.0
100.0
200.0
300.0
400.0
-200.0
-100.0
0.0
100.0
200.0
RADIUS (CM)

Figure 10

Liquid Hydrogen and Vapor

Liquid Filled=30% $t = 1.80 \times 10^{2}$ s

$g = -1.50 \times 10^{-3} g_0$

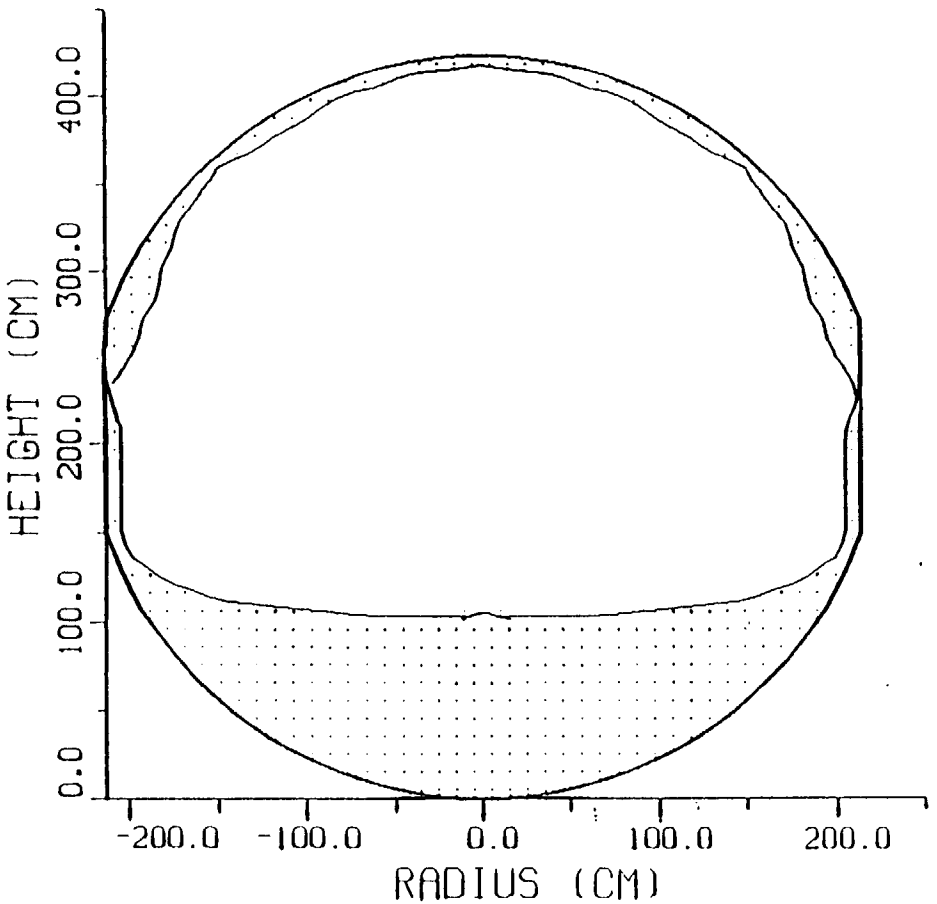

Figure 11

(B) Full-Scale Simulation

Liquid Filled: 30%

Settling Acceleration: 3.0×10^{-3} g_0

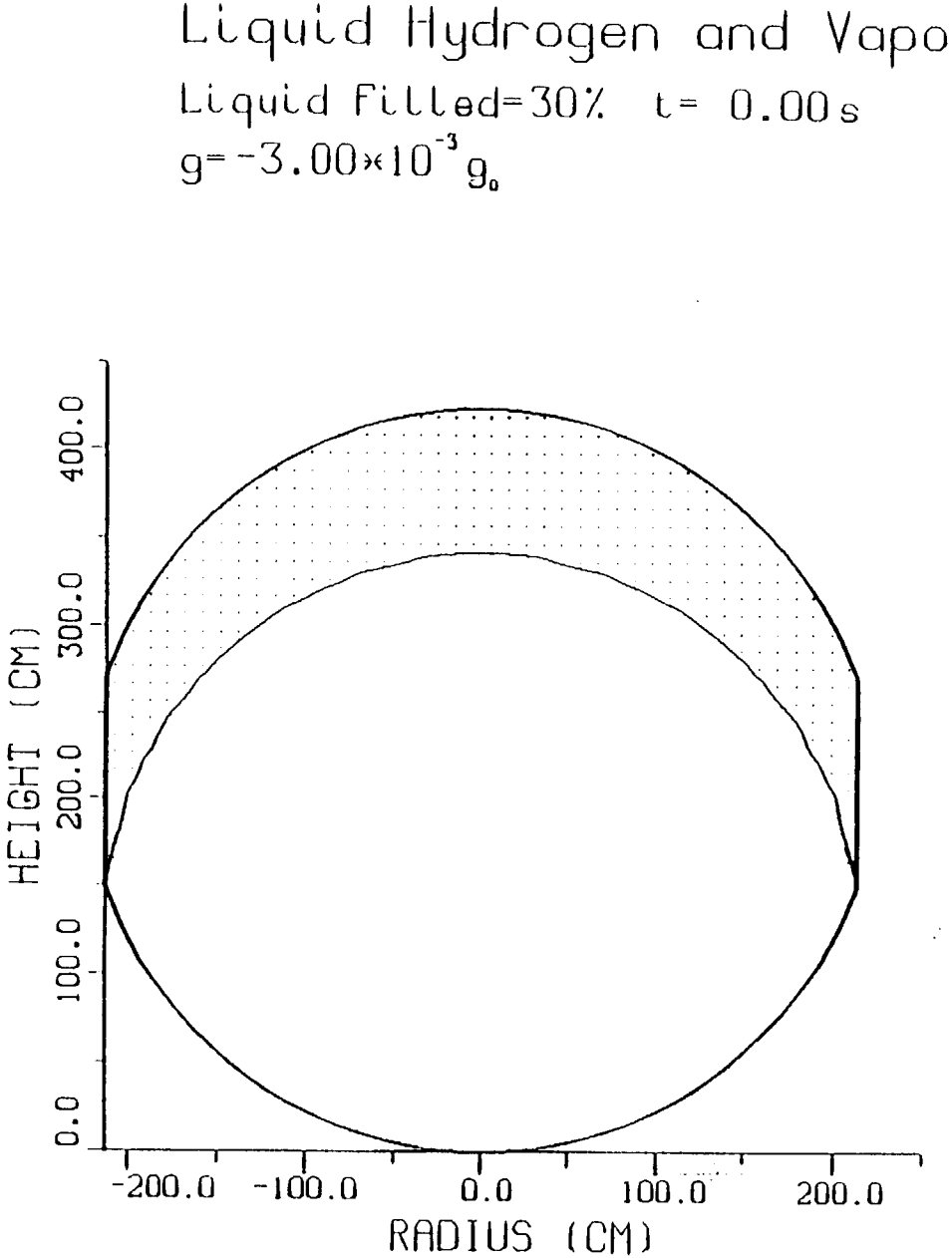
Liquid Hydrogen and Vapor
Liquid Filled=30% t= 0.00 s
g=-3.00×10^-3 g0
HEIGHT (CM)
0.0
100.0
200.0
300.0
400.0
-200.0
-100.0
0.0
100.0
200.0
RADIUS (CM)

Figure 12

Liquid Hydrogen and Vapor

Liquid Filled=30% $t = 2.88 \times 10^{1}$ s

$g = -3.00 \times 10^{-3} g_0$

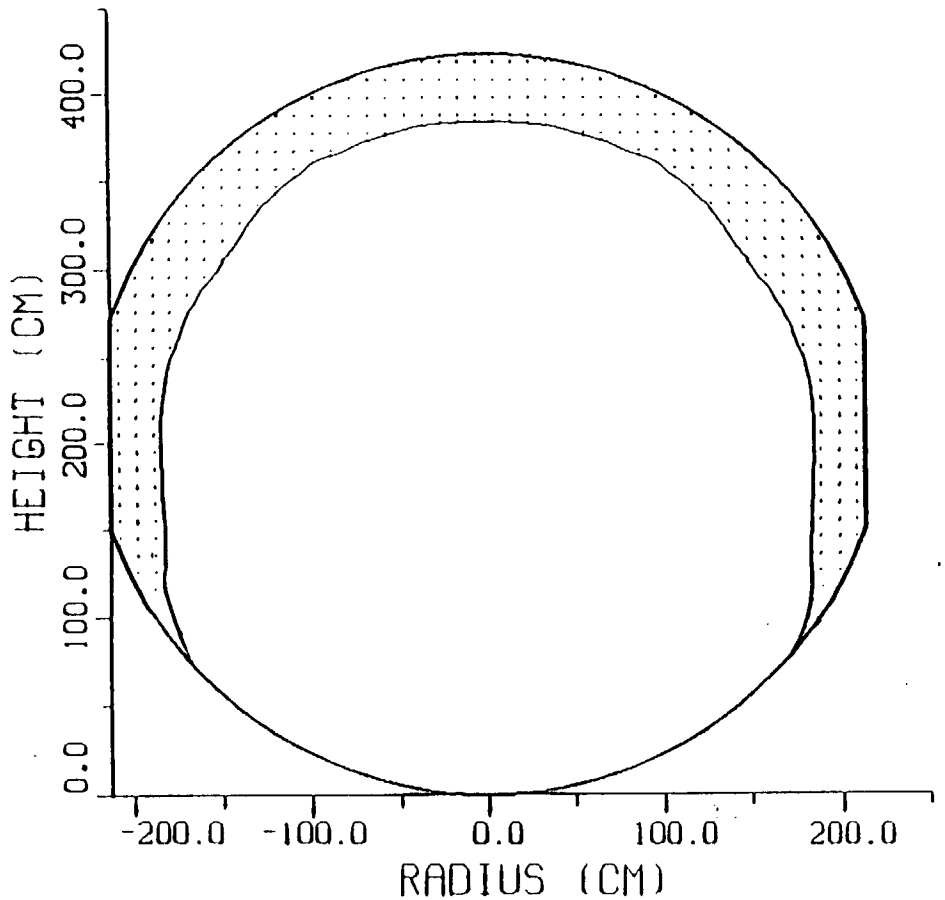

Figure 13

Liquid Hydrogen and Vapor

Liquid Filled=30% $t = 5.77 \times 10^{1}$ s

$g = -3.00 \times 10^{-3} g_o$

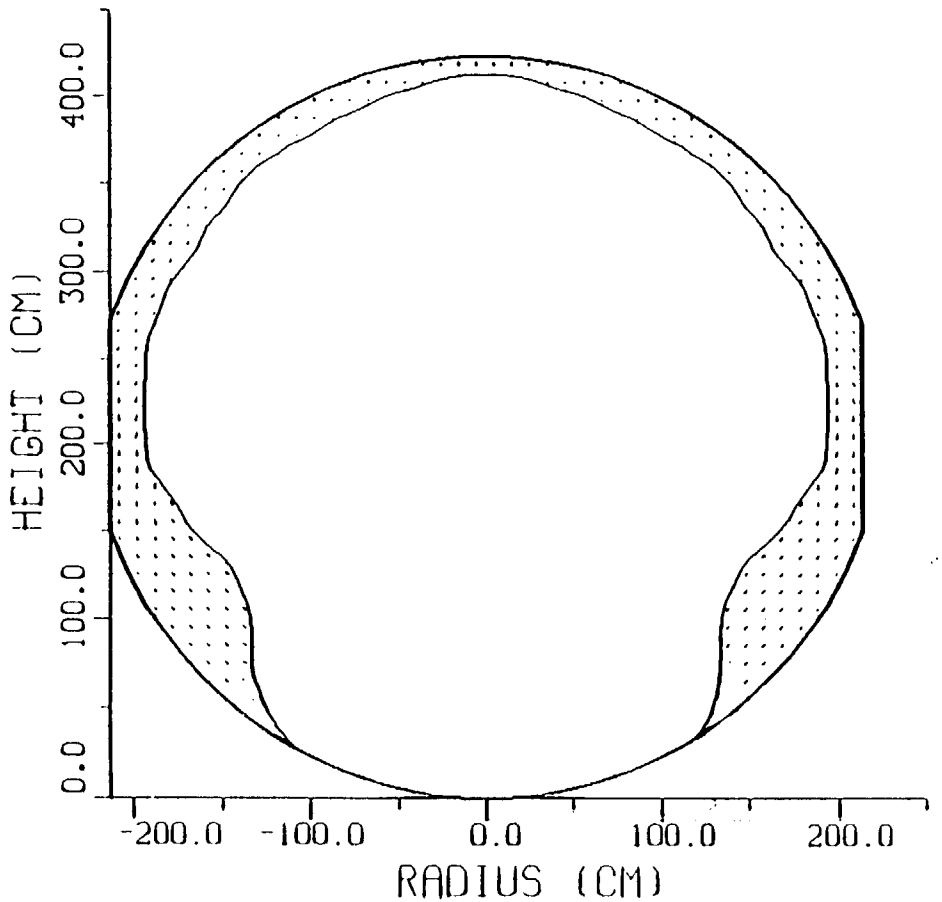

Figure 14

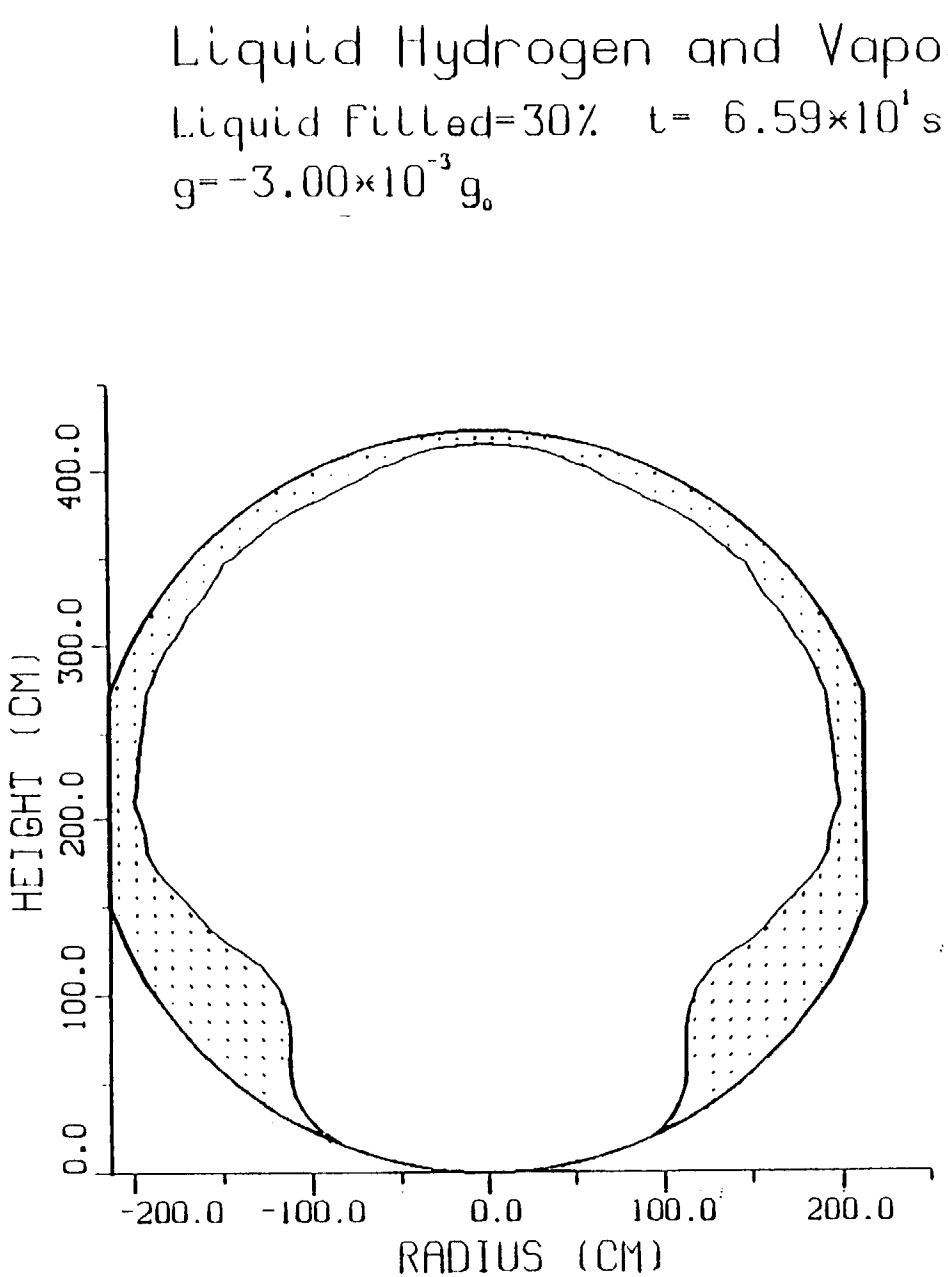
Liquid Hydrogen and Vapor
Liquid Filled=30% t= 6.59×10¹ s
g=-3.00×10⁻³ g₀
HEIGHT (CM)
0.0
100.0
200.0
300.0
400.0
-200.0
-100.0
0.0
100.0
200.0
RADIUS (CM)

Figure 15

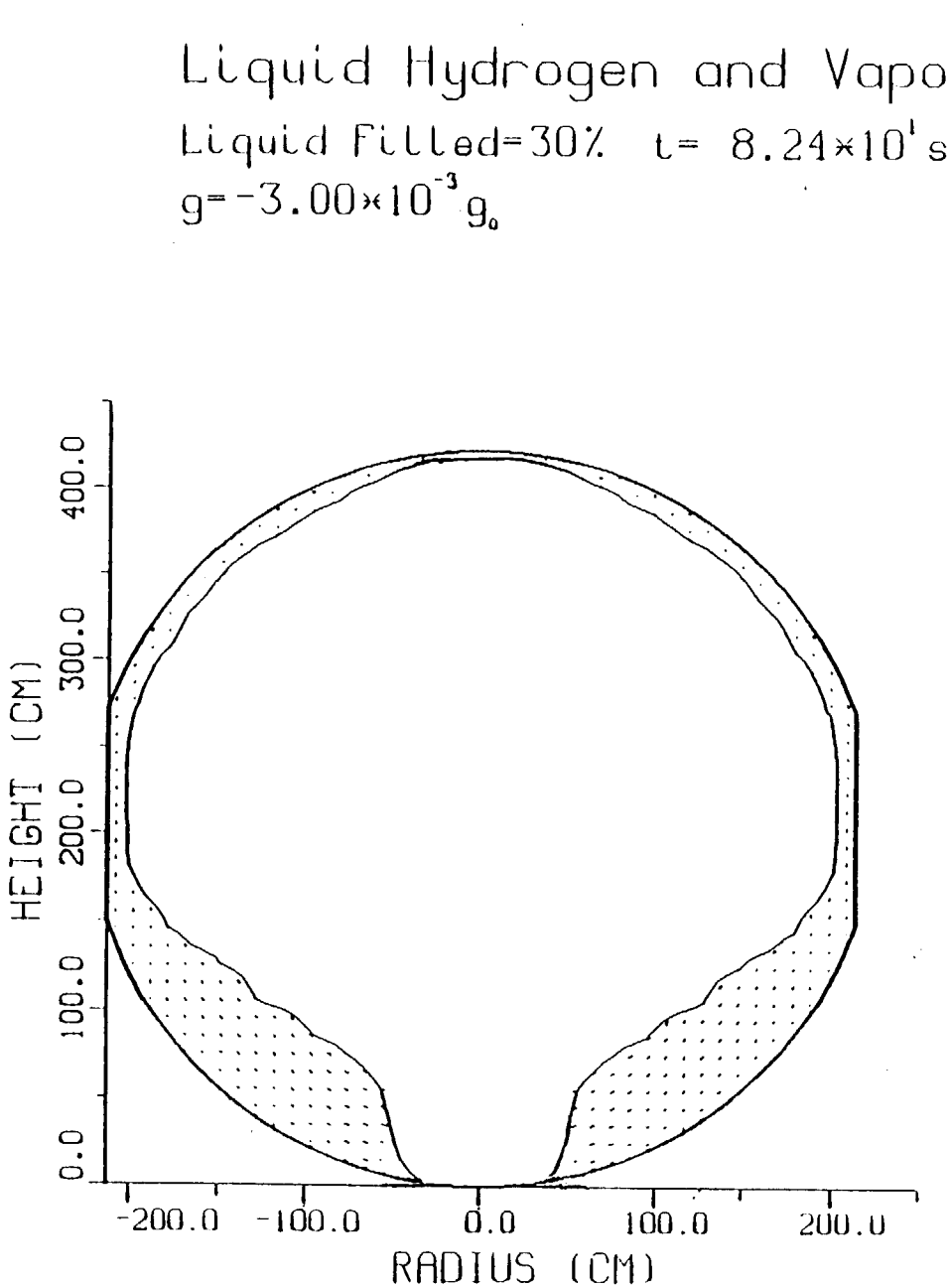
Liquid Hydrogen and Vapor
Liquid Filled=30% t= 8.24×10¹ s
g=-3.00×10⁻³ g₀
HEIGHT (CM)
0.0
100.0
200.0
300.0
400.0
-200.0
-100.0
0.0
100.0
200.0
RADIUS (CM)

Figure 16

Liquid Hydrogen and Vapor

Liquid Filled=30% $t = 8.57 \times 10^{1}$ s

$g = -3.00 \times 10^{-3} g_o$

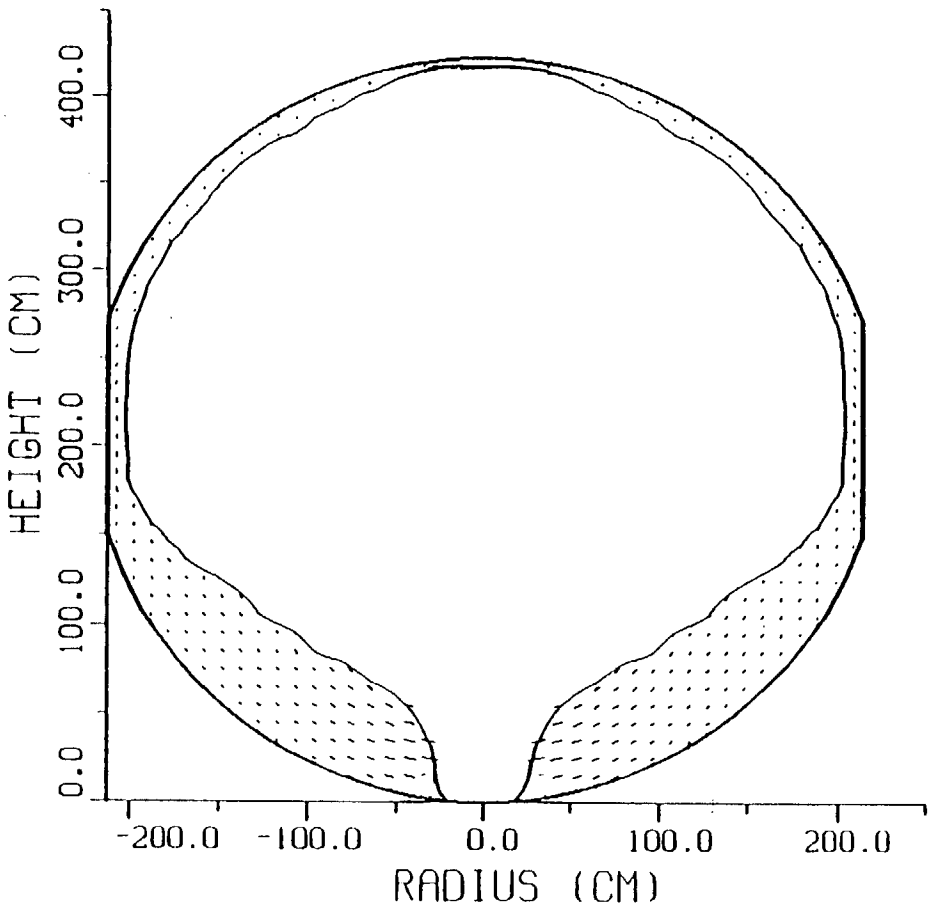

Figure 17

Liquid Hydrogen and Vapor

Liquid Filled=30% $t = 9.39 \times 10^{1}$ s

$g = -3.00 \times 10^{-3} g_o$

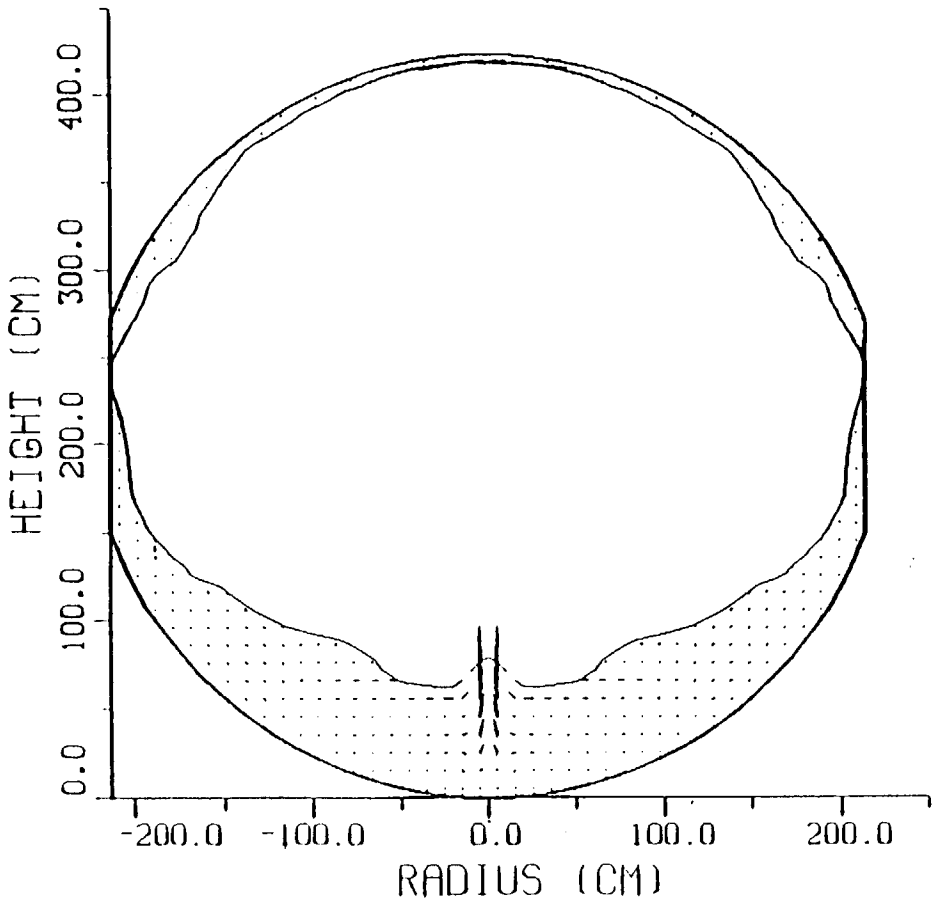

Figure 18

Liquid Hydrogen and Vapor

Liquid Filled=30% $t = 9.72 \times 10^{1}$ s

$g = -3.00 \times 10^{-3} g_0$

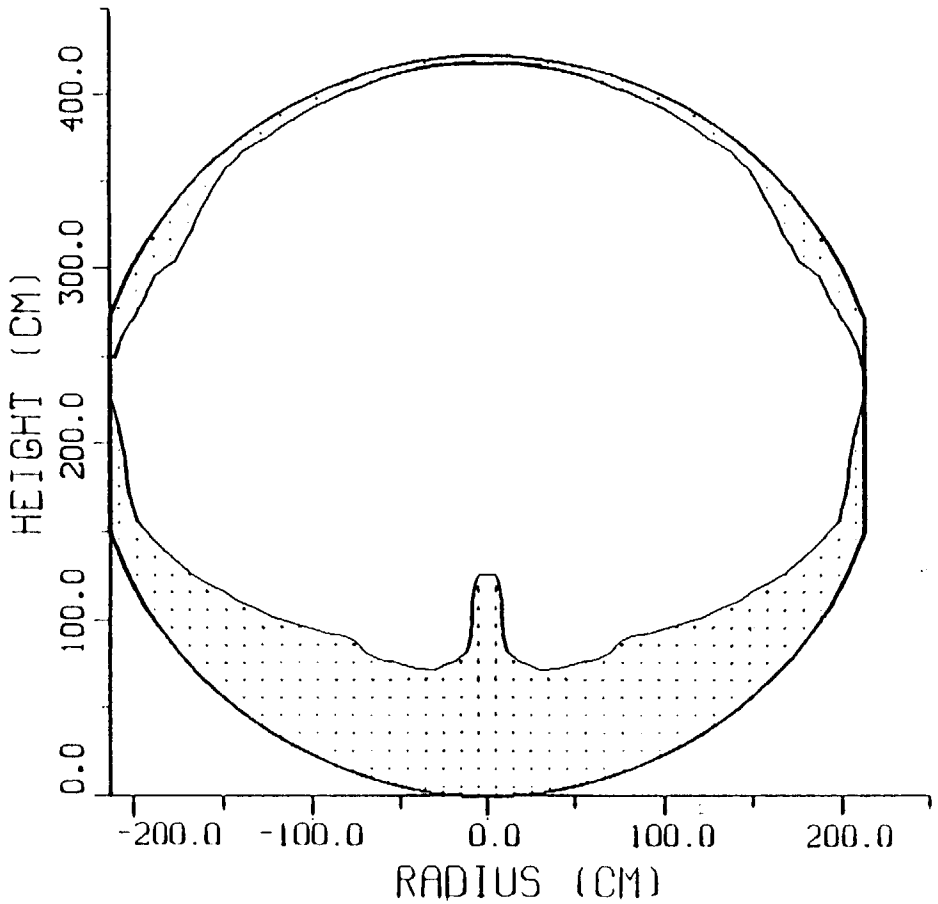

Figure 19

Liquid Hydrogen and Vapor

Liquid Filled=30% $t = 1.17 \times 10^{2}$ s

$g = -3.00 \times 10^{-3} g_0$

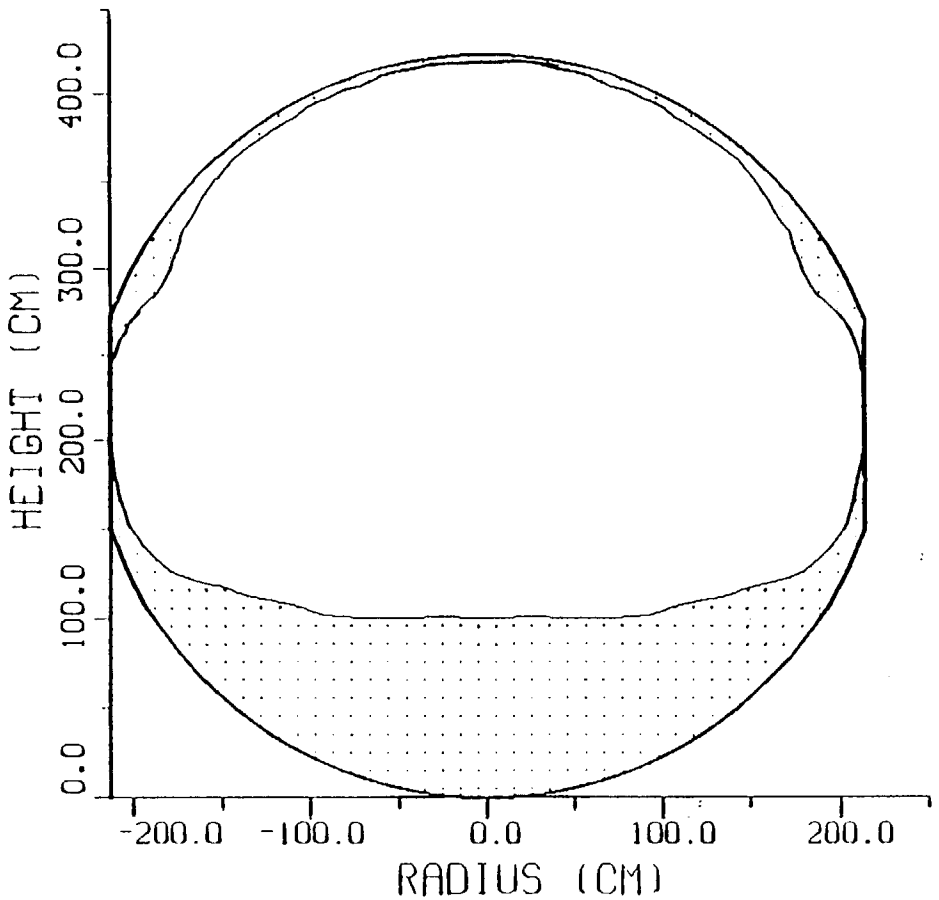

Figure 20

Liquid Hydrogen and Vapor

Liquid Filled=30% t= 1.33×10^{2} s

g= -3.00×10^{-3} g_o

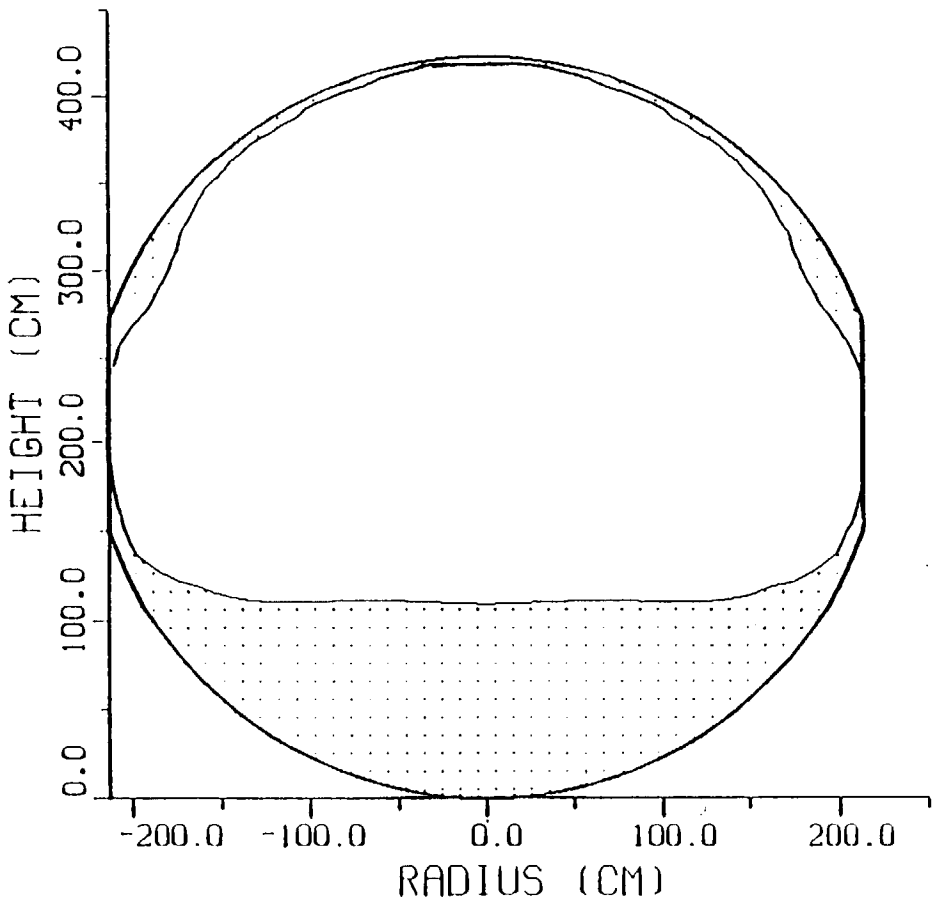

Figure 21

(C) Full-Scale Simulation

Liquid Filled: 70%

Settling Acceleration: 1.5×10^{-3} g_0

Liquid Hydrogen and Vapor

Liquid Filled=70% t= 0.00s

$g = -1.50 \times 10^{-3} g_o$

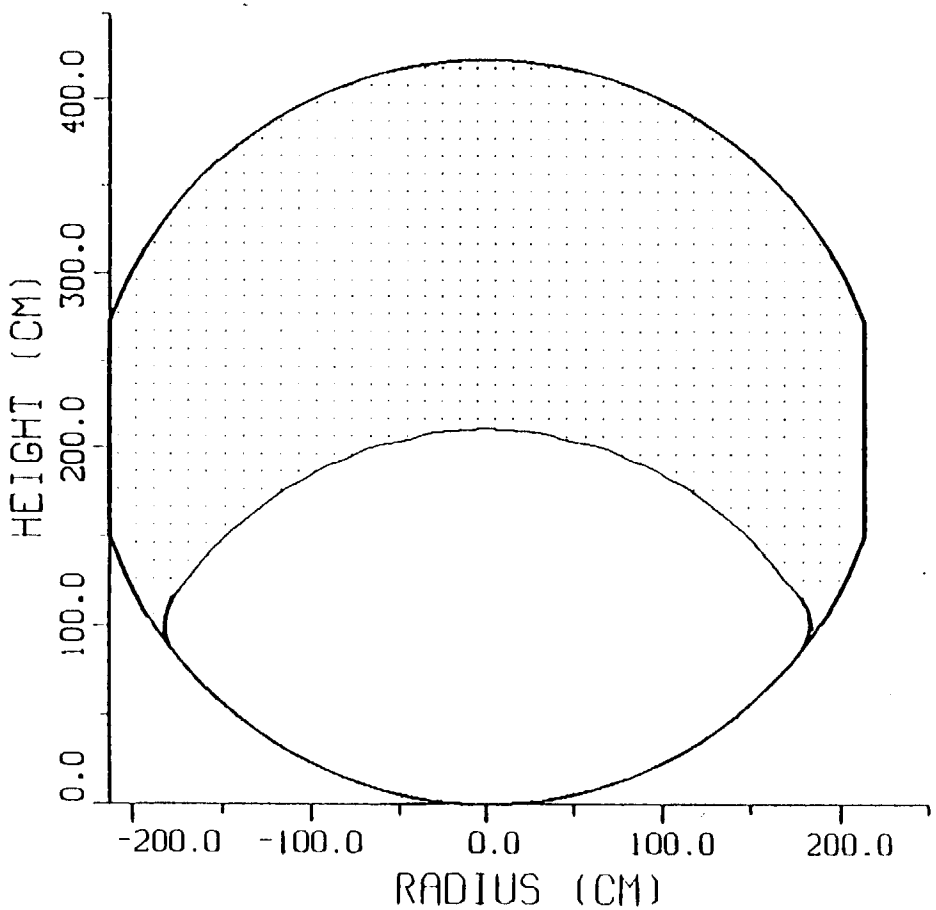

Figure 22

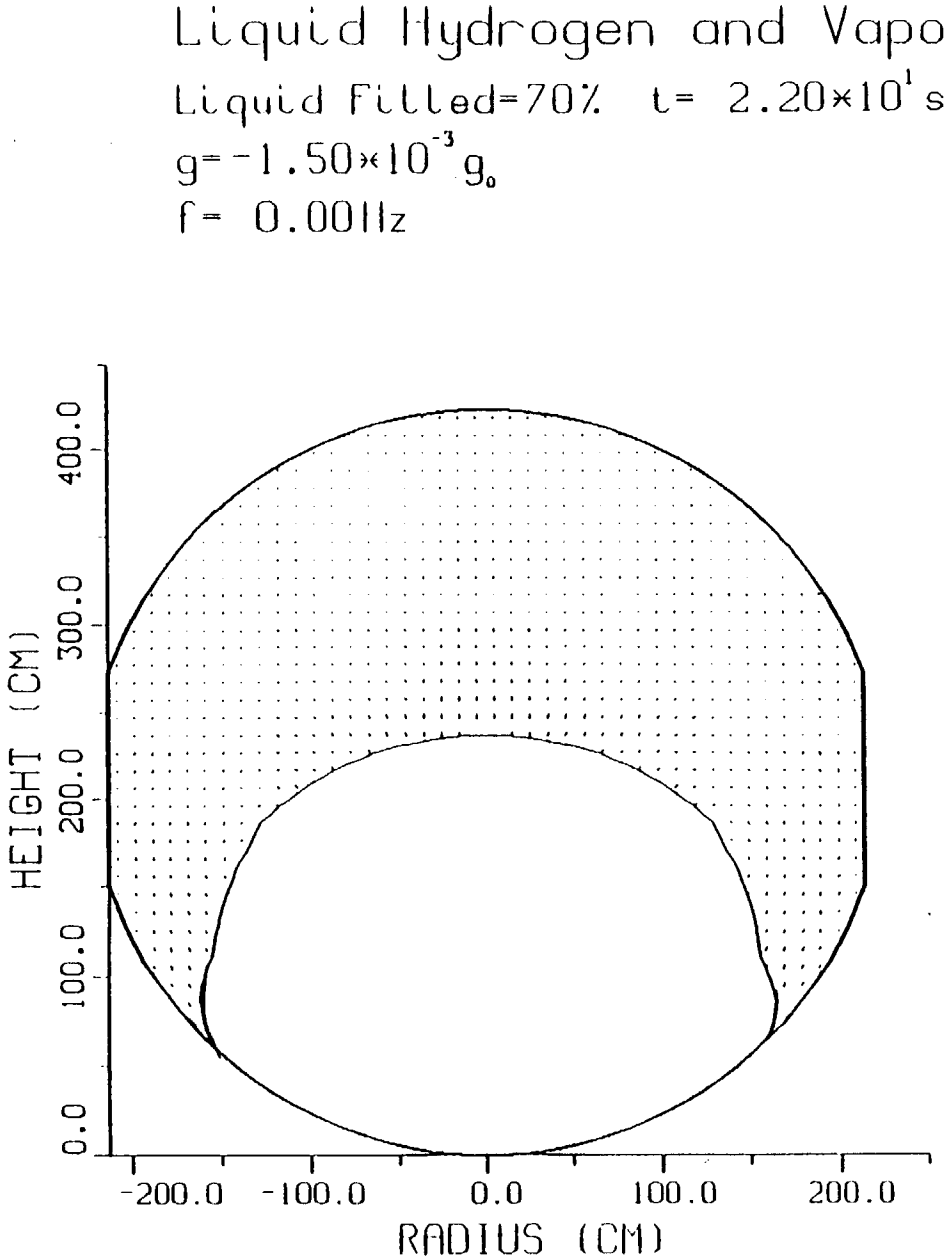
Liquid Hydrogen and Vapor
Liquid Filled=70% t= 2.20×10^1 s
g=-1.50×10^-3 g_o
f= 0.001Hz
HEIGHT (CM)
0.0
100.0
200.0
300.0
400.0
-200.0
-100.0
0.0
100.0
200.0
RADIUS (CM)

Figure 23

Liquid Hydrogen and Vapor

Liquid Filled=70% $t = 6.60 \times 10^{1}$ s

$g = -1.50 \times 10^{-3} g_0$

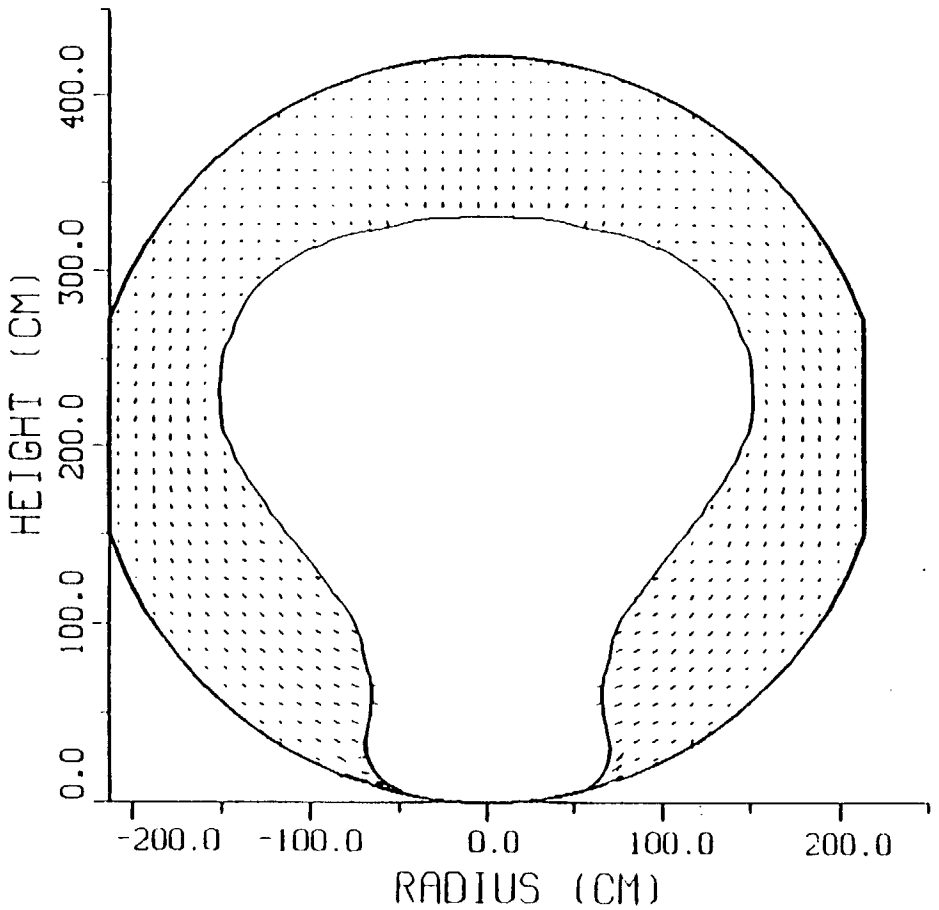

Figure 24

Liquid Hydrogen and Vapor

Liquid Filled=70% $t = 8.71 \times 10^{1}$ s

$g = -1.50 \times 10^{-3} g_0$

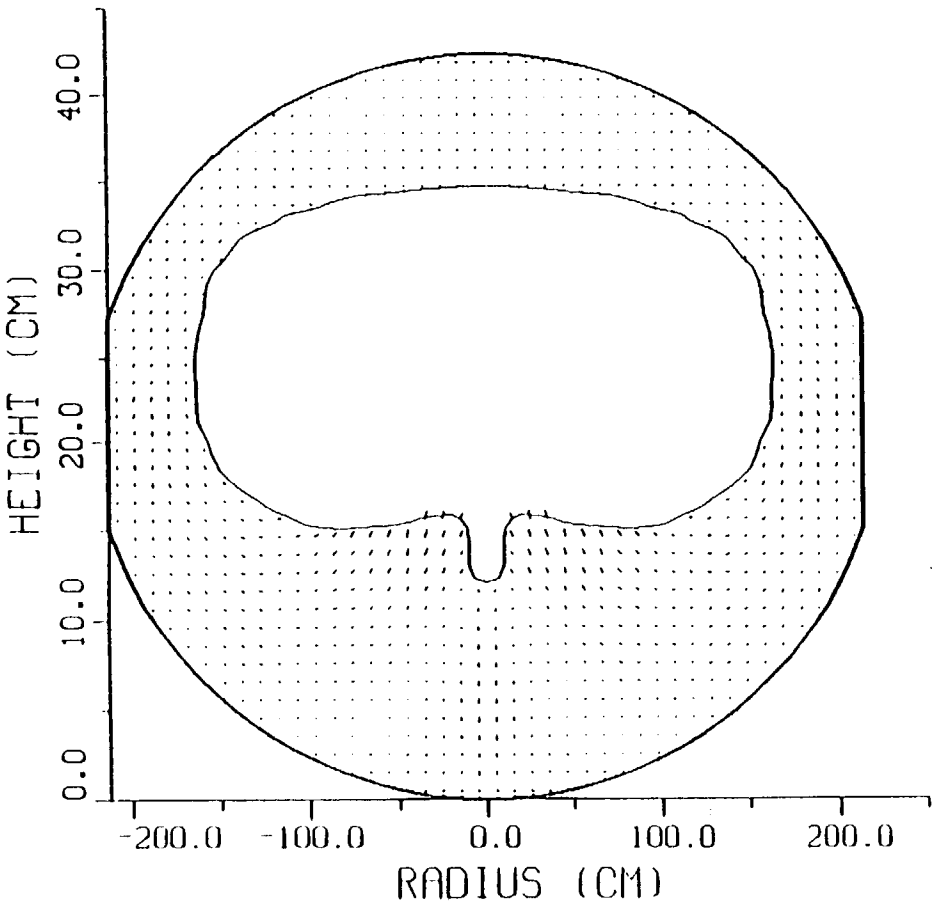

Figure 25

Liquid Hydrogen and Vapor

Liquid Filled=70% t= 1.01×10^{2} s

$g = -1.50 \times 10^{-3} g_o$

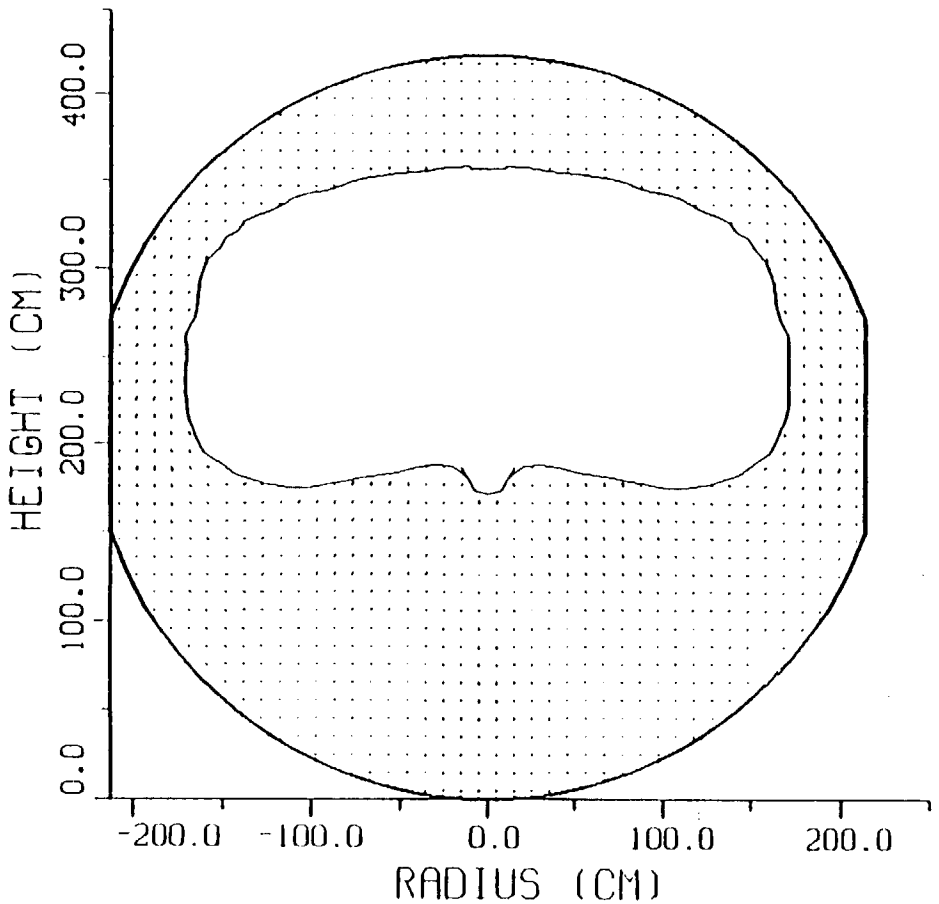

Figure 26

Liquid Hydrogen and Vapor

Liquid Filled=70% $t = 1.06 \times 10^{2}$ s

$g = -1.50 \times 10^{-3} g_0$

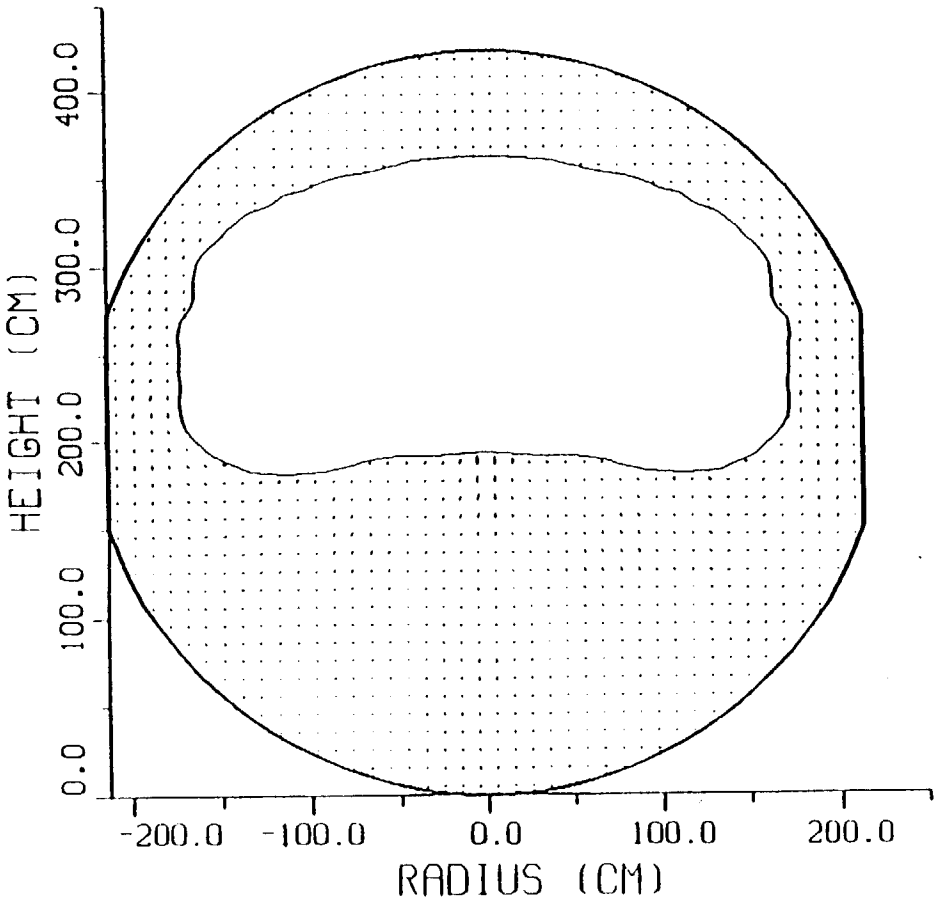

Figure 27

Liquid Hydrogen and Vapor

Liquid Filled=70% $t = 1.14 \times 10^2$ s

$g = -1.50 \times 10^{-3} g_o$

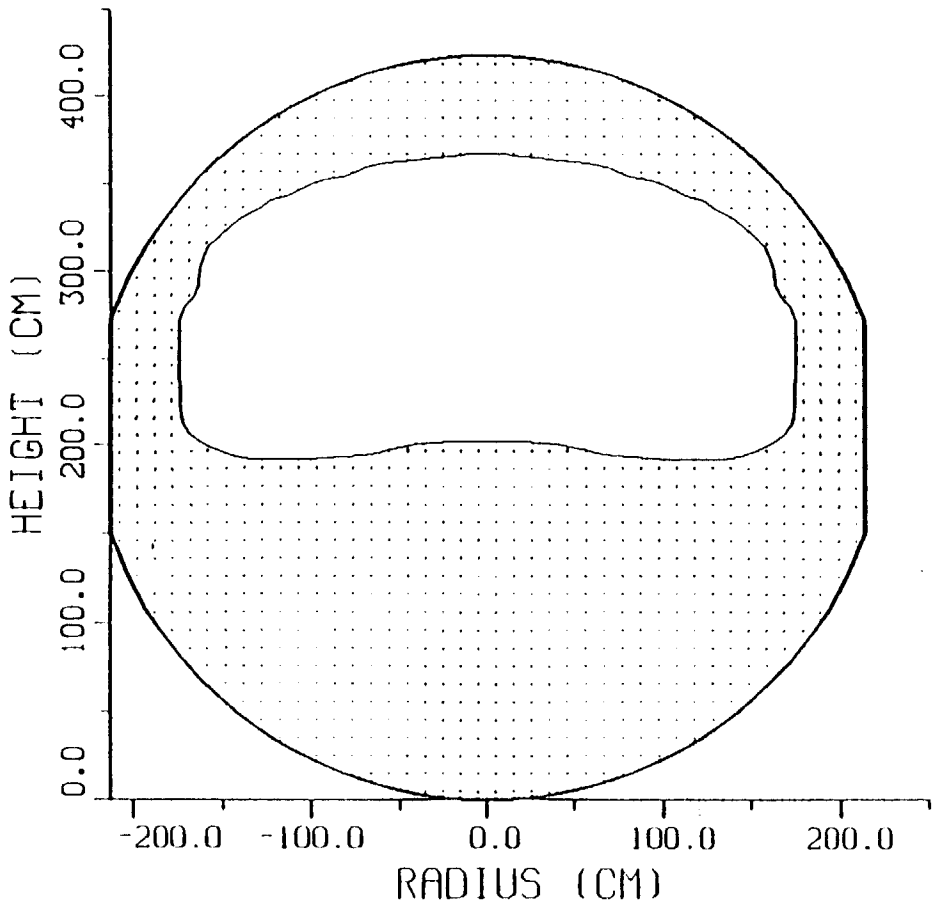

Figure 28

Liquid Hydrogen and Vapor

Liquid Filled=70% $t = 1.72 \times 10^2$ s

$g = -1.50 \times 10^{-3} g_o$

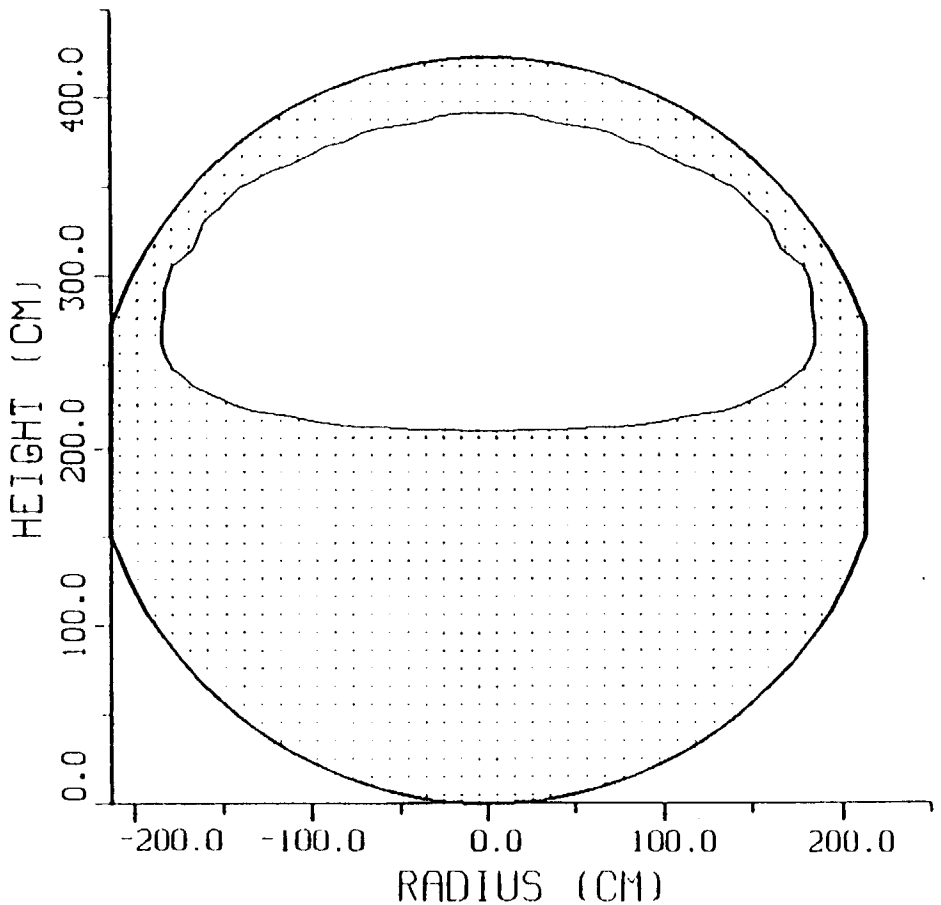

Figure 29

Liquid Hydrogen and Vapor

Liquid Filled=70% $t = 1.98 \times 10^{2}$ s

$g = -1.50 \times 10^{-3} g_o$

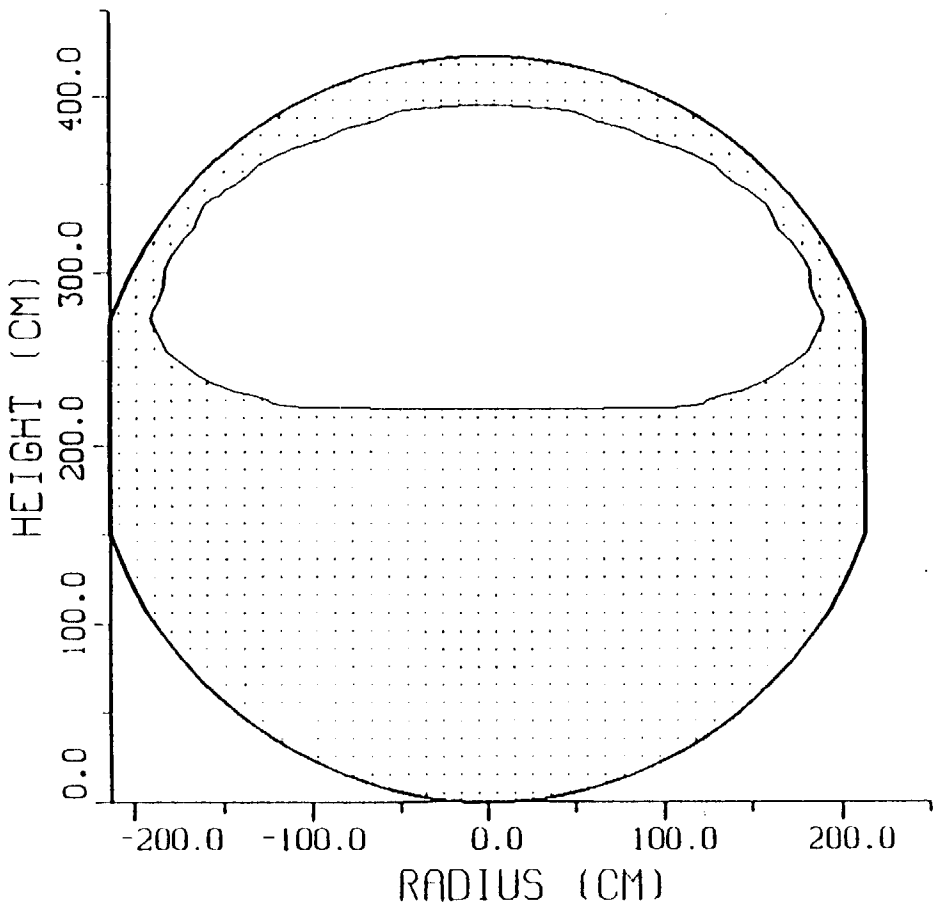

Figure 30

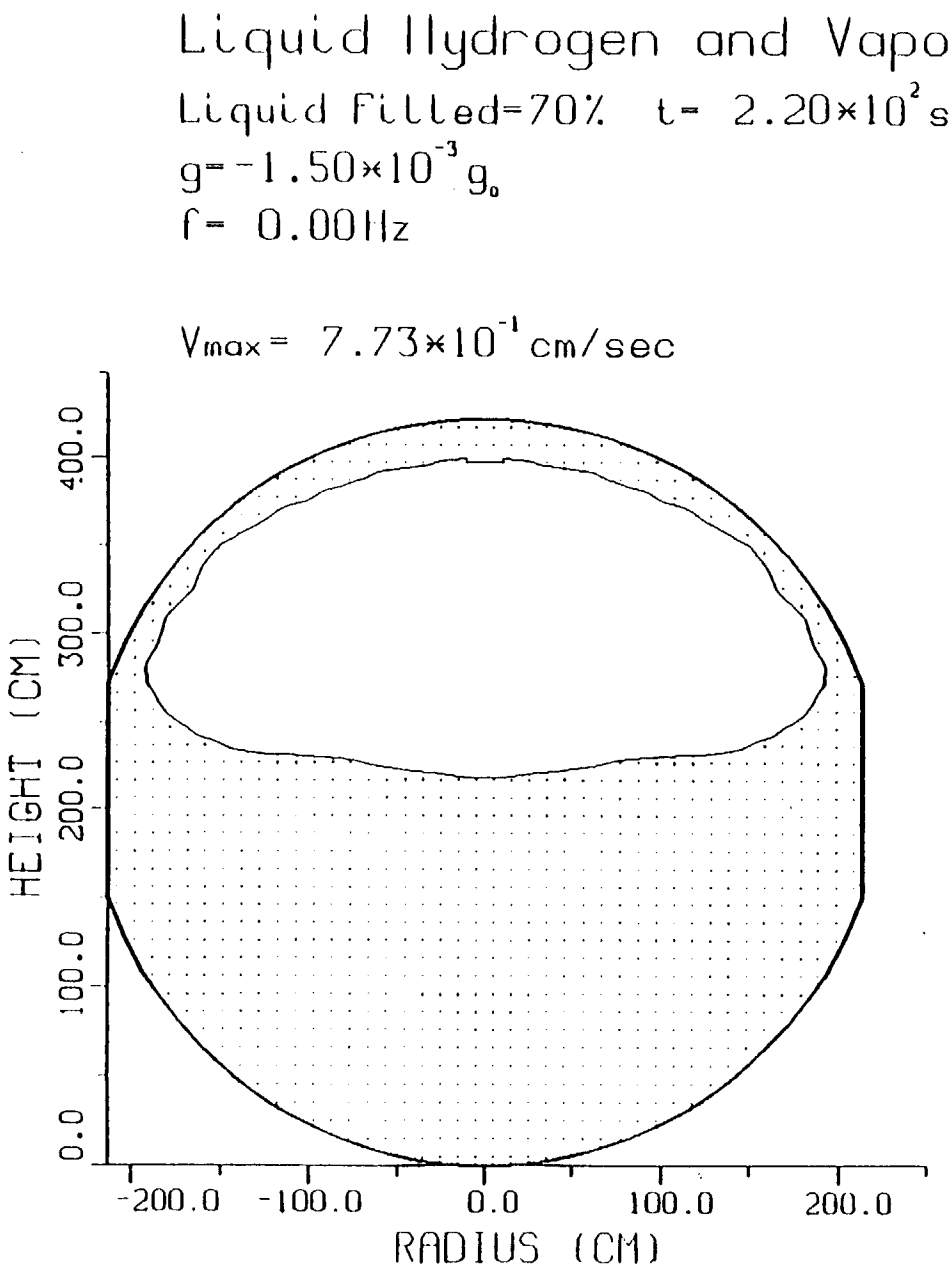
Liquid Hydrogen and Vapor
Liquid Filled=70% t= 2.20×10^2 s
g= -1.50×10^-3 g0
f= 0.001Hz
Vmax= 7.73×10^-1 cm/sec
HEIGHT (CM)
0.0
100.0
200.0
300.0
400.0
-200.0
-100.0
0.0
100.0
200.0
RADIUS (CM)

Figure 31

(D) Full-Scale Simulation

Liquid Filled: 70%

Settlinng Accleration: 3.0×10^{-3} g_0

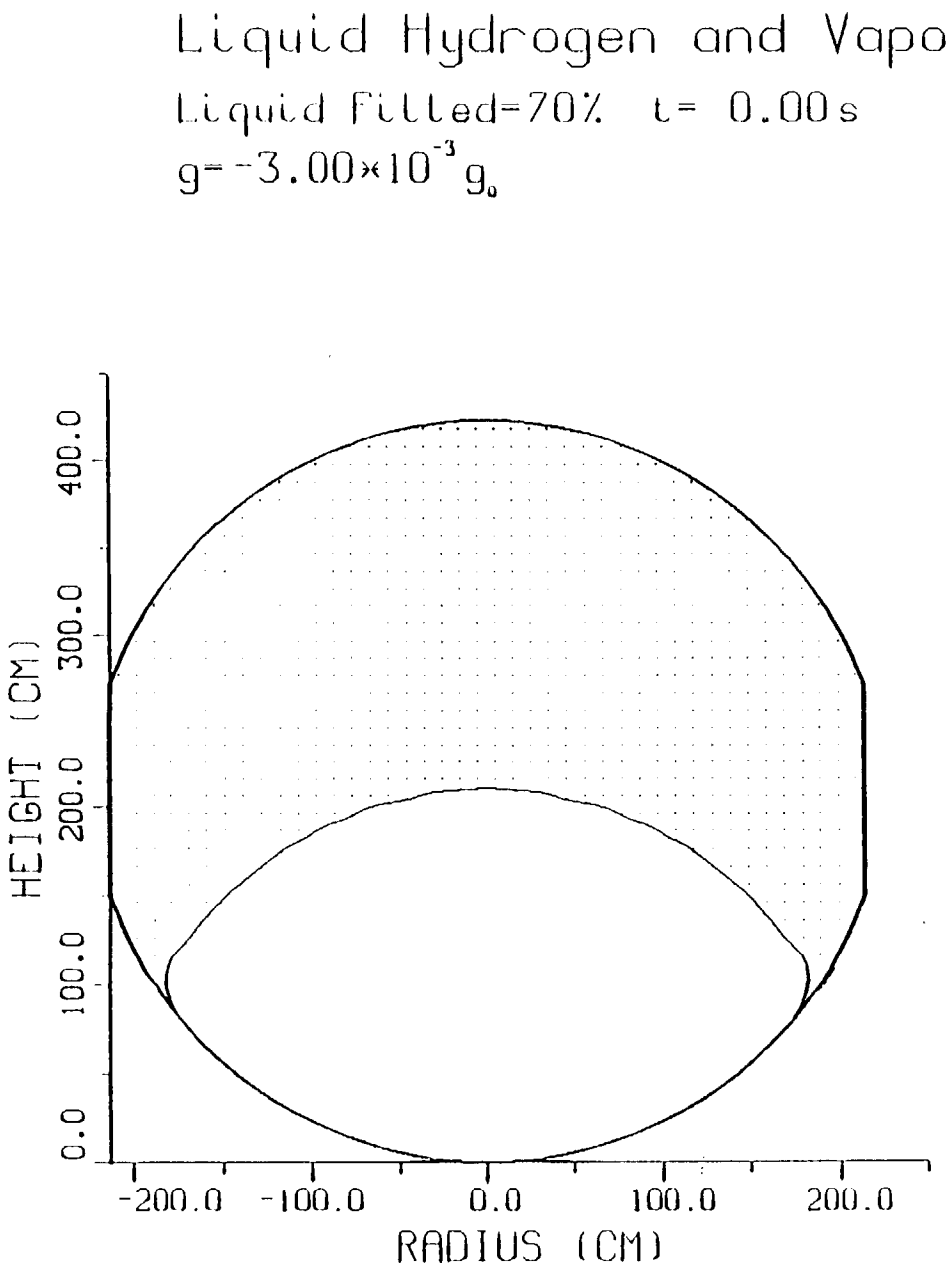
Liquid Hydrogen and Vapor
Liquid Filled=70% t= 0.00s
g=-3.00×10^-3 g0
HEIGHT (CM)
0.0
100.0
200.0
300.0
400.0
-200.0
-100.0
0.0
100.0
200.0
RADIUS (CM)

Figure 32

Liquid Hydrogen and Vapor

Liquid Filled=70% $t = 1.40 \times 10^{1}$ s

$g = -3.00 \times 10^{-3} g_o$

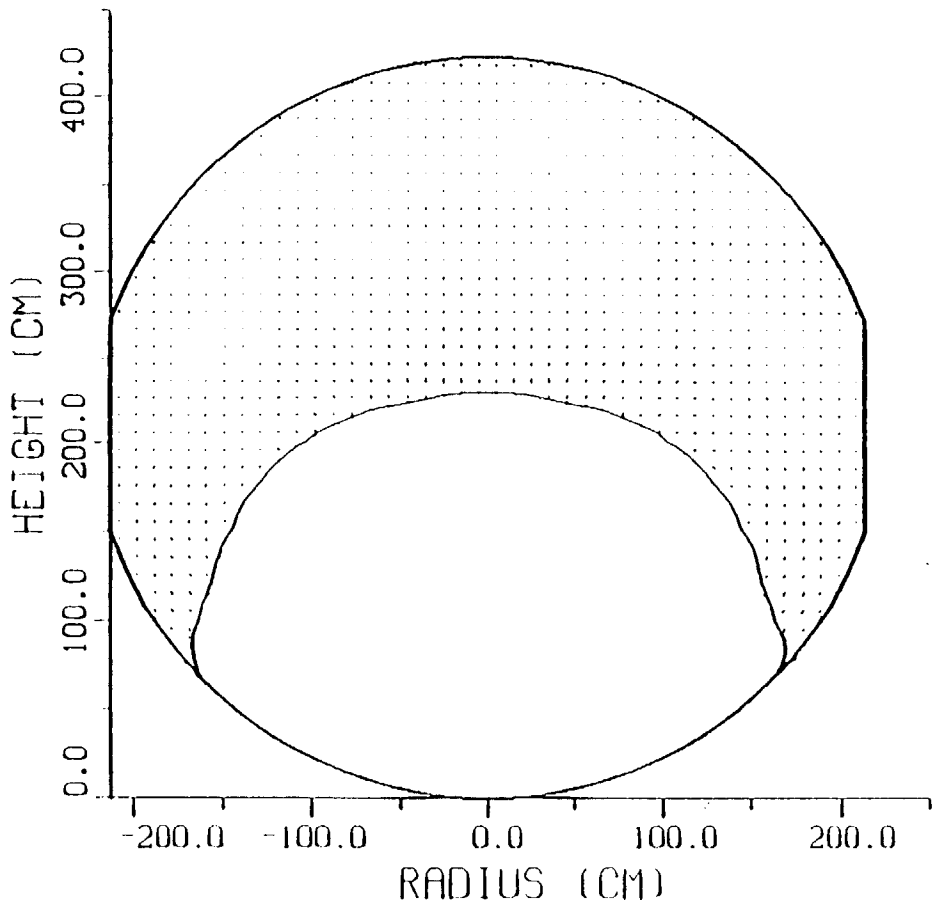

Figure 33

Liquid Hydrogen and Vapor

Liquid Filled=70% $t = 3.74 \times 10^{1}$ s

$g = -3.00 \times 10^{-3} g_0$

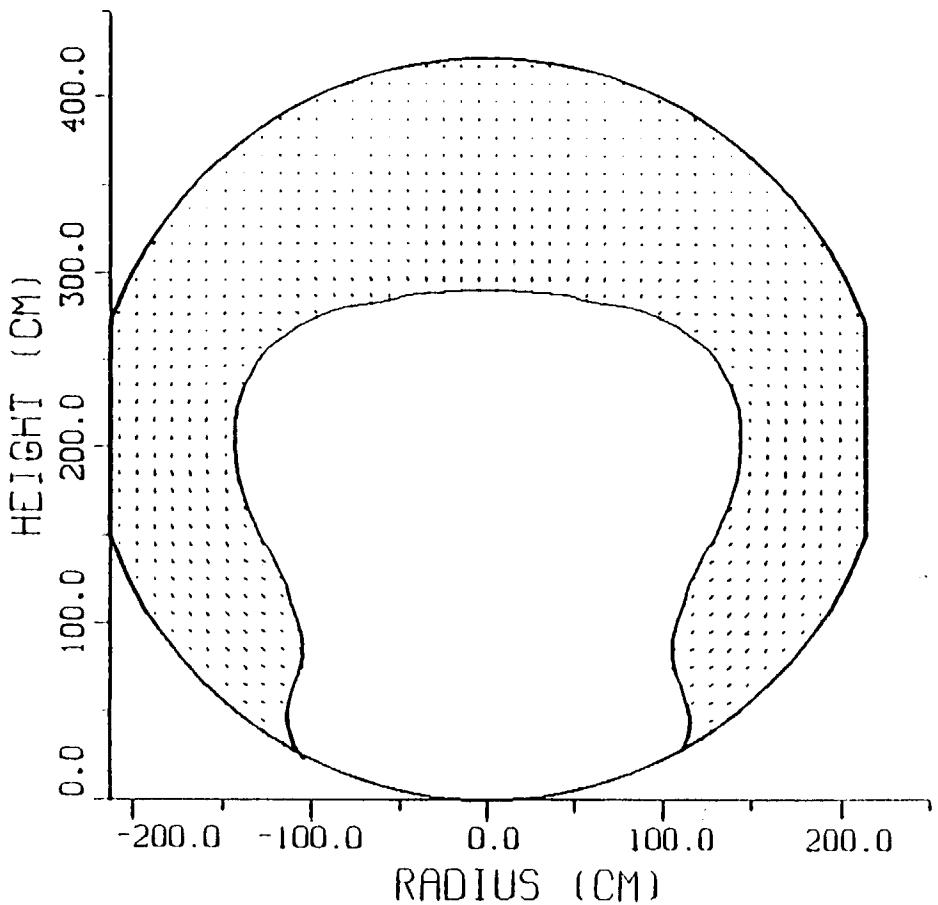

Figure 34

Liquid Hydrogen and Vapor

Liquid Filled=70% $t = 4.21 \times 10^{1}$ s

$g = -3.00 \times 10^{-3} g_0$

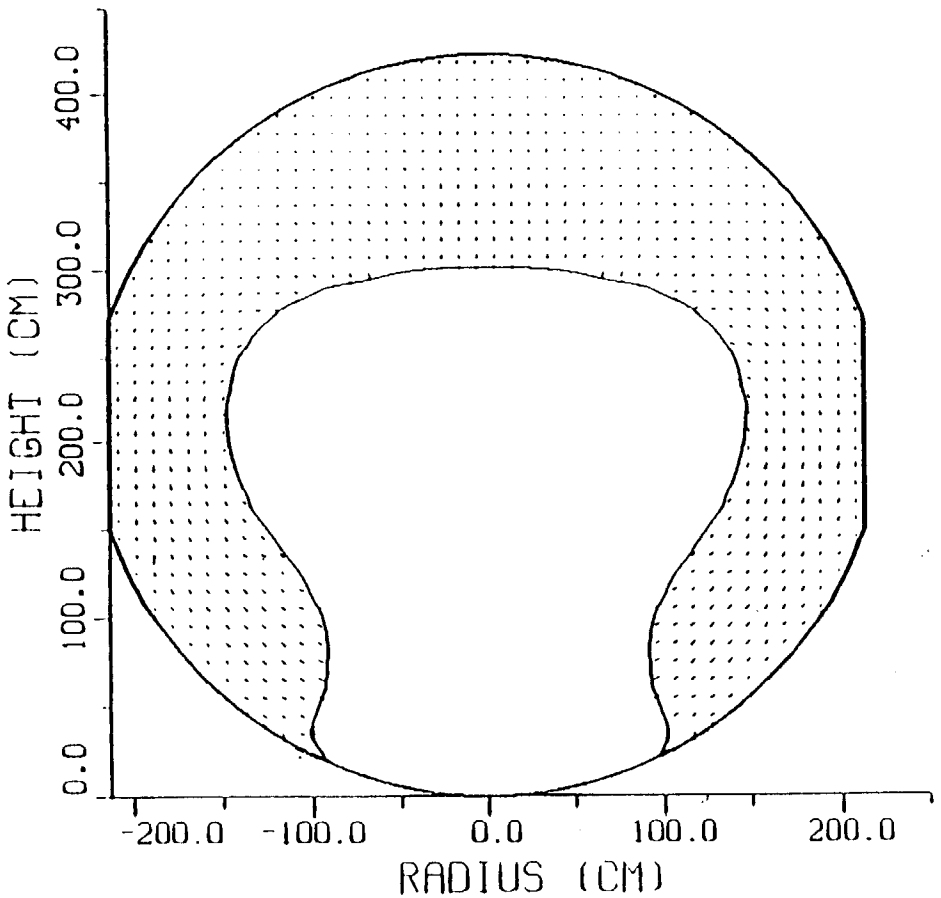

Figure 35

Liquid Hydrogen and Vapor

Liquid Filled=70% $t = 5.14 \times 10^{1}$ s

$g = -3.00 \times 10^{-3} g_0$

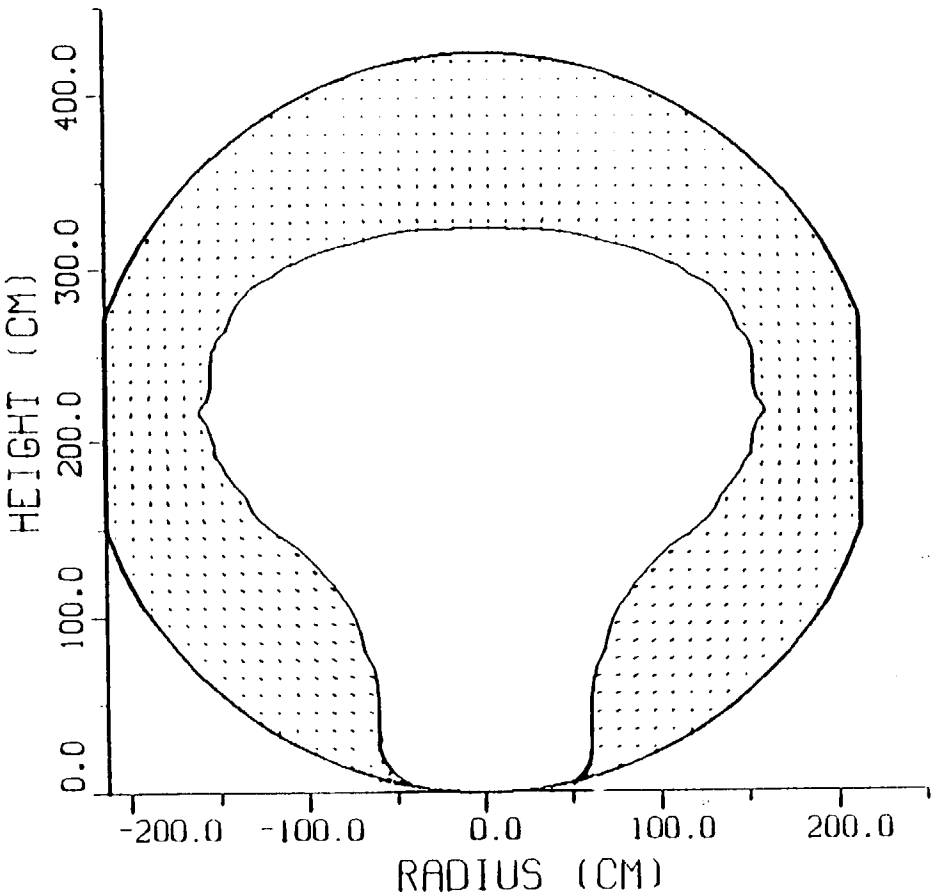

Figure 36

Liquid Hydrogen and Vapor

Liquid Filled=70% $t = 8.39 \times 10^{1}$ s

$g = -3.00 \times 10^{-3} g_0$

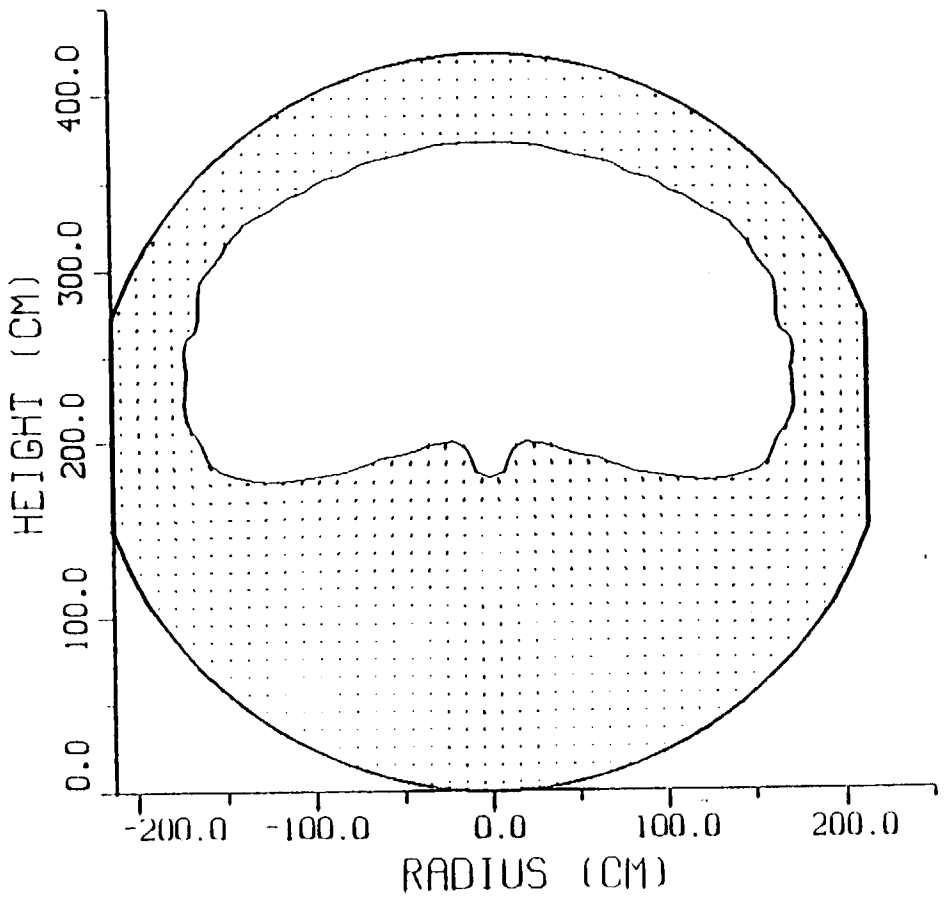

Figure 37

Liquid Hydrogen and Vapor

Liquid Filled=70% $t = 8.86 \times 10^{1}$ s

$g = -3.00 \times 10^{-3} g_0$

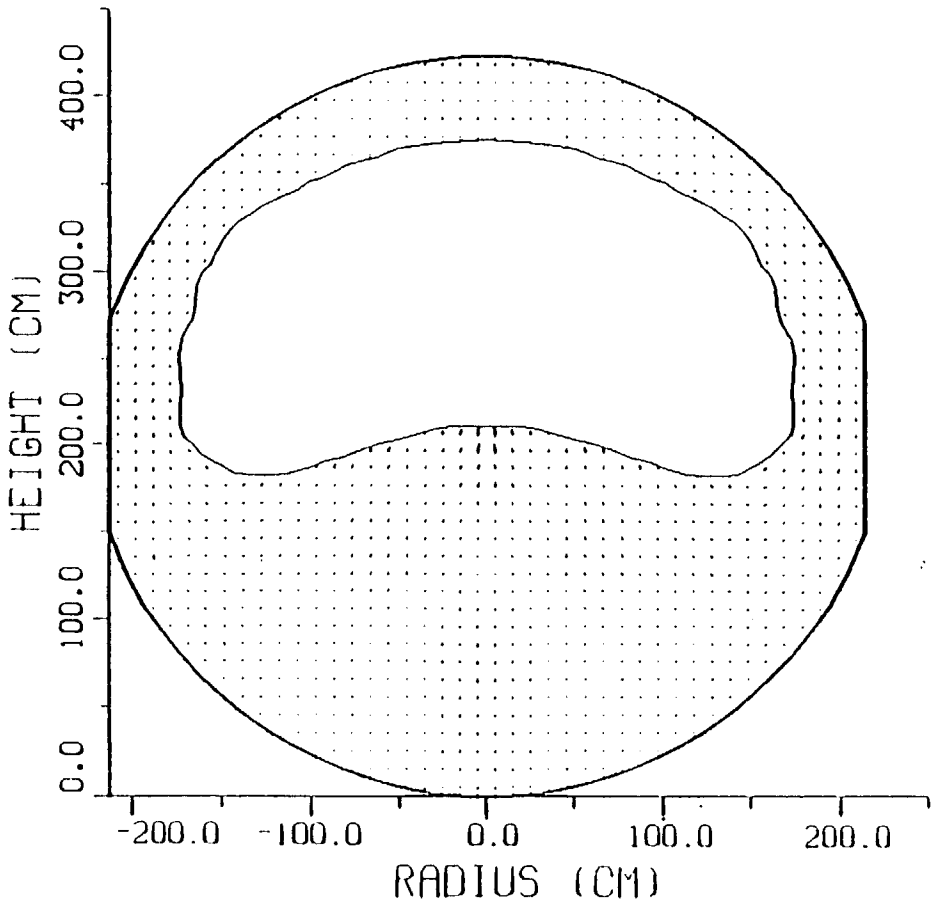

Figure 38

Liquid Hydrogen and Vapor

Liquid Filled=70% $t = 1.45 \times 10^{2}$ s

$g = -3.00 \times 10^{-3} g_0$

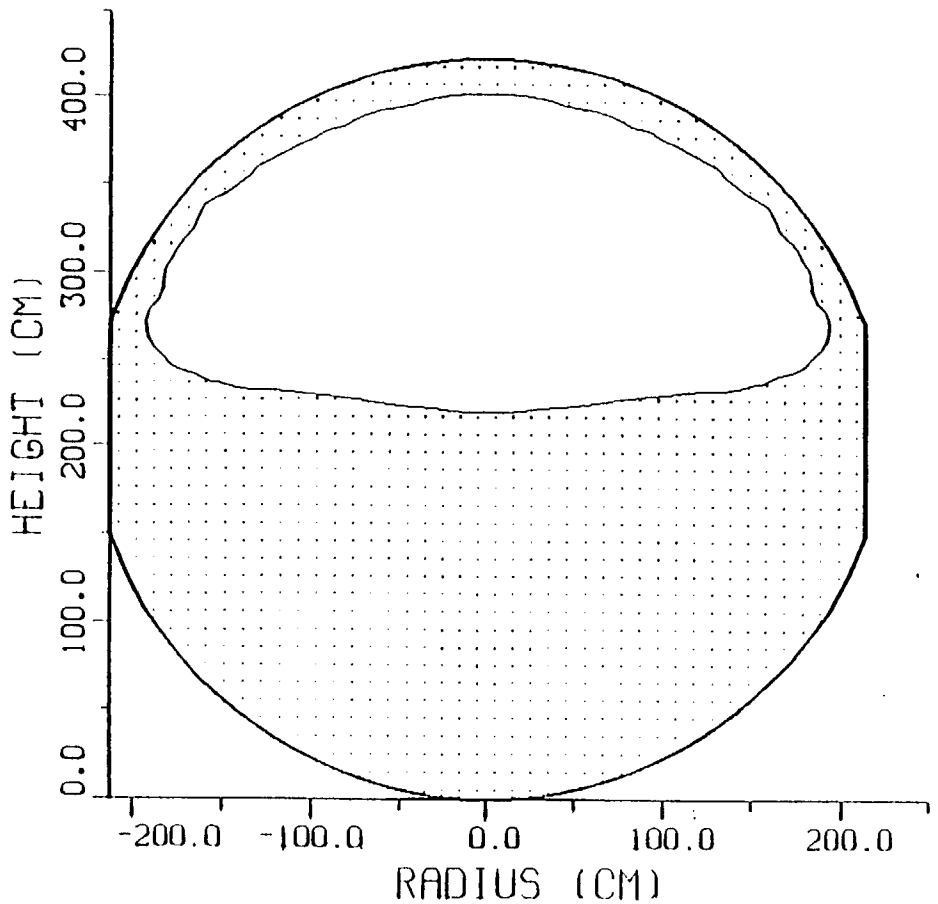

Figure 39

Liquid Hydrogen and Vapor

Liquid Filled=70% $t = 1.73 \times 10^{2}$ s

$g = -3.00 \times 10^{-3} g_0$

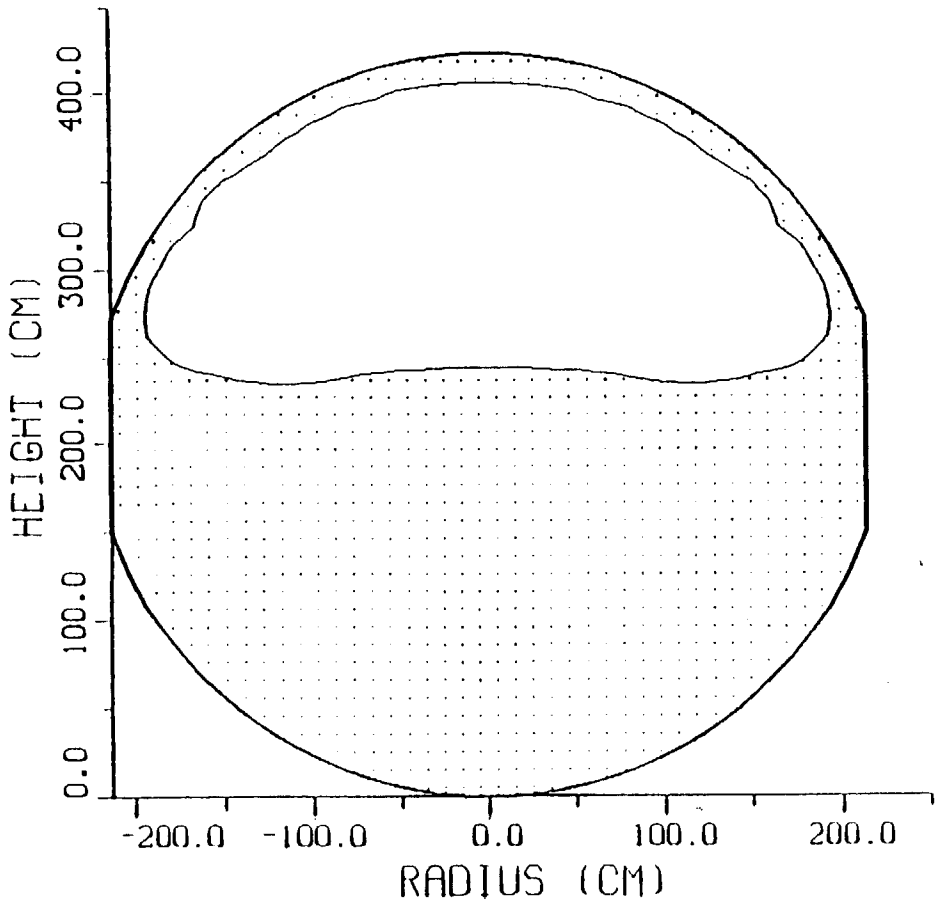

Figure 40

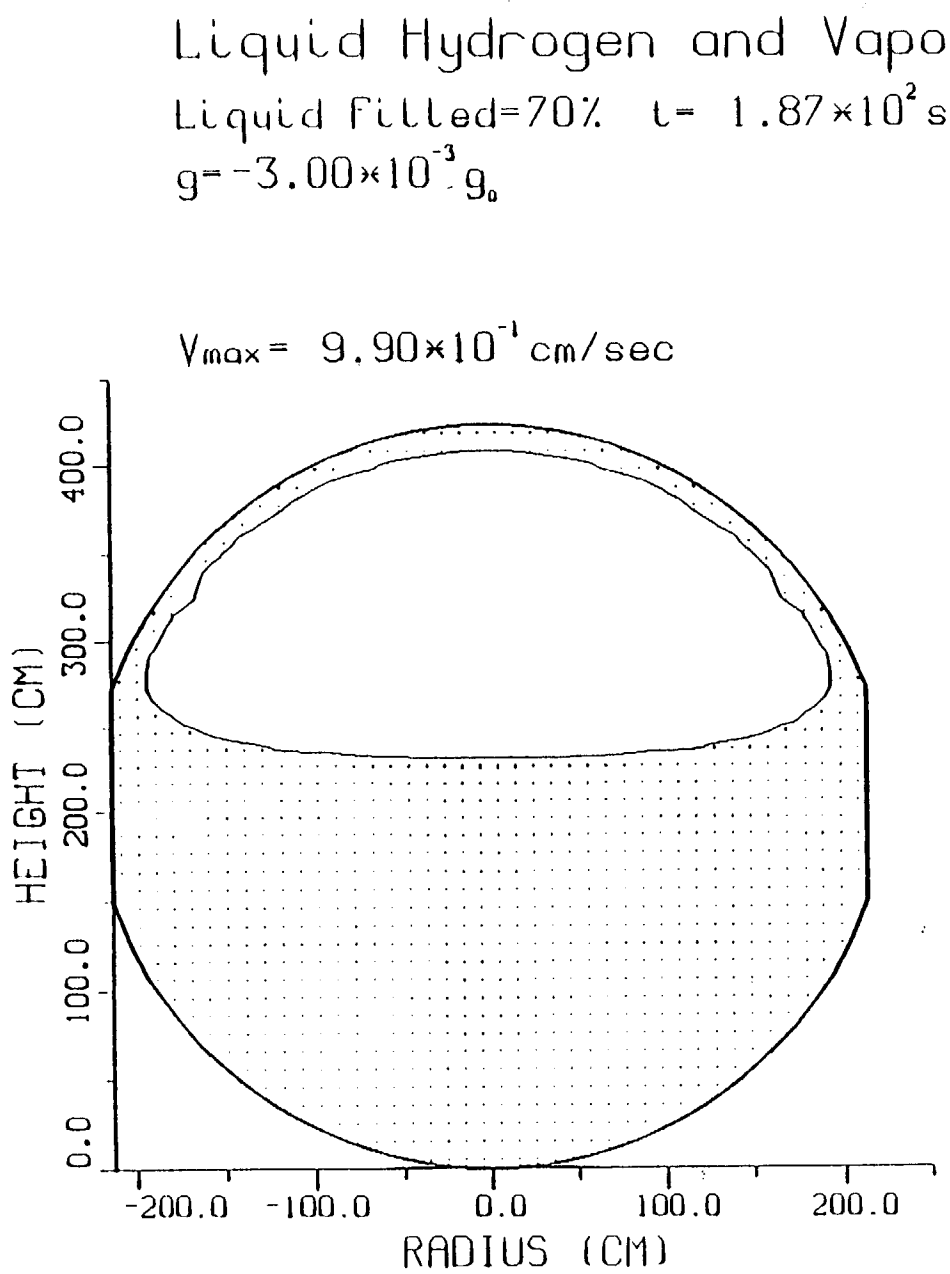
Liquid Hydrogen and Vapor
Liquid Filled=70% t= 1.87×10^2 s
g=-3.00×10^-3 g0
Vmax= 9.90×10^-1 cm/sec
HEIGHT (CM)
400.0
300.0
200.0
100.0
0.0
-200.0
-100.0
0.0
100.0
200.0
RADIUS (CM)

Figure 41

(IV) Sub-Scale Simulation for Liquid Reorientation and Resettlement

In the sub-scale STV propellant tank liquid hydrogen reorientation we have accomplished the following four cases of numerical simulation: (E) Cryogenic liquid hydrogen reoreintation activated by constant settling acceleration of geyser initiation; (F) Cryogenic liquid hydrogen reorientation activated by low frequency impulsive settling acceleration of geyser initiation; (G) Cryogenic liquid hydrogen reorientation activated by medium frequency impulsive settling acceleration of geyser initiation; and (H) Cryogenic liquid hydrogen reorientation activated by high frequency impulsive settling acceleration of geyser initiation.

(E) Cryogenic Liquid Hydrogen Reorientation Activated by Constant Settling Acceleration of Geyser Initiation

Abstract

A key objective of the cryogenic fluid management of the spacecraft propulsion system is to develop the technology necessary for acquisition or positioning of liquid outflow or vapor venting. In this paper, numerical simulation of positive liquid acquisition is attempted by introducing reverse gravity acceleration, resulting from the propulsive thrust of auxiliary engines, which exceeds critical value for the initiation of geyser. Based on the computer simulation of flow fields during the course of fluid reorientation, six dimensionless parameters resulted in this study. It shows that these parameters hold near constant values through the entire ranges of liquid filled levels, from 30% to 80%, during the course of fluid reorientation.

Nomenclature

a_g = geyser initiation acceleration (cm/s^2)

a_m = scale flow acceleration associated with maximum velocity (cm/s^2), defined by Eq (5)

D = diameter of propellant tank (cm)

f = frequency of impulsive thrust (H_z)

g_i = geyser initiation gravity-level (g_0)

g_0 = normal Earth gravitational acceleration = 9.81 m/s^2

$\bar{h}$ = average liquid height (cm)

h_m = maximum liquid height (cm)

L = height of propellant tank (cm)

L_m = scale length of maximum liquid height (cm/s), defined by Eq (4)

STV = Space Transfer Vehicle

$\bar{t}_f$ = average free fall time (s)

t_m = time for observing maximum flow velocity (s)

t_R = liquid reaching tank bottom time (s)

V_{fm} = free fall velocity from maximum liquid height (cm/s), defined by Eq (3)

$\bar{V}_f$ = average free fall velocity (cm/s), defined by Eq (2)

V_m = maximum flow velocity (cm/s)

I. Introduction

In spacecraft design, the requirements for a settled propellant are different for tank pressurization, engine restart, venting, or propellant transfer. Prepressurization requires that heat and mass transfer effects be minimized; otherwise, a process of chill down of tank, venting of noncondensing gases, etc., may have to carry out for the cryogenic system. For engine restart, it is necessary to have the liquid settle with no bubbles near the tank outlet so that the initial flow of propellant will not carry vapor to the pump or engine. The slosh wave amplitude should be relatively low to keep the center of mass shifts within an acceptable range and wave motion low enough to avoid pressure collapse caused by interface agitation .

Bubble and globule formation as a result of liquid impact with the aft end of the tank could lead to propellant loss for the spacecraft during venting. Globules could be entrained in the vented ullage gas or bubbles rising through the liquid and expanding because of the decreasing tank pressure could cause a spray of globules to be vented. Liquid level rise, vent liquid loss, fluid freezing, and vehicle dynamics are all affected by the microgravity levels.

A key objective of the cryogenic fluid management of spacecraft propulsion system, such as a Space Transfer Vehicle[1] (STV), is to develop the technology necessary for acquisition or positioning of liquid and vapor within a tank in reduced gravity to enable liquid outflow or vapor venting. Liquid acquisition techniques can be divided into two general categories: (1) Active liquid acquisition by the creation of a positive acceleration environment resulting from

the propulsive thrust of small auxiliary engines, and (2) Passive liquid acquisition utilizing the liquid capillary forces provided by using solid baffles of liquid traps made of fine mesh screen material. In this study, active liquid acquisition is aimed for numerically simulating the resettlement of cryogenic liquid hydrogen. Liquid hydrogen, which, in general, poses more severe technical challenges than liquid oxygen, is used as the test bed working fluid in this study.

Recently Lesie[2] was able to measure and to numerically compute the bubble shapes at various ratios of centrifugal force to surface tension force in the microgravity environment. Hung and Leslie[3] extended Leslie's work[2] to rotating free surfaces influenced by gravity with higher rotating speeds when the bubble intersects with both the top and bottom walls of the cylinder. Hung et al.[4,5] further extended the work to include rotating speeds which resulted with bubbles intersecting and/or without intersecting the top, bottom and side walls of the cylinder.

An analysis of time-dependent dynamical behavior of surface tension on partially-filled rotating fluids in both low gravity and microgravity environments was carried out by numerically solving the Navier-Stokes equations subjected to the initial and the boundary conditions[4,6]. The initial condition for the bubble profiles was adopted from steady-state formulations developed by Hung and Leslie[3], and Hung et al.[6] for rotating cylinder tank; and by Hung et al.[5,7] for the dewar-shaped container to be used in the Gravity Probe-B Spacecraft[8]. Some of the steady-state formulations of bubble

shapes, in particular for bubbles intersecting at the top wall of the cylinder, were compared with the experiment carried out by Leslie[2] in a free-fallinng aircraft (KC-135) with an excellent agreement.

An efficient propellant settling technique should minimize propellant usage and weight penalties. This can be accomplished by providing optimal acceleration to the spacecraft such that the propellant is reoriented over the tank outlet without any vapor entrainment, any excessive geysering, or any other undesirable fluid motion.

Production of geyser during the propellant reorientation is not a desirable motion for the space fluid management. It is because geyser is always accompanied by the vapor entrainment and globule formation. Geyser is observed at reverse gravity acceleration greater than certain critical values of acceleration during the course of liquid reorientation. In other words, geyser will not be observed at very low reverse gravity level, and it will be detected when the reverse gravity level is greater than the certain critical level. In this paper, numerical simulation of positive liquid acquisition is attemted by introducing reverse gravity acceleration, resulting from the propulsive thrust of small auxiliary engines which exceeds the critical value for geyser initiation. The reverse gravity acceleration is starting with a small value and increases gradually till the initiation of geyser is detected in the computer simulation for the liquid reorientation of propellant tank with various liquid-filled levels.

In this study, time-dependent computations have been carried out

to investigate the dynamical behavior of fluid reorientation or resettling of propellant prior to main engine firing for spacecraft restart at the net reverse gravity acceleration which is great enough to initiate geyser during the liquid reorientation. The computation extends to the study of the characteristics of fluid resettlement due to the reversal of lowest artificial gravity fields which is great enough to initiate geyser with and without various frequencies of impulsive acceleration. This frequency of impulsive acceleration is generally termed "gravity jitters". Gravity jitters are produced by spacecraft attitude motion, machinery (turbine, pump, engine) vibrations, thruster firing, thruster shutdown, etc.[9] Positioning of liquid propellant over the tank outlet can be carried out by using small auxiliary thrusters which provide a thrust parallel to the tank's major axis in the direction of flight.

II. Numerical Simulation of Liquid Hydorgen Reorientation at the Reverse Gravity Acceleration of Geyser Initiation

Propellant tank of liquid-filled levels of 30, 50, 65, 70 and 80% are considered in this study. Time-dependent axial symmetry mathematical formulation are adopted. Detailed description of mathematical formulation, initial and boundary conditions suitable for the analysis of cryogenic fluid management under microgravity environment are given in our earlier studies.[4,6,10-12] The initial profiles of liquid-vapor interface are determined from computations based on algorithms developed for the steady state formultion of microgravity fluid management.[3-7]

A staggered grid for the velocity components is used in this

computer program. The method was first developed by Harlow and Welch[13] for their MAC (marker and cell) method of studying fluid flows along free surface. The finite difference method employed in this numerical study was the "Hybrid Scheme" developed by Spalding.[14] The formulation for this method is valid for any arbitrary interface location between the grid points is not limited to middle point interfaces.[15] An algorithm for semi-implicit method[16] was used as the procedure for modeling the flow field. The time step is determined automatically based on the size of the grid points and the velocity of flow fields. Detailed description of the computational algorithm applicable to microgravity fluid management are illustrated in our earlier studies.[4,6,10-12] Fig 1(A) shows the distribution of grid points in the radial-axial plane of cylindrical coordinates.

For the purpose of facilitating easy comparison between computational resuslts and experimental measurement, a model of 0.01 size prototype is adopted in the computer simulation. Fig 1(B) shows a model size for computation. The size of prototype is height, L = 166.8" (423.672 cm), and diameter, D = 168" (426.72 cm). Model size is L = 4.23672 cm and D = 4.2672 cm, as shown in Fig 1(B). If the spacecraft had been coasting for a long time, aligned with its direction of motion, the most signigicant force, drag, would be axial and with acceleration of $10^{-4}g_0$ along upward direction. The hydrogen vapor is, thus, originally positioned at the bottom of the tank. The requirement to settle or to position liquid fuel over the outlet end of the spacecraft propellant tank prior to main engine restart poses a

microgravity fluid behavior problem.[10] Retromaneuvers of spacecraft, such as STV, require settling or reorientation of the propellant to main engine firing.[1,10] Cryogenic liquid propellant shall be positioned over the tank outlet by using auxiliary thrusters (or idle-mode thrusters from the main engine) which provide a thrust parallel to the tank's major axis in the direction of flight. In the present study of computer simulation, a small value of reverse gravity acceleration (downward direction) is provided by the propulsive thrust of small auxiliary engine to initiate the reorientation of liquid propellant. This small value of reverse gravity acceleration of propulsive thrust increases gradually till reaching the critical value on which initiation of geyser is detected during the time period of fluid resettlement. We term this reverse gravity acceleration of propulsive thrust, which is capable to initiate geyser, as "geyser initiation gravity-level". This geyser initiation gravity level has been investigated through the method of trial and error for the various liquid-filled levels of propellant tank as a base to simulate following cases of reduced gravity fluid behaviors during the reorientation: (A) constant reverse gravity acceleration, (B) impulsive reverse gravity acceleration with a frequency of 0.1 H_z, (C) impulsive reverse gravity acceleration with a frequency of 1.0 H_z, and (D) impulsive reverse gravity acceleration with a frequency of 10 H_z. Cases (B) to (D) for the impulsive reverse gravity acceleration with various frequencies will be discussed in the subsequent papers. Liquid filled level of 30, 50, 65, 70 and 80% have been considered in this study. Cryogenic liquid hydrogen at temperature of 20K is

considered. Hydrogen density of 0.071 g/cm^3; surface tension coefficient at the interface between liquid hydrogen and hydrogen vapor of 1.9 dyne/cm; hydrogen viscosity coefficient of 1.873×10^{-3} cm^2/s; and contact angle of 0.5^0 are used in the computer simulation.

Reorientation of cryogenic liquid hydrogen activated by geyser initiation reverse gravity acceleration produced by propulsive thrust has been investigated for various liquid filled levels of propellant tank. It is found that these geyser initiation gravity levels are 5.5×10^{-2}, 6.52×10^{-2}, 6.6×10^{-2}, 6.7×10^{-2} and $8.2 \times 10^{-2} g_0$ for liquid filled levels of 30, 50, 65, 70, and 80%, respectively. To illustrate some examples Figs 2 and 3 show the selected sequences of time evolution of fluid reorientation for cryogenic hydrogen with liquid filled levels of 30, and 80%, respectively. Each figure contains four sub-figures. Subfigure (A) is initial profile of liquid-vapor interface at the moment of the starting of fluid reorientation at time $t = 0$; subfigure (B), the flow profile during the course of fluid reorientation before the initation of geysering motion; subfigure (C), the flow profile with geysering motion; and subfigure (D), the flow profile after the ending of geysering motion.

Figs 2 and 3 illustrate following flow behaviors: (1) The liquid starts to flow in an annular sheet along the solid wall of tank and gradually pushes the vapor toward the central portion of the lower dome of tank as the net acceleration, reversing the direction of gravity field, which is applied toward the downward direction of tank's major axis, by using small auxiliary thrusters; (2) As the

downward fluid annular sheet along the tank wall reaches the central bottom dome side of the tank, a geysering flow is observed; and (3) The vapor is thus pushed upward centrally into the liquid and the geysering disappears.

Table 1 shows the characteristics of cryogenic liquid hydrogen resettlement activated by reverse gravity acceleration at geyser initiation gravity level. Average liquid height $\bar{h}$, and maximum liquid height h_m are shown in Fig 1(B). Average free fall velocity $\bar{V}_f$, average free fall time $\bar{t}_f$, and free fall velocity from maximum liquid height V_{fm} are computed from the following equations:

$$\bar{V}_f = (2g_i\bar{h})^{1/2} \qquad (1)$$

$$\bar{t}_f = \left(\frac{2\bar{h}}{g_i}\right)^{1/2} \qquad (2)$$

$$V_{fm} = (2g_i h_m)^{1/2} \qquad (3)$$

where g_i denotes geyser initiation reverse gravity acceleration. Values of maximum flow velocity V_m, time for observing maximum flow velocity t_m, and time for reorienting liquid flowing down and reaching the bottom of propellant tank t_R, are obtained from the numerical computation of flow field. Scale length of maximum flow velocity L_m, and scale flow acceleration associated with maximum velocity a_m, are computed from the following parameters:

$$L_m = V_m t_m \qquad (4)$$

$$a_m = \frac{V_m}{t_m} \qquad (5)$$

Following dimensionless parameters are introduced: $V_m/\bar{V}_f$, $t_R/\bar{t}_f$, $t_m/\bar{t}_f$, a_m/a_g, $L_m/\bar{h}$ and V_m/V_{fm} where a_g stands geyser initiation acceleration (cm/s^2) for corresponding geyser initiation gravity level g_i.

Figs 4 to 6 show the variations of dimensionless parameters in terms of liquid filled levels. Denominators of these six dimensionless parameters are either predetermined from the geometry of liquid fill levels or can be deduced from the corresponding calculations associated with the geyser initiation gravity levels. Characteristics of these near constant values dimensionless parameters can provide a good understanding of the physics of microgravity fluid behaviors, in particular the active category of liquid acquisition or positioning, and also the design criteria of on-orbit spacecraft propulsion system at the critical value of reverse gravity acceleration of propulsive thrust which is capable to inititiate geyser.

Fig 4(A) shows the ratio of maximum flow velocity to average free fall flow velocity $V_m/\bar{V}_f$ and its associated parameters of V_m and $\bar{V}_f$ in terms of liquid filled levels. It shows that the ratio of $V_m/\bar{V}_f$ varies in the range of 4.3 to 4.9 in the entire liquid filled levels while V_m and $\bar{V}_f$ vary from 62.0 to 73.6 cm/s (decreasing with increasing liquid filled levels) and from 12.5 to 17.0 cm/s (also decreasing with increasing liquid filled levels), respectively. As $\bar{V}_f$ can be predetermined from geyser initiation gravity level and average liquid

height, shown in Eq (1), one can make an approximate prediction of maximum flow velocity during the liquid reorientation for the various liquid filled levels.

Fig 4(B) shows the ratio of liquid reaching bottom time to average free fall time $t_R/\bar{t}_f$ and its associated parameters of t_R and $\bar{t}_f$ in terms of liquid filled levels. It shows that the ratio of $t_R/\bar{t}_f$ varies in the range of 1.21 to 1.30 in the entire liquid filled levels while t_R and $\bar{t}_f$ vary from 0.20 to 0.40 s (decreasing with increasing liquid filled levels) and from 0.15 to 0.32 s (also decreasing with increasing liquid filled levels), respectively. As $\bar{t}_f$ can be predetermined from geyser initiation gravity level and average liquid height, shown in Eq (2), one can predict the time reorienting liquid fluid flowing down from the original position and reaching the bottom of propellant tank for the various liquid filled levels at the reverse gravity acceleration capable for the initiation of geyser.

Fig 5(A) shows the ratio of time for observing maximum flow velocity to average free fall time $t_m/\bar{t}_f$ and its associated parameters of t_m and $\bar{t}_f$ in terms of liquid filled levels. It shows that the ratio of $t_m/\bar{t}_f$ varies in the range of 1.2 to 1.3 in the entire liquid filled levels while t_m and $\bar{t}_f$ vary from 0.20 to 0.42 s (decreasing with increasing liquid filled levels) and from 0.15 to 0.32 s (also decreasing with increasing liquid filled levels), resectively. As we indicated in 4, $\bar{t}_f$ can be predetermined, one can predict the time for observing maximum flow velocity for various liquid filled levels at the reverse gravity acceleration capable for the initiation of geyser.

Fig 5(B) shows the ratio of scale flow acceleration associated with maximum velocity to geyser initiation acceleration for corresponding geyser initiation gravity level a_m/a_g and its associated parameters of a_m and a_g in terms of liquid filled levels. It shows that the ratio of a_m/a_g varies in the range of 3.3 to 3.9 in the entire liquid filled levels while a_m and a_g vary from 175 to 310 cm/s^2 (increasing with increasing liquid filled levels) and from 53.9 to 80.4 cm/s^2 (also increasing with increasing liquid filled levels), respectively. As a_g can be predetermined from geyser initiation gravity level, one can make an approximate prediction of scale flow acceleration associated with maximum velocity, which is defined in Eq (5), at the reverse gravity acceleration capable for the initiation of geyser.

Fig 6(A) shows the ratio of scale length of maximum flow velocity to average liquid height $L_m/\bar{h}$ and its associated parameters of L_m and $\bar{h}$ in terms of liquid filled levels. It shows that the ratio of $L_m/\bar{h}$ varies in the range of 11.6 to 13.0 in the entire liquid filled levels while L_m and $\bar{h}$ vary from 12.4 to 30.9 cm (decreasing with increasing liquid filled levels) and from 0.93 to 2.67 cm (also decreasing with increasing liquid filled levels), respectively. As $\bar{h}$ can be predetermined from the geometry of liquid filled levels, one can make an approximate prediction of scale length of maximum flow velocity, which is defined in Eq (4), at the reverse gravity acceleration capable for the initiation of geyser.

Fig 6(B) shows the ratio of maximum flow velocity to free fall velocity from maximum liquid height V_m/V_{fm} and its associated

parameters of V_m and V_{fm} in terms of liquid filled levels. It shows that the ratio of V_m/V_{fm} varies in the range of 3.8 to 4.0 in the entire liquid filled levels while V_m and V_{fm} vary from 62.0 to 73.6 cm/s (decreasing with increasing liquid filled levels) and from 16.4 to 19.2 cm/s (also decreasing with increasing liquid filled levels), respectively. As V_{fm} can be predetermined from geyser initiation gravity level and maximum liquid height, shown in Eq (3), one can make an approximate prediction of maximum flow velocity at the reverse gravity acceleration capable for the initiation of geyser.

Six dimensionless parameters presented in this study show that the parameters hold near constant values through the entire ranges of liquid filled levels during the course of reorientation of liquid hydrogen activated by the reverse gravity acceleration which is great enough to initiate geysering flow. As the denominators of these six dimensionless parameters are either predetermined from the geometry of liquid filled levels or can be deduced from the corresponding calculations associated with the geyser initiation gravity levels, one can predict the flow parameters from these relations.

III. Discussion and Conclusions

The efficient management of subcritical cryogenic propellants is one of the key technology drivers for the on-orbit spacecraft. Cryogenic liquids are essential for the spacecraft as reactants, coolants, and propellants. The requirement to settle or to position liquid fuel over the outlet end of the spacecraft propellant tank prior to main engine restart poses a microgravity fluid behavior problem. Retromaneuvers of spacecraft require settling or

reorientation of the propellant prior to main engine firing. Cryogenic liquid propellant is positioned over the tank outlet by using small auxiliary thrusters (or idle-mode thrusters from the main engine) which provide a thrust parallel to the tank's major axis in the direction of flight.

The results of the study of fluid reorientation have to be evaluated in terms of how well they can be managed efficiently. An efficient propellant settling technique should minimize propellant usage and weight penalties through the operation of small thrusters (or idle-mode thrusters from the main engine). This can be accomplished by providing optimal acceleration to the spacecraft such that the propellant is reoriented over the tank outlet without any vapor entrainment, any excessive geysering, or any other undesirable fluid motion.

Production of geyser during the propellant reorientation is not a desirable motion for the space fluid management under microgravity environment. In this paper, numerical simulation of positive liquid acquisition is attempted by introducing reverse gravity acceleration, resulting from the propulsive thrust of auxiliary engines, which exceeds critical value for the intiation of geyser.

Flow profile simulations, in particular the time evolution of liquid-vapor interface during the course of fluid reorientation, for the selected various liquid filled levels are shown in Figs 2 and 3. Table 1 and Figs 4 to 6 show the characteristics of dimensionless flow parameters and their associated flow fields during the course of fluid reorientation with geyser initiation. Computer simulation of flow

fields disclose the following results: (1) Geyser initiation gravity level is high (low) for high (low) liquid filled level; (2) Average liquid height is high (low) for low (high) liquid filled level; (3) Average free fall flow velocity is high (low) for low (high) liquid filled level; (4) Maximum flow velocity is high (low) for low (high) liquid filled level; (5) Average free fall time is longer (shorter) for low (high) liquid filled level; (6) Time for liquid falling from original position to liquid reaching bottom time is longer (shorter) for low (high) liquid filled level; (7) Time for observing maximum flow velocity is longer (shorter) for low (high) liquid filled level; (8) Scale length of maximum flow velocity is longer (shorter) for low (high) liquid filled level; (9) Scale flow acceleration associated with maximum velocity is low (high) for low (high) liquid filled level; (10) Maximum liquid height is high (low) for low (high) liquid filled level; and (11) Free fall velocity from maximum liquid height is high (low) for low (high) liquid filled level.

Based on the computer simulation of flow fields during the course of fluid reorientation, six dimensionless parameters are presented in this study. It is shown, in Figs 4 to 6, that these parameters hold near constant values through the entire ranges of liquid filled levels during the course of fluid reorientation activated by the reverse gravity acceleration great enough to initiate geyser. As the denominators of these dimensionless parameters are either predetermined from the geometry of liquid filled levels or can be deduced from the corresponding calculations associated with the

geyser intiation gravity levels, one can predict the values of these flow parameters from the relationship shown in Eqs (1) to (5).

Any fluid capable of motion relative to the spacecraft will be subject to an acceleration relative to the mass center of the spacecraft that arises from the gravity gradient of the Earth[17,18]. In addition to the Earth's gravitational force, the interaction between the particle mass of fluids and the spacecraft mass due to gravity gradient accelerations[17] have also been taken into consideration in this microgravity fluid management study.

To conclude, we have demonstrated that, the computer algorithm presented, can be used to simulate fluid behavior in a microgravity environment, in particular the development of technology necessary for acquisition or positioning of liquid and vapor within a tank to enable liquid outflow or vapor venting through active liquid acquisition by the creation of a positive acceleration environment resulting from propulsive thrust. Better understanding of the full pictures of flow fields during the course of fluid reorientation can provide the proper design techniques for handling and managing the cryogenic liquid propellants to be used in on-orbit spacecraft propulsion.

Acknowledgement

The authors appreciate the support recieved from the National Aeronautics and Space Administration Headquarters through the NASA Grant NAGW-812, and NASA Marshall Space Flight Center through the NASA Contract NAS8-36955/Delivery Order No. 69.

Reference

1. NASA Office of Aeronautics and Space Technology, Technology for Future NASA Missions: Civil Space Technology Initiative and Pathfinder, NASA CP-3016,National Aeronautics and Space Administration, Washington, D.C., 1988, pp. 568.

2. Leslie, F. W., "Measurements of Rotating Bubble Shapes in a Low Gravity Environment," Journal of Fluid Mechanics, Vol. 161, Dec. 1985, pp. 269-279.

3. Hung, R. J., and Leslie, F. W., "Bubble Shape in a Liquid Filled Rotating Container Under Low Gravity," Journal of Spacecraft and Rockets, Vol. 25, Jan.-Feb. 1988, pp. 70-74.

4. Hung, R. J., Tsao, Y.D., Hong, B. B., and Leslie, F. W., "Time Dependent Dynamical Behavior of Surface Tension on Rotating Fluids under Microgravity Environment," Advances in Space Research, Vol. 8, No. 12, 1988, pp. 205-213.

5. Hung, R. J., Tsao, Y. D., Hong, B. B., and Leslie, F. W., "Bubble Behaviors in a Slowly Rotating Helium Dewar in Gravity Probe-B Spacecraft Experiment," Journal of Spacecraft and Rockets, Vol. 26, May-June 1989, pp. 167-172.

6. Hung, R. J., Tsao, Y. D., Hong, B. B., and Leslie, F. W., "Dynamical Behavior of Surface Tension on Rotating Fluids in Low and Microgravity Environments," International Journal for Microgravity Research and Applications, Vol. 11, June 1989, pp. 81-95.

7. Hung, R. J., Tsao, Y. D., Hong, B. B., and Leslie F. W., "Axisymmetric Bubble Profiles in a Slwowly Rotating Helium

Dewar Under Low and Microgravity Environments," Acta Astronautica, Vol. 19, May 1989, pp. 411-426.

8. "Stanford Relativity Gyroscope Experiment (NASA Gravity Probe-B)," Proceedings of Society of Photo-Optical Instrumentation Engineers, Vol. 619, Society of Photo-Optical Instrumentation Engineers, Bellingham, WA, 1986, pp. 1-165.

9. Kamotani, Y., Prasad, A., and Ostrach, S., "Thermal Convection in an Enclosure Due to Vibrations Aboard a Spacecraft," AIAA Journal, Vol. 19, Apr. 1981, pp. 511-516.

10. Hung, R. J., Lee, C. C., and Shyu, K. L., "Reorientation of Rotating Fluid in Microgravity Environment with and without Gravity Jitters," Journal of Spacecraft and Rockets, Vol. 27, 1990, in press.

11. Hung, R. J., Lee, C. C., and Leslie, F. W. "Effects of G-Jitters on the Stability of Rotating Bubble Under Microgravity Environment,"Acta Astronautica, Vol. 20, 1990, in press.

12. Hung, R. J., Lee, C. C., and Leslie, F. W., "Response of Gravity Level Fluctuations on the Gravity Probe-B Spacecraft Propellant System," Journal of Propulsion and Power, Vol. 6, 1990, in press.

13. Harlow, F. H., and Welch, F. E., "Numerical Calculation of Time-Dependent Viscous Incompressible Flow of Fluid with Free Surface," Physics of Fluids, Vol. 8, Dec. 1965, pp. 2182-2189.

14. Spalding, D. B. "A Novel Finite-Difference Formulation for Differential Expressions Involving Both First and Second Derivatives," International Journal of Numerical Methods in Engineering, Vol. 4, July-Aug. 1972, pp. 551-559.

15. Patanker, S. V., Numerical Heat Transfer and Fluid Flow, Hemisphere-Mcgraw-Hill, New York, NY, 1980, pp. 197.

16. Patanker, S. V., and Spalding, S. D., "A Calculation Procedure for Heat, Mass and Momentum Transfer in Three Dimensional Parabolic Flows," Internationsl Journal of Heat Mass Transfer, Vol. 15, Nov.-Dec. 1972, pp. 1787-1805.

17. Misner, C. W., Thorne, K. S., and Wheeler, J. A., "Gravitation", W. H. Freeman and Co., San Francisco, CA, 1973, pp. 1-1279.

18. Forward, R. L., "Flattening Space-Time Near the Earth, "Physical Review, Series D, Vol. 26, Aug. 1982, pp. 735-744.

Table 1 CHARACTERISTICS OF CRYOGENIC HYDROGEN REORIENTATION
(Frequency of Impulsive Acceleration = 0.0 Hz)

Liquid Filled Level (%)	30	50	65	70	80
Geyser Initiation Gravity-Level, g_i (10^{-2} g_o)	5.5	6.52	6.6	6.7	8.2
Geyser Initiation Acceleration, a_g (cm/s^2)	53.9	63.9	64.7	65.7	80.4
Average Liquid Height, $\bar{h}$ (cm)	2.67	2.05	1.52	1.35	0.93
Average Free Fall Flow Velocity, $\bar{V}_f$ (cm/s)	17.0	16.2	14.0	13.3	12.5
Maximum Flow Velocity, V_m (cm/s)	73.6	72.6	68.5	65.7	62.0
$V_m/\bar{V}_f$	4.3	4.5	4.8	4.9	4.9
Average Free Fall Time, $\bar{t}_f$ (s)	0.32	0.25	0.22	0.20	0.15
Liquid Reaching Bottom Time, t_R (s)	0.40	0.31	0.27	0.25	0.20
$t_R/\bar{t}_f$	1.25	1.21	1.25	1.25	1.30

Table 1 CHARACTERISTICS OF CRYOGENIC HYDROGEN REORIENTATION
(Frequency of Impulsive Acceleration = 0.0 Hz) (continued)

Liquid Filled Level (%)	30	50	65	70	80
Time for Observing Maximum Flow Velocity, t_m (s)	0.42	0.31	0.28	0.25	0.20
Scale Length of Maximum Flow Velocity, L_m ($= V_m t_m$) (cm)	30.9	23.2	19.2	16.7	12.4
$L_m/\bar{h}$	11.6	11.6	12.4	12.3	13.0
$t_m/\bar{t}_f$	1.3	1.2	1.3	1.3	1.3
Scale Flow Acceleration Associated with Maximum Velocity, a_m ($= V_m/t_m$) (cm/s^2)	175	232	244	257	310
a_m/a_g	3.3	3.6	3.7	3.9	3.8
Maximum Liquid Height, h_m (cm)	3.41	2.79	2.26	2.09	1.67
Free Fall Velocity from Maximum Liquid Height V_{fm} (cm/s)	19.2	18.9	17.1	16.6	16.4
V_m/V_{fm}	3.9	3.8	4.0	3.9	3.8

Figure Captions

Fig 1. (A) Distribution of grid points in the radial-axial plane of cylindrical coordinate for propellant tank, and (B) Model size propellant tank adopted for numerical simulation with geometrical description.

Fig 2. Selected sequences of time evolution of fluid reorientation with liquid filled level of 30%, (A) initial profile, (B) flow profile before the initiation of geyser, (C) flow profile with geyser, and (D) flow profile after the ending of geyser.

Fig 3. Selected sequences of time evolution of fluid reorientation with liquid filled levels of 80%, (A) initial profile, (B) flow profile before the initiation of geyser, (C) flow profile with geyser, and (D) flow profile after the ending of geyser.

Fig 4. (A) Ratio of $V_m/\bar{V}_f$ and its associated parameters in terms of liquid filled levels, (B) Ratio of $t_R/\bar{t}_f$ and its associated parameters in terms of liquid filled levels.

Fig 5. (A) Ratio of $t_m/\bar{t}_f$ and its associated parameters in terms of liquid filled levels, (B) Ratio of a_m/a_g and its associated parameters in terms of liquid filled levels.

Fig 6. (A) Ratio of $L_m/\bar{h}$ and its associated parameters in terms of liquid filled levels, (B) Ratio of V_m/V_{fm} and its associated parameters in terms of liquid filled levels.

(A)

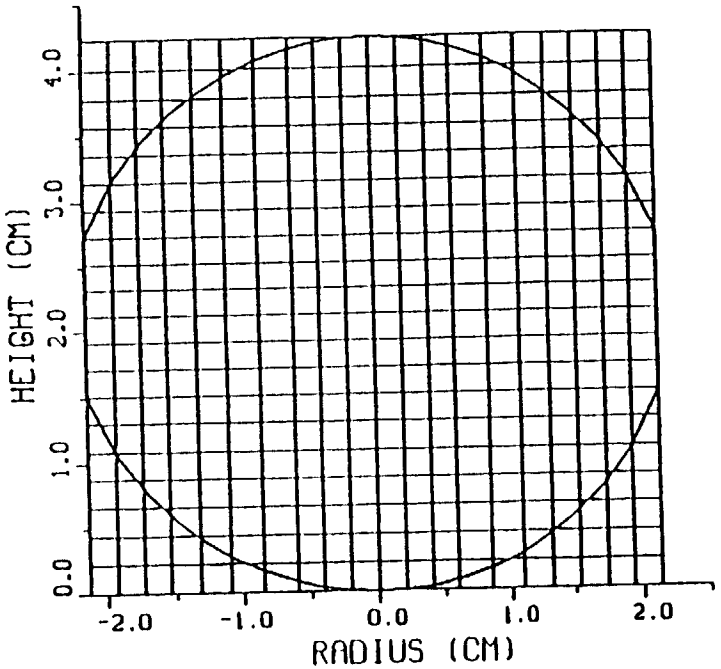

(B)

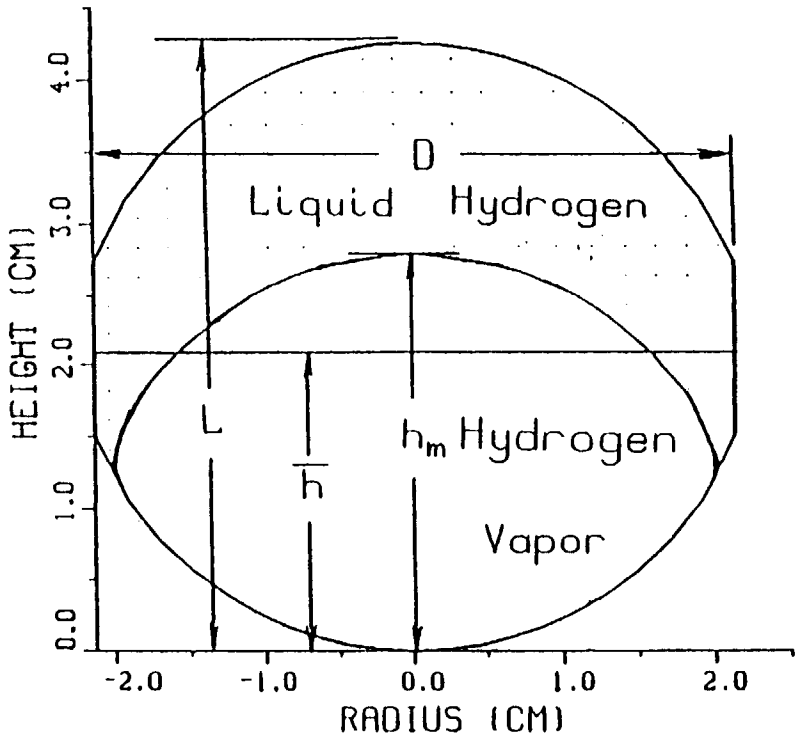

D-4.26720 CM, L-4.23672 CM

Fig 1

A. Liquid Hydrogen and Vapor
Liquid Filled-30% t- 0.00s
g--5.50×10^{-2}g$_o$
f- 0.00Hz

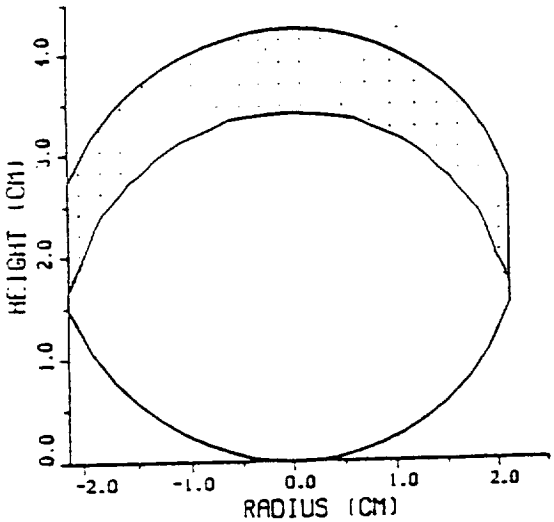

B. Liquid Hydrogen and Vapor
Liquid Filled-30% t- 3.00×10^{-1}s
g--5.50×10^{-2}g$_o$
f- 0.00Hz

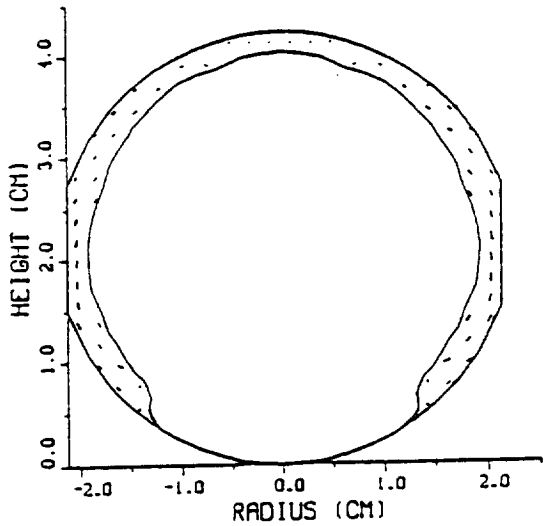

C. Liquid Hydrogen and Vapor
Liquid Filled-30% t- 5.27×10^{-1}s
g--5.50×10^{-2}g$_o$
f- 0.00Hz

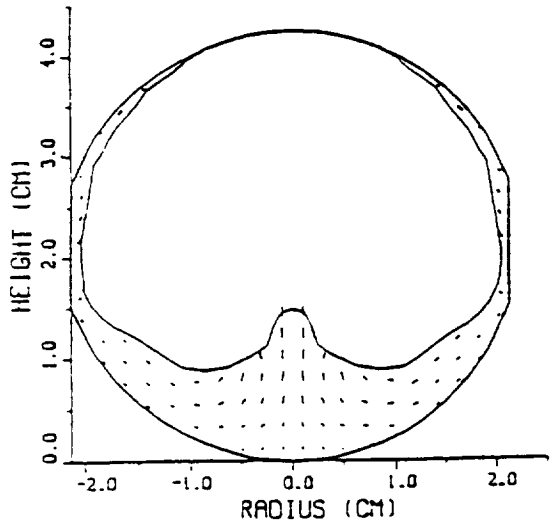

D. Liquid Hydrogen and Vapor
Liquid Filled-30% t- 9.47×10^{-1}s
g--5.50×10^{-2}g$_o$
f- 0.00Hz

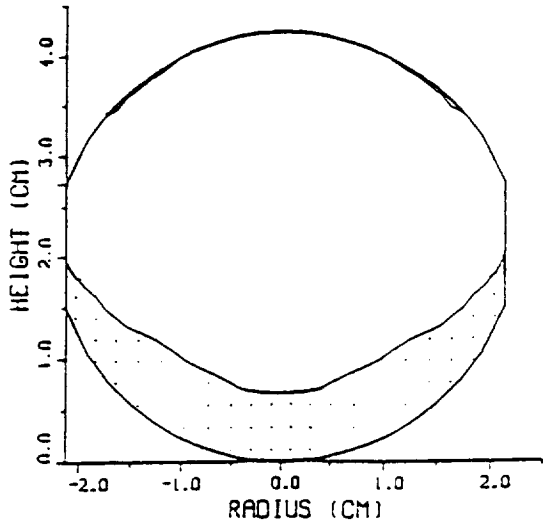

Fig 2

A. Liquid Hydrogen and Vapor
Liquid Filled-50% t= 0.00s
g=-6.52×10^{-2}g$_o$
f= 0.00Hz

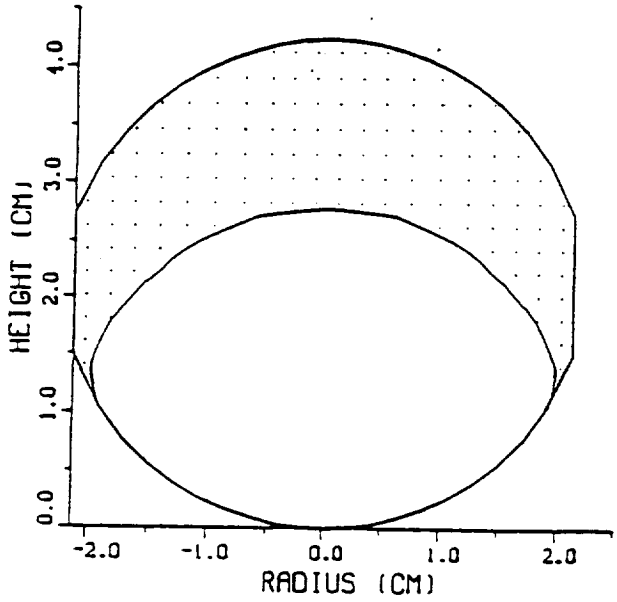

B. Liquid Hydrogen and Vapor
Liquid Filled-50% t= 2.40×10^{-1}s
g=-6.52×10^{-2}g$_o$
f= 0.00Hz

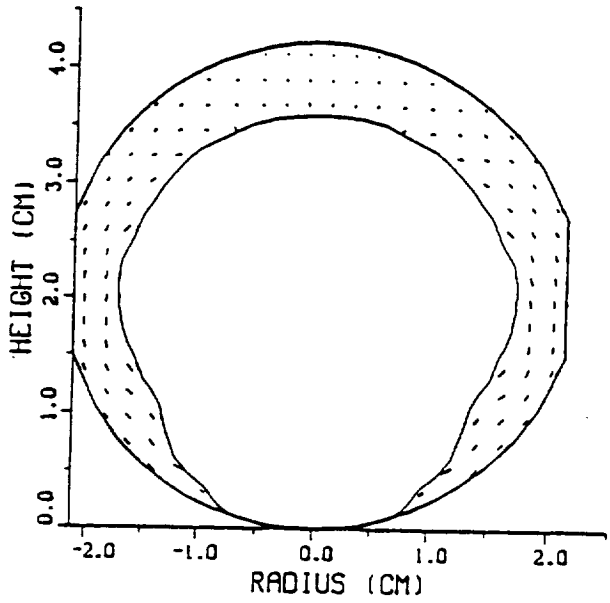

C. Liquid Hydrogen and Vapor
Liquid Filled-50% t= 4.04×10^{-1}se
g=-6.52×10^{-2}g$_o$
f= 0.00Hz

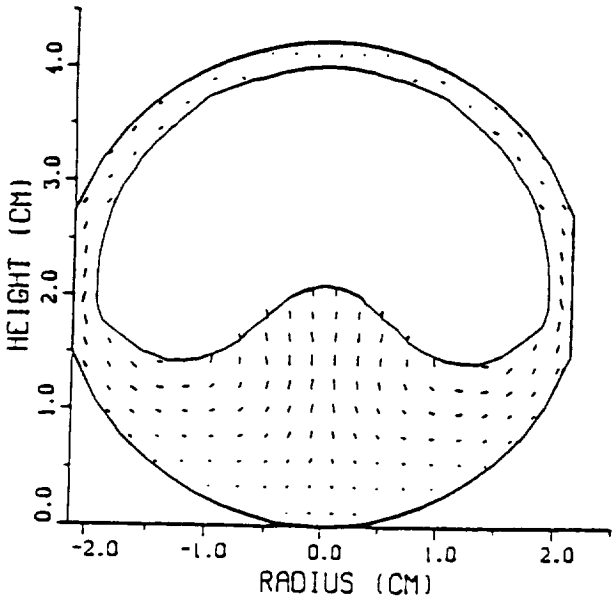

D. Liquid Hydrogen and Vapor
Liquid Filled-50% t= 5.24×10^{-1}s
g=-6.52×10^{-2}g$_o$
f= 0.00Hz

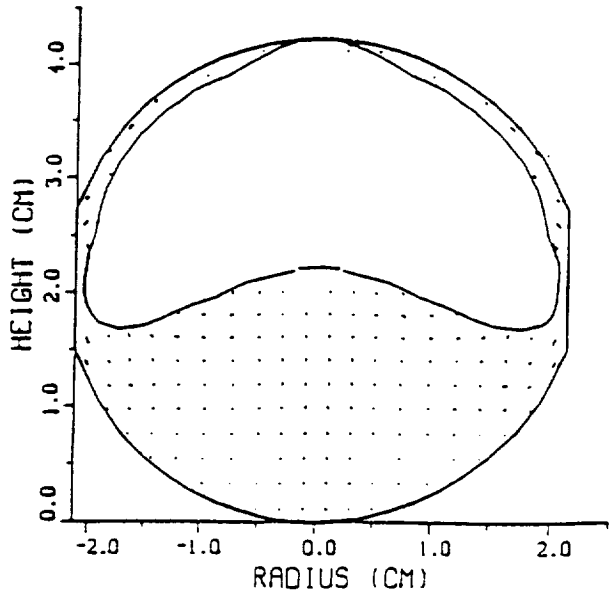

Fig 3

A. Liquid Hydrogen and Vapor
Liquid Filled-65% t= 0.00s
g=-6.60×10^{-2}g$_o$
f= 0.00Hz

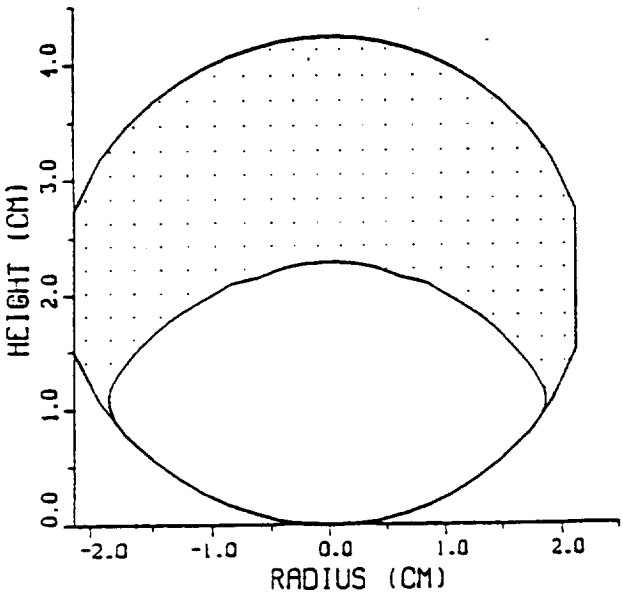

B. Liquid Hydrogen and Vapor
Liquid Filled-65% t= 2.40×10^{-1}s
g=-6.60×10^{-2}g$_o$
f= 0.00Hz

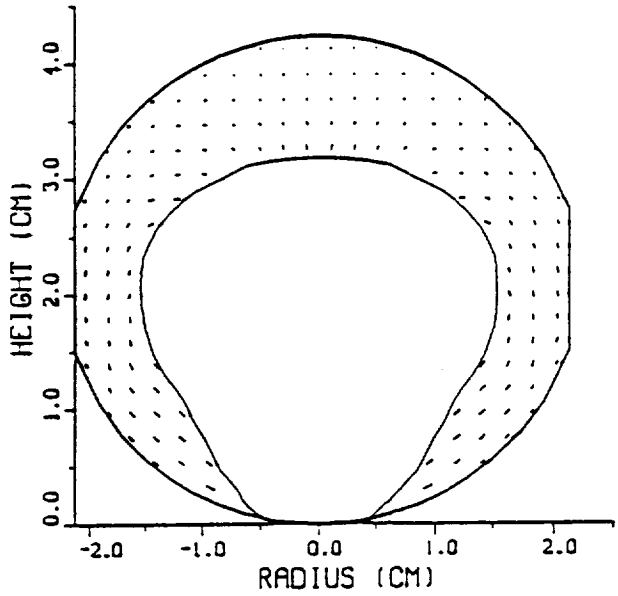

C. Liquid Hydrogen and Vapor
Liquid Filled-65% t= 4.61×10^{-1}s
g=-6.60×10^{-2}g$_o$
f= 0.00Hz

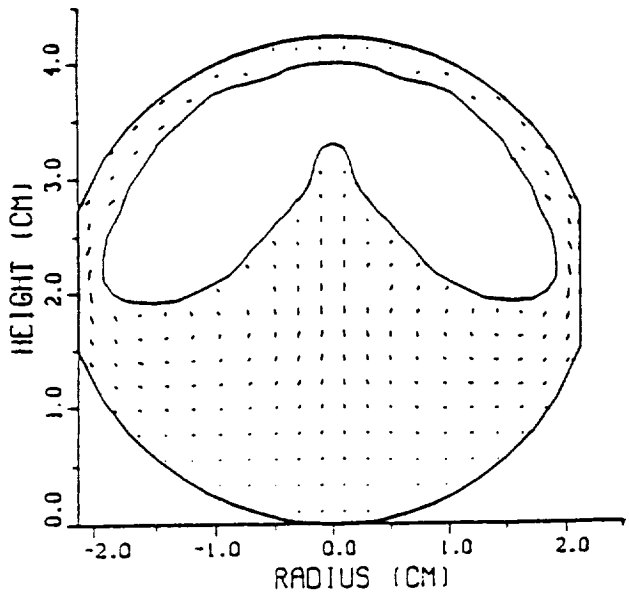

D. Liquid Hydrogen and Vapor
Liquid Filled-65% t= 7.61×10^{-1}s
g=-6.60×10^{-2}g$_o$
f= 0.00Hz

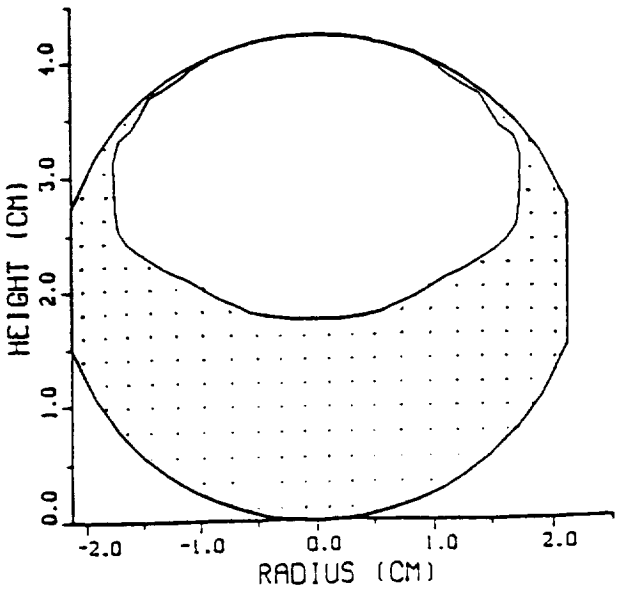

Fig 4

A. Liquid Hydrogen and Vapor
Liquid Filled=70% t= 0.00s
g=-6.70×10^{-2}g$_o$
f= 0.00Hz

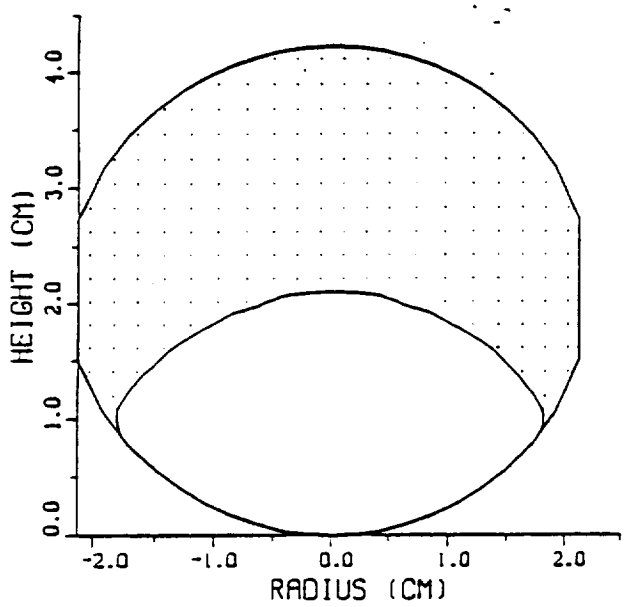

B. Liquid Hydrogen and Vapor
Liquid Filled=70% t= 1.80×10^{-1}s
g=-6.70×10^{-2}g$_o$
f= 0.00Hz

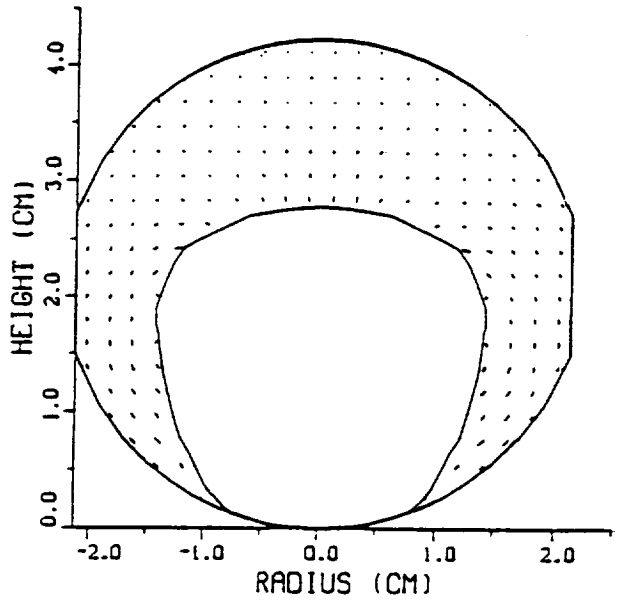

C. Liquid Hydrogen and Vapor
Liquid Filled=70% t= 2.84×10^{-1}s
g=-6.70×10^{-2}g$_o$
f= 0.00Hz

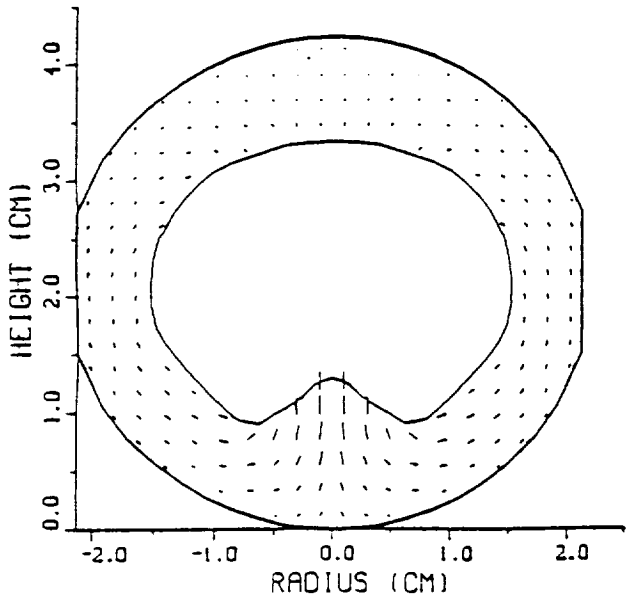

D. Liquid Hydrogen and Vapor
Liquid Filled=70% t= 1.18×10^{0}s
g=-6.70×10^{-2}g$_o$
f= 0.00Hz

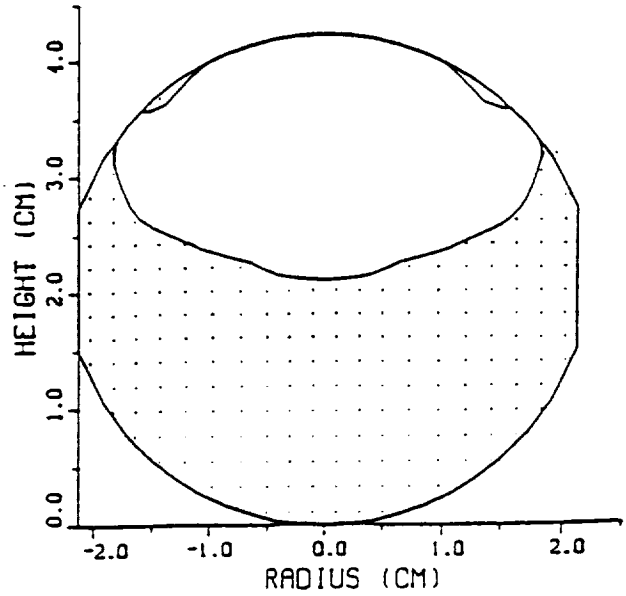

Fig 5

A. Liquid Hydrogen and Vapor
Liquid Filled-80% t= 0.00s
g=-8.20×10^{-2}g$_o$
f= 0.00Hz

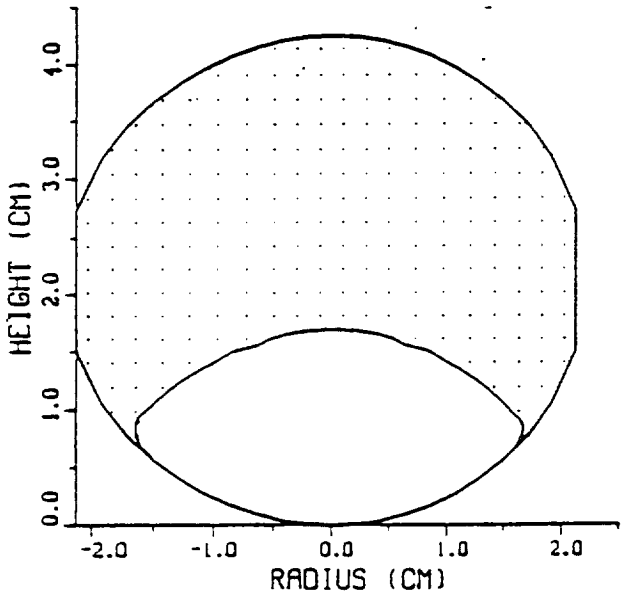

B. Liquid Hycrogen and Vapor
Liquid Filled-80% t= 1.80×10^{-1}s
g=-8.20×10^{-2}g$_o$
f= 0.00Hz

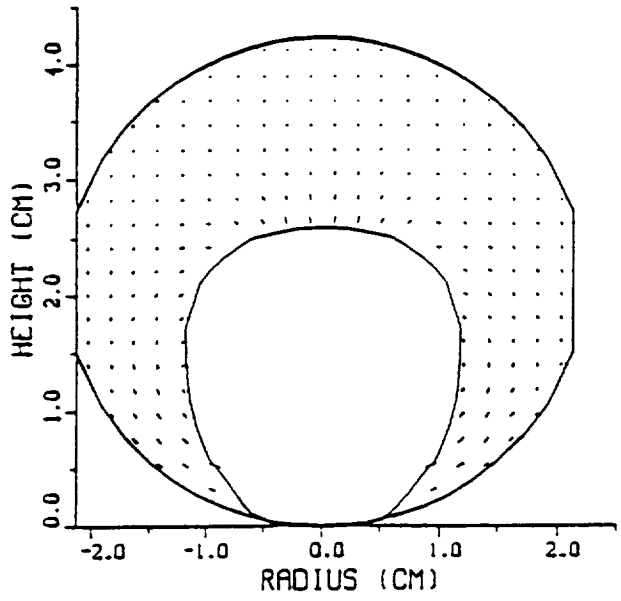

C. Liquid Hydrogen and Vapor
Liquid Filled-80% t= 2.77×10^{-1}s
g=-8.20×10^{-2}g$_o$
f= 0.00Hz

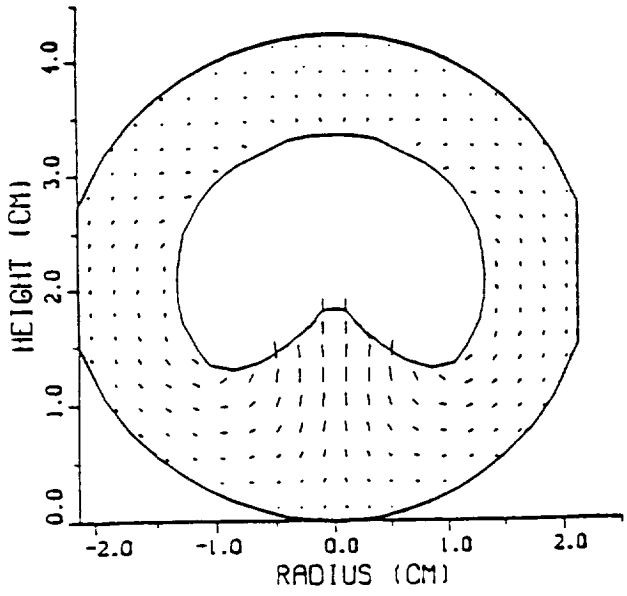

D. Liquid Hydrogen and Vapor
Liquid Filled-80% t= 7.57×10^{-1}s
g=-8.20×10^{-2}g$_o$
f= 0.00Hz

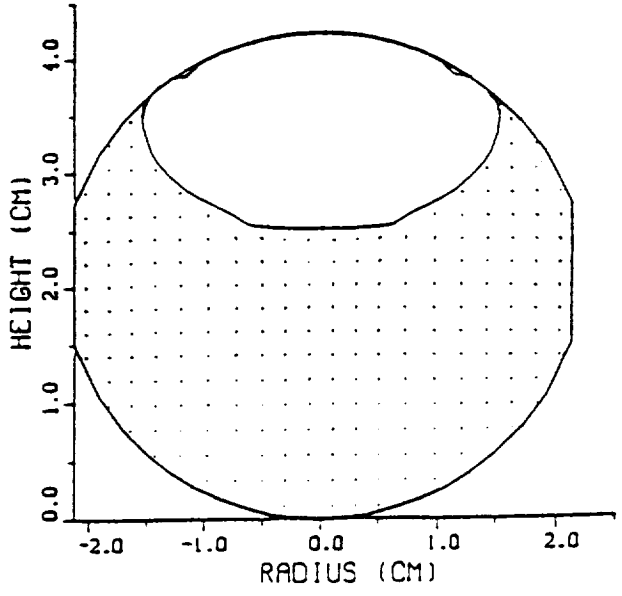

Fig 6

(A)

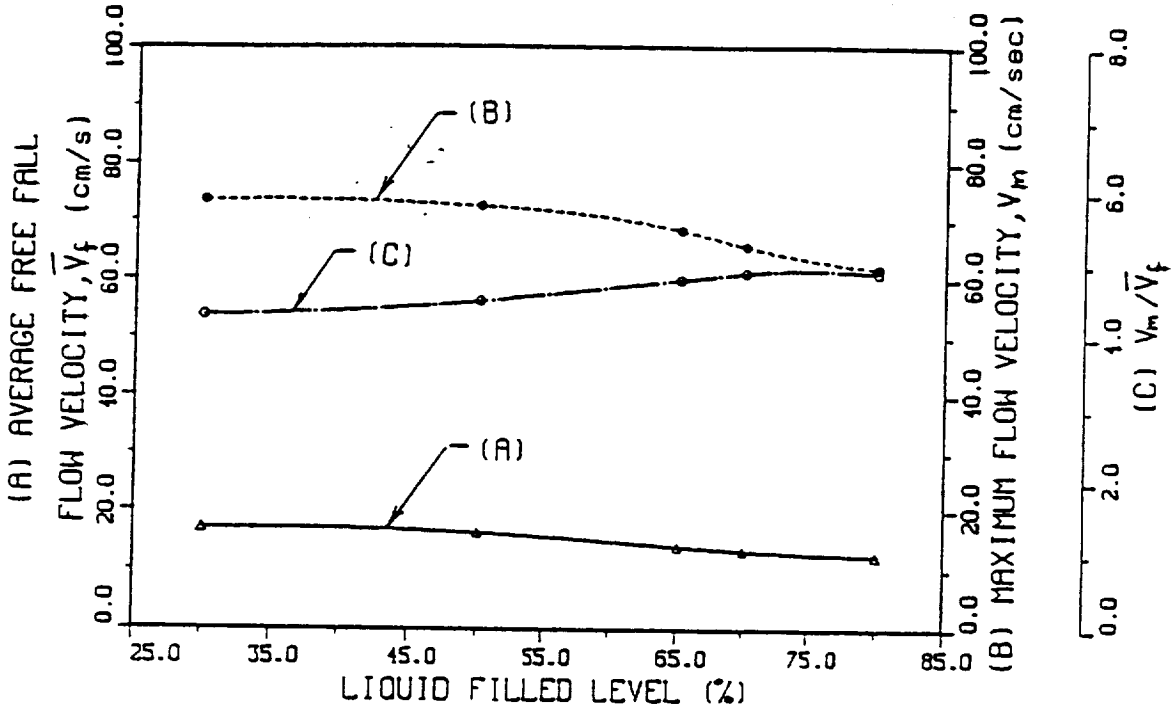
(A) AVERAGE FREE FALL FLOW VELOCITY, $\bar{V}_f$ (cm/s)
(B) MAXIMUM FLOW VELOCITY, V_m (cm/sec)
(C) $V_m/\bar{V}_f$
LIQUID FILLED LEVEL (%)
(A)
(B)
(C)
0.0
20.0
40.0
60.0
80.0
100.0
25.0
35.0
45.0
55.0
65.0
75.0
85.0
1.0
2.0
6.0
8.0

(B)

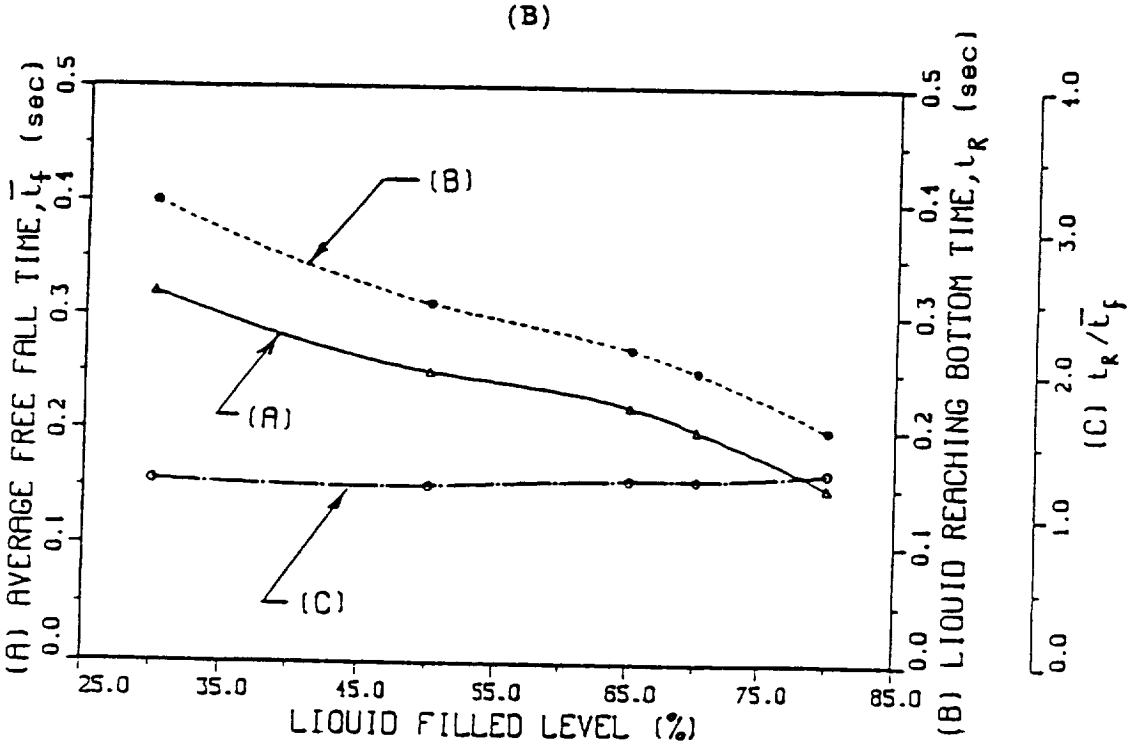
(A) AVERAGE FREE FALL TIME, $\bar{t}_f$ (sec)
(B) LIQUID REACHING BOTTOM TIME, t_R (sec)
(C) $t_R/\bar{t}_f$
LIQUID FILLED LEVEL (%)
(A)
(B)
(C)
0.0
0.1
0.2
0.3
0.4
0.5
25.0
35.0
45.0
55.0
65.0
75.0
85.0
1.0
2.0
3.0
4.0

Fig 7(A,B)

(A)

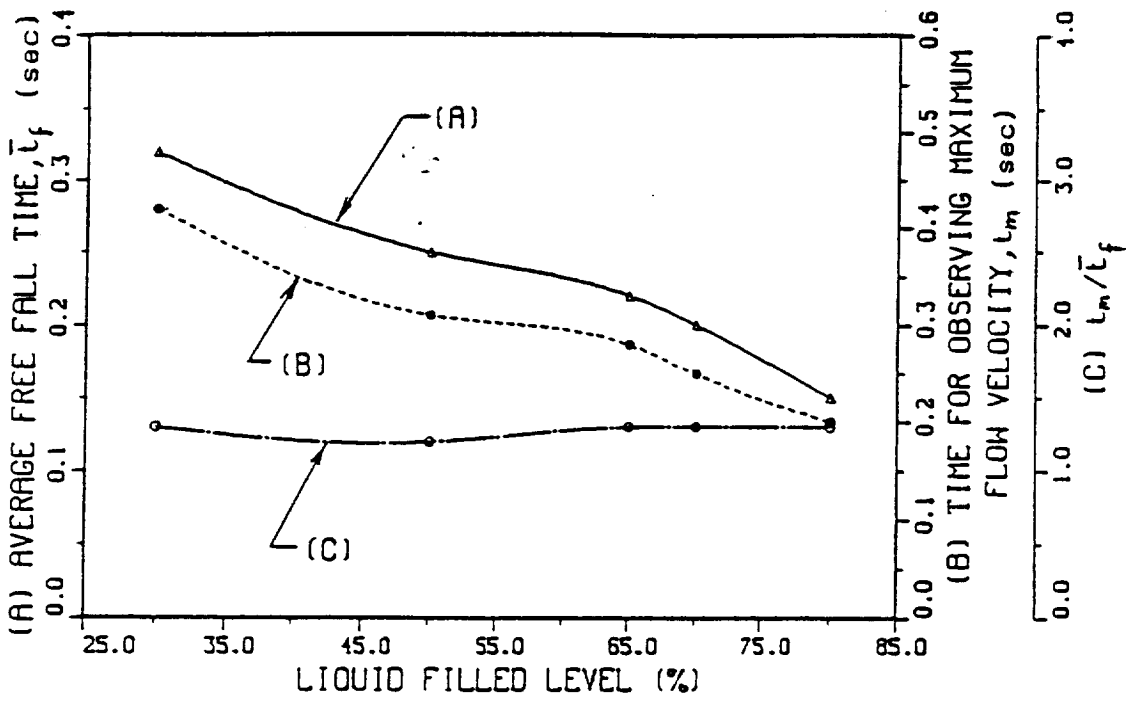
(A) AVERAGE FREE FALL TIME, $\bar{t}_f$ (sec)
(B) TIME FOR OBSERVING MAXIMUM FLOW VELOCITY, t_m (sec)
(C) $t_m/\bar{t}_f$
LIQUID FILLED LEVEL (%)
(A)
(B)
(C)
0.0
0.1
0.2
0.3
0.4
0.6
0.5
1.0
2.0
3.0
25.0
35.0
45.0
55.0
65.0
75.0
85.0

(B)

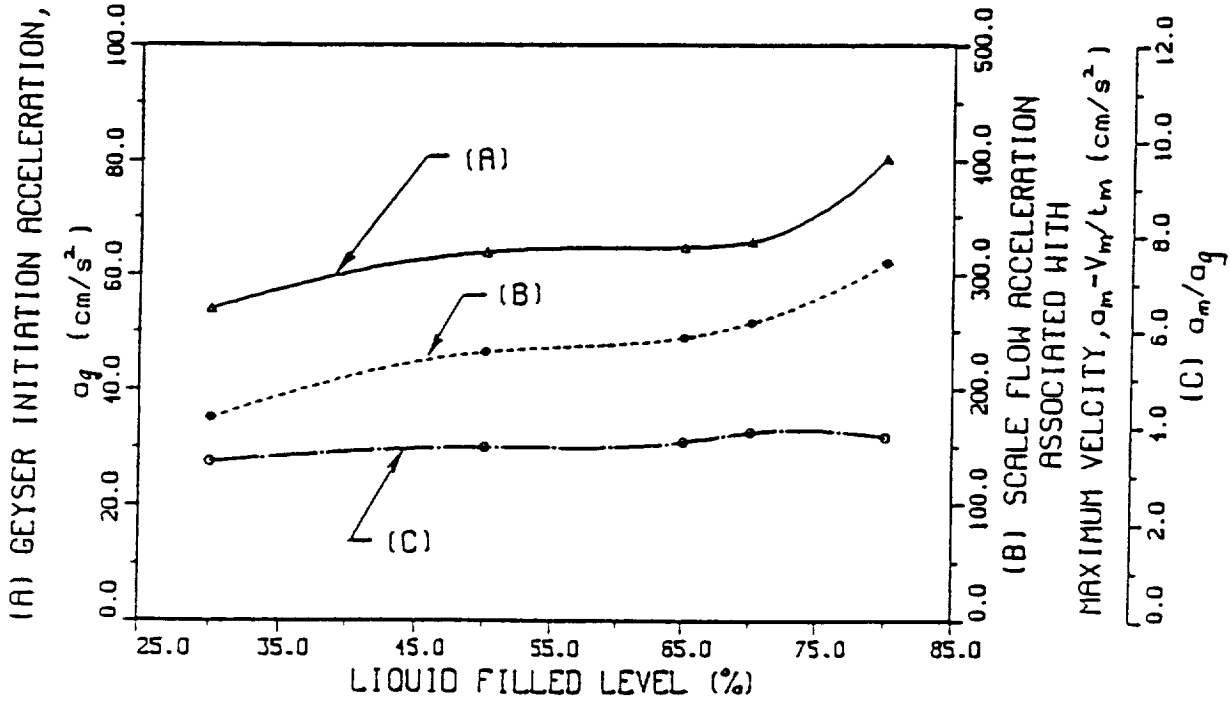
(A) GEYSER INITIATION ACCELERATION, a_g (cm/s^2)
(B) SCALE FLOW ACCELERATION ASSOCIATED WITH MAXIMUM VELCITY, a_m-V_m/t_m (cm/s^2)
(C) a_m/a_g
LIQUID FILLED LEVEL (%)
(A)
(B)
(C)
0.0
20.0
40.0
60.0
80.0
100.0
100.0
200.0
300.0
400.0
500.0
2.0
4.0
6.0
8.0
10.0
12.0
25.0
35.0
45.0
55.0
65.0
75.0
85.0

Fig 8(A,B)

(A)

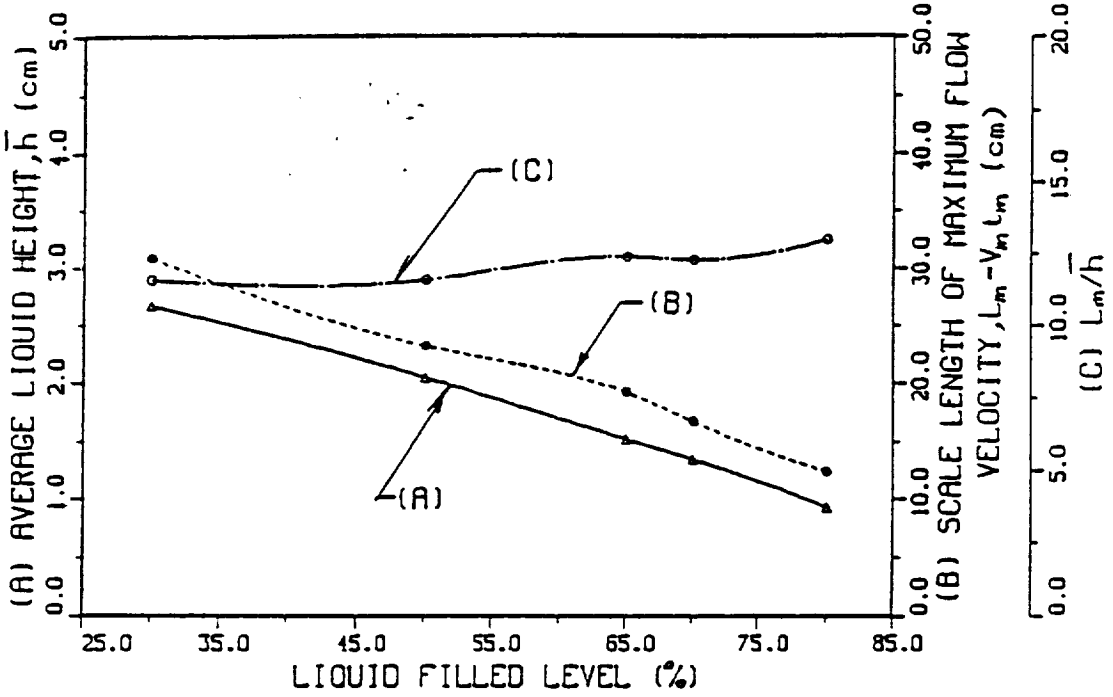
(A) AVERAGE LIQUID HEIGHT, $\bar{h}$ (cm)
(B) SCALE LENGTH OF MAXIMUM FLOW VELOCITY, $L_m - V_m L_m$ (cm)
(C) $L_m/\bar{h}$
LIQUID FILLED LEVEL (%)
(A)
(B)
(C)
0.0
1.0
2.0
3.0
4.0
5.0
10.0
20.0
30.0
40.0
50.0
5.0
15.0
25.0
35.0
45.0
55.0
65.0
75.0
85.0

(B)

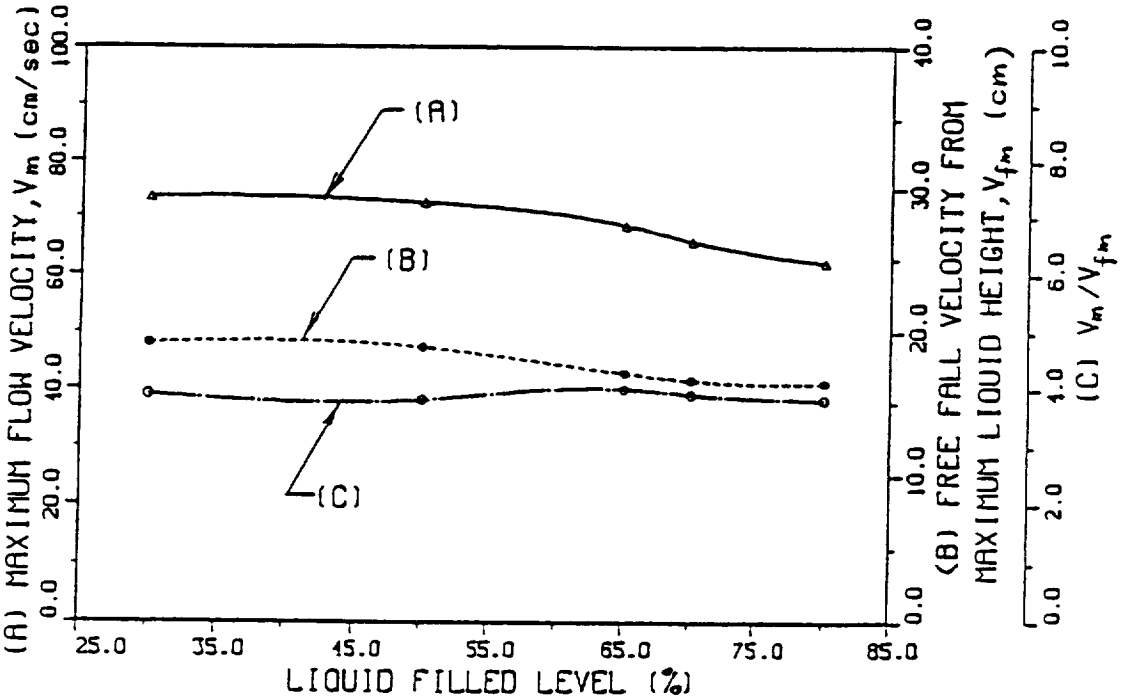
(A) MAXIMUM FLOW VELOCITY, V_m (cm/sec)
(B) FREE FALL VELOCITY FROM MAXIMUM LIQUID HEIGHT, V_{fm} (cm)
(C) V_m/V_{fm}
LIQUID FILLED LEVEL (%)
(A)
(B)
(C)
0.0
20.0
40.0
60.0
80.0
100.0
10.0
30.0
2.0
4.0
6.0
8.0
25.0
35.0
45.0
55.0
65.0
75.0
85.0

Fig 9(A,B)

(F) Cryogenic Liquid Hydrogen Reorientation Activated by Low Frequency Impulsive Settling Acceleration of Geyser Initiation

ABSTRACT

The requirement to settle or to position liquid fluid over the outlet end of spacecraft propellant tank prior to main engine restart poses a microgravity fluid behavior problem. Resettlement or reorintation of liquid propellant can be accomplished by providing optimal acceleration to the spacecraft such that the propellant is reorientaed over the tank oulet without any vapor entrainment, any excessive geysering, or any other undesirable fluid motion for the space fluid management under microgravity environment. The purpose of present study is to investigate most efficient technique for propellant resettling through the minimization of propellant usage and weight penalties. Comparison between the constant reverse gravtiy acceleration and impulsive reverse gravity acceleration to be used for the activation of propellant resettlement, it shows that impulsive reverse gravity thrust is superior to constant reverse gravity thrust for liquid reorientation in a reduced gravity environment.

I. Introduction

In spacecraft design, the requirements for a settled propellant are different for tank pressurization, engine restart, venting, or propellant transfer. Prepressurization requires that heat and mass transfer effects be minimized; otherwise, a process of chill down of tank, venting of noncondensing gases, etc., may have to carry out for the cryogenic system. For engine restart, it is necessary to have the liquid settle with no bubbles near the tank outlet so that the initial flow of propellant will not carry vapor to the pump or engine. The slosh wave amplitude should be relatively low to keep the center of mass shifts within an acceptable range and wave motion low enough to avoid pressure collapse caused by interface agitation . For venting, it is probably necessary that virtually all bubbles be displaced from the bulk liquid so that a two-phase mixture is not vented. Propellant transfer requires that the liquid be completely settled with virtually no bubbles. Outflow of a liquid near the tank outlet can result in the prematrue ingestion of gas while a signigicant amount of liquid is still in the tank under microgravity environment. This phenomenon is termed "suction dip". Slosh wave motion must be minimal because the combination of "suction dip" and sloshing could cause gas pull-through to occur more readily in microgravity than if the surface were essentially quiescent.

During the prepressurization of a cryogenic propellant in microgravity, significant heat and mass transfer will occur if the liquid interface is disturbed. Interface disturbances may result from (a) impingement of the gas on the liquid surface at a mass flow

rate sufficient to cause Kelvin-Helmholtz instability, (b) globule formation from breaking waves caused by wave motion over baffles or internal hardware, (c) globule and surface froth formation resulting from movement of bubbles through the liquid to the surface, and (d) surface froth formation because of gas impingement.

Bubble and globule formation as a result of liquid impact with the aft end of the tank could lead to propellant loss for the spacecraft during venting. Globules could be entrained in the vented ullage gas or bubbles rising through the liquid and expanding because of the decreasing tank pressure could cause a spray of globules to be vented. Liquid level rise, vent liquid loss, fluid freezing, and vehicle dynamics are all affected by the microgravity levels.

A key objective of the cryogenic fluid management of spacecraft propulsion system, such as a Space Transfer Vehicle[1] (STV), is to develop the technology necessary for acquisition or positioning of liquid and vapor within a tank in reduced gravity to enable liquid outflow or vapor venting. Liquid acquisition techniques can be divided into two general categories: (1) Active liquid acquisition by the creation of a positive acceleration environment resulting from the propulsive thrust of small auxiliary engines, and (2) Passive liquid acquisition utilizing the liquid capillary forces provided by using solid baffles of liquid traps made of fine mesh screen material. In this series of study, active liquid acquisition is aimed for numerically simulating the resettlement of cryogenic liquid hydrogen. Liquid hydrogen, which, in general, poses more severe technical challenges than liquid oxygen, is used as the test bed

working fluid in this study.

Recently Lesie[2] was able to measure and to numerically compute the bubble shapes at various ratios of centrifugal force to surface tension force in 2, 4 and 6.3 cm deep cylinders in the microgravity environment. The results showed excellent agreement between model computation and measurements. Hung and Leslie[3] extended Leslie's work[2] to rotating free surfaces influenced by gravity with higher rotating speeds when the bubble intersects with both the top and bottom walls of the cylinder. Hung et al.[4,5] further extended the work to include rotating speeds which resulted with bubbles intersecting and/or without intersecting the top, bottom and side walls of the cylinder.

An analysis of time-dependent dynamical behavior of surface tension on partially-filled rotating fluids in both low gravity and microgravity environments was carried out by numerically solving the Navier-Stokes equations subjected to the initial and the boundary conditions[4,6]. At the interface between the liquid and the gaseous fluids, both the kinematic surface boundary condition, and the interface stress conditions for components tangential and normal to the interface, were applied. The initial condition for the bubble profiles was adopted from steady-state formulations developed by Hung and Leslie[3], and Hung et al.[6] for rotating cylinder tank; and by Hung et al.[5,7] for the dewar-shaped container to be used in the Gravity Probe-B Spacecraft[8]. Some of the steady-state formulations of bubble shapes, in particular for bubbles intersecting at the top wall of the cylinder, were compared with the experiment carried out by

Leslie[2] in a free-fallinng aircraft (KC-135). Comparisons of time-dependent results between numerical computations and experiments were unavailable. This was because the calibration of the recordings of time-dependent gravity variations in a KC-135 aircraft during the short time periods of microgravity environment is very difficult. There was also an unavailability of accelerometer data for measuring the actual levels of microgravity during the experiment.

An efficient propellant settling technique should minimize propellant usage and weight penalties. This can be accomplished by providing optimal acceleration to the spacecraft such that the propellant is reoriented over the tank outlet without any vapor entrainment, any excessive geysering, or any other undesirable fluid motion.

Production of geyser during the propellant reorientation is not a desirable motion for the space fluid management. It is because geyser is always accompanied by the vapor entrainment and globule formation. Geyser is observed at reverse gravity thrust greater than certain critical values of acceleration during the course of liquid reorientation. In other words, geyser will not be observed at very low reverse gravity level, and it will be detected when the reverse gravity level is greater than the certain critical value. In this series of study, numerical simulation of positive liquid acquisition is attemted by introducing reverse gravity acceleration, resulting from the propulsive thrust of small auxiliary engines which exceeds the critical value for geyser initiation. The reverse gravity acceleration is starting with a small value and increases gradually

till the initiation of geyser is detected in the computer simulation for the liquid reorientation of propellant tank with various liquid-filled levels.

In this series of studies, time-dependent computations have been carried out to investigate the dynamical behavior of fluid reorientation or resettling of propellant prior to main engine firing for spacecraft restart at the net reverse gravity acceleration which is great enough to initiate geyser during the liquid reorientation. First paper of present study (Paper I)[9] investigates the characteristics of fluid resettlement due to the reversal of lowest constant reverse gravity acceleration which is great enough to initiate geyser without any impulsive acceleration. The frequency of impulsive acceleration is generally termed "gravity jitters". Gravity jitters are produced by spacecraft attitude motion, machinery (turbine, pump, engine) vibrations, thruster firing, thruster shutdown, impulsive engine acceleration, etc.[10] Positioning of liquid propellant over the tank outlet can be carried out by using small auxiliary thrusters which provide a thrust parallel to the tank's major axis in the direction of flight.

Computer simulation of flow field based on Paper I[9] during the course of fluid reorientation induced by constant reverse gravity acceleration show that six dimensionless parameters are abtained in the study. These parameters hold near constant values through the entire ranges of liquid filled levels during the course of fluid reorientation activated by the reverse gravity acceleration great enough to initiate geyser. As the denominators of these

dimensionless parameters are either predetermined from the geometry of liquid filled levels or can be deduced from the corresponding calculations associated with the geyser initiation gravity levels. One can predict the values of these flow parameters. These predictable parameters include maximum flow velocity V_m, time for observing maximum flow velocity t_m, time for reorienting liquid flowing down and reaching the bottom of propellant tank t_R, scale length of maximum flow velocity L_m, and scale flow acceleration associated with maximum velocity a_m.

Instead of applying constant reverse gravity acceleration as we described in Paper I[9], this paper adopts impulsive reverse gravity acceleration with a low frequency of 0.1 Hz for the activation of fluid reorientation with liquid filled levels of 30, 50, 65, 70 and 80%.

II. Numerical Simulation of Liquid Hydrogen Reorientation with Geyser Initiation at Low Frequency Impulsive Reverse Gravity Acceleration of 0.1 Hz

The present study examines time-dependent fluid behaviors, in particular the dynamics of liquid hydrogen and hydrogen vapor reorientation induced by reverse gravity acceleration which is great enough to introduce geyser initiation. As in Paper I[9], time-dependent axial symmetry mathematical formulation are adopted. Detailed description of mathematical formulation, initial and boundary conditions suitable for the analysis of cryogenic fluid management under microgravity environment are given in our earlier

studies.[4,6,11-13] The initial profiles of liquid-vapor interface are determined from computations based on algorithms developed for the steady state formultion of microgravity fluid management.[3-7]

Detailed description of computational algorithm applicable to microgravity fluid management are illustrated in Paper I[9] and our earlier studies.[4,6,11-13] As we have indicated in Paper I[9], for the purpose of facilitating easy comparison between computational resuslts and experimental measurement, a model of 0.01 size prototype is adopted in the computer simulation. Model size is height L = 4.23672 cm and diameter D = 4.2672 cm. If the spacecraft had been coasting for a long time, aligned with its direction of motion, the most signigicant force, drag, would be axial and with acceleration of $10^{-4}g_0$ along upward direction. The hydrogen vapor is, thus, originally positioned at the bottom of the tank. The requirement to settle or to position liquid fuel over the outlet end of the spacecraft propellant tank prior to main engine restart poses a microgravity fluid behavior problem.[11] Retromaneuvers of spacecraft, such as STV, require settling or reorientation of the propellant prior to main engine firing.[1,11] Cryogenic liquid propellant shall be positioned over the tank outlet by using auxiliary thrusters (or idle-mode thrusters from the main engine) which provide a thrust parallel to the tank's major axis in the direction of flight. Similar to Paper I[9], a small value of reverse gravity acceleration (downward direction) is provided by the propulsive thrust of small auxiliary engine to initiate the reorientation of liquid propellant. This small value of reverse gravity acceleration of propulsive thrust increases

gradually till reaching the critical value on which initiation of geyser is detected during the time period of fluid resettlement. We term this reverse gravity acceleration of propulsive thrust, which is capable to initiate geyser, as "geyser initiation gravity-level". This geyser initiation gravity level has been investigated through the method of trial and error for the various liquid-filled levels as a base to simulate impulsive reverse gravity acceleration with frequencies of 0.1, 1.0 and 10 Hz. As we have indicated in Paper I[9], cryogenic liquid hydrogen at temperature of 20K is considered. Hydrogen density of 0.071 g/cm^3; surface tension coefficient at the interface between liquid hydrogen and hydrogen vapor of 1.9 dyne/cm; hydrogen viscosity coefficient of 1.873×10^{-3} cm^2/s; and contact angle of 0.5^0 are used in the computer simulation.

In this paper, among three categories of impulsive reverse gravity acceleration with frequencies of 0.1, 1.0 and 10 Hz, reorientation of cryogenic liquid hydrogen activated by geyser initiation impulsive reverse gravity acceleration with a low frequency of 0.1 Hz produced by propulsive thrust will be investigated for various liquid filled levels of propellant tank. Paper I shows that these geyser initiation gravity levels are 5.5×10^{-2}, 6.52×10^{-2}, 6.6×10^{-2}, 6.7×10^{-2} and $8.2 \times 10^{-2} g_0$ for liquid filled levels of 30, 50, 65, 70, and 80%, respectively.

Table 1 shows some basic geometrys and characteristics of cryogenic liquid hydrogen resettlement activated by reverse gravity acceleration at geyser initiation gravity level. Average liquid height $\bar{h}$, and maximum liquid height h_m are shown in Figure 1. Average

free fall velocity $\bar{V}_f$, average free fall time $\bar{t}_f$, and free fall velocity from maximum liquid height V_{fm} are computed from the following equations:

$$\bar{V}_f = (2g_{io}\bar{h})^{1/2} \qquad (1)$$

$$\bar{t}_f = \left(\frac{2\bar{h}}{g_{io}}\right)^{1/2} \qquad (2)$$

$$V_{fm} = (2g_{io}h_m)^{1/2} \qquad (3)$$

where g_{io} denotes geyser initiation reverse gravity acceleration.

To show examples of the selected sequences of time evolution of fluid reorientation for cryogenic hydrogen, Figures 2, 3, 4, 5, and 6 show time evolution of fluid reorientation activated by geyser initiation impulse reverse gravity acceleration with a frequency of 0.1 Hz for liquid filled levels of 30, 50, 65, 70 and 80 %, respectively. Each figure contains four sub-figures. Subfigure (A) is initial profile of liquid-vapor interface at the moment of the starting of fluid reorientation at time t = 0; subfigure (B), the flow profile during the course of fluid reorientation before the initiation of geysering motion; subfigure (C), the flow profile with geysering motion; and subfigure (D), the flow profile after the ending of geysering motion.

Examples of selected sequences of time evolution of fluid reorientation illustrate following flow behaviors: (1) The liquid starts to flow in an annular sheet along the solid wall of tank and gradually pushes the vapor toward the central portion of the lower dome of tank as the net acceleration, reversing the direction of gravity field, which is applied toward the downward direction of the

tank's major axis, by using small auxiliary thrusters; (2) As the downward fluid annular sheet along the tank wall reaches the central bottom dome side of the tank, a geysering flow is observed; and (3) The vapor is thus pushed upward centrally into the liquid and the geysering disappears.

Based on the computer simulation of flow field values of maximum flow velocity V_m, time for observing maximum flow velocity t_m, and time for reorienting liquid flowing down and reaching the bottom of propellant tank t_R, are obtained and illustrated in Table 2 for reverse gravity acceleration with impulsive frequency of 0.1 Hz. Scale length of maximum flow velocity L_m, and scale flow acceleration associated with maximum velocity a_m, can be computed from the following parameters:

$$L_m = V_m t_m \tag{4}$$

$$a_m = \frac{V_m}{t_m} \tag{5}$$

Following dimensionless parameters are introduced: $V_m/\bar{V}_f$, $t_R/\bar{t}_f$, $t_m/\bar{t}_f$, a_m/a_g, $L_m/\bar{h}$ and V_m/V_{fm} where a_g stands geyser initiation acceleration (cm/s^2) for corresponding geyser initiation gravity level g_{io}. Impulsive reverse gravity acceleration, g_i with frequency f Hz is defined as follows:

$$g_i = g_{io}\left(1 + \frac{1}{2}\sin 2\pi ft\right) \tag{6}$$

Figures 7 to 9 show the variations of dimensionless parameters in terms of liquid filled levels for impulsive acceleration with frequency of 0.1 Hz. Denominators of these six dimensionless

parameters are either predetermined from the geometry of liquid fill levels or can be deduced from the corresponding calculations associated with the geyser initiation gravity levels. Characteristics of these near constant values dimensionless parameters can provide a good understanding of the physics of microgravity fluid behaviors, in particular the active category of liquid acquisition or positioning, and also the design criteria of on-orbit spacecraft propulsion system at the critical value of reverse gravity acceleration of propulsive thrust which is capable to initiate geyser.

An efficient propellant settling technique should minimize propellant usage and weight penalties. This can be accomplished by providing optimal acceleration to the spacecraft such that the propellant is reoriented over the tank outlet without any vapor entrainment, any excessive geysering, or any other undesirable fluid motion. In particular, it is important to study how well the impulsive acceleration can provide higher efficient propellant settling technique than the constant acceleration thrust technique. Also, what is the most optimal choice of impulsive frequency which can achieve the best fluid acquisition management being the goal of our research.

Figure 7(A) shows the ratio of maximum flow velocity to average free fall flow velocity $V_m/\bar{V}_f$ and its associated parameters of V_m and $\bar{V}_f$ in terms of liquid filled levels for impulsive acceleration with frequency of 0.1 Hz. It shows that the ratio of $V_m/\bar{V}_f$ varies in the range of 5.0 to 5.1 in the entire liquid filled levels while V_m and $\bar{V}_f$

vary from 64.0 to 85.3 cm/s (decreasing with increasing liquid filled levels) and from 12.5 to 17.0 cm/s (also decreasing with increasing liquid filled levels), respectively. As $\bar{V}_f$ can be predetermined from geyser initiation gravity level and average liquid height, shown in Equation (1), one can make an approximate prediction of maximum flow velocity during the liquid reorientation for the various liquid filled levels. In comparison between impulsive acceleration with frequency of 0.1 Hz and constant thrust acceleration, it shows that impulsive acceleration can produce higher maximum flow velocity ($V_m/\bar{V}_f$ = 5.0 to 5.1) than that of constant thrust acceleration ($V_m/\bar{V}_f$ = 4.3 to 4.9).

Figure 7(B) shows the ratio of liquid reaching bottom time to average free fall time $t_R/\bar{t}_f$ and its associated parameters of t_R and $\bar{t}_f$ in terms of liquid filled levels for impulsive acceleration with frequency of 0.1 Hz. It shows that the ratio of $t_R/\bar{t}_f$ varies in the range of 1.1 to 1.2 in the entire liquid filled levels while t_R and $\bar{t}_f$ vary from 0.19 to 0.36 s (decreasing with increasing liquid filled levels) and from 0.15 to 0.32 s (also decreasing with increasing liquid filled levels), respectively. As $\bar{t}_f$ can be predetermined from geyser initiation gravity level and average liquid height, shown in Equation (2), one can predict the time reorienting liquid fluid flowing down from the original position and reaching the bottom of propellant tank for the various liquid filled levels at the reverse gravity acceleration capable for the initiation of geyser. In comparison between impulsive acceleration with frequency of 0.1 Hz and constant thrust acceleration, it shows that impulsive

C-2

acceleration activate the flow which takes shorter time for flow to reach the tank bottom ($t_R/\bar{t}_f$ = 1.1 to 1.2) than that of constant thrust acceleration ($t_R/\bar{t}_f$ = 1.21 to 1.30).

Figure 8(A) shows the ratio of time for observing maximum flow velocity to average free fall time $t_m/\bar{t}_f$ and its associated parameters of t_m and $\bar{t}_f$ in terms of liquid filled levels for impulsive acceleration with frequency of 0.1 Hz. It shows that the ratio of $t_m/\bar{t}_f$ varies in the range of 1.2 to 1.3 in the entire liquid filled levels while t_m and $\bar{t}_f$ vary from 0.18 to 0.39 s (decreasing with increasing liquid filled levels) and from 0.15 to 0.32 s (also decreasing with increasing liquid filled levels), resectively. As we indicated in Figure 7(B), $\bar{t}_f$ can be predetermined, one can predict the time for observing maximum flow velocity for various liquid filled levels at the reverse gravity acceleration capable for the initiation of geyser. In comparison between impulsive acceleration with frequency of 0.1 Hz and constant thrust acceleration, it shows that impulsive acceleration can activate higher maximum flow velocity within a shorter period of time (0.18 to 0.39 s) than that of constant thrust acceleration (0.20 to 0.425).

Figure 8(B) shows the ratio of scale flow acceleration associated with maximum velocity to geyser initiation acceleration for corresponding geyser initiation gravity level a_m/a_g and its associated parameters of a_m and a_g in terms of liquid filled levels for impulsive acceleration with frequency of 0.1 Hz. It shows that the ratio of a_m/a_g varies in the range of 4.1 to 4.4 in the entire liquid filled levels while a_m and a_g vary from 218 to 355 cm/s^2 (increasing

with increasing liquid filled levels) and from 53.9 to 80.4 cm/s^2 (also increasing with increasing liquid filled levels), respectively. As a_g can be predetermined from geyser initiation gravity level, one can make an approximate prediction of scale flow acceleration associated with maximum velocity, which is defined in Equation (5), at the reverse gravity acceleration capable for the initiation of geyser. In comparison between impulsive acceleration with frequency of 0.1 Hz and constant thrust acceleration, it shows that impulsive acceleration can produce higher scale flow acceleration associated with maximum flow velocity (a_m/a_g = 4.1 to 4.4) than that of constant thrust acceleration (a_m/a_g = 3.3 to 3.8).

Figure 9(A) shows the ratio of scale length of maximum flow velocity to average liquid height $L_m/\bar{h}$ and its associated parameters of L_m and $\bar{h}$ in terms of liquid filled levels for impulsive acceleration with frequency of 0.1 Hz. It shows that the ratio of $L_m/\bar{h}$ varies in the range of 12.3 to 12.6 in the entire liquid filled levels while L_m and $\bar{h}$ vary from 11.5 to 33.2 cm (decreasing with increasing liquid filled levels) and from 0.93 to 2.67 cm (also decreasing with increasing liquid filled levels), respectively. As $\bar{h}$ can be predetermined from the geometry of liquid filled levels, one can make an approximate prediction of scale length of maximum flow velocity, which is defined in Equation (4), at the reverse gravity acceleration capable for the initiation of geyser. In comparison between impulsive acceleration with frequency of 0.1 Hz and constant thrust acceleration, it shows that impulsive acceleration can produce longer scale length of maximum flow velocity (L_m = 11.5 to 33.2 cm) than that

of constant thrust acceleration (L_m = 12.4 to 30.9).

Figure 9(B) shows the ratio of maximum flow velocity to free fall velocity from maximum liquid height V_m/V_{fm} and its associated parameters of V_m and V_{fm} in terms of liquid filled levels for impulsive acceleration with frequency of 0.1 Hz. It shows that the ratio of V_m/V_{fm} varies in the range of 4.0 to 4.4 in the entire liquid filled levels while V_m and V_{fm} vary from 64.0 to 85.3 cm/s (decreasing with increasing liquid filled levels) and from 16.4 to 19.2 cm/s (also decreasing with increasing liquid filled levels), respectively. As V_{fm} can be predetermined from geyser initiation gravity level and maximum liquid height, shown in Equation (3), one can make an approximate prediction of maximum flow velocity at the reverse gravity acceleration capable for the initiation of geyser. In comparison between impulsive acceleration with frequency of 0.1 Hz and constant thrust acceleration, it shows that impulsive acceleration can produce higher maximum velocity (V_m/V_{fm} = 4.0 to 4.4) than that of constant thrust acceleration (V_m/V_{fm} = 3.8 to 4.0).

As we have illustrated in Paper I[9], six dimensionless parameters presented in this study show that the parameters hold near constant values through the entire ranges of liquid filled levels during the course of reorientation of liquid hydrogen activated by the reverse gravity acceleration which is great enough to initiate geysering flow. As the purpose of present study is to investigate an efficient propellant settling technique which is able to minimize propellant usage and weight penalties, comparison of flow parameters between impulsive acceleration with frequency of 0.1 Hz and that of constant

thrust acceleration have been made toward this objective. It shows that the operation of auxiliary engine with impulsive acceleration of 0.1 Hz frequency is better than that of constant thrust acceleration in terms of introducing a higher maximum flow velocity, a shorter time period to reach maximum flow velocity, a shorter time period for flow to reach the tank bottom (tank outlet) for resettling, a longer scale length of maximum flow velocity, and a higher flow acceleration associated with maximum flow velocity.

IV. Discussion and Conclusions

The requirement to settle or to position liquid fluid over the outlet end of the spacecraft propellant tank prior to main engine restart poses a microgravity fluid behavior problem. Retromaneuvers of spacecraft require settling or reorientation of the propellant prior to main engine firing. Cryogenic liquid propellant is positioned over the tank outlet by using small auxiliary thrusters (or idle-mode thrusters from the main engine) which provide a thrust parallel to the tank's major axis in the direction of flight.

The results of the study of fluid reorientation have to be evaluated in terms of how well they can be managed efficiently. An efficient propellant settling technique should minimize propellant usage and weight penalties through the operation of small thrusters (or idle-mode thrusters from the main engine). This can be accomplished by providing optimal acceleration to the spacecraft such that the propellant is reoriented over the tank outlet without any vapor entrainment, any excessive geysering, or any other undesirable fluid motion.

Production of geyser during the propellant reorientation is not a desirable motion for the space fluid management under microgravity environment. It is because geyser is always accompanied by the vapor entrainment and globule formation. Geyser is observed at reverse gravity acceleration greater than certain critical values of acceleration during the course of liquid reorientation. In this paper, numerical simulation of positive liquid acquisition is attempted by introducing reverse gravity acceleration, resulting from the propulsive thrust with high impulsive frquency of 0.1 Hz auxiliary engine, which exceeds critical value for the initiation of geyser.

Evaluation of performance is based on how efficient the impulsive&a+60Hreverse gravity with 0.1 Hz frequency in comparison wit constant thrust acceleration can activate following flow parameters at the same background thrust accelerations: (A) a higher maximum flow velocity, (B) a shorter time period for flow to reach maximum velocity, (C) a shorter time period for flow to reach tank bottom (tank outlet) for fluid resettling, (D) a larger length scale of maximum flow velocity, and (E) a higher flow acceleration associated with maximum flow velocity. Comparison between the results of present study for impulsive thrust with 0.1 Hz frequency and that of constant thrust, shown in Paper I[9], it shows that impulsive thrust, is superior than the constant reverse thrust in terms of efficient operation of fluid reorientation.

Based on the computer simulation of flow fields during the course of fluid reorientation, six dimensionless parameters are presented

both in Paper I[9] and this study. It is shown that these parameters hold near constant values through the entire ranges of liquid filled levels during the course of fluid reorientation activated by the reverse gravity acceleration in both constant and impulsive thrusts great enough to initiate geyser. As the denominators of these dimensionless parameters are either predetermined from the geometry of liquid filled levels, as shown in Table 1, or can be deduced from the corresponding calculations associated with the geyser initiation gravity levels, one can predict the values of these flow parameters. Present study can greatly enhance our understanding in the behaviors of cryogenic fluid resettlement under reduced gravity environment. This is particularly important for liquid acquisition technique to be used in on-orbit spacecraft design.

Any fluid capable of motion relative to the spacecraft will be subject to an acceleration relative to the mass center of the spacecraft that arises from the gravity gradient of the Earth[14,15]. In addition to the Earth's gravitational force, the interaction between the particle mass of fluids and the spacecraft mass due to gravity gradient acceleration[14] have also been taken into consideration in this microgravity fluid management study.

To conclude, we have demonstrated that, the computer algorithm presented, can be used to simulate fluid behavior in a microgravity environment, in particular the development of technology necessary for acquisition or positioning of liquid and vapor within a tank to enable liquid outflow or vapor venting through active liquid acquisition by the creation of a positive acceleration environment

resulting from propulsive thrust. Better understanding of the full pictures of flow fields in both constant and impulsive thrusts, during the course of fluid reorientation can provide the proper design techniques for handling and managing the cryogenic liquid propellants to be used in on-orbit spacecraft propulsion. It is important to emphasize that impulsive reverse gravity thrust is superior to constant reverse gravity thrust for the activation of liquid necessary for the resettlement of liquid in a reduced gravity environement.

Acknowledgement

The authors appreciate the support recieved from the National Aeronautics and Space Administration Headquarters through the NASA Grant NAGW-812, and NASA Marshall Space Flight Center through the NASA Contract NAS8-36955/Delivery Order No. 69. The authors would like to acknowledge the great help recieved through discussions from Lee Jones, Leon Hastings, George Schmidt, and James Martin of Space Propulsion Branch of NASA Marshall Space Flight Center.

Reference

1. NASA Office of Aeronautics and Space Technology, Technology for Future NASA Missions: Civil Space Technology Initiative and Pathfinder, NASA CP-3016,National Aeronautics and Space Administration, Washington, D.C., 1988, pp. 568.

2. Leslie, F. W., "Measurements of Rotating Bubble Shapes in a Low Gravity Environment," Journal of Fluid Mechanics, Vol. 161, Dec. 1985, pp. 269-279.

3. Hung, R. J., and Leslie, F. W., "Bubble Shape in a Liquid Filled Rotating Container Under Low Gravity," Journal of Spacecraft and Rockets, Vol. 25, Jan.-Feb. 1988, pp. 70-74.

4. Hung, R. J., Tsao, Y.D., Hong, B. B., and Leslie, F. W., "Time Dependent Dynamical Behavior of Surface Tension on Rotating Fluids under Microgravity Environment," Advances in Space Research, Vol. 8, No. 12, 1988, pp. 205-213.

5. Hung, R. J., Tsao, Y. D., Hong, B. B., and Leslie, F. W., "Bubble Behaviors in a Slowly Rotating Helium Dewar in Gravity Probe-B Spacecraft Experiment," Journal of Spacecraft and Rockets, Vol. 26, May-June 1989, pp. 167-172.

6. Hung, R. J., Tsao, Y. D., Hong, B. B., and Leslie, F. W., "Dynamical Behavior of Surface Tension on Rotating Fluids in Low and Microgravity Environments," International Journal for Microgravity Research and Applications, Vol. 11, June 1989, pp. 81-95.

7. Hung, R. J., Tsao, Y. D., Hong, B. B., and Leslie F. W., "Axisymmetric Bubble Profiles in a Slwowly Rotating Helium

Dewar Under Low and Microgravity Environments," Acta Astronautica, Vol. 19, May 1989, pp. 411-426.

8. "Stanford Relativity Gyroscope Experiment (NASA Gravity Probe-B)," Proceedings of Society of Photo-Optical Instrumentation Engineers, Vol. 619, Society of Photo-Optical Instrumentation Engineers, Bellingham, WA, 1986, pp. 1-165.

9. Hung, R. J., and Shyu, K. L., "Cryogenic Liquid Hydrogen Reorientation Activated by Constant Reverse Gravity Acceleration of Geyser Initiation," AIAA Paper No. 90-3712, 1990.

10. Kamotani, Y., Prasad, A., and Ostrach, S., "Thermal Convection in an Enclosure Due to Vibrations Aboard a Spacecraft," AIAA Journal, Vol. 19, Apr. 1981, pp. 511-516.

11. Hung, R. J., Lee, C. C., and Shyu, K. L., "Reorientation of Rotating Fluid in Microgravity Environment with and without Gravity Jitters," Journal of Spacecraft and Rockets, Vol. 27, 1990, in press.

12. Hung, R. J., Lee, C. C., and Leslie, F. W. "Effects of G-Jitters on the Stability of Rotating Bubble Under Microgravity Environment," Acta Astronautica, Vol. 20, 1990, in press.

13. Hung, R. J., Lee, C. C. and Leslie F. W., "Response of Gravity Level Fluctuations on the Gravity Probe-B Spacecraft Propellant System," Journal of Propulsion and Power, Vol. 6, 1990, in press.

14. Misner, C. W., Thorne, K. S., and Wheeler, J. A., "Gravitation",

W. H. Freeman and Co., San Francisco, CA, 1973, pp. 1-1279.

15. Forward, R. L., "Flattening Space-Time Near the Earth, "Physical Review, Series D, Vol. 26, Aug. 1982, pp. 735-744.

TABLE 1 SOME BASIC GEOMETRYS AND CHARACTERISTICS
OF CRYOGENIC LIQUID HYDROGEN REORIENTATION

Liquid Filled Level (%)	30	50	65	70	80
Geyser Initiation Gravity-Level, $g_{io}(10^{-2}\ g_o)$	5.5	6.52	6.6	6.7	8.2
Geyser Initiation Acceleration, a_g (cm/s^2)	53.9	63.9	64.7	65.7	80.4
Average Liquid Height, $\bar{h}$ (cm)	2.67	2.05	1.52	1.35	0.93
Average Free Fall Flow Velocity, $\bar{V}_f$ (cm/s)	17.0	16.2	14.0	13.3	12.5
Maximum Liquid Height, h_m (cm)	3.41	2.79	2.26	2.09	1.67
Free Fall Velocity from Maximum Liquid Height V_{fm} (cm/s)	19.2	18.9	17.1	16.6	16.4

Table 2 CHARACTERISTICS OF CRYOGENIC HYDROGEN REORIENTATION
(Frequency of Impulsive Acceleration = 0.1 Hz)

Liquid Filled Level (%)	30	50	65	70	80
Maximum Flow Velocity, V_m (cm/s)	85.3	83.6	72.8	69.8	64.0
$V_m/\bar{V}_f$	5.0	5.1	5.2	5.2	5.1
Liquid Reaching Bottom Time, t_R (s)	0.36	0.30	0.27	0.23	0.19
$t_R/\bar{t}_f$	1.1	1.2	1.2	1.1	1.2
Time for Observing Maximum Velocity, t_m (s)	0.39	0.31	0.26	0.24	0.18
Scale Length of Maximum Flow Velocity L_m (= $V_m t_m$) (cm)	33.2	25.9	18.9	16.7	11.5
$L_m/\bar{h}$	12.4	12.6	12.4	12.3	12.3
$t_m/\bar{t}_f$	1.2	1.2	1.3	1.2	1.2
Scale Flow Acceleration Associated with Maximum Velocity, a_m (=$V_m t_m$) (cm/s^2)	218	269	280	290	355
a_m/a_g	4.1	4.2	4.3	4.4	4.4
V_m/V_{fm}	4.4	4.4	4.3	4.2	4.0

Figure Captions

Figure 1. (A) Distribution of grid points in the radial-axial plane of cylindrical coordinate for propellant tank, and (B) Model size propellant tank adopted for numerical simulation with geometrical description.

Figure 2. Selected sequences of time evolution of fluid reorientation with liquid filled level of 30% for impulsive acceleration with frequency of 0.1 Hz, (A) initial profile, (B) flow profile before the initiation of geyser, (C) flow profile with geyser, and (D) flow profile after the ending of geyser.

Figure 3. Selected sequences of time evolution of fluid reorientation with liquid filled level of 50% for impulsive acceleration with frequency of 0.1 Hz, (A) initial profile, (B) flow profile before the initiation of geyser, (C) flow profile with geyser, and (D) flow profile after the ending of geyser.

Figure 4. Selected sequences of time evolution of fluid reorientation with liquid filled level of 65% for impulsive acceleration with frequency of 0.1 Hz, (A) initial profile, (B) flow profile before the initiation of geyser, (C) flow profile with geyser, and (D) flow profile after the ending of geyser.

Figure 5. Selected sequences of time evolution of fluid reorientation with liquid filled level of 70% for impulsive acceleration with frequency of 0.1 Hz, (A)

initial profile, (B) flow profile before the initiation of geyser, (C) flow profile with geyser, and (D) flow profile after the ending of geyser.

Figure 6. Selected sequences of time evolution of fluid reorientation with liquid filled levels of 80% for impulsive acceleration with frequency of 0.1 Hz, (A) initial profile, (B) flow profile before the initiation of geyser, (C) flow profile with geyser, and (D) flow profile after the ending of geyser.

Figure 7. (A) Ratio of $V_m/\bar{V}_f$ and its associated parameters in terms of liquid filled levels, (B) Ratio of $t_R/\bar{t}_f$ and its associated parameters in terms of liquid filled levels.

Figure 8. (A) Ratio of $t_m/\bar{t}_f$ and its associated parameters in terms of liquid filled levels, (B) Ratio of a_m/a_g and its associated parameters in terms of liquid filled levels.

Figure 9. (A) Ratio of $L_m/\bar{h}$ and its associated parameters in terms of liquid filled levels, (B) Ratio of V_m/V_{fm} and its associated parameters in terms of liquid filled levels.

(A)

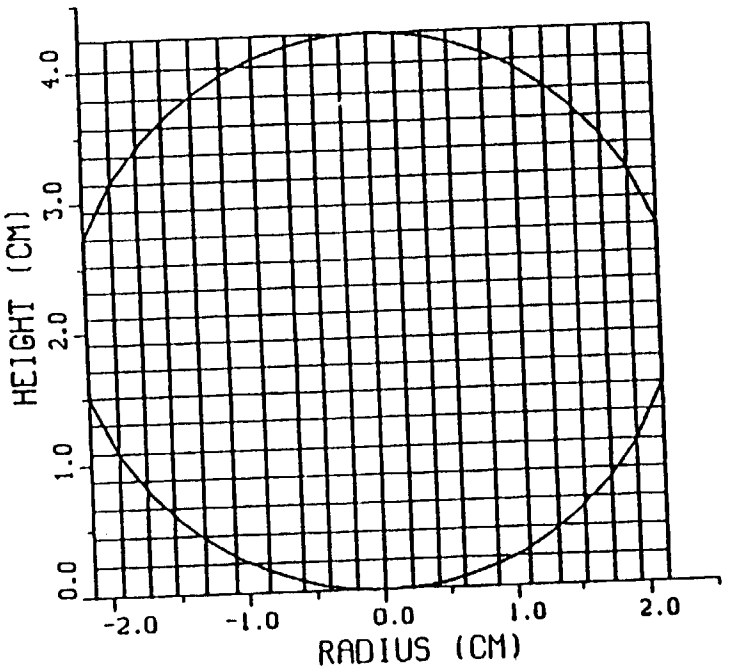

(B)

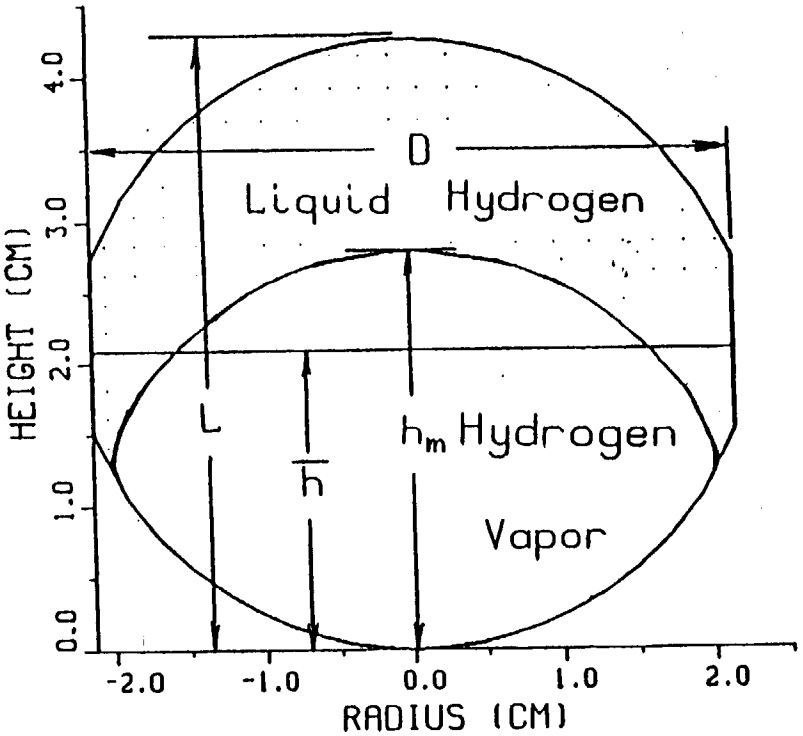

D-4.26720 CM, L-4.23672 CM

Fig 1

A. Liquid Hydrogen and Vapor
Liquid Filled=30% t= 0.00s
g=-5.50×10^{-2}g$_o$
f= 1.00×10^{-1}Hz

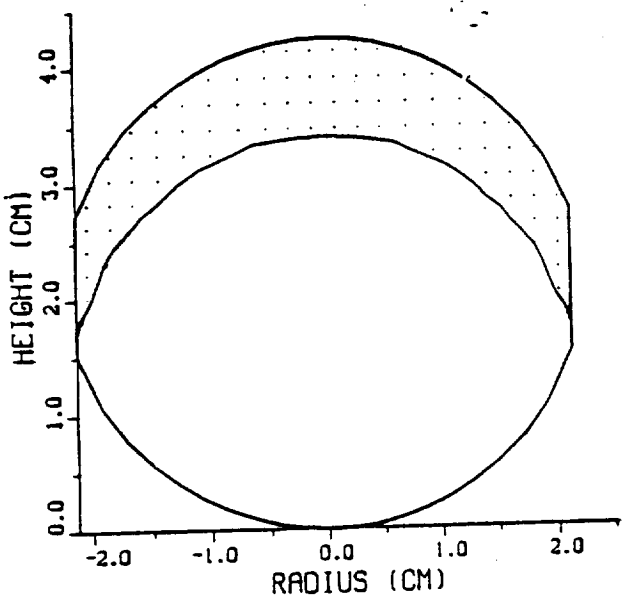

B. Liquid Hydrogen and Vapor
Liquid Filled=30% t= 2.40×10^{-1}s
g=-5.50×10^{-2}g$_o$
f= 1.00×10^{-1}Hz

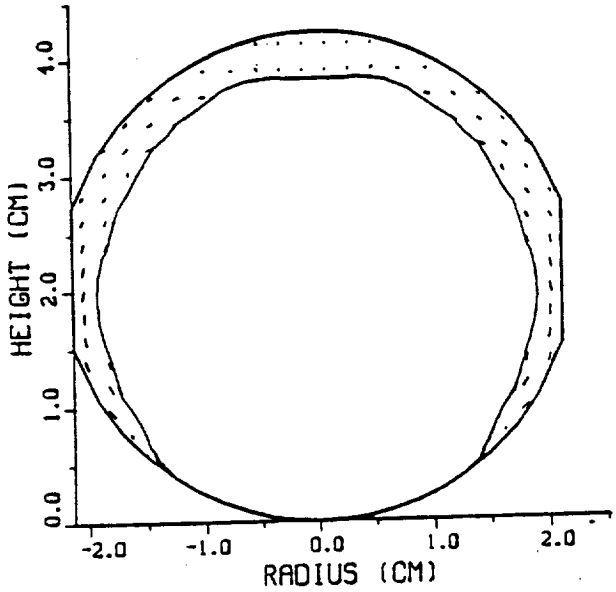

C. Liquid Hydrocen and Vapor
Liquid Filled=30% t= 5.27×10^{-1}s
g=-5.50×10^{-2}g$_o$
ω= 0.00rpm
f= 1.00×10^{-1}Hz

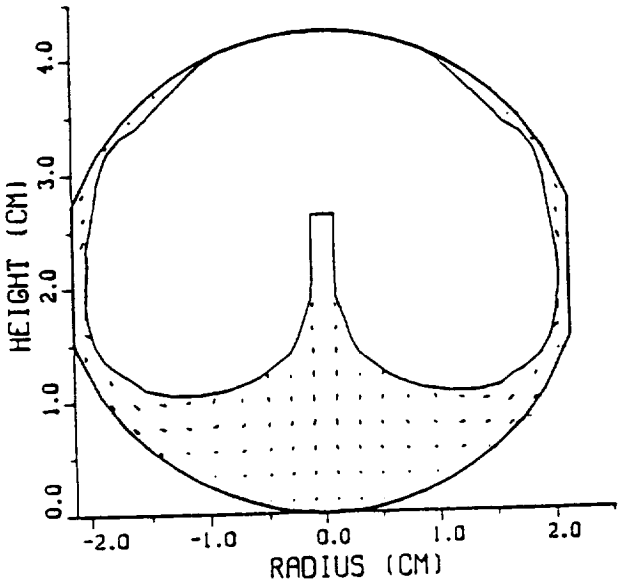

D. Liquid Hydrogen and Vapor
Liquid Filled=30% t= 8.27×10^{-1}s
g=-5.50×10^{-2}g$_o$
f= 1.00×10^{-1}Hz

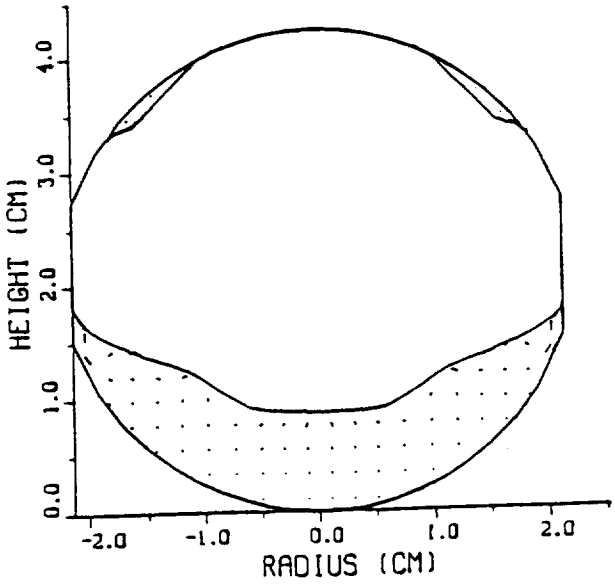

Fig 2

A. Liquid Hydrogen and Vapor
Liquid Filled=50% t= 0.00s
g=-6.52×10^{-2}g$_o$
f= 1.00×10^{-1}Hz

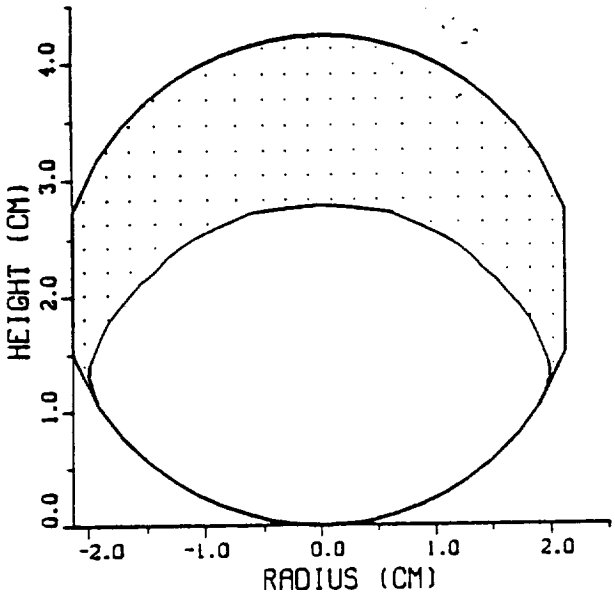

B. Liquid Hydrogen and Vapor
Liquid Filled=50% t= 2.40×10^{-1}s
g=-6.52×10^{-2}g$_o$
f= 1.00×10^{-1}Hz

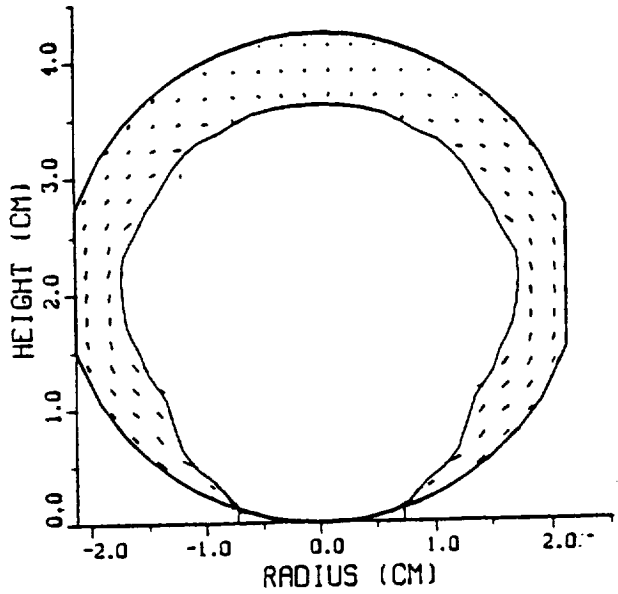

C. Liquid Hydrogen and Vapor
Liquid Filled=50% t= 4.58×10^{-1}s
g=-6.52×10^{-2}g$_o$
f= 1.00×10^{-1}Hz

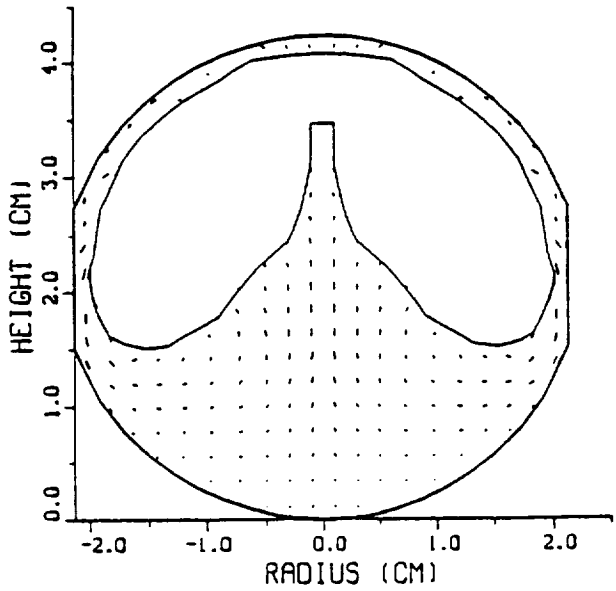

D. Liquid Hydrogen and Vapor
Liquid Filled=50% t= 1.90×10^{0}s
g=-6.52×10^{-2}g$_o$
f= 1.00×10^{-1}Hz

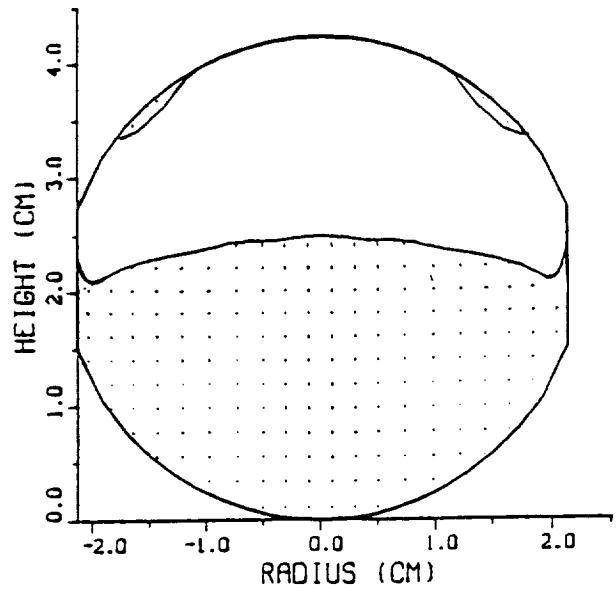

Fig 3

A. Liquid Hydrogen and Vapor
Liquid Filled-65% t= 0.00s
g=-6.60×10^{-2}g$_o$
f= 1.00×10^{-1}Hz

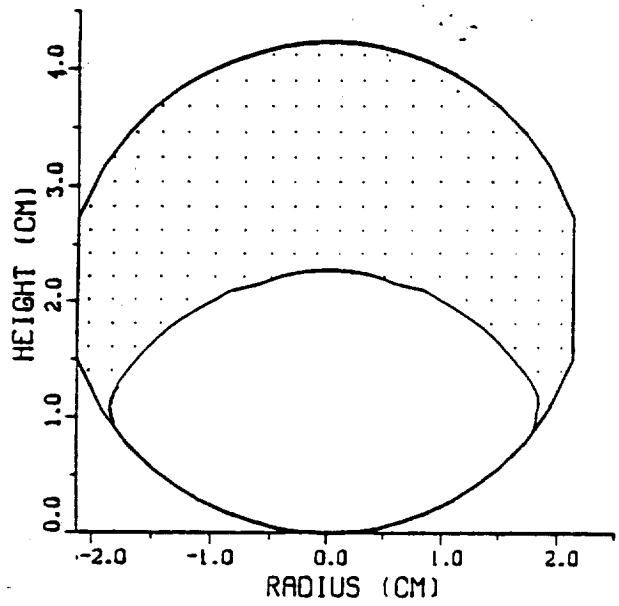

B. Liquid Hydrogen and Vapor
Liquid Filled-65% t= 2.40×10^{-1}s
g=-6.60×10^{-2}g$_o$
f= 1.00×10^{-1}Hz

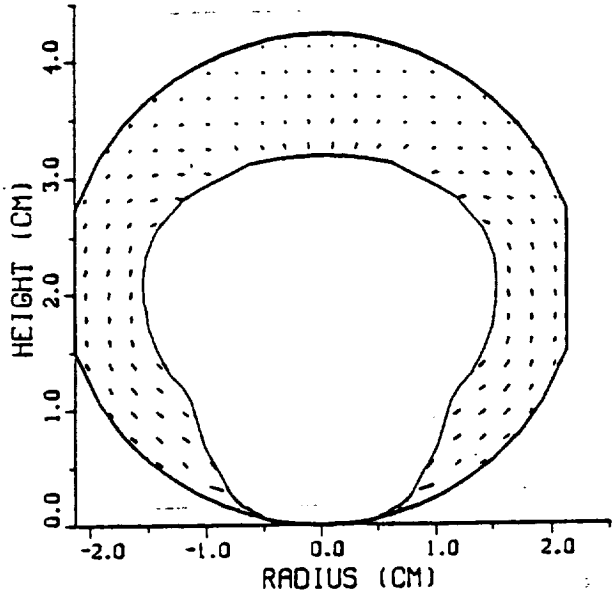

C. Liquid Hydrogen and Vapor
Liquid Filled-65% t= 3.90×10^{-1}s
g=-6.60×10^{-2}g$_o$
f= 1.00×10^{-1}Hz

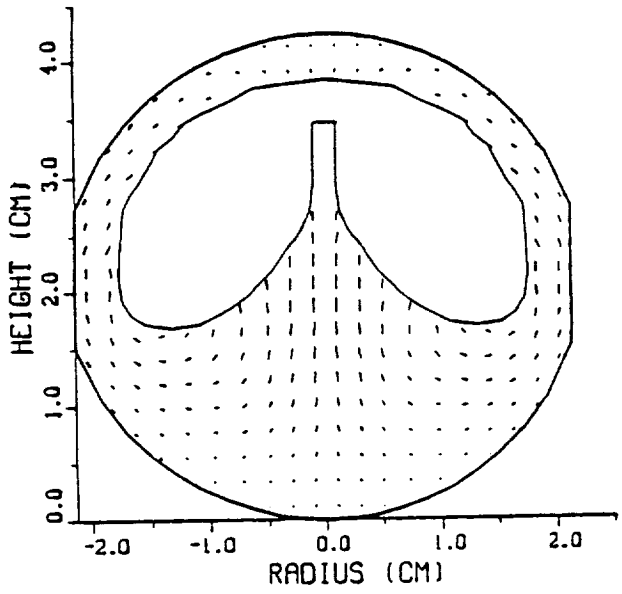

D. Liquid Hydrogen and Vapor
Liquid Filled-65% t= 7.50×10^{-1}s
g=-6.60×10^{-2}g$_o$
f= 1.00×10^{-1}Hz

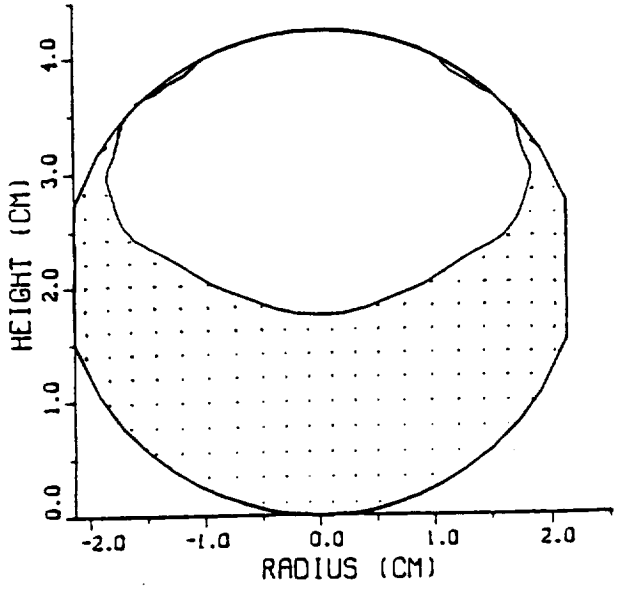

Fig 4

A. Liquid Hydrogen and Vapor
Liquid Filled-70% t= 0.00s
g=-7.00×10^{-2}g$_o$
f= 1.00×10^{-1}Hz

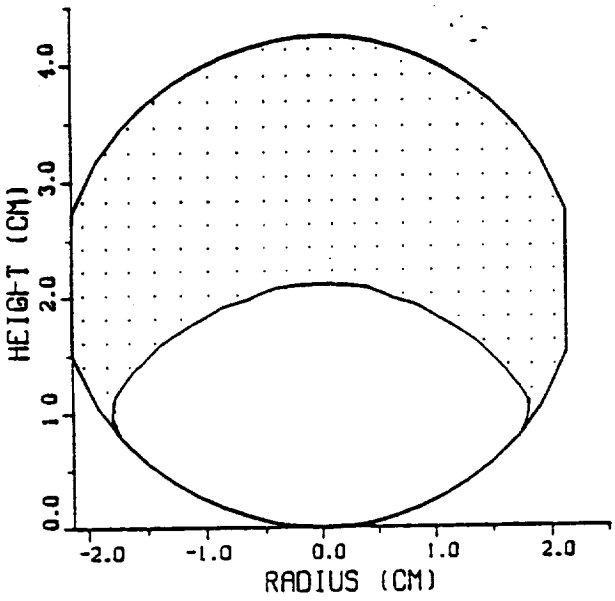

B. Liquid Hydrogen and Vapor
Liquid Filled-70% t= 1.80×10^{-1}s
g=-7.00×10^{-2}g$_o$
f= 1.00×10^{-1}Hz

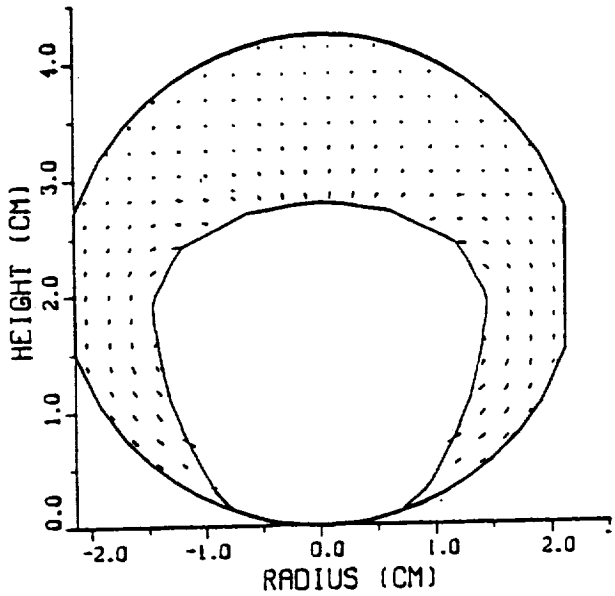

C. Liquid Hydroger and Vapor
Liquid Filled-70% t= 3.35×10^{-1}s
g=-7.00×10^{-2}g$_o$
f= 1.00×10^{-1}Hz

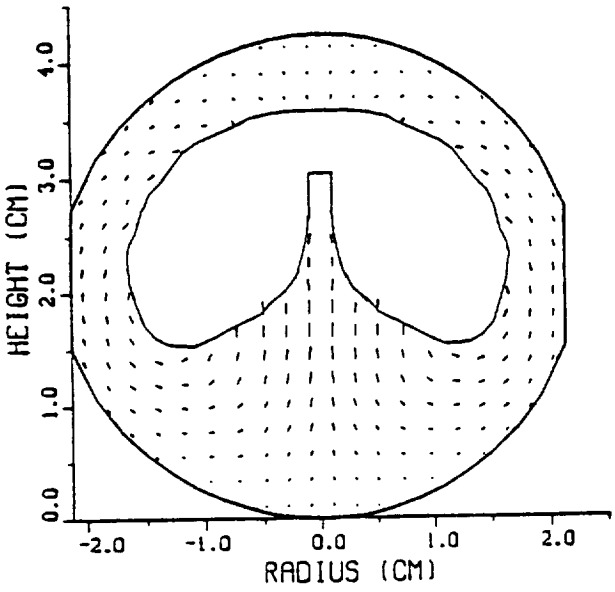

D. Liquid Hydrogen and Vapor
Liquid Filled-70% t= 8.75×10^{-1}s
g=-7.00×10^{-2}g$_o$
f= 1.00×10^{-1}Hz

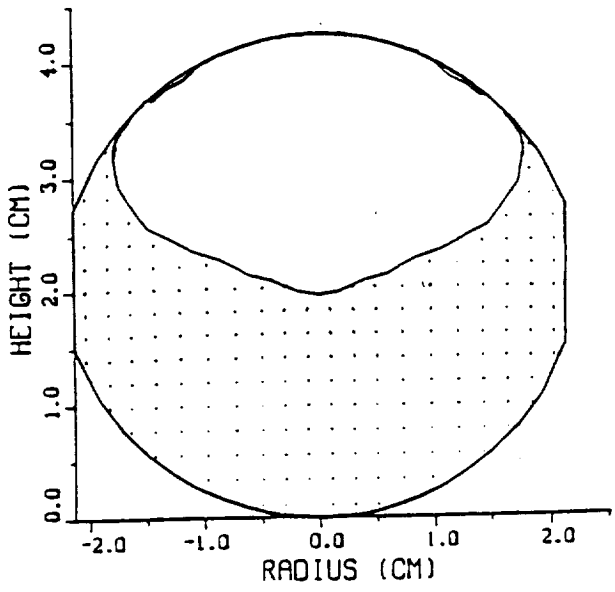

Fig 5

A. Liquid Hydrogen and Vapor
Liquid Filled-80% t= 0.00s
g=-8.20×10^{-2} g$_e$
f= 1.00×10^{-1} Hz

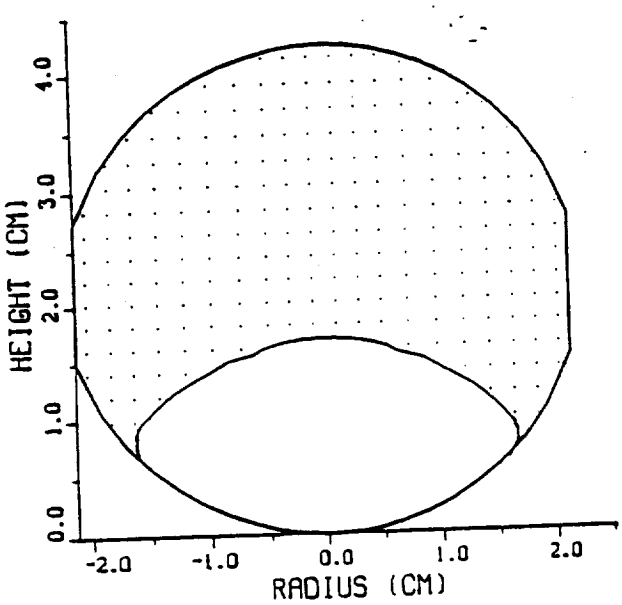

B. Liquid Hydrogen and Vapor
Liquid Filled-80% t= 1.80×10^{-1} s
g=-8.20×10^{-2} g$_e$
f= 1.00×10^{-1} Hz

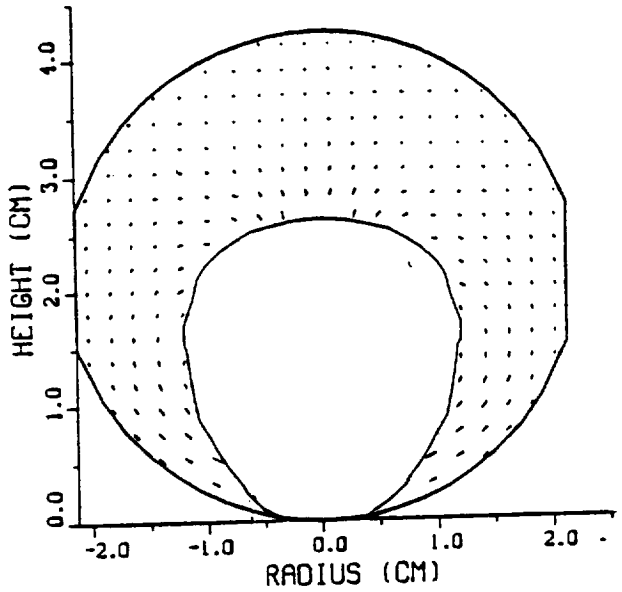

C. Liquid Hydrogen and Vapor
Liquid Filled-80% t= 3.32×10^{-1} s
g=-8.20×10^{-2} g$_e$
f= 1.00×10^{-1} Hz

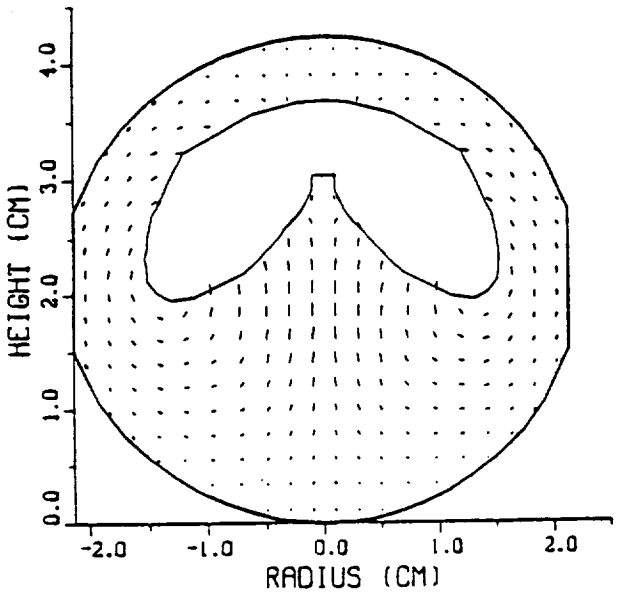

D. Liquid Hydrogen and Vapor
Liquid Filled-80% t= 6.92×10^{-1} s
g=-8.20×10^{-2} g$_e$
f= 1.00×10^{-1} Hz

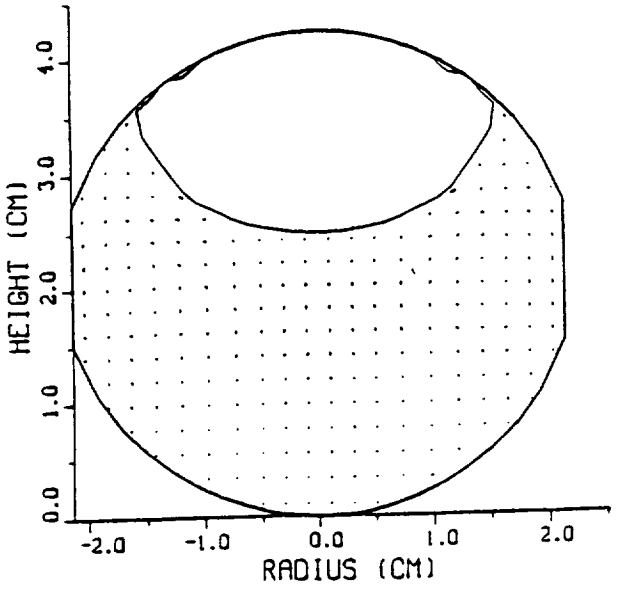

Fig 6

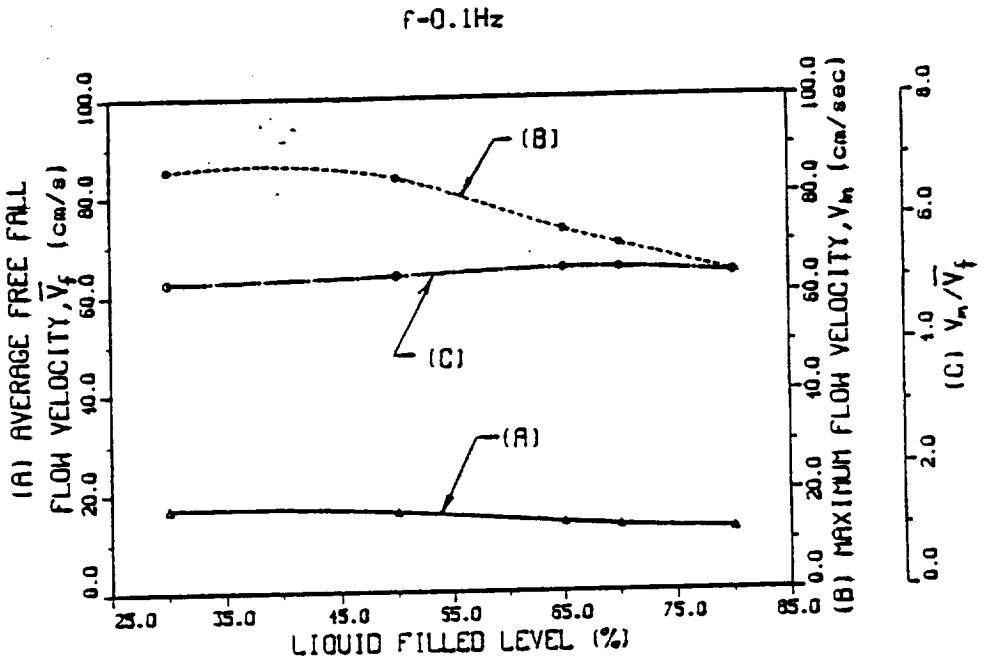
f-0.1Hz
(A) AVERAGE FREE FALL FLOW VELOCITY, $\bar{V}_f$ (cm/s)
(B) MAXIMUM FLOW VELOCITY, V_m (cm/sec)
(C) $V_m/\bar{V}_f$
(B)
(C)
(A)
LIQUID FILLED LEVEL (%)

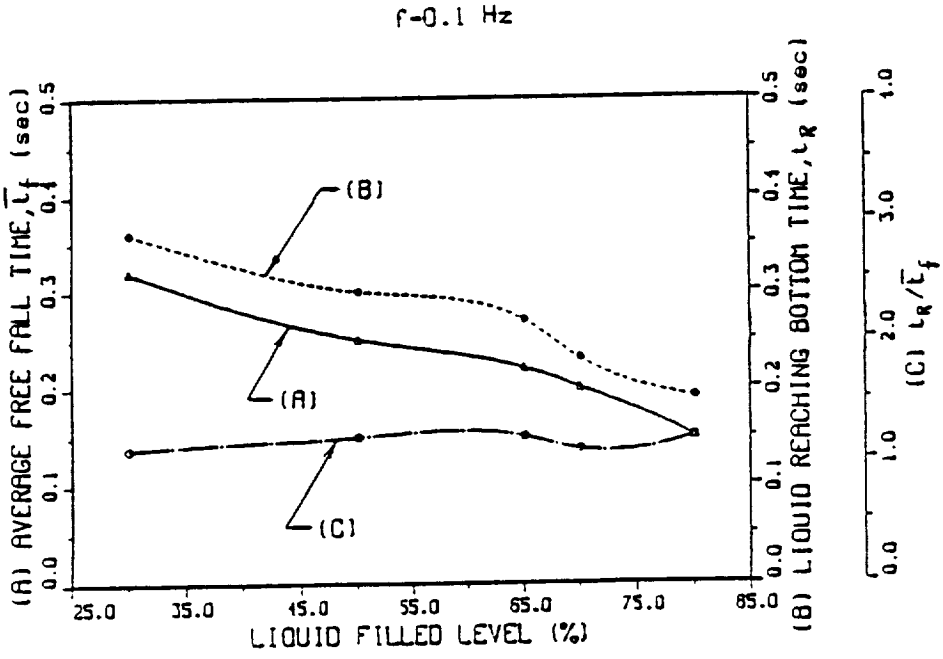
f-0.1 Hz
(A) AVERAGE FREE FALL TIME, $\bar{t}_f$ (sec)
(B) LIQUID REACHING BOTTOM TIME, t_R (sec)
(C) $t_R/\bar{t}_f$
(B)
(A)
(C)
LIQUID FILLED LEVEL (%)

Fig 7 (A,B)

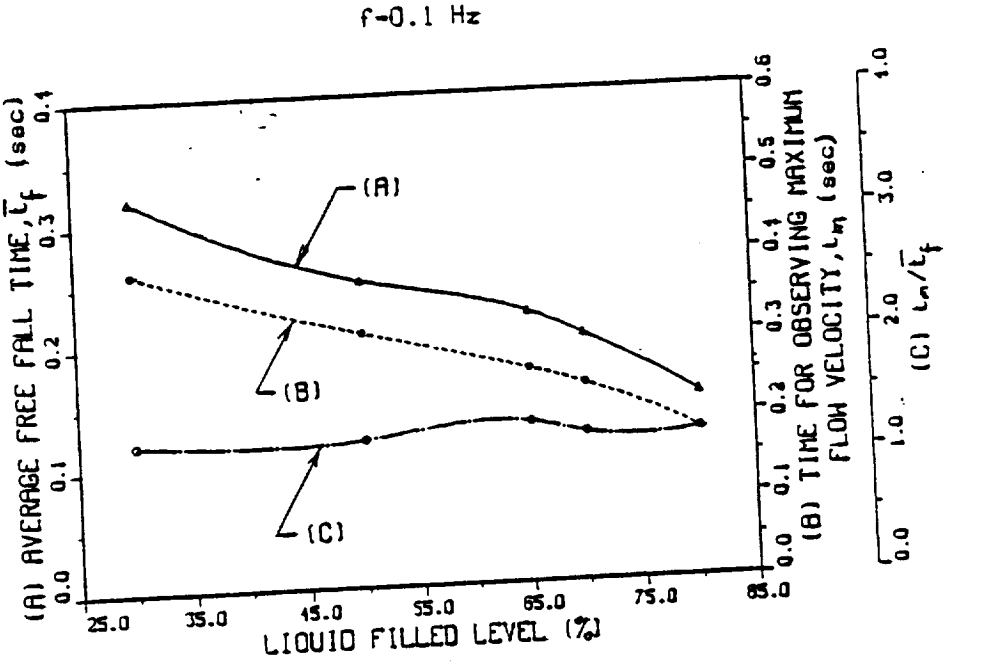
f=0.1 Hz
(A) AVERAGE FREE FALL TIME, $\bar{t}_f$ (sec)
(B) TIME FOR OBSERVING MAXIMUM FLOW VELOCITY, t_m (sec)
(C) $t_m/\bar{t}_f$
(A)
(B)
(C)
LIQUID FILLED LEVEL (%)

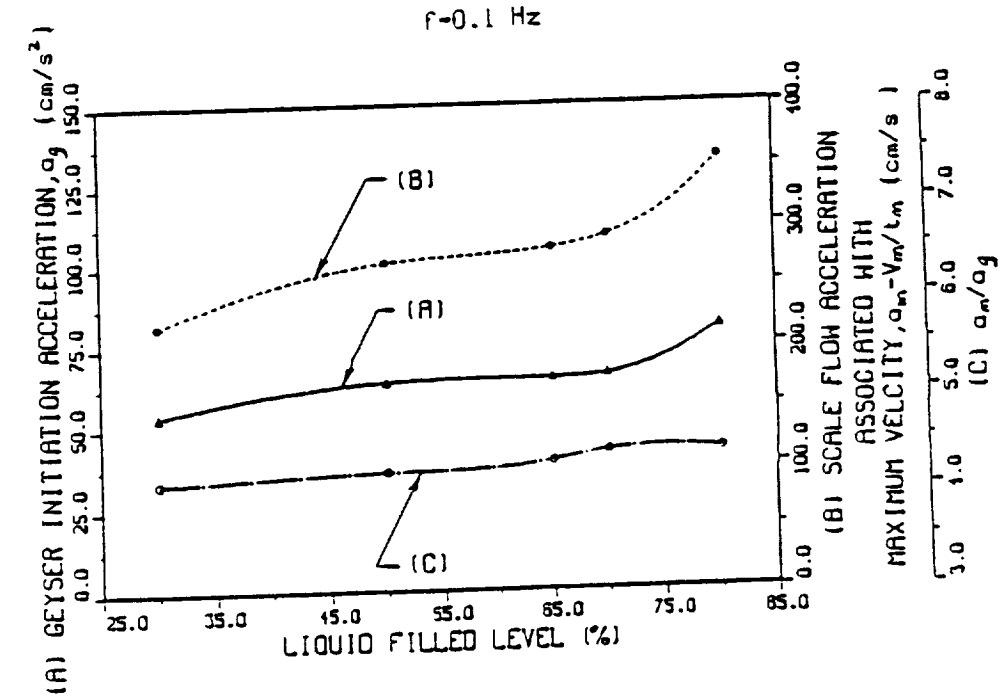
f=0.1 Hz
(A) GEYSER INITIATION ACCELERATION, a_g (cm/s²)
(B) SCALE FLOW ACCELERATION ASSOCIATED WITH MAXIMUM VELCITY, a_m-V_m/t_m (cm/s²)
(C) a_m/a_g
(B)
(A)
(C)
LIQUID FILLED LEVEL (%)

Fig 8 (A,B)

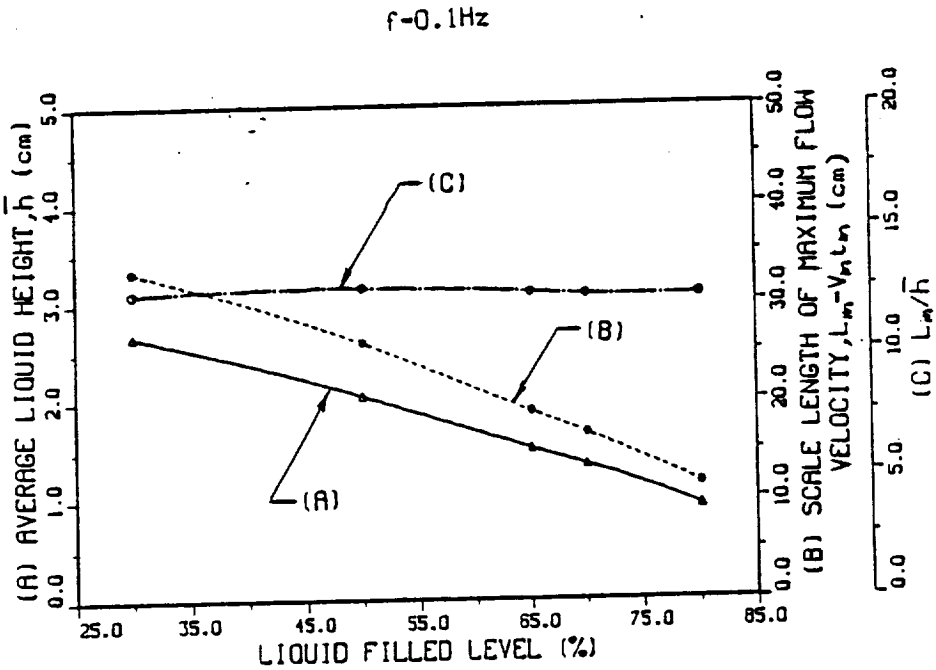
f-0.1Hz
(A) AVERAGE LIQUID HEIGHT, $\bar{h}$ (cm)
(B) SCALE LENGTH OF MAXIMUM FLOW VELOCITY, L_m-$V_m t_m$ (cm)
(C) $L_m/\bar{h}$
(A)
(B)
(C)
LIQUID FILLED LEVEL (%)
25.0
35.0
45.0
55.0
65.0
75.0
85.0

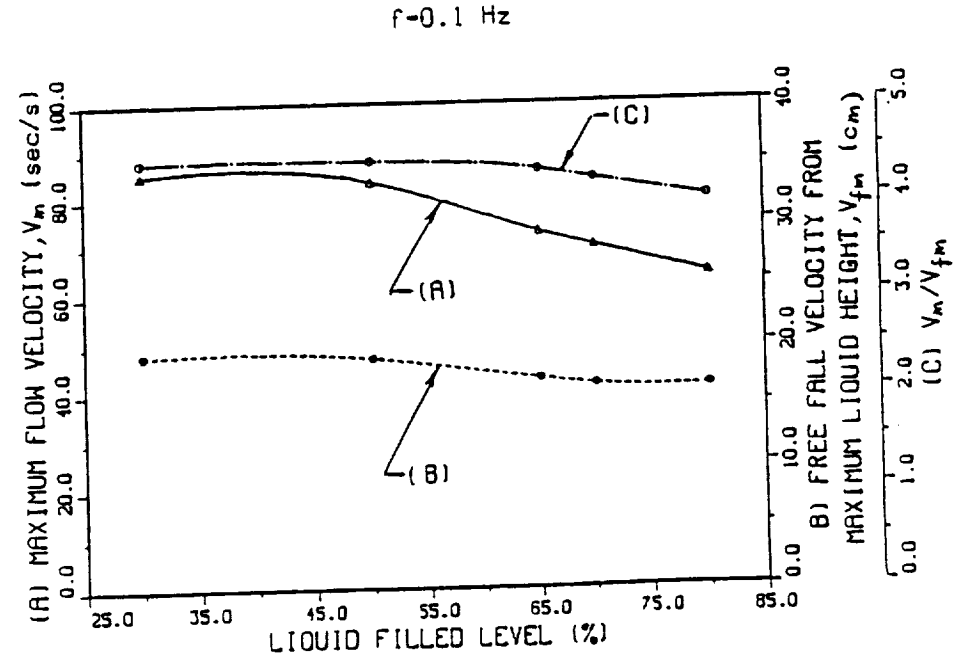
f-0.1 Hz
(A) MAXIMUM FLOW VELOCITY, V_m (sec/s)
B) FREE FALL VELOCITY FROM MAXIMUM LIQUID HEIGHT, V_{fm} (cm)
(C) V_m/V_{fm}
(A)
(B)
(C)
LIQUID FILLED LEVEL (%)
25.0
35.0
45.0
55.0
65.0
75.0
85.0

Fig 9 (A,B)

(G) Cryogenic Liquid Hydrogen Reorientation Activated by Medium Freuqency Impulsive Settling Acceleration of Geyser Initiation

ABSTRACT

The requirement to settle or to position liquid fluid over the outlet end of spacecraft propellant tank prior to main engine restart poses a microgravity fluid behavior problem. Resettlement or reorintation of liquid propellant can be accomplished by providing optimal acceleration to the spacecraft such that the propellant is reorientaed over the tank oulet without any vapor entrainment, any excessive geysering, or any other undesirable fluid motion for the space fluid management under microgravity environment. The purpose of present study is to investigate most efficient technique for propellant resettling through the minimization of propellant usage and weight penalties. Comparison between the constant reverse gravtiy acceleration and impulsive reverse gravity acceleration to be used for the activation of propellant resettlement, it shows that impulsive reverse gravity thrust is superior to constant reverse gravity thrust for liquid reorientation in a reduced gravity environment. Comparison among impulsive reverse gravity thrust with 0.1, 1.0 and 10 Hz frequencies for liquid filled level in the range between 30 to 80 %, it shows that the selection of 1.0 Hz frequency impulsive thrust over the other frequency ranges of impulsive thrust is most proper based on the present study.

Nomenclature

a_g = geyser initiation acceleration (cm/s^2)

a_m = scale flow acceleration associated with maximum velocity (cm/s^2), defined by Equation (5)

D = diameter of propellant tank (cm)

f = frequency of impulsive thrust (H_z)

g_i = impulsive reverse gravity acceleration, defined by Equation (6)

g_{io} = geyser initiation gravity-level (g_0)

g_0 = normal Earth gravitational acceleration = 9.81 m/s^2

$\bar{h}$ = average liquid height (cm)

h_m = maximum liquid height (cm)

L = height of propellant tank (cm)

L_m = scale length of maximum liquid height (cm/s), defined by Equation (4)

STV = Space Transfer Vehicle

$\bar{t}_f$ = average free fall time (s)

t_m = time for observing maximum flow velocity (s)

t_R = liquid reaching tank bottom time (s)

V_{fm} = free fall velocity from maximum liquid height (cm/s), defined by Equation (3)

$\bar{V}_f$ = average free fall velocity (cm/s), defined by Equation (2)

V_m = maximum flow velocity (cm/s)

I. Introduction

In spacecraft design, the requirements for a settled propellant are different for tank pressurization, engine restart, venting, or propellant transfer. Prepressurization requires that heat and mass transfer effects be minimized; otherwise, a process of chill down of tank, venting of noncondensing gases, etc., may have to carry out for the cryogenic system. For engine restart, it is necessary to have the liquid settle with no bubbles near the tank outlet so that the initial flow of propellant will not carry vapor to the pump or engine. The slosh wave amplitude should be relatively low to keep the center of mass shifts within an acceptable range and wave motion low enough to avoid pressure collapse caused by interface agitation . For venting, it is probably necessary that virtually all bubbles be displaced from the bulk liquid so that a two-phase mixture is not vented. Propellant transfer requires that the liquid be completely settled with virtually no bubbles. Outflow of a liquid near the tank outlet can result in the prematrue ingestion of gas while a signigicant amount of liquid is still in the tank under microgravity environment. This phenomenon is termed "suction dip". Slosh wave motion must be minimal because the combination of "suction dip" and sloshing could cause gas pull-through to occur more readily in microgravity than if the surface were essentially quiescent.

During the prepressurization of a cryogenic propellant in microgravity, significant heat and mass transfer will occur if the liquid interface is disturbed. Interface disturbances may result from (a) impingement of the gas on the liquid surface at a mass flow

rate sufficient to cause Kelvin-Helmholtz instability, (b) globule formation from breaking waves caused by wave motion over baffles or internal hardware, (c) globule and surface froth formation resulting from movement of bubbles through the liquid to the surface, and (d) surface froth formation because of gas impingement.

Bubble and globule formation as a result of liquid impact with the aft end of the tank could lead to propellant loss for the spacecraft during venting. Globules could be entrained in the vented ullage gas or bubbles rising through the liquid and expanding because of the decreasing tank pressure could cause a spray of globules to be vented. Liquid level rise, vent liquid loss, fluid freezing, and vehicle dynamics are all affected by the microgravity levels.

A key objective of the cryogenic fluid management of spacecraft propulsion system, such as a Space Transfer Vehicle[1] (STV), is to develop the technology necessary for acquisition or positioning of liquid and vapor within a tank in reduced gravity to enable liquid outflow or vapor venting. Liquid acquisition techniques can be divided into two general categories: (1) Active liquid acquisition by the creation of a positive acceleration environment resulting from the propulsive thrust of small auxiliary engines, and (2) Passive liquid acquisition utilizing the liquid capillary forces provided by using solid baffles of liquid traps made of fine mesh screen material. In this series of study, active liquid acquisition is aimed for numerically simulating the resettlement of cryogenic liquid hydrogen. Liquid hydrogen, which, in general, poses more severe technical challenges than liquid oxygen, is used as the test bed

working fluid in this study.

Recently Lesie[2] was able to measure and to numerically compute the bubble shapes at various ratios of centrifugal force to surface tension force in 2, 4 and 6.3 cm deep cylinders in the microgravity environment. The results showed excellent agreement between model computation and measurements. Hung and Leslie[3] extended Leslie's work[2] to rotating free surfaces influenced by gravity with higher rotating speeds when the bubble intersects with both the top and bottom walls of the cylinder. Hung et al.[4,5] further extended the work to include rotating speeds which resulted with bubbles intersecting and/or without intersecting the top, bottom and side walls of the cylinder.

An analysis of time-dependent dynamical behavior of surface tension on partially-filled rotating fluids in both low gravity and microgravity environments was carried out by numerically solving the Navier-Stokes equations subjected to the initial and the boundary conditions[4,6]. At the interface between the liquid and the gaseous fluids, both the kinematic surface boundary condition, and the interface stress conditions for components tangential and normal to the interface, were applied. The initial condition for the bubble profiles was adopted from steady-state formulations developed by Hung and Leslie[3], and Hung et al.[6] for rotating cylinder tank; and by Hung et al.[5,7] for the dewar-shaped container to be used in the Gravity Probe-B Spacecraft[8]. Some of the steady-state formulations of bubble shapes, in particular for bubbles intersecting at the top wall of the cylinder, were compared with the experiment carried out by

Leslie[2] in a free-fallinng aircraft (KC-135). Comparisons of time-dependent results between numerical computations and experiments were unavailable. This was because the calibration of the recordings of time-dependent gravity variations in a KC-135 aircraft during the short time periods of microgravity environment is very difficult. There was also an unavailability of accelerometer data for measuring the actual levels of microgravity during the experiment.

An efficient propellant settling technique should minimize propellant usage and weight penalties. This can be accomplished by providing optimal acceleration to the spacecraft such that the propellant is reoriented over the tank outlet without any vapor entrainment, any excessive geysering, or any other undesirable fluid motion.

Production of geyser during the propellant reorientation is not a desirable motion for the space fluid management. It is because geyser is always accompanied by the vapor entrainment and globule formation. Geyser is observed at reverse gravity thrust greater than certain critical values of acceleration during the course of liquid reorientation. In other words, geyser will not be observed at very low reverse gravity level, and it will be detected when the reverse gravity level is greater than the certain critical value. In this series of study, numerical simulation of positive liquid acquisition is attemted by introducing reverse gravity acceleration, resulting from the propulsive thrust of small auxiliary engines which exceeds the critical value for geyser initiation. The reverse gravity acceleration is starting with a small value and increases gradually

till the initiation of geyser is detected in the computer simulation for the liquid reorientation of propellant tank with various liquid-filled levels.

In this series of studies, time-dependent computations have been carried out to investigate the dynamical behavior of fluid reorientation or resettling of propellant prior to main engine firing for spacecraft restart at the net reverse gravity acceleration which is great enough to initiate geyser during the liquid reorientation. First paper of present study (Paper I)[9] investigates the characteristics of fluid resettlement due to the reversal of lowest constant reverse gravity acceleration which is great enough to initiate geyser without any impulsive acceleration. The frequency of impulsive acceleration is generally termed "gravity jitters". Gravity jitters are produced by spacecraft attitude motion, machinery (turbine, pump, engine) vibrations, thruster firing, thruster shutdown, impulsive engine acceleration, etc.[10] Positioning of liquid propellant over the tank outlet can be carried out by using small auxiliary thrusters which provide a thrust parallel to the tank's major axis in the direction of flight.

Computer simulation of flow field based on Paper I[9] during the course of fluid reorientation induced by constant reverse gravity acceleration show that six dimensionless parameters are abtained in the study. These parameters hold near constant values through the entire ranges of liquid filled levels during the course of fluid reorientation activated by the reverse gravity acceleration great enough to initiate geyser. As the denominators of these

dimensionless parameters are either predetermined from the geometry of liquid filled levels or can be deduced from the corresponding calculations associated with the geyser initiation gravity levels. One can predict the values of these flow parameters. These predictable parameters include maximum flow velocity V_m, time for observing maximum flow velocity t_m, time for reorienting liquid flowing down and reaching the bottom of propellant tank t_R, scale length of maximum flow velocity L_m, and scale flow acceleration associated with maximum velocity a_m.

Instead of applying constant reverse gravity acceleration as we described in Paper I[9], this paper adopts impulsive reverse gravity acceleration with a medium frequency of 1.0 Hz for the activation of fluid reorientation with liquid filled levels of 30, 50, 65, 70 and 80%.

II. Numerical Simulation of Liquid Hydrogen Reorientation with Geyser Initiation at Medium Frequency Impulsive Reverse Gravity Acceleration of 1.0 Hz

The present study examines time-dependent fluid behaviors, in particular the dynamics of liquid hydrogen and hydrogen vapor reorientation induced by reverse gravity acceleration which is great enough to introduce geyser initiation. As in Paper I[9], time-dependent axial symmetry mathematical formulation are adopted. Detailed description of mathematical formulation, initial and boundary conditions suitable for the analysis of cryogenic fluid

management under microgravity environment are given in our earlier studies.[4,6,11-13] The initial profiles of liquid-vapor interface are determined from computations based on algorithms developed for the steady state formulation of microgravity fluid management.[3-7]

Detailed description of computational algorithm applicable to microgravity fluid management are illustrated in Paper I[9] and our earlier studies.[4,6,11-13] As we have indicated in Paper I[9], for the purpose of facilitating easy comparison between computational resuslts and experimental measurement, a model of 0.01 size prototype is adopted in the computer simulation. Model size is height L = 4.23672 cm and diameter D = 4.2672 cm. If the spacecraft had been coasting for a long time, aligned with its direction of motion, the most signigicant force, drag, would be axial and with acceleration of $10^{-4}g_0$ along upward direction. The hydrogen vapor is, thus, originally positioned at the bottom of the tank. The requirement to settle or to position liquid fuel over the outlet end of the spacecraft propellant tank prior to main engine restart poses a microgravity fluid behavior problem.[11] Retromaneuvers of spacecraft, such as STV, require settling or reorientation of the propellant prior to main engine firing.[1,11] Cryogenic liquid propellant shall be positioned over the tank outlet by using auxiliary thrusters (or idle-mode thrusters from the main engine) which provide a thrust parallel to the tank's major axis in the direction of flight. Similar to Paper I[9], a small value of reverse gravity acceleration (downward direction) is provided by the propulsive thrust of small auxiliary engine to initiate the reorientation of liquid propellant. This small value of

reverse gravity acceleration of propulsive thrust increases gradually till reaching the critical value on which initiation of geyser is detected during the time period of fluid resettlement. We term this reverse gravity acceleration of propulsive thrust, which is capable to initiate geyser, as "geyser initiation gravity-level". This geyser initiation gravity level has been investigated through the method of trial and error for the various liquid-filled levels as a base to simulate impulsive reverse gravity acceleration with frequencies of 0.1, 1.0 and 10 Hz. As we have indicated in Paper I[9], cryogenic liquid hydrogen at temperature of 20K is considered. Hydrogen density of 0.071 g/cm^3; surface tension coefficient at the interface between liquid hydrogen and hydrogen vapor of 1.9 dyne/cm; hydrogen viscosity coefficient of 1.873×10^{-3} cm^2/s; and contact angle of 0.5^0 are used in the computer simulation.

In this paper, among three categories of impulsive reverse gravity acceleration with frequencies of 0.1, 1.0 and 10 Hz, reorientation of cryogenic liquid hydrogen activated by geyser initiation impulsive reverse gravity acceleration with a frequency of 1.0 Hz produced by propulsive thrust will be investigated for various liquid filled levels of propellant tank. Paper I shows that these geyser initiation gravity levels are 5.5×10^{-2}, 6.52×10^{-2}, 6.6×10^{-2}, 6.7×10^{-2} and $8.2 \times 10^{-2} g_0$ for liquid filled levels of 30, 50, 65, 70, and 80%, respectively.

Table 1 shows some basic geometrys and characteristics of cryogenic liquid hydrogen resettlement activated by reverse gravity acceleration at geyser initiation gravity level. Average liquid

height $\bar{h}$, and maximum liquid height h_m are shown in Figure 1. Average free fall velocity $\bar{V}_f$, average free fall time $\bar{t}_f$, and free fall velocity from maximum liquid height V_{fm} are computed from the following equations:

$$\bar{V}_f = (2g_{io}\bar{h})^{1/2} \qquad (1)$$

$$\bar{t}_f = \left(\frac{2\bar{h}}{g_{io}}\right)^{1/2} \qquad (2)$$

$$V_{fm} = (2g_{io}h_m)^{1/2} \qquad (3)$$

where g_{io} denotes geyser initiation reverse gravity acceleration.

To show examples of the selected sequences of time evolution of fluid reorientation for cryogenic hydrogen, Figures 2, 3, 4, 5, and 6 show time evolution of fluid reorientation activated by geyser initiation impulse reverse gravity acceleration with a frequency of 1.0 Hz for liquid filled levels of 30, 50, 65, 70 and 80 %, respectively. Each figure contains four sub-figures. Subfigure (A) is initial profile of liquid-vapor interface at the moment of the starting of fluid reorientation at time t = 0; subfigure (B), the flow profile during the course of fluid reorientation before the initiation of geysering motion; subfigure (C), the flow profile with geysering motion; and subfigure (D), the flow profile after the ending of geysering motion.

Examples of selected sequences of time evolution of fluid reorientation illustrate following flow behaviors: (1) The liquid starts to flow in an annular sheet along the solid wall of tank and gradually pushes the vapor toward the central portion of the lower dome of tank as the net acceleration, reversing the direction of

gravity field, which is applied toward the downward direction of the tank's major axis, by using small auxiliary thrusters; (2) As the downward fluid annular sheet along the tank wall reaches the central bottom dome side of the tank, a geysering flow is observed; and (3) The vapor is thus pushed upward centrally into the liquid and the geysering disappears.

Based on the computer simulation of flow field values of maximum flow velocity V_m, time for observing maximum flow velocity t_m, and time for reorienting liquid flowing down and reaching the bottom of propellant tank t_R, are obtained and illustrated in Table 2 for reverse gravity acceleration with impulsive frequency of 1.0 Hz. Scale length of maximum flow velocity L_m, and scale flow acceleration associated with maximum velocity a_m, can be computed from the following parameters:

$$L_m = V_m t_m \tag{4}$$

$$a_m = \frac{V_m}{t_m} \tag{5}$$

Following dimensionless parameters are introduced: $V_m/\bar{V}_f$, $t_R/\bar{t}_f$, $t_m/\bar{t}_f$, a_m/a_g, $L_m/\bar{h}$ and V_m/V_{fm} where a_g stands geyser initiation acceleration (cm/s^2) for corresponding geyser initiation gravity level g_{io}. Impulsive reverse gravity acceleration, g_i with frequency f Hz is defined as follows:

$$g_i = g_{io}\left(1 + \frac{1}{2}\sin 2\pi ft\right) \tag{6}$$

Figures 7 to 9 show the variations of dimensionless parameters in terms of liquid filled levels for impulsive acceleration with

frequency of 1.0 Hz. Denominators of these six dimensionless parameters are either predetermined from the geometry of liquid fill levels or can be deduced from the corresponding calculations associated with the geyser initiation gravity levels. Characteristics of these near constant values dimensionless parameters can provide a good understanding of the physics of microgravity fluid behaviors, in particular the active category of liquid acquisition or positioning, and also the design criteria of on-orbit spacecraft propulsion system at the critical value of reverse gravity acceleration of propulsive thrust which is capable to initiate geyser.

An efficient propellant settling technique should minimize propellant usage and weight penalties. This can be accomplished by providing optimal acceleration to the spacecraft such that the propellant is reoriented over the tank outlet without any vapor entrainment, any excessive geysering, or any other undesirable fluid motion. In particular, it is important to study how well the impulsive acceleration can provide higher efficient propellant settling technique than the constant acceleration thrust technique. Also, what is the most optimal choice of impulsive frequency which can achieve the best fluid acquisition management being the goal of our research.

Figure 7(A) shows the ratio of maximum flow velocity to average free fall flow velocity $V_m/\bar{V}_f$ and its associated parameters of V_m and $\bar{V}_f$ in terms of liquid filled levels for impulsive acceleration with frequency of 1.0 Hz. It shows that the ratio of $V_m/\bar{V}_f$ varies in the

range of 6.6 to 6.7 in the entire liquid filled levels while V_m and $\bar{V}_f$ vary from 82.5 to 112.2 cm/s (decreasing with increasing liquid filled levels) and from 12.5 to 17.0 cm/s (also decreasing with increasing liquid filled levels), respectively. As $\bar{V}_f$ can be predetermined from geyser initiation gravity level and average liquid height, shown in Equation (1), one can make an approximate prediction of maximum flow velocity during the liquid reorientation for the various liquid filled levels. In comparison between impulsive acceleration with frequency of 1.0 Hz and with frequencies of 0.1 and 10 Hz, it shows that the former case of thrust can activate higher maximum flow velocity ($V_m/\bar{V}_f$ = 6.6 to 6.7) than that of the latter two cases of thrust accelerations ($V_m/\bar{V}_f$ = 5.0 to 5.2 for f= 0.1 Hz; and = 5.1 to 5.3 for f = 10 Hz).

Figure 7(B) shows the ratio of liquid reaching bottome time to average free fall time $t_R/\bar{t}_f$ and its associated parameters of t_R and $\bar{t}_f$ in terms of liquid filled levels for impulsive acceleration with frequency of 1.0 Hz. It shows that the ratio of $t_R/\bar{t}_f$ varies in the range of 1.1 to 1.2 in the entire liquid filled levels while t_R and $\bar{t}_f$ vary from 0.19 to 0.35 s (decreasing with increasing liquid filled levels), respectively. As $\bar{t}_f$ can be predetermined from geyser initiation gravity level and average liquid height, shown in Equation (2), one can predict the time for reorienting liquid fluid flowing down from the original position and reaching the bottom of propellant tank for the various liquid filled levels at the reverse gravity acceleration capable for the initiation of geyser. In comparison between impulsive acceleration with frequency of 1.0 Hz and with

frequencies of 0.1 and 10 Hz, it shows that the former case of thrust can activate the flow which takes slightly shorter time period for flow to reach the tank bottom (t_R = 0.19 to 0.35 s) than that of the latter two cases of acceleration (t_R = 0.19 to 0.36 s for f = 0.1 Hz; and = 0.18 to 0.37 s for f =10 Hz).

Figure 8(A) shows the ratio of time for observing maximum flow velocity to average free fall time $t_m/\bar{t}_f$ and its associated parameters of t_m and $\bar{t}_f$ in terms of liquid filled levels. It shows that the ratio of $t_m/\bar{t}_f$ varies in the range of 1.1 to 1.2 in the entire liquid filled levels while t_m and $\bar{t}_f$ vary from 0.18 to 0.35 s (decreasing with increasing liquid filled levels) and from 0.15 to 0.32 s (also decreasing with increasing liquid filled levels), respectively. As we indicated in Figure 7(B), $\bar{t}_f$ can be predetermined, one can predict the time for observing maximum flow velocity for various liquid filled levels at the reverse gravity acceleration capable for the initiation of geyser. In comparison between impulsive acceleration with frequency of 1.0 Hz and with frequencies of 0.1 and 10 Hz, it shows that the former case of thrust can produce higher maximum flow velocity with a slightly shorter period of time (t_m = 0.18 to 0.35 s) than that of the latter two cases of acceleration (t_m = 0.18 to 0.39 s for both f = 0.1 and 10 Hz).

Figure 8(B) shows the ratio of scale flow acceleration associated with maximum velocity to geyser initiation acceleration for corresponding geyser initiation gravity level a_m/a_g and its associated parameters of a_m and a_g in terms of liquid filled levels for impulsive aceeleration with frequency of 1.0 Hz. It shows that the

ratio of a_m/a_g varies in the range of 5.7 to 6.1 in the entire liquid filled levels while a_m and a_g vary from 320 to 458 cm/s^2 (increasing with increasing liquid filled levels) and from 53.9 to 80.4 cm/s^2 (also increasing with increasing liquid filled levels), respectively. As a_g can be predetermined from geyser initiation gravity level, one can make an approximate prediction of scale flow acceleration associated with maximum velocity, which is defined in Equation (5), at the reverse gravity acceleration capable for the initiation of geyser. In comparison between impulsive acceleration with frequency ot 1.0 Hz and with frequencies of 0.1 and 10 Hz, it shows that the former case of thrust can activate higher scale flow acceleration associated with maximum flow velocity (a_m/a_g = 5.7 to 6.1) than that of the latter two cases of acceleration (a_m/a_g = 4.1 to 4.4 for f= 0.1 Hz; and = 4.2 to 4.3 for f = 10 Hz).

Figure (9A) shows the ratio of scale length of maximum flow velocity to average liquid height $L_m/\bar{h}$ and its associated parameters of L_m and $\bar{h}$ in terms of liquid levels for impulsive acceleration with frequency of 1.0 Hz. It shows that the ratio of $L_m/\bar{h}$ varies in the range of 14.7 to 15.9 in the entire liquid filled levels while L_m and $\bar{h}$ vary from 14.8 to 39.3 cm (decreasing with increasing liquid filled levels) and from 0.93 to 2.67 cm (also decreasing with increasing liquid filled levels), respectively. As $\bar{h}$ can be predetermined from the geometry of liquid filled levels, one can make an approximate prediction of scale length of maximum flow velocity, which is defined in Equation (4), at the reverse gravity acceleration capable for the initiation of geyser. In comparison between impulsive acceleration

with frequency of 1.0 Hz and with frequencies of 0.1 and 10 Hz, it shows that the former case of thrust can activate larger scale length of maximum flow velocity ($L_m/\bar{h}$ = 14.7 to 15.9) than that of the latter two cases of acceleration ($L_m/\bar{h}$ = 12.3 to 12.6 for f = 0.1 Hz and = 12.1 to 13.1 for f = 10 Hz).

Figure 9(B) shows the ratio of maximum flow velocity to free fall velocity from maximum liquid height V_m/V_{fm} and its associated parameters of V_m and V_{fm} in terms of liquid filled levels for impulsive acceleration with frequency of 1.0 Hz. It shows that the ratio of V_m/V_{fm} varies in the range of 5.2 to 5.8 in the entire liquid filled levels while V_m and V_{fm} vary from 82.5 to 112.2 cm/s (decreasing with increasing liquid filled levels) and from 16.4 to 19.2 cm/s (also decreasing with increasing liquid filled levels), respectively. As V_{fm} can be predetermined from geyser initiation gravity level and maximum liquid height, shown in Equation (3), one can make an approximate prediction of maximum flow velocity at the reverse gravity acceleration capable for the initiation of geyser. In comparison between impulsive acceleration with frequency of 1.0 Hz and with frequencies of 0.1 and 10 Hz, it shows that the former case of thrust can activate higher maximum flow velocity (V_m/V_{fm} = 5.2 to 5.8) than that of the latter two cases of acceleration (V_m/V_{fm} = 4.0 to 4.4 for f = 0.1 Hz; and = 3.9 to 4.6 for f = 10 Hz).

As we have mentioned in Paper I[9], six dimensionless parameters presented in this study show that the parameters hold near constant values through the entire ranges of liquid filled levels during the course of reorientation of liquid hydrogen activated by the reverse

gravity acceleration with impulsive thrust frequency of 1.0 Hz, which is great enough to initiate geysering flow. As the purpose of present study is to investigate an efficient propellant settling technique which is able to minimize propellant usage and weight penalties, comparison of flow parameters between impulsive acceleration with frequency of 1.0 Hz and that of 0.1 and 10 Hzs have been made toward this objective. It shows that the operation of auxiliary engine with impulsive acceleration of 1.0 Hz frequency is better than that of 0.1 and 10 Hz frequency impulsive thrust acceleration in terms of introducing a higher maximum flow velocity, a shorter time period fo flow to reach maximum flow velocity, a shorter time period for flow to reach the tank bottom (tank outlet) for fluid resettling, a larger scale length of maximum flow velocity, and a higher flow acceleration associated with maximum flow velocity. It is shown that the impulsive acceleration with frequencies of 0.1 and 10 Hz can provide a higher efficient propellant resettling technique than that of the constant thrust acceleration based on same arguments mentioned earlier. It can be ranked in the order of efficienty that the impulsive acceleration with frequency of 1.0 Hz, followed by that with impulsive frequencies of 0.1 and 10 Hz which are about the same order, and then by constant thrust acceleration based on priority of selecting higher efficient propellant resettling technique.

IV. Discussion and Conclusions

The requirement to settle or to position liquid fluid over the outlet end of the spacecraft propellant tank prior to main engine restart poses a microgravity fluid behavior problem. Retromaneuvers

of spacecraft require settling or reorientation of the propellant prior to main engine firing. Cryogenic liquid propellant is positioned over the tank outlet by using small auxiliary thrusters (or idle-mode thrusters from the main engine) which provide a thrust parallel to the tank's major axis in the direction of flight.

The results of the study of fluid reorientation have to be evaluated in terms of how well they can be managed efficiently. An efficient propellant settling technique should minimize propellant usage and weight penalties through the operation of small thrusters (or idle-mode thrusters from the main engine). This can be accomplished by providing optimal acceleration to the spacecraft such that the propellant is reoriented over the tank outlet without any vapor entrainment, any excessive geysering, or any other undesirable fluid motion.

Production of geyser during the propellant reorientation is not a desirable motion for the space fluid management under microgravity environment. It is because geyser is always accompanied by the vapor entrainment and globule formation. Geyser is observed at reverse gravity acceleration greater than certain critical values of acceleration during the course of liquid reorientation. In this paper, numerical simulation of positive liquid acquisition is attempted by introducing reverse gravity acceleration, resulting from the propulsive thrust with impulsive frquencies of 0.1, 1.0 and 10 Hz auxiliary engines, which exceeds critical value for the initiation of geyser.

Evaluation of performance is based on how efficient the

impulsive reverse gravity with various frequencies can activate following flow parameters at the same background thrust accelerations: (A) a higher maximum flow velocity, (B) a shorter time period for flow to reach maximum velocity, (C) a shorter time period for flow to reach tank bottom (tank outlet) for fluid resettling, (D) a larger length scale of maximum flow velocity, and (E) a higher flow acceleration associated with maximum flow velocity. In summary, it is shown that impulsive reverse gravity with various frequencies is the most efficient choice for the reverse thrust to be operated at auxiliary engine for the purpose of fluid reorientation. Comparison between the results of present study for impulsive thrust with various frequencies and that of constant thrust, shown in Paper I[9], it shows that impulsive thrust, regardless of frequency range, is always superior than the constant reverse thrust in terms of efficient operation of fluid reorientation.

Based on the computer simulation of flow fields during the course of fluid reorientation, six dimensionless parameters are presented both in Paper I[9] and this study. It is shown that these parameters hold near constant values through the entire ranges of liquid filled levels during the course of fluid reorientation activated by the reverse gravity acceleration in both constant and impulsive thrusts great enough to initiate geyser. As the denominators of these dimensionless parameters are either predetermined from the geometry of liquid filled levels, as shown in Table 1, or can be deduced from the corresponding calculations associated with the geyser initiation gravity levels, one can predict

the values of these flow parameters. Present study can greatly enhance our understanding in the behaviors of cryogenic fluid resettlement under reduced gravity environment. This is particularly important for liquid acquisition technique to be used in on-orbit spacecraft design.

Any fluid capable of motion relative to the spacecraft will be subject to an acceleration relative to the mass center of the spacecraft that arises from the gravity gradient of the Earth[14,15]. In addition to the Earth's gravitational force, the interaction between the particle mass of fluids and the spacecraft mass due to gravity gradient acceleration[14] have also been taken into consideration in this microgravity fluid management study.

To conclude, we have demonstrated that, the computer algorithm presented, can be used to simulate fluid behavior in a microgravity environment, in particular the development of technology necessary for acquisition or positioning of liquid and vapor within a tank to enable liquid outflow or vapor venting through active liquid acquisition by the creation of a positive acceleration environment resulting from propulsive thrust. Better understanding of the full pictures of flow fields in both constant and impulsive thrusts, during the course of fluid reorientation can provide the proper design techniques for handling and managing the cryogenic liquid propellants to be used in on-orbit spacecraft propulsion. It is important to emphasize that impulsive reverse gravity thrust is superior to constant reverse gravity thrust for the activation of liquid necessary for the resettlement of liquid in a reduced gravity

environement. It is also worthwhile to mention that the selection of 1.0 Hz frequency impulsive thrust over the other frequency ranges is most proper based on the present study.

Acknowledgement

The authors appreciate the support recieved from the National Aeronautics and Space Administration Headquarters through the NASA Grant NAGW-812, and NASA Marshall Space Flight Center through the NASA Contract NAS8-36955/Delivery Order No. 69. The authors would like to acknowledge the great help recieved through discussions from Lee Jones, Leon Hastings, George Schmidt, and James Martin of Space Propulsion Branch of NASA Marshall Space Flight Center.

Reference

1. NASA Office of Aeronautics and Space Technology, Technology for Future NASA Missions: Civil Space Technology Initiative and Pathfinder, NASA CP-3016,National Aeronautics and Space Administration, Washington, D.C., 1988, pp. 568.

2. Leslie, F. W., "Measurements of Rotating Bubble Shapes in a Low Gravity Environment," Journal of Fluid Mechanics, Vol. 161, Dec. 1985, pp. 269-279.

3. Hung, R. J., and Leslie, F. W., "Bubble Shape in a Liquid Filled Rotating Container Under Low Gravity," Journal of Spacecraft and Rockets, Vol. 25, Jan.-Feb. 1988, pp. 70-74.

4. Hung, R. J., Tsao, Y.D., Hong, B. B., and Leslie, F. W., "Time Dependent Dynamical Behavior of Surface Tension on Rotating Fluids under Microgravity Environment," Advances in Space Research, Vol. 8, No. 12, 1988, pp. 205-213.

5. Hung, R. J., Tsao, Y. D., Hong, B. B., and Leslie, F. W., "Bubble Behaviors in a Slowly Rotating Helium Dewar in Gravity Probe-B Spacecraft Experiment," Journal of Spacecraft and Rockets, Vol. 26, May-June 1989, pp. 167-172.

6. Hung, R. J., Tsao, Y. D., Hong, B. B., and Leslie, F. W., "Dynamical Behavior of Surface Tension on Rotating Fluids in Low and Microgravity Environments," International Journal for Microgravity Research and Applications, Vol. 11, June 1989, pp. 81-95.

7. Hung, R. J., Tsao, Y. D., Hong, B. B., and Leslie F. W., "Axisymmetric Bubble Profiles in a Slwowly Rotating Helium

Dewar Under Low and Microgravity Environments," Acta Astronautica, Vol. 19, May 1989, pp. 411-426.

8. "Stanford Relativity Gyroscope Experiment (NASA Gravity Probe-B)," Proceedings of Society of Photo-Optical Instrumentation Engineers, Vol. 619, Society of Photo-Optical Instrumentation Engineers, Bellingham, WA, 1986, pp. 1-165.

9. Hung, R. J., and Shyu, K. L., "Cryogenic Liquid Hydrogen Reorientation Activated by Constant Reverse Gravity Acceleration of Geyser Initiation," AIAA Paper No. 90-3712, 1990.

10. Kamotani, Y., Prasad, A., and Ostrach, S., "Thermal Convection in an Enclosure Due to Vibrations Aboard a Spacecraft," AIAA Journal, Vol. 19, Apr. 1981, pp. 511-516.

11. Hung, R. J., Lee, C. C., and Shyu, K. L., "Reorientation of Rotating Fluid in Microgravity Environment with and without Gravity Jitters," Journal of Spacecraft and Rockets, Vol. 27, 1990, in press.

12. Hung, R. J., Lee, C. C., and Leslie, F. W. "Effects of G-Jitters on the Stability of Rotating Bubble Under Microgravity Environment," Acta Astronautica, Vol. 20, 1990, in press.

13. Hung, R. J., Lee, C. C. and Leslie F. W., "Response of Gravity Level Fluctuations on the Gravity Probe-B Spacecraft Propellant System," Journal of Propulsion and Power, Vol. 6, 1990, in press.

14. Misner, C. W., Thorne, K. S., and Wheeler, J. A., "Gravitation",

W. H. Freeman and Co., San Francisco, CA, 1973, pp. 1-1279.

15. Forward, R. L., "Flattening Space-Time Near the Earth, "Physical Review, Series D, Vol. 26, Aug. 1982, pp. 735-744.

TABLE 1 SOME BASIC GEOMETRYS AND CHARACTERISTICS
OF CRYOGENIC LIQUID HYDROGEN REORIENTATION

Liquid Filled Level (%)	30	50	65	70	80
Geyser Initiation Gravity-Level, $g_{io}(10^{-2}\ g_o)$	5.5	6.52	6.6	6.7	8.2
Geyser Initiation Acceleration, a_g (cm/s^2)	53.9	63.9	64.7	65.7	80.4
Average Liquid Height, $\bar{h}$ (cm)	2.67	2.05	1.52	1.35	0.93
Average Free Fall Flow Velocity, $\bar{V}_f$ (cm/s)	17.0	16.2	14.0	13.3	12.5
Maximum Liquid Height, h_m (cm)	3.41	2.79	2.26	2.09	1.67
Free Fall Velocity from Maximum Liquid Height V_{fm} (cm/s)	19.2	18.9	17.1	16.6	16.4

Table 2 CHARACTERISTICS OF CRYOGENIC HYDROGEN REORIENTATION
(Frequency of Impulsive Acceleration = 1.0 Hz)

Liquid Filled Level (%)	30	50	65	70	80
Maximum Flow Velocity, V_m (cm/s)	112.2	107.0	94.8	89.5	82.5
$V_m/\bar{V}_f$	6.6	6.6	6.7	6.7	6.6
Liquid Reaching Bottom Time, t_R (s)	0.35	0.28	0.24	0.22	0.19
$t_R/\bar{t}_f$	1.1	1.1	1.1	1.1	1.2
Time for Observing Maximum Velocity, t_m (s)	0.35	0.30	0.24	0.22	0.18
Scale Length of Maximum Flow Velocity, L_m ($= V_m t_m$) (cm)	39.3	32.1	22.8	19.7	14.8
$L_m/\bar{h}$	14.7	15.6	15.0	14.6	15.9
$t_m/\bar{t}_f$	1.1	1.2	1.1	1.1	1.2
Scale Flow Acceleration Associated with Maximum Velocity, a_m ($= V_m/t_m$) (cm/s^2)	320	356	395	407	458
a_m/a_g	5.9	5.7	6.1	6.1	5.7
V_m/V_{fm}	5.8	5.7	5.6	5.6	5.2

Figure Captions

Figure 1. (A) Distribution of grid points in the radial-axial plane of cylindrical coordinate for propellant tank, and (B) Model size propellant tank adopted for numerical simulation with geometrical description.

Figure 2. Selected sequences of time evolution of fluid reorientation with liquid filled level of 30% for impulsive acceleration with frequency of 1.0 Hz, (A) initial profile, (B) flow profile before the initiation of geyser, (C) flow profile with geyser, and (D) flow profile after the ending of geyser.

Figure 3. Selected sequences of time evolution of fluid reorientation with liquid filled level of 50% for impulsive acceleration with frequency of 1.0 Hz, (A) initial profile, (B) flow profile before the initiation of geyser, (C) flow profile with geyser, and (D) flow profile after the ending of geyser.

Figure 4. Selected sequences of time evolution of fluid reorientation with liquid filled level of 65% for impulsive acceleration with frequency of 1.0 Hz, (A) initial profile, (B) flow profile before the initiation of geyser, (C) flow profile with geyser, and (D) flow profile after the ending of geyser.

Figure 5. Selected sequences of time evolution of fluid reorientation with liquid filled level of 70% for impulsive acceleration with frequency of 1.0 Hz, (A)

initial profile, (B) flow profile before the initiation of geyser, (C) flow profile with geyser, and (D) flow profile after the ending of geyser.

Figure 6. Selected sequences of time evolution of fluid reorientation with liquid filled levels of 80% for impulsive acceleration with frequency of 1.0 Hz, (A) initial profile, (B) flow profile before the initiation of geyser, (C) flow profile with geyser, and (D) flow profile after the ending of geyser.

Figure 7. (A) Ratio of $V_m/\bar{V}_f$ and its associated parameters in terms of liquid filled levels, (B) Ratio of $t_R/\bar{t}_f$ and its associated parameters in terms of liquid filled levels.

Figure 8. (A) Ratio of $t_m/\bar{t}_f$ and its associated parameters in terms of liquid filled levels, (B) Ratio of a_m/a_g and its associated parameters in terms of liquid filled levels.

Figure 9. (A) Ratio of $L_m/\bar{h}$ and its associated parameters in terms of liquid filled levels, (B) Ratio of V_m/V_{fm} and its associated parameters in terms of liquid filled levels.

(A)

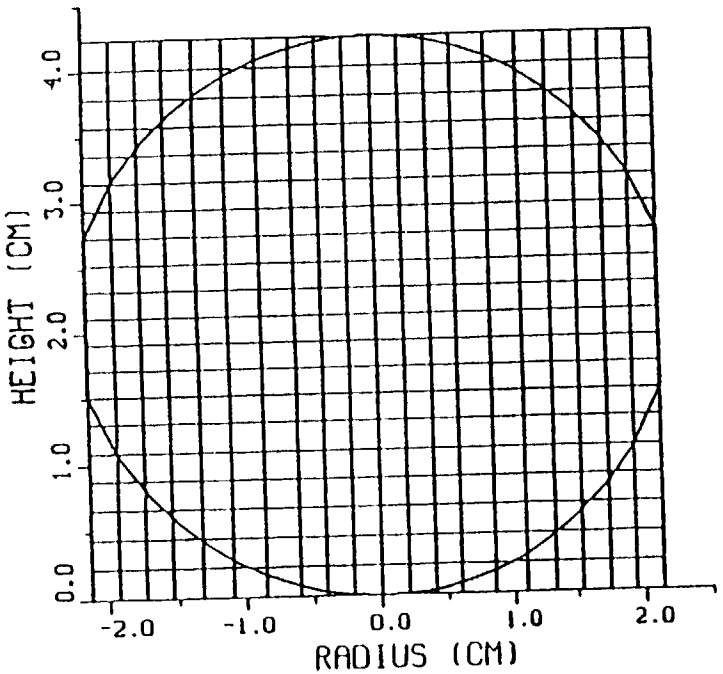

(B)

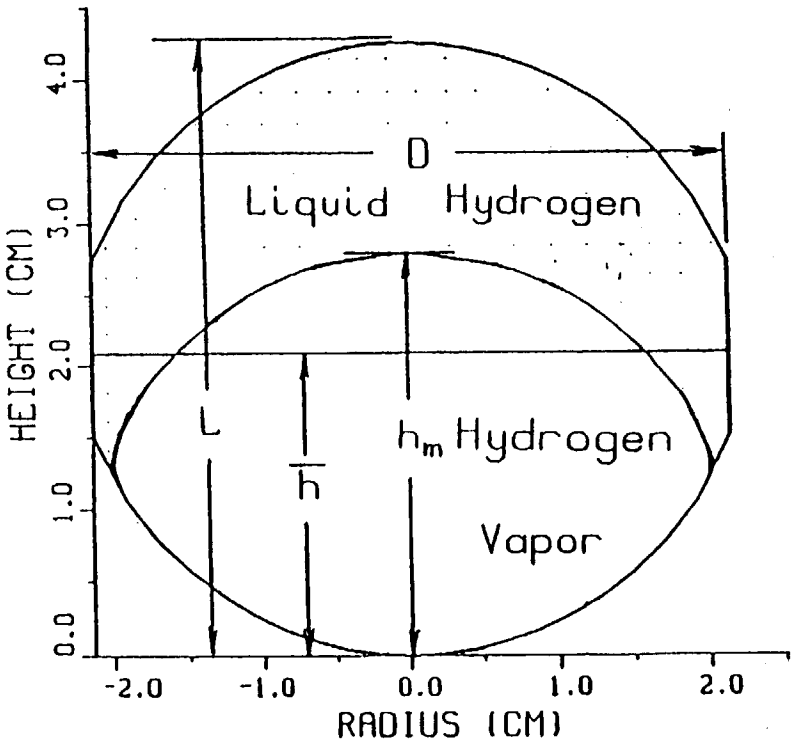

D-4.26720 CM, L-4.23672 CM

Fig 1

A. Liquid Hydrogen and Vapor
Liquid Filled=30% t= 0.00 s
g=-5.50×10^{-2} g$_o$
f= 1.00×10^{0} Hz

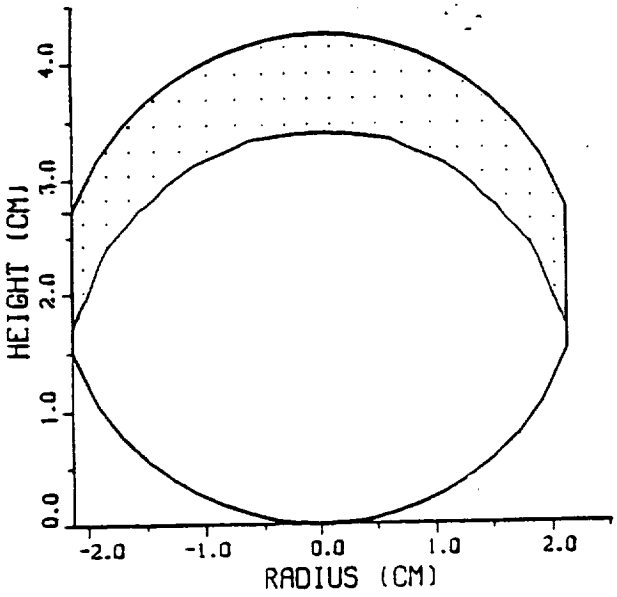

B. Liquid Hydrogen and Vapor
Liquid Filled=30% t= 3.00×10^{-1} s
g=-5.50×10^{-2} g$_o$
f= 1.00×10^{0} Hz

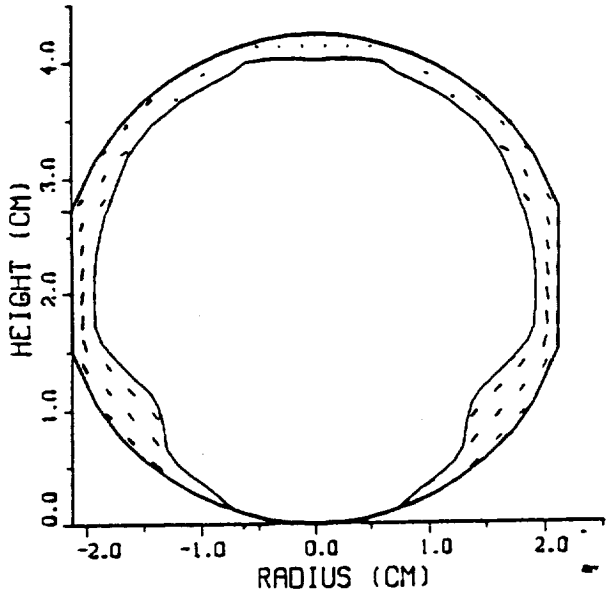

C. Liquid Hydrogen and Vapor
Liquid Filled=30% t= 5.13×10^{-1} s
g=-5.50×10^{-2} g$_o$
f= 1.00×10^{0} Hz

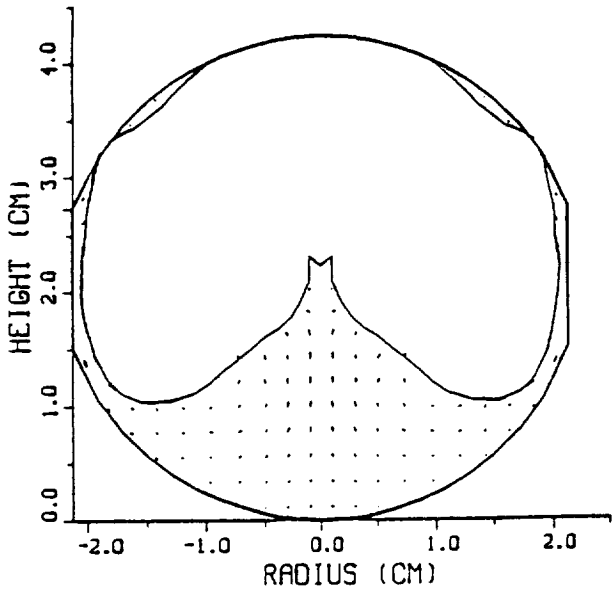

D. Liquid Hydrogen and Vapor
Liquid Filled=30% t= 9.93×10^{-1} s
g=-5.50×10^{-2} g$_o$
f= 1.00×10^{0} Hz

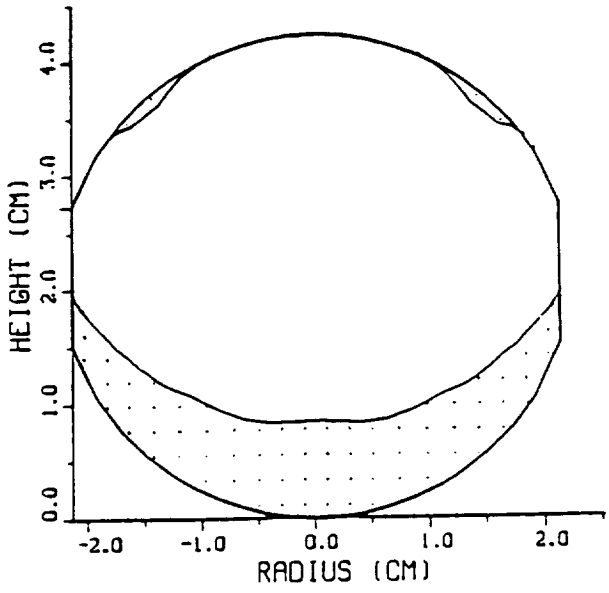

Fig 2

A. Liquid Hydrogen and Vapor
Liquid Filled-50% t= 0.00s
g=-6.52×10^{-2}g$_o$
f= 1.00×10^{0}Hz

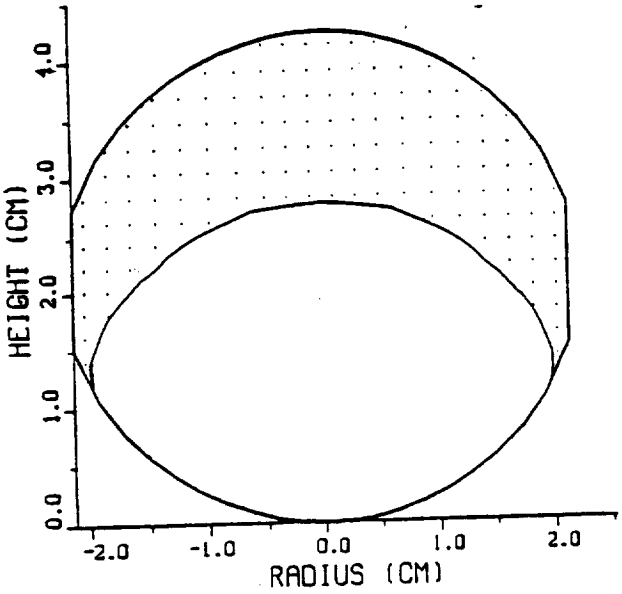

B. Liquid Hydrogen and Vapor
Liquid Filled-50% t= 2.40×10^{-1}s
g=-6.52×10^{-2}g$_o$
f= 1.00×10^{0}Hz

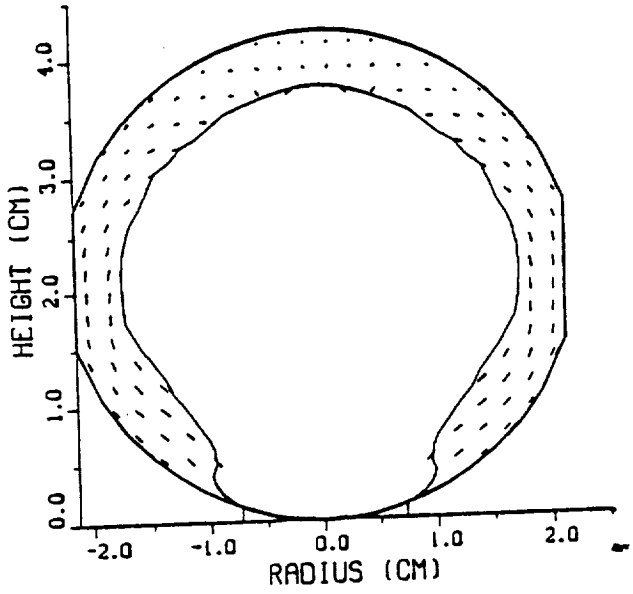

C. Liquid Hydrogen and Vapor
Liquid Filled-50% t= 3.22×10^{-1}s
g=-6.52×10^{-2}g$_o$
f= 1.00×10^{0}Hz

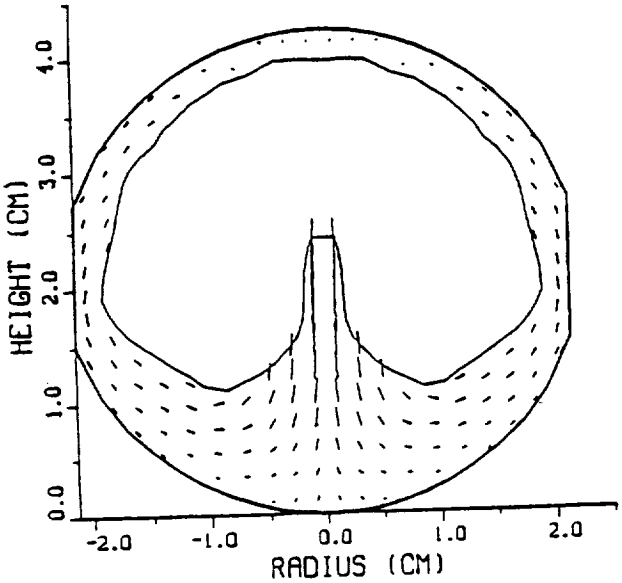

D. Liquid Hydrogen and Vapor
Liquid Filled-50% t= 6.17×10^{-1}s
g=-6.52×10^{-4}g$_o$
f= 1.00×10^{0}Hz

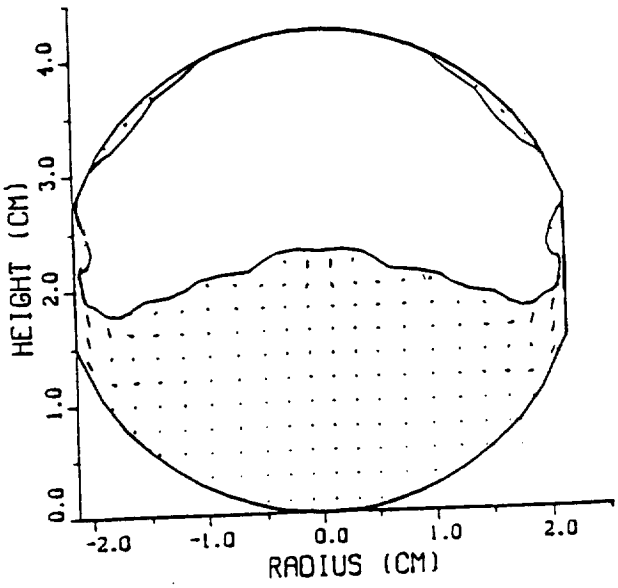

Fig 3

A. Liquid Hydrogen and Vapor
Liquid Filled-70% t= 0.00s
g=-7.00×10^{-2} g_o
f= 1.00×10^{0} Hz

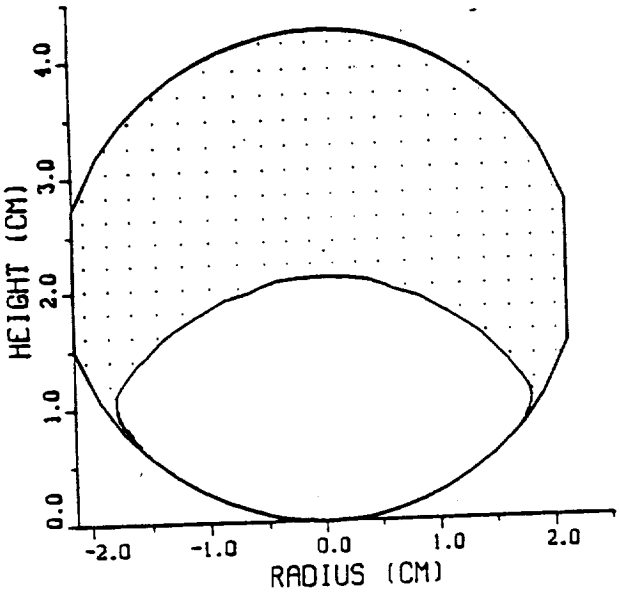

B. Liquid Hydrogen and Vapor
Liquid Filled-70% t= 1.80×10^{-1} s
g=-7.00×10^{-2} g_o
f= 1.00×10^{0} Hz

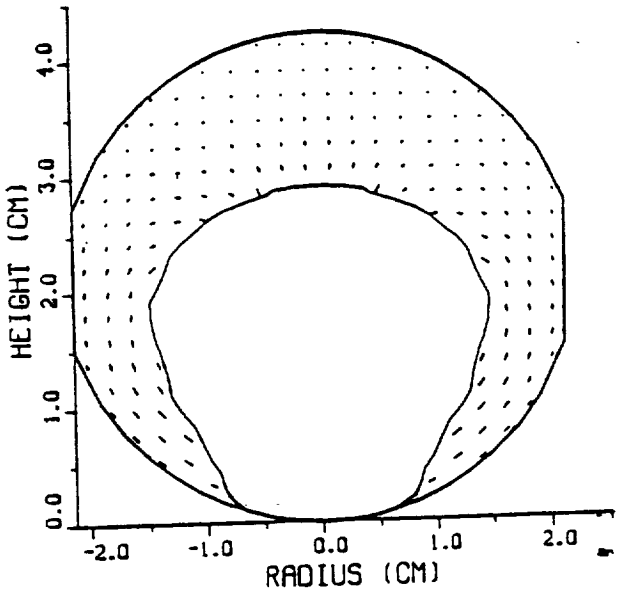

C. Liquid Hydrogen and Vapor
Liquid Filled-70% t= 3.20×10^{-1} s
g=-7.00×10^{-2} g_o
f= 1.00×10^{0} Hz

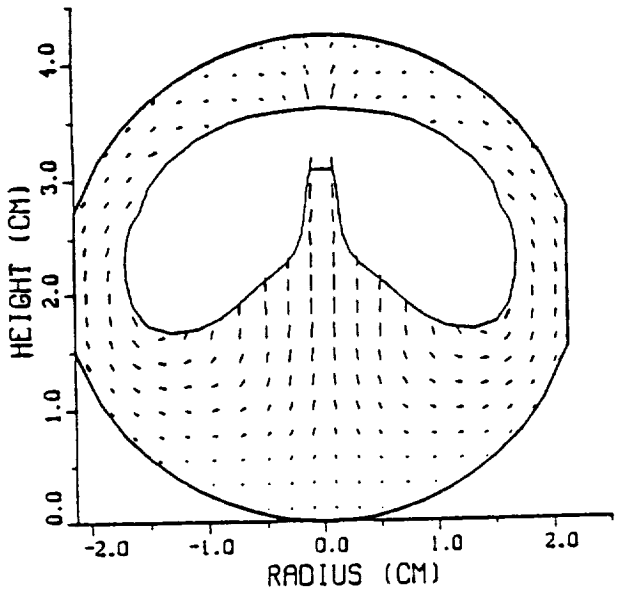

D. Liquid Hydrogen and Vapor
Liquid Filled-70% t= 8.00×10^{-1} s
g=-7.00×10^{-2} g_o
f= 1.00×10^{0} Hz

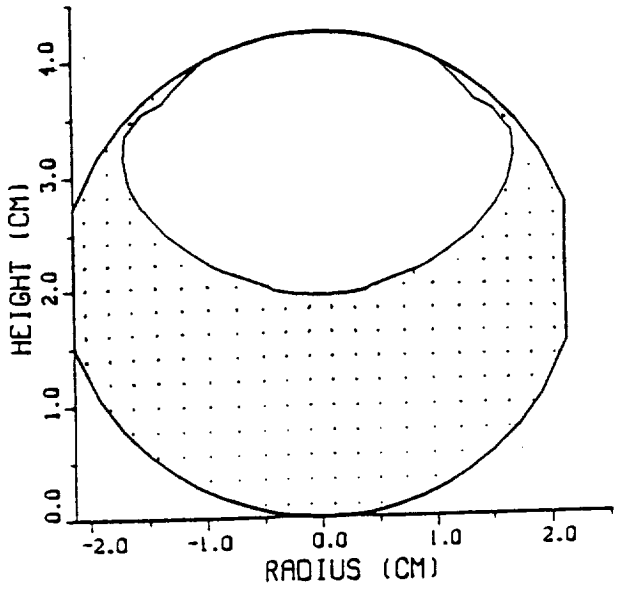

Fig 4

A. Liquid Hydrogen and Vapor
Liquid Filled-65% t= 0.00s
g=-6.60×10^{-2}g$_o$
f= 1.00×10^{0}Hz

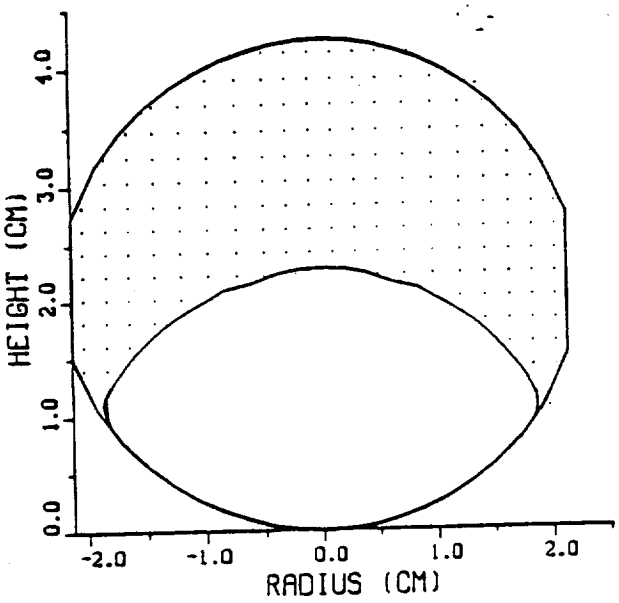

B. Liquid Hydrogen and Vapor
Liquid Filled-65% t= 1.80×10^{-1}s
g=-6.60×10^{-2}g$_o$
f= 1.00×10^{0}Hz

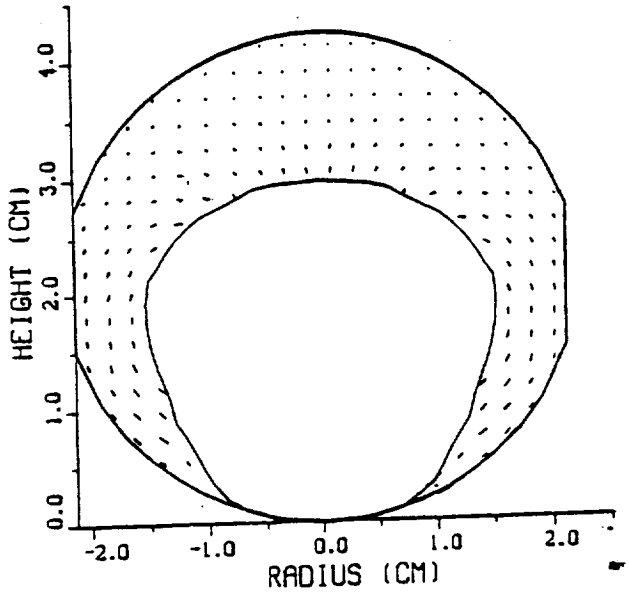

C. Liquid Hydrogen and Vapor
Liquid Filled-65% t= 3.86×10^{-1}s
g=-6.60×10^{-2}g$_o$
f= 1.00×10^{0}Hz

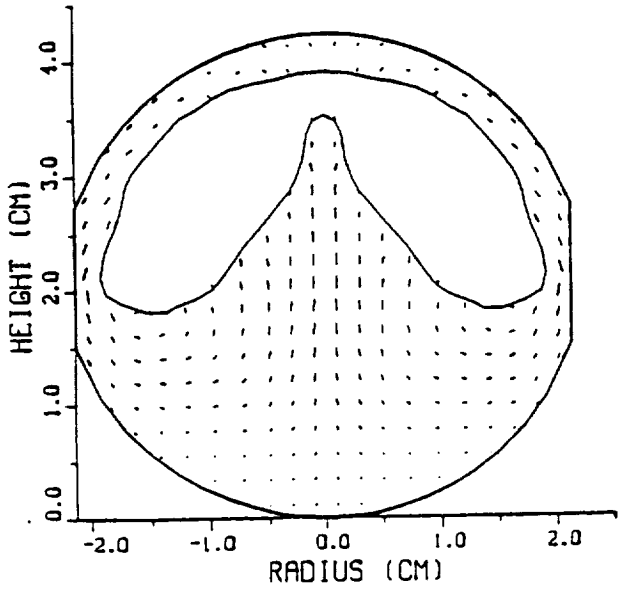

D. Liquid Hydrogen and Vapor
Liquid Filled-65% t= 7.46×10^{-1}s
g=-6.60×10^{-2}g$_o$
f= 1.00×10^{0}Hz

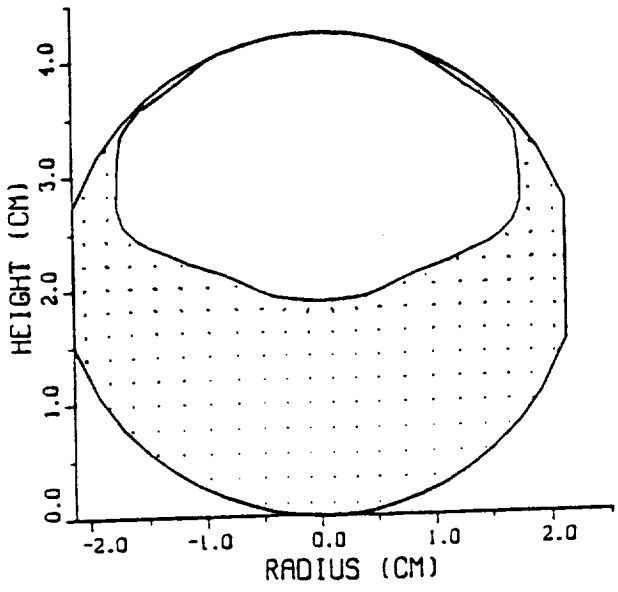

Fig 5

A. Liquid Hydrogen and Vapor
Liquid Filled-80% t= 0.00s
g=-8.20×10^{-2} g$_o$
f= 1.00×10^{0} Hz

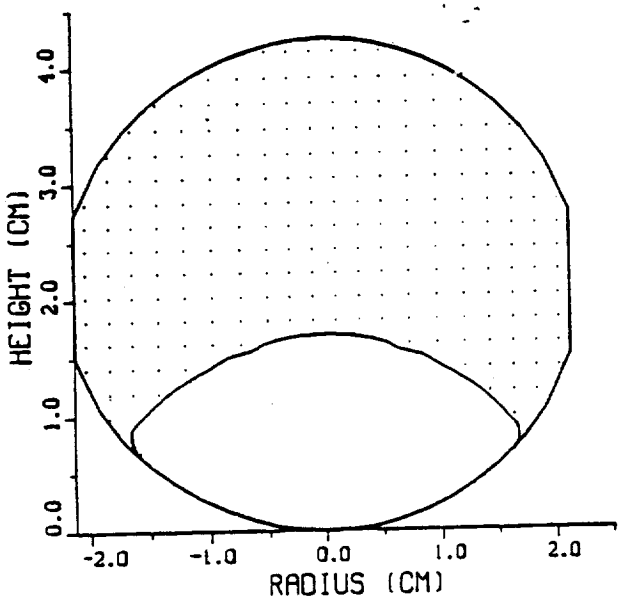

B. Liquid Hydrogen and Vapor
Liquid Filled-80% t= 1.80×10^{-1} s
g=-8.20×10^{-2} g$_o$
f= 1.00×10^{0} Hz

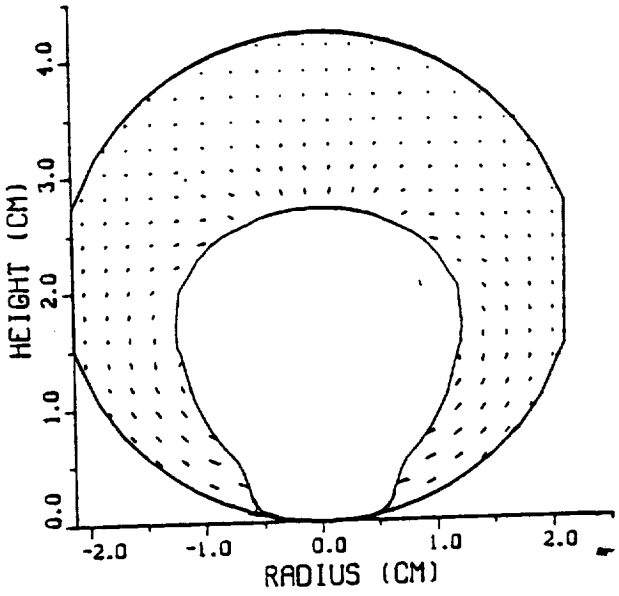

C. Liquid Hydrogen and Vapor
Liquid Filled-80% t= 2.68×10^{-1} s
g=-8.20×10^{-2} g$_o$
f= 1.00×10^{0} Hz

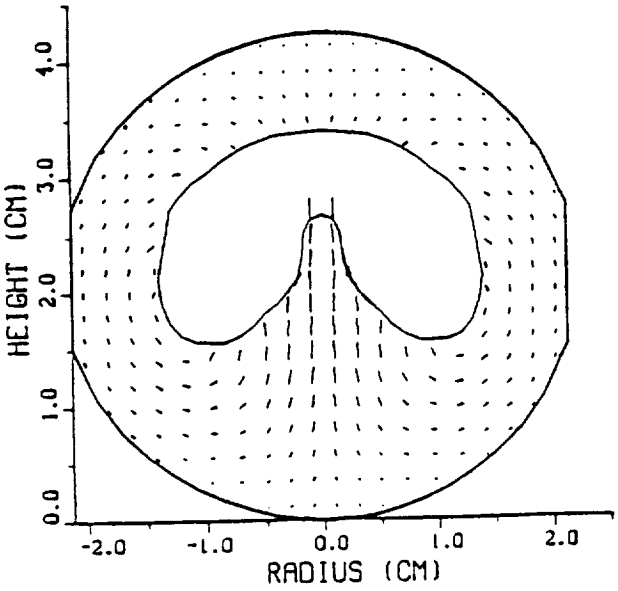

D. Liquid Hydrogen and Vapor
Liquid Filled-80% t= 8.08×10^{-1} s
g=-8.20×10^{-2} g$_o$
f= 1.00×10^{0} Hz

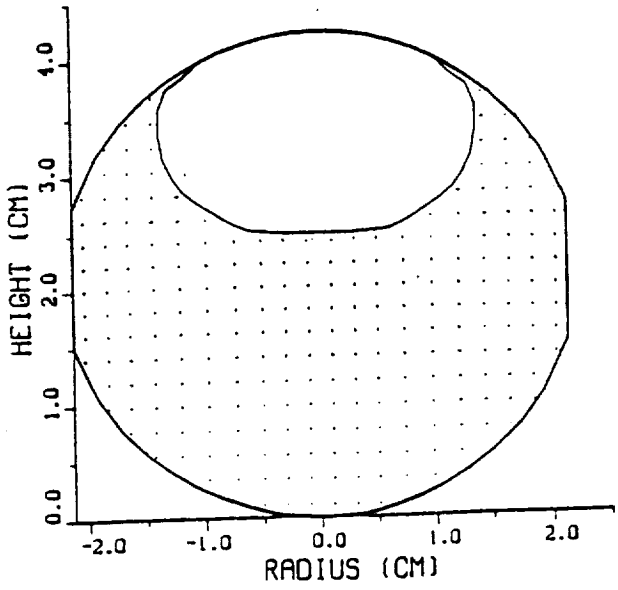

Fig 6

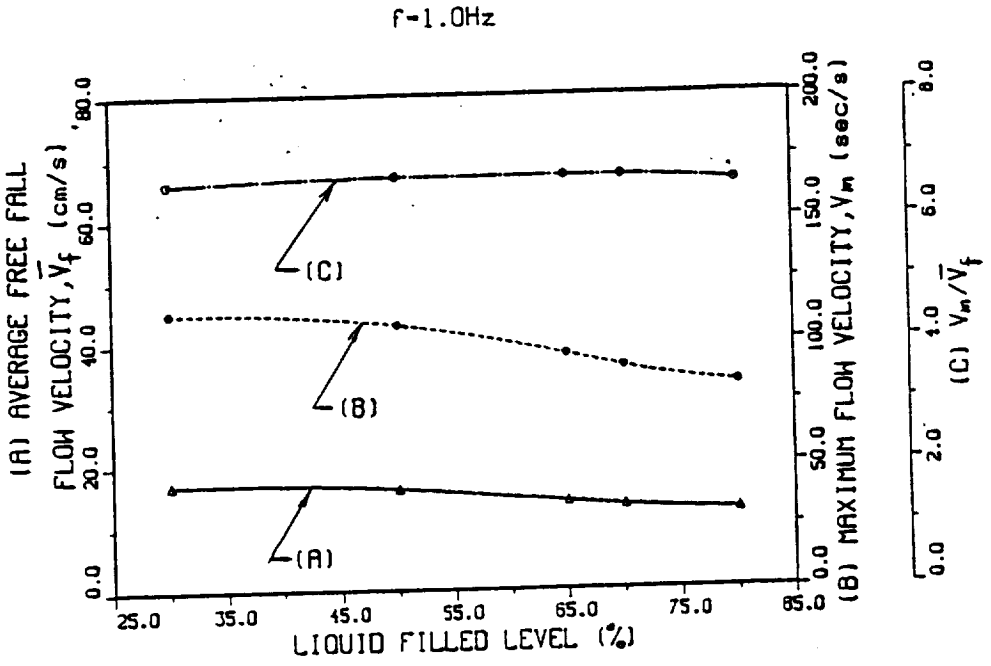
f=1.0Hz
(A) AVERAGE FREE FALL FLOW VELOCITY, $\bar{V}_f$ (cm/s)
(B) MAXIMUM FLOW VELOCITY, V_m (sec/s)
(C) $V_m/\bar{V}_f$
(C)
(B)
(A)
LIQUID FILLED LEVEL (%)

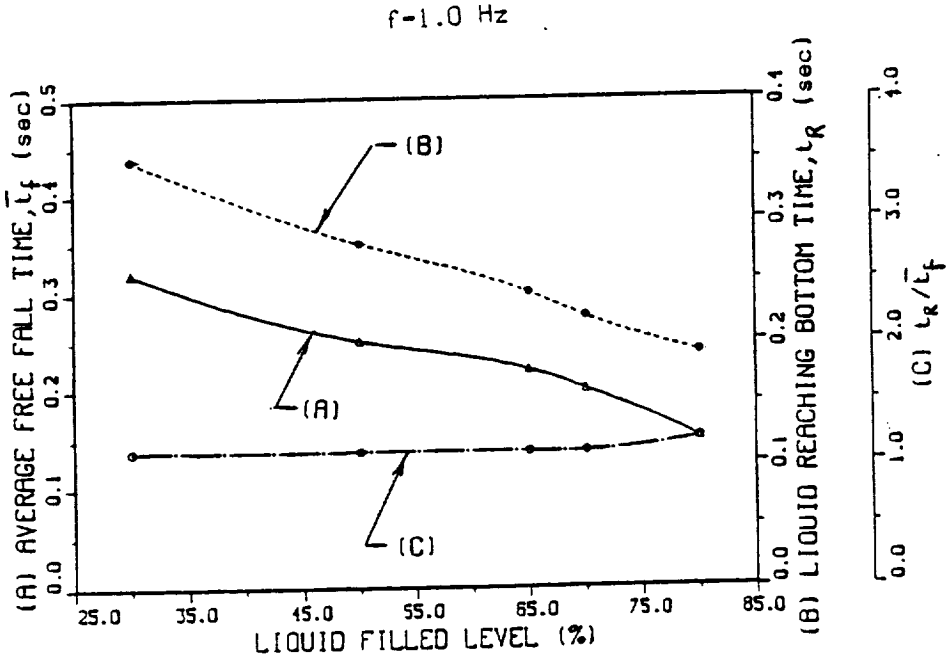
f=1.0 Hz
(A) AVERAGE FREE FALL TIME, $\bar{t}_f$ (sec)
(B) LIQUID REACHING BOTTOM TIME, t_R (sec)
(C) $t_R/\bar{t}_f$
(B)
(A)
(C)
LIQUID FILLED LEVEL (%)

Fig 7 (A,B)

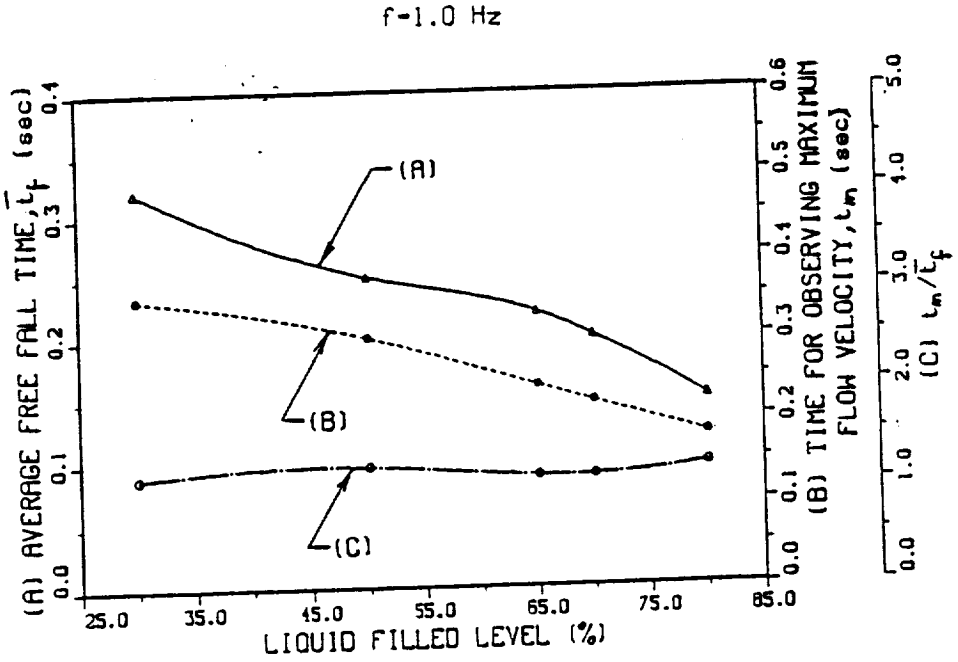
f=1.0 Hz
(A) AVERAGE FREE FALL TIME, $\bar{t}_f$ (sec)
(B) TIME FOR OBSERVING MAXIMUM FLOW VELOCITY, t_m (sec)
(C) $t_m/\bar{t}_f$
(A)
(B)
(C)
LIQUID FILLED LEVEL (%)

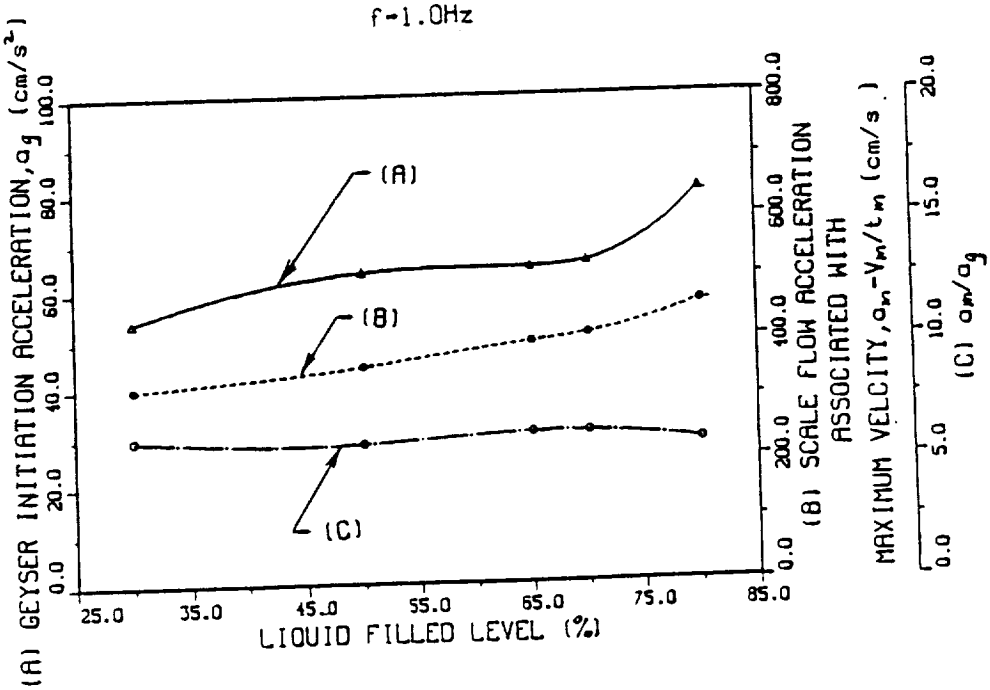
f=1.0Hz
(A) GEYSER INITIATION ACCELERATION, a_g (cm/s²)
(B) SCALE FLOW ACCELERATION ASSOCIATED WITH MAXIMUM VELOCITY, a_m-V_m/t_m (cm/s²)
(C) a_m/a_g
(A)
(B)
(C)
LIQUID FILLED LEVEL (%)

Fig 8 (A,B)

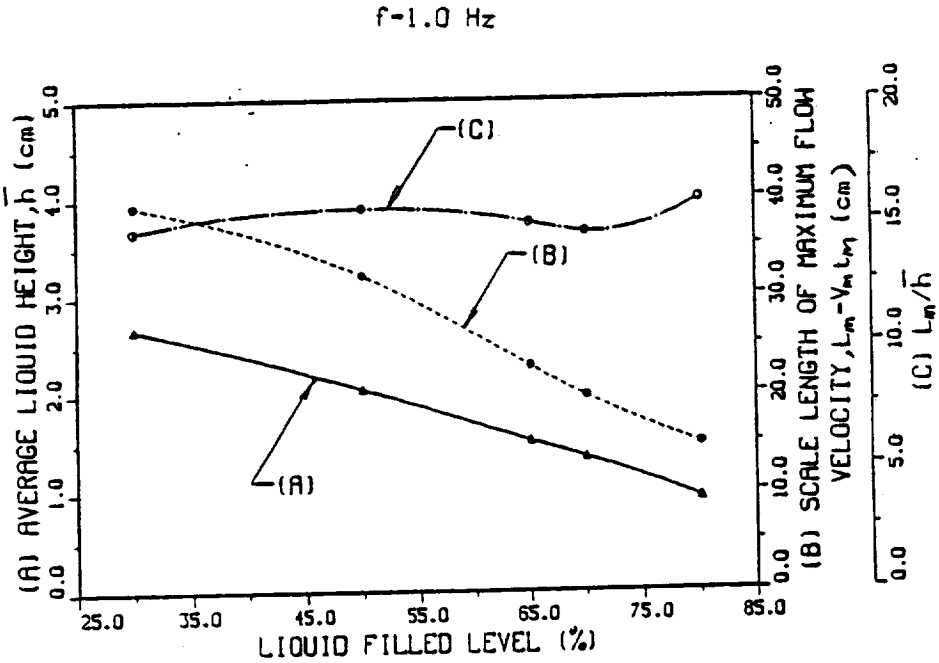
f-1.0 Hz
(A) AVERAGE LIQUID HEIGHT, $\bar{h}$ (cm)
(B) SCALE LENGTH OF MAXIMUM FLOW VELOCITY, $L_m - V_m t_m$ (cm)
(C) $L_m/\bar{h}$
(A)
(B)
(C)
LIQUID FILLED LEVEL (%)

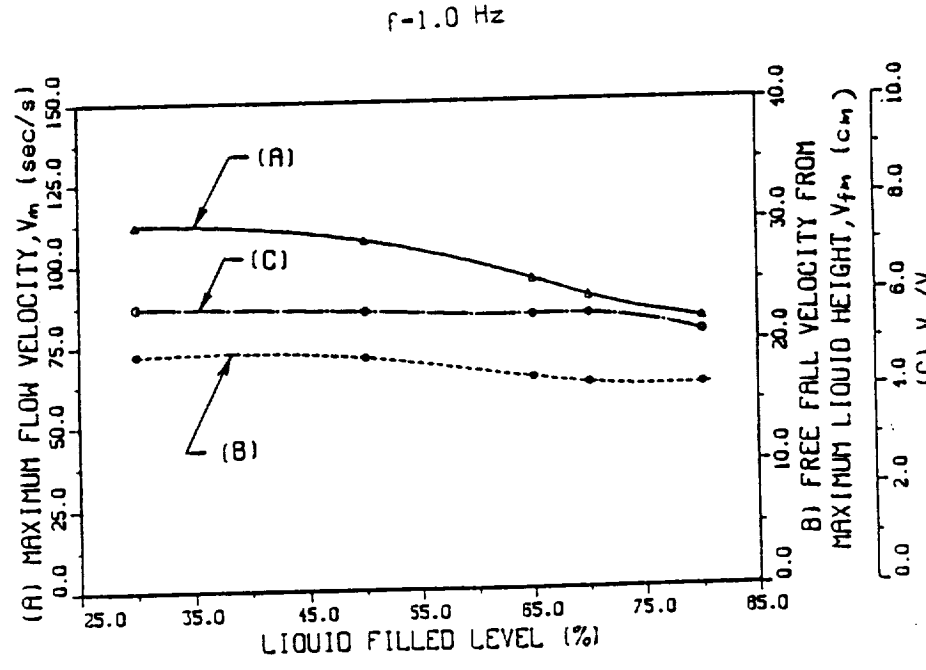
f-1.0 Hz
(A) MAXIMUM FLOW VELOCITY, V_m (sec/s)
B) FREE FALL VELOCITY FROM MAXIMUM LIQUID HEIGHT, V_{fm} (cm)
(C) V_m/V_{fm}
(A)
(B)
(C)
LIQUID FILLED LEVEL (%)

Fig 9 (A,B)

(H) Cryogenic Liquid Hydrogen Reorientation Activated by High Frequency Impulsive Acceleration of Geyser Initiation

Abstract

The requirement to settle or to position liquid fluid over the outlet end of spacecraft propellant tank prior to main engine restart poses a microgravity fluid behavior problem. Resettlement or reorintation of liquid propellant can be accomplished by providing optimal acceleration to the spacecraft such that the propellant is reorientaed over the tank oulet without any vapor entrainment, any excessive geysering, or any other undesirable fluid motion for the space fluid management under microgravity environment. The purpose of present study is to investigate most efficient technique for propellant resettling through the minimization of propellant usage and weight penalties. Comparison between the constant reverse gravtiy acceleration and impulsive reverse gravity acceleration to be used for the activation of propellant resettlement, it shows that impulsive reverse gravity thrust is superior to constant reverse gravity thrust for liquid reorientation in a reduced gravity environment.

I. Introduction

In spacecraft design, the requirements for a settled propellant are different for tank pressurization, engine restart, venting, or propellant transfer. Prepressurization requires that heat and mass transfer effects be minimized; otherwise, a process of chill down of tank, venting of noncondensing gases, etc., may have to carry out for the cryogenic system. For engine restart, it is necessary to have the liquid settle with no bubbles near the tank outlet so that the initial flow of propellant will not carry vapor to the pump or engine. The slosh wave amplitude should be relatively low to keep the center of mass shifts within an acceptable range and wave motion low enough to avoid pressure collapse caused by interface agitation . For venting, it is probably necessary that virtually all bubbles be displaced from the bulk liquid so that a two-phase mixture is not vented. Propellant transfer requires that the liquid be completely settled with virtually no bubbles. Outflow of a liquid near the tank outlet can result in the prematrue ingestion of gas while a signigicant amount of liquid is still in the tank under microgravity environment. This phenomenon is termed "suction dip". Slosh wave motion must be minimal because the combination of "suction dip" and sloshing could cause gas pull-through to occur more readily in microgravity than if the surface were essentially quiescent.

During the prepressurization of a cryogenic propellant in microgravity, significant heat and mass transfer will occur if the liquid interface is disturbed. Interface disturbances may result from (a) impingement of the gas on the liquid surface at a mass flow

rate sufficient to cause Kelvin-Helmholtz instability, (b) globule formation from breaking waves caused by wave motion over baffles or internal hardware, (c) globule and surface froth formation resulting from movement of bubbles through the liquid to the surface, and (d) surface froth formation because of gas impingement.

Bubble and globule formation as a result of liquid impact with the aft end of the tank could lead to propellant loss for the spacecraft during venting. Globules could be entrained in the vented ullage gas or bubbles rising through the liquid and expanding because of the decreasing tank pressure could cause a spray of globules to be vented. Liquid level rise, vent liquid loss, fluid freezing, and vehicle dynamics are all affected by the microgravity levels.

A key objective of the cryogenic fluid management of spacecraft propulsion system, such as a Space Transfer Vehicle[1] (STV), is to develop the technology necessary for acquisition or positioning of liquid and vapor within a tank in reduced gravity to enable liquid outflow or vapor venting. Liquid acquisition techniques can be divided into two general categories: (1) Active liquid acquisition by the creation of a positive acceleration environment resulting from the propulsive thrust of small auxiliary engines, and (2) Passive liquid acquisition utilizing the liquid capillary forces provided by using solid baffles of liquid traps made of fine mesh screen material. In this series of study, active liquid acquisition is aimed for numerically simulating the resettlement of cryogenic liquid hydrogen. Liquid hydrogen, which, in general, poses more severe technical challenges than liquid oxygen, is used as the test bed

working fluid in this study.

Recently Lesie[2] was able to measure and to numerically compute the bubble shapes at various ratios of centrifugal force to surface tension force in 2, 4 and 6.3 cm deep cylinders in the microgravity environment. The results showed excellent agreement between model computation and measurements. Hung and Leslie[3] extended Leslie's work[2] to rotating free surfaces influenced by gravity with higher rotating speeds when the bubble intersects with both the top and bottom walls of the cylinder. Hung et al.[4,5] further extended the work to include rotating speeds which resulted with bubbles intersecting and/or without intersecting the top, bottom and side walls of the cylinder.

An analysis of time-dependent dynamical behavior of surface tension on partially-filled rotating fluids in both low gravity and microgravity environments was carried out by numerically solving the Navier-Stokes equations subjected to the initial and the boundary conditions[4,6]. At the interface between the liquid and the gaseous fluids, both the kinematic surface boundary condition, and the interface stress conditions for components tangential and normal to the interface, were applied. The initial condition for the bubble profiles was adopted from steady-state formulations developed by Hung and Leslie[3], and Hung et al.[6] for rotating cylinder tank; and by Hung et al.[5,7] for the dewar-shaped container to be used in the Gravity Probe-B Spacecraft[8]. Some of the steady-state formulations of bubble shapes, in particular for bubbles intersecting at the top wall of the cylinder, were compared with the experiment carried out by

Leslie[2] in a free-fallinng aircraft (KC-135). Comparisons of time-dependent results between numerical computations and experiments were unavailable. This was because the calibration of the recordings of time-dependent gravity variations in a KC-135 aircraft during the short time periods of microgravity environment is very difficult. There was also an unavailability of accelerometer data for measuring the actual levels of microgravity during the experiment.

An efficient propellant settling technique should minimize propellant usage and weight penalties. This can be accomplished by providing optimal acceleration to the spacecraft such that the propellant is reoriented over the tank outlet without any vapor entrainment, any excessive geysering, or any other undesirable fluid motion.

Production of geyser during the propellant reorientation is not a desirable motion for the space fluid management. It is because geyser is always accompanied by the vapor entrainment and globule formation. Geyser is observed at reverse gravity thrust greater than certain critical values of acceleration during the course of liquid reorientation. In other words, geyser will not be observed at very low reverse gravity level, and it will be detected when the reverse gravity level is greater than the certain critical value. In this series of study, numerical simulation of positive liquid acquisition is attemted by introducing reverse gravity acceleration, resulting from the propulsive thrust of small auxiliary engines which exceeds the critical value for geyser initiation. The reverse gravity acceleration is starting with a small value and increases gradually

till the initiation of geyser is detected in the computer simulation for the liquid reorientation of propellant tank with various liquid-filled levels.

In this series of studies, time-dependent computations have been carried out to investigate the dynamical behavior of fluid reorientation or resettling of propellant prior to main engine firing for spacecraft restart at the net reverse gravity acceleration which is great enough to initiate geyser during the liquid reorientation. First paper of present study (Paper I)[9] investigates the characteristics of fluid resettlement due to the reversal of lowest constant reverse gravity acceleration which is great enough to initiate geyser without any impulsive acceleration. The frequency of impulsive acceleration is generally termed "gravity jitters". Gravity jitters are produced by spacecraft attitude motion, machinery (turbine, pump, engine) vibrations, thruster firing, thruster shutdown, impulsive engine acceleration, etc.[10] Positioning of liquid propellant over the tank outlet can be carried out by using small auxiliary thrusters which provide a thrust parallel to the tank's major axis in the direction of flight.

Computer simulation of flow field based on Paper I[9] during the course of fluid reorientation induced by constant reverse gravity acceleration show that six dimensionless parameters are abtained in the study. These parameters hold near constant values through the entire ranges of liquid filled levels during the course of fluid reorientation activated by the reverse gravity acceleration great enough to initiate geyser. As the denominators of these

dimensionless parameters are either predetermined from the geometry of liquid filled levels or can be deduced from the corresponding calculations associated with the geyser initiation gravity levels. One can predict the values of these flow parameters. These predictable parameters include maximum flow velocity V_m, time for observing maximum flow velocity t_m, time for reorienting liquid flowing down and reaching the bottom of propellant tank t_R, scale length of maximum flow velocity L_m, and scale flow acceleration associated with maximum velocity a_m.

Instead of applying constant reverse gravity acceleration as we described in Paper I[9], this paper adopts impulsive reverse gravity acceleration with a high frequency of 10 Hz for the activation of fluid reorientation with liquid filled levels of 30, 50, 65, 70 and 80%.

II. Mathematical Model

The present study examines time-dependent fluid behaviors, in particular the dynamics of liquid hydrogen and hydrogen vapor reorientation induced by reverse gravity acceleration which is great enough to introduce geyser initiation. As in Paper I[9], time-dependent axial symmetry mathematical formulation are adopted.

Consider a closed circular cylinder of radius, a, with length, L, which is partially filled with a cryogenic liquid hydrogen of constant density ρ and kinematic viscosity ν. Let us use cylindrical coordinates (r, θ, z), with corresponding velocity components (u, v, w). The gravitational acceleration, g, is along the z-axis. For the

case of axial symmetry, the θ-dependency vanishes. The governing equations are shown as follows:

(A) Continuity Equation

$$\frac{1}{r}\frac{\partial}{\partial r}(ru) + \frac{\partial w}{\partial z} = 0 \qquad (2\text{-}1)$$

(B) Momentum Equations

$$\frac{Du}{Dt} - \frac{v^2}{r} = -\frac{1}{\rho}\frac{\partial P}{\partial r} + \nu\left(\nabla^2 u - \frac{u}{r^2}\right) \qquad (2\text{-}2)$$

$$\frac{Dv}{Dt} + \frac{uv}{r} = \nu\left(\nabla^2 v - \frac{v}{r^2}\right) \qquad (2\text{-}3)$$

$$\frac{Dw}{Dt} = -\frac{1}{\rho}\frac{\partial P}{\partial z} - g + \nu\nabla^2 w \qquad (2\text{-}4)$$

where,

$$\frac{D}{Dt} = \frac{\partial}{\partial t} + u\frac{\partial}{\partial r} + w\frac{\partial}{\partial z} \qquad (2\text{-}5)$$

$$\nabla^2 = \frac{1}{r}\frac{\partial}{\partial r}\left(r\frac{\partial}{\partial r}\right) + \frac{\partial^2}{\partial z^2} \qquad (2\text{-}6)$$

Let the profile of the interface between gaseous and liquid fluids be given by:

$$\eta\ (t,\ r,\ z) = 0,\ \text{or}\ r = \eta(t,z) \qquad (2\text{-}7)$$

The initial condition of the profile of interface between gaseous and liquid fluids at $t = t_0$ is assigned explicitly, and is given by:

$$\eta(t = t_0,\ r,\ z) = 0,\ \text{or}\ r = \eta_0(z) = \eta(t_0,z) \qquad (2\text{-}8)$$

A set of boundary conditions has to be supplied for solving the

equations. These initial interface profiles used in this study have been given explicitly through the steady state computations made by Hung and Leslie[3] and Hung et al[4] which were checked by the experiments carried over by Leslie[2]. These boundary conditions are as follows:

(1) At the container wall, no-penetration and no-slip conditions assure that both the tangential and the normal components of the velocity along the solid walls will vanish. In the numerical calculation of bubble profiles for ethanol and air, a constant contact angle is present when the free surface of liquid ethanol intersects the container wall.

(2) Along the interface between the liquid and gaseous fluids, the following two conditions apply:

(a) Kinematic surface boundary condition: The liquid (or gaseous) surface moves with the liquid (or gas) which implies

$$\left.\begin{aligned} &\frac{D\eta}{Dt} = 0, \text{ or} \\ &\frac{\partial \eta}{\partial t} + u\frac{\partial \eta}{\partial r} + w\frac{\partial \eta}{\partial z} = 0 \\ &\text{on } \eta = \eta(t = t_i,\ r,\ z) \end{aligned}\right\} \qquad (2\text{-}9)$$

(b) Interface stress condition: At the interface, the stress must be continuous. These can be decomposed to the components normal and tangential to the interface. For the component tangential

to the interface between liquid and gaseous fluids

$$\left[\tau \cdot n - (n \cdot \tau \cdot n) \right]_{liquid} = \left[\tau \cdot n - (n \cdot \tau \cdot n) \right]_{gas} \qquad (2\text{-}10)$$

must hold. Here

$$\tau_{ij} = \mu \left(\frac{\partial u_i}{\partial x_j} + \frac{\partial u_j}{\partial x_i} + \frac{2}{3} \frac{\partial u_k}{\partial x_k} \delta_{ij} \right) + \zeta \frac{\partial u_k}{\partial x_k} \delta_{ij}$$

is the viscous stress tensor; μ, the viscous coefficient of the first kind; ζ, the viscous coefficient of the second kind; n, the unit vector normal to the interface and δ_{ij}, the Dirac delta function. For the component normal to the interface between the liquid and gaseous fluids, the expression becomes Laplace's formula which is

$$P_G - P_L - (n \cdot \tau \cdot n)_{gas} + (n \cdot \tau \cdot n)_{liquid} = - \frac{\sigma}{r} \frac{d}{dr} \left[\frac{r\phi}{(1 + \phi^2)^{1/2}} \right] \qquad (2\text{-}11)$$

Here P_L denotes the liquid pressure at the interface; P_G, the gaseous pressure at the interface; σ, the surface tension of the interface; and ϕ, the tangent of the interface which is defined by:

$$\phi = \frac{dz}{dr} \quad \text{on} \quad \eta_i = \eta(t_i, r, z) \qquad (2\text{-}12)$$

Detailed description of computational algorithm applicable to

microgravity fluid management are illustrated in Paper I[9] and our earlier studies.[4,6,11-13] As we have indicated in Paper I[9], for the purpose of facilitating easy comparison between computational resuslts and experimental measurement, a model of 0.01 size prototype is adopted in the computer simulation. Model size is height L = 4.23672 cm and diameter D = 4.2672 cm. If the spacecraft had been coasting for a long time, aligned with its direction of motion, the most signigicant force, drag, would be axial and with acceleration of $10^{-4}g_0$ along upward direction. The hydrogen vapor is, thus, originally positioned at the bottom of the tank. The requirement to settle or to position liquid fuel over the outlet end of the spacecraft propellant tank prior to main engine restart poses a microgravity fluid behavior problem.[11] Retromaneuvers of spacecraft, such as STV, require settling or reorientation of the propellant prior to main engine firing.[1,11] Cryogenic liquid propellant shall be positioned over the tank outlet by using auxiliary thrusters (or idle-mode thrusters from the main engine) which provide a thrust parallel to the tank's major axis in the direction of flight. Similar to Paper I[9], a small value of reverse gravity acceleration (downward direction) is provided by the propulsive thrust of small auxiliary engine to initiate the reorientation of liquid propellant. This small value of reverse gravity acceleration of propulsive thrust increases gradually till reaching the critical value on which initiation of geyser is detected during the time period of fluid resettlement. We term this reverse gravity acceleration of propulsive thrust, which is capable to initiate geyser, as "geyser initiation gravity-level".

This geyser initiation gravity level has been investigated through the method of trial and error for the various liquid-filled levels as a base to simulate impulsive reverse gravity acceleration with frequencies of 0.1, 1.0 and 10 Hz. As we have indicated in Paper I[9], cryogenic liquid hydrogen at temperature of 20K is considered. Hydrogen density of 0.071 g/cm^3; surface tension coefficient at the interface between liquid hydrogen and hydrogen vapor of 1.9 dyne/cm; hydrogen viscosity coefficient of 1.873×10^{-3} cm^2/s; and contact angle of 0.5^0 are used in the computer simulation.

III. Numerical Simulation of Liquid Hydrogen Reorientation With Geyser Initiation at High Frequency Impulsive Reverse Gravity Acceleration With Frequency of 10 Hz

In this paper, among three categories of impulsive gravity acceleration with frequencies of 0.1, 1.0 and 10 Hz, reorientation of cryogenic liquid hydrogen activated by geyser initiation impulsive reverse gravity acceleration with a high frequency of 10 Hz produced by propulsive thrust will be investigated for various liquid filled levels of propellant tank. Paper I shows that these geyser initiation gravity levels are 5.5×10^{-2}, 6.52×10^{-2}, 6.6×10^{-2}, 6.7×10^{-2} and $8.2 \times 10^{-2} g_0$ for liquid filled levels of 30, 50, 65, 70, and 80%, respectively.

Table 1 shows some basic geometrys and characteristics of cryogenic liquid hydrogen resettlement activated by reverse gravity acceleration at geyser initiation gravity level. Average liquid

height $\bar{h}$, and maximum liquid height h_m are shown in Figure 1. Average free fall velocity $\bar{V}_f$, average free fall time $\bar{t}_f$, and free fall velocity from maximum liquid height V_{fm} are computed from the following equations:

$$\bar{V}_f = (2g_{io}\bar{h})^{1/2} \qquad (3\text{-}1)$$

$$\bar{t}_f = \left(\frac{2\bar{h}}{g_{io}}\right)^{1/2} \qquad (3\text{-}2)$$

$$V_{fm} = (2g_{io}h_m)^{1/2} \qquad (3\text{-}3)$$

where g_{io} denotes geyser initiation reverse gravity acceleration.

To show examples of the selected sequences of time evolution of fluid reorientation for cryogenic hydrogen, Figures 2, 3, 4, 5, and 6 show time evolution of fluid reorientation activated by geyser initiation impulse reverse gravity acceleration with a frequency of 10 Hz for liquid filled levels of 30, 50, 65, 70, and 80%, respectively. Each figure contains four sub-figures. Subfigure (A) is initial profile of liquid-vapor interface at the moment of the starting of fluid reorientation at time t = 0; subfigure (B), the flow profile during the course of fluid reorientation before the initiation of geysering motion; subfigure (C), the flow profile with geysering motion; and subfigure (D), the flow profile after the ending of geysering motion.

Examples of selected sequences of time evolution of fluid reorientation illustrate following flow behaviors: (1) The liquid starts to flow in an annular sheet along the solid wall of tank and gradually pushes the vapor toward the central portion of the lower dome of tank as the net acceleration, reversing the direction of

gravity field, which is applied toward the downward direction of the tank's major axis, by using small auxiliary thrusters; (2) As the downward fluid annular sheet along the tank wall reaches the central bottom dome side of the tank, a geysering flow is observed; and (3) The vapor is thus pushed upward centrally into the liquid and the geysering disappears.

Based on the computer simulation of flow field values of maximum flow velocity V_m, time for observing maximum flow velocity t_m, and time for reorienting liquid flowing down and reaching the bottom of propellant tank t_R, are obtained and illustrated in Table 2 for reverse gravity acceleration with impulsive frequency of 10 Hz. Scale length of maximum flow velocity L_m, and scale flow acceleration associated with maximum velocity a_m, can be computed from the following parameters:

$$L_m = V_m t_m \qquad (3\text{-}4)$$

$$a_m = \frac{V_m}{t_m} \qquad (3\text{-}5)$$

Following dimensionless parameters are introduced: $V_m/\bar{V}_f$, $t_R/\bar{t}_f$, $t_m/\bar{t}_f$, a_m/a_g, $L_m/\bar{h}$ and V_m/V_{fm} where a_g stands geyser initiation acceleration (cm/s^2) for corresponding geyser initiation gravity level g_{io}. Impulsive reverse gravity acceleration, g_i with frequency f Hz is defined as follows:

$$g_i = g_{io}\left(1 + \frac{1}{2}\sin 2\pi ft\right) \qquad (3\text{-}6)$$

Figures 7 to 9 show the variations of dimensionless parameters in terms of liquid filled levels for impulsive acceleration with

frequency of 10 Hz. Denominators of these six dimensionless parameters are either predetermined from the geometry of liquid fill levels or can be deduced from the corresponding calculations associated with the geyser initiation gravity levels. Characteristics of these near constant values dimensionless parameters can provide a good understanding of the physics of microgravity fluid behaviors, in particular the active category of liquid acquisition or positioning, and also the design criteria of on-orbit spacecraft propulsion system at the critical value of reverse gravity acceleration of propulsive thrust which is capable to initiate geyser.

An efficient propellant settling technique should minimize propellant usage and weight penalties. This can be accomplished by providing optimal acceleration to the spacecraft such that the propellant is reoriented over the tank outlet without any vapor entrainment, any excessive geysering, or any other undesirable fluid motion. In particular, it is important to study how well the impulsive acceleration can provide higher efficient propellant settling technique than the constant acceleration thrust technique. Also, what is the most optimal choice of impulsive frequency which can achieve the best fluid acquisition management being the goal of our research.

Figure 7(A) shows the ratio of maximum flow velocity to average free fall flow velocity $V_m/\bar{V}_f$ and its associated parameters of V_m and $\bar{V}_f$ in terms of liquid filled levels for impulsive acceleration with frequency of 10 Hz. It shows that the ratio of $V_m/\bar{V}_f$ varies in the

range of 5.1 to 5.3 in the entire liquid filled levels while V_m and $\bar{V}_f$ vary from 63.0 to 89.3 cm/s (decreasing with increasing liquid filled levels) and from 12.5 to 17.0 cm/s (also decreasing with increasing liquid filled levels), respectively. As $\bar{V}_f$ can be predetermined from geyser initiation gravity level and average liquid height, shown in Equation (3-1), one can make an approximate prediction of maximum flow velocity during the liquid reorientation for the various liquid filled levels. In comparison for impulsive frequency acceleration and constant reverse thrust acceleration in terms of the performance of capability to induce higher maximum flow velocity to accomplish flow reorientation, it shows that impulsive frequency of 10 Hz reverse thrust is better than that of constant thrust acceleration in which the maximum flow velocity induced are in the range of 62.0 to 73 cm/s in the entire liquid filled levels.

Figure 7(B) shows the ratio of liquid reaching bottome time to average free fall time $t_R/\bar{t}_f$ and its associated parameters of t_R and $\bar{t}_f$ in terms of liquid filled levels for impulsive acceleration with frequency of 10 Hz. It shows that the ratio of $t_R/\bar{t}_f$ varies in the range of 1.1 to 1.2 in the entire liquid filled levels while t_R and $\bar{t}_f$ vary from 0.18 to 0.37 s (decreasing with increasing liquid filled levels), respectively. As $\bar{t}_f$ can be predetermined from geyser initiation gravity level and average liquid height, shown in Equation (3-2), one can predict the time for reorienting liquid fluid flowing down from the original position and reaching the bottom of propellant tank for the various liquid filled levels at the reverse gravity acceleration capable for the intiation of geyser. In comparison for

impulsive frequency of 10 Hz reverse thrust acceleration and constant thrust acceleration, in terms of the performance of capability to induce the flow which can reach the tank bottom with a minimum time, it shows that the performance for impulsive acceleration with 10 Hz is better than that of constant thrust acceleration in which t_R is in the range of 0.20 to 0.40 s for the entire liquid filled levels.

Figure 8(A) shows the ratio of time for observing maximum flow velocity to average free fall time $t_m/\bar{t}_f$ and its associated parameters of t_m and $\bar{t}_f$ in terms of liquid filled levels. It shows that the ratio of $t_m/\bar{t}_f$ is in a value of 1.2 in the entire liquid filled levels while t_m and $\bar{t}_f$ vary from 0.19 to 0.39 s (decreasing with increasing liquid filled levels) and form 0.15 to 0.32 s (also decreasing with increasing liquid filled levels), respectively. As we indicated in Figure 7(B), $\bar{t}_f$ can be predetermined, one can predict the time for observing maximum flow velocity for various liquid filled levels at the reverse gravity acceleration capable for the initiation of geyser. In comparison for impulsive frequency of 10 Hz reverse thrust acceleration and constant thrust accelerattion, in terms of performance of capability to imduce maximum flow velocity in a short period of time, it shows that the perfromance for impulsive acceleration with 10 Hz is better than that of constant thrust acceleration in which t_m is in the range of 0.20 to 0.42 s for the entire liquid filled levels.

Figure 8(B) shows the ratio of scale flow acceleration associated with maximum velocity to geyser intiation acceleration for corresponding geyser intiation gravity level a_m/a_g and its associated

parameters of a_m and a_g in terms of liquid filled levels for impulsive aceeleration with frequency of 10 Hz. It shows that the ratio of a_m/a_g vary from 4.2 to 4.3 in entire liquid filled levels while a_m and a_g vary from 228.9 to 331.6 cm/s^2 (increasing with increasing liquid filled levels) and from 53.9 to 80.4 cm/s^2 (also increasing with increasing liquid filled levels), respectively. As a_g can be predetermined from geyser initiation gravity level, one can make an approximate prediction of scale flow acceleration associated with maximum velocity, which is defined in Equation (3-5), at the reverse gravity acceleration capable for the initiation of geyser. In comparison for impulsive frequency of 10 Hz reverse thrust acceleration and constant thrust acceleration, in terms of the performance of capability to induce higher scale flow acceleration associated with maximum flow velocity, it shows that the performance for impulsive acceleration with 10 Hz is better than that of constant thrust acceleration in which a_m is in the range of 175 to 310 cm/s^2 for the entire liquid filled levels.

Figure (9A) shows the ratio of scale length of maximum flow velocity to average liquid height $L_m/\bar{h}$ and its associated parameters of L_m and $\bar{h}$ in terms of liquid levels for impulsive acceleration with frequency of 10 Hz. It shows that the ratio of $L_m/\bar{h}$ varies in the range of 12.8 to 13.0 in the entire liquid filled levels while L_m and $\bar{h}$ vary from 11.9 to 34.8 cm (decreasing with increasing liquid filled levels) and from 0.93 to 2.67 cm (also decreasing with increasing liquid filled levels), respectively. As $\bar{h}$ can be predetermined from the geometry of liquid filled levels, one can make an approximate

prediction of scale length of maximum flow velocity, which is defined in Equation (3-4), at the reverse gravity acceleration capable for the initiation of geyser. In comparison for impulsive frequency of 10 Hz reverse thrust acceleration and constant thrust acceleration, in terms of the performance of capability to produce larger scale length of maximum flow velocity, it shows that the scale length produced by impulsive acceleration with 10 Hz is longer than that of constant thrust acceleration in which L_m is in the range of 12.6 to 30.9 cm for the entire liquid filled levels.

Figure 9(B) shows the ratio of maximum flow velocity to free fall velocity from maximum liquid height V_m/V_{fm} and its associated parameters of V_m and V_{fm} in terms of liquid filled levels for impulsive acceleration with frequency of 10 Hz. It shows that the ratio of V_m/V_{fm} varies in the range of 3.9 to 4.6 in the entire liquid filled levels while V_m and V_{fm} vary from 63.0 to 89.3 cm/s (decreasing with increasing liquid filled levels) and from 16.4 to 19.2 cm/s (also decreasing with increasing liquid filled levels), respectively. As V_{fm} can be predetermined from geyser initiation gravity level and maximum liquid height, shown in Equation (3-3), one can make an approximate prediction of maximum flow velocity at the reverse gravity acceleration capable for the initiation of geyser. In comparison for impulsive frequency of 10 Hz reverse thrust acceleration and constant thrust acceleration, in terms of producing higher maximum flow velocity, it shows that the maximum flow velocity produced by impulsive acceleration with 10 Hz produce higher maximum flow velocity than that of the constant thrust acceleration in which

V_m is in the range of 62.0 to 73.6 cm/s for the entire liquid filled levels.

Similar to Paper I[9] for constant reverse gravity acceleration, six dimensionless parameters presented in this study show that the parameters hold near constant values through the entire ranges of liquid filled levels during the course of reorientation of liquid hydrogen activated by the reverse gravity acceleration with impulsive thrust frequency of 10 Hz, which is great enough to initiate geysering flow. As the purpose of present study is to investigate an efficient propellant resettling technique which is able to minimize propellant usage and weight penalties, comparison of flow parameters induced by the impulsive acceleration with frequency of 10 Hz and constant thrust acceleration toward these goals have been made. It shows that the operation of auxiliary engine with impulsive thrust acceleration of 10 Hz is better than that of the constant thrust acceleration.

IV. Discussion and Conclusions

The requirement to settle or to position liquid fluid over the outlet end of the spacecraft propellant tank prior to main engine restart poses a microgravity fluid behavior problem. Retromaneuvers of spacecraft require settling or reorientation of the propellant prior to main engine firing. Cryogenic liquid propellant is positioned over the tank outlet by using small auxiliary thrusters (or idle-mode thrusters from the main engine) which provide a thrust parallel to the tank's major axis in the direction of flight.

The results of the study of fluid reorientation have to be evaluated in terms of how well they can be managed efficiently. An

efficient propellant settling technique should minimize propellant usage and weight penalties through the operation of small thrusters (or idle-mode thrusters from the main engine). This can be accomplished by providing optimal acceleration to the spacecraft such that the propellant is reoriented over the tank outlet without any vapor entrainment, any excessive geysering, or any other undesirable fluid motion.

Production of geyser during the propellant reorientation is not a desirable motion for the space fluid management under microgravity environment. It is because geyser is always accompanied by the vapor entrainment and globule formation. Geyser is observed at reverse gravity acceleration greater than certain critical values of acceleration during the course of liquid reorientation. In this paper, numerical simulation of positive liquid acquisition is attempted by introducing reverse gravity acceleration, resulting from the propulsive thrust with high impulsive frquency of 10 Hz auxiliary engine, which exceeds critical value for the initiation of geyser.

Evaluation of performance is based on how efficient the impulsive reverse gravity with 10 Hz frequency in comparison with constant thrust acceleration can activate following flow parameters at the same background thrust accelerations: (A) a higher maximum flow velocity, (B) a shorter time period for flow to reach maximum velocity, (C) a shorter time period for flow to reach tank bottom (tank outlet) for fluid resettling, (D) a larger length scale of maximum flow velocity, and (E) a higher flow acceleration associated with

maximum flow velocity. Comparison between the results of present study for impulsive thrust with 10 Hz frequency and that of constant thrust, shown in Paper I[9], it shows that impulsive thrust is superior than the constant thrust in terms of efficient operation of fluid reorientation.

Based on the computer simulation of flow fields during the course of fluid reorientation, six dimensionless parameters are presented both in Paper I[9] and this study. It is shown that these parameters hold near constant values through the entire ranges of liquid filled levels during the course of fluid reorientation activated by the reverse gravity acceleration in both constant and impulsive thrusts great enough to initiate geyser. As the denominators of these dimensionless parameters are either predetermined from the geometry of liquid filled levels, as shown in Table 1, or can be deduced from the corresponding calculations associated with the geyser initiation gravity levels, one can predict the values of these flow parameters. Present study can greatly enhance our understanding in the behaviors of cryogenic fluid resettlement under reduced gravity environment. This is particularly important for liquid acquisition technique to be used in on-orbit spacecraft design.

Any fluid capable of motion relative to the spacecraft will be subject to an acceleration relative to the mass center of the spacecraft that arises from the gravity gradient of the Earth[14,15]. In addition to the Earth's gravitational force, the interaction between the particle mass of fluids and the spacecraft mass due to gravity gradient acceleration[14] have also been taken into

consideration in this microgravity fluid management study.

To conclude, we have demonstrated that, the computer algorithm presented, can be used to simulate fluid behavior in a microgravity environment, in particular the development of technology necessary for acquisition or positioning of liquid and vapor within a tank to enable liquid outflow or vapor venting through active liquid acquisition by the creation of a positive acceleration environment resulting from propulsive thrust. Better understanding of the full pictures of flow fields in both constant and impulsive thrusts, during the course of fluid reorientation can provide the proper design techniques for handling and managing the cryogenic liquid propellants to be used in on-orbit spacecraft propulsion. It is important to emphasize that impulsive reverse gravity thrust is superior to constant reverse gravity thrust for the activation of liquid necessary for the resettlement of liquid in a reduced gravity environement.

Acknowledgement

The authors appreciate the support recieved from the National Aeronautics and Space Administration Headquarters through the NASA Grant NAGW-812, and NASA Marshall Space Flight Center through the NASA Contract NAS8-36955/Delivery Order No. 69. The authors would like to acknowledge the great help recieved through discussions from Lee Jones, Leon Hastings, George Schmidt, and James Martin of Space Propulsion Branch of NASA Marshall Space Flight Center.

Reference

1. NASA Office of Aeronautics and Space Technology, Technology for Future NASA Missions: Civil Space Technology Initiative and Pathfinder, NASA CP-3016,National Aeronautics and Space Administration, Washington, D.C., 1988, pp. 568.

2. Leslie, F. W., "Measurements of Rotating Bubble Shapes in a Low Gravity Environment," Journal of Fluid Mechanics, Vol. 161, Dec. 1985, pp. 269-279.

3. Hung, R. J., and Leslie, F. W., "Bubble Shape in a Liquid Filled Rotating Container Under Low Gravity," Journal of Spacecraft and Rockets, Vol. 25, Jan.-Feb. 1988, pp. 70-74.

4. Hung, R. J., Tsao, Y.D., Hong, B. B., and Leslie, F. W., "Time Dependent Dynamical Behavior of Surface Tension on Rotating Fluids under Microgravity Environment," Advances in Space Research, Vol. 8, No. 12, 1988, pp. 205-213.

5. Hung, R. J., Tsao, Y. D., Hong, B. B., and Leslie, F. W., "Bubble Behaviors in a Slowly Rotating Helium Dewar in Gravity Probe-B Spacecraft Experiment," Journal of Spacecraft and Rockets, Vol. 26, May-June 1989, pp. 167-172.

6. Hung, R. J., Tsao, Y. D., Hong, B. B., and Leslie, F. W., "Dynamical Behavior of Surface Tension on Rotating Fluids in Low and Microgravity Environments," International Journal for Microgravity Research and Applications, Vol. 11, June 1989, pp. 81-95.

7. Hung, R. J., Tsao, Y. D., Hong, B. B., and Leslie F. W., "Axisymmetric Bubble Profiles in a Slwowly Rotating Helium

Dewar Under Low and Microgravity Environments," Acta Astronautica, Vol. 19, May 1989, pp. 411-426.

8. "Stanford Relativity Gyroscope Experiment (NASA Gravity Probe-B)," Proceedings of Society of Photo-Optical Instrumentation Engineers, Vol. 619, Society of Photo-Optical Instrumentation Engineers, Bellingham, WA, 1986, pp. 1-165.

9. Hung, R. J., and Shyu, K. L., "Cryogenic Liquid Hydrogen Reorientation Activated by Constant Reverse Gravity Acceleration of Geyser Initiation," AIAA Paper No. 90-3712, 1990.

10. Kamotani, Y., Prasad, A., and Ostrach, S., "Thermal Convection in an Enclosure Due to Vibrations Aboard a Spacecraft," AIAA Journal, Vol. 19, Apr. 1981, pp. 511-516.

11. Hung, R. J., Lee, C. C., and Shyu, K. L., "Reorientation of Rotating Fluid in Microgravity Environment with and without Gravity Jitters," Journal of Spacecraft and Rockets, Vol. 27, 1990, in press.

12. Hung, R. J., Lee, C. C., and Leslie, F. W. "Effects of G-Jitters on the Stability of Rotating Bubble Under Microgravity Environment," Acta Astronautica, Vol. 20, 1990, in press.

13. Hung, R. J., Lee, C. C. and Leslie F. W., "Response of Gravity Level Fluctuations on the Gravity Probe-B Spacecraft Propellant System," Journal of Propulsion and Power, Vol. 6, 1990, in press.

14. Misner, C. W., Thorne, K. S., and Wheeler, J. A., "Gravitation",

W. H. Freeman and Co., San Francisco, CA, 1973, pp. 1-1279.

15. Forward, R. L., "Flattening Space-Time Near the Earth, "Physical Review, Series D, Vol. 26, Aug. 1982, pp. 735-744.

TABLE 1 SOME BASIC GEOMETRYS AND CHARACTERISTICS
OF CRYOGENIC LIQUID HYDROGEN REORIENTATION

Liquid Filled Level (%)	30	50	65	70	80
Geyser Initiation Gravity-Level, $g_{io}(10^{-2}\ g_o)$	5.5	6.52	6.6	6.7	8.2
Geyser Initiation Acceleration, a_g (cm/s^2)	53.9	63.9	64.7	65.7	80.4
Average Liquid Height, $\bar{h}$ (cm)	2.67	2.05	1.52	1.35	0.93
Average Free Fall Flow Velocity, $\bar{V}_f$ (cm/s)	17.0	16.2	14.0	13.3	12.5
Maximum Liquid Height, h_m (cm)	3.41	2.79	2.26	2.09	1.67
Free Fall Velocity from Maximum Liquid Height V_{fm} (cm/s)	19.2	18.9	17.1	16.6	16.4

Table 2 CHARACTERISTICS OF CRYOGENIC HYDROGEN REORIENTATION
(Frequency of Impulsive Acceleration = 10 Hz)

Liquid Filled Level (%)	30	50	65	70	80
Maximum Flow Velocity, V_m (cm/s)	89.3	82.6	74.2	68	63
$V_m/\bar{V}_f$	5.25	5.1	5.3	5.1	5.1
Liquid Reaching Bottom Time, t_R (s)	0.37	0.29	0.27	0.23	0.18
$t_R/\bar{t}_f$	1.1	1.1	1.2	1.1	1.2
Time for Observing Maximum Velocity, t_m (s)	0.39	0.30	0.27	0.24	0.19
Scale Length of Maximum Flow Velocity, L_m ($= V_m t_m$) (cm)	34.8	24.8	20.0	16.3	11.9
$L_m/\bar{h}$	13.0	12.1	13.1	12.1	12.8
$t_m/\bar{t}_f$	1.2	1.2	1.2	1.2	1.2
Scale Flow Acceleration Associated with Maximum Velocity, a_m ($= V_m/t_m$) (cm/s^2)	228.9	274.3	274.8	283.3	331.6
a_m/a_g	4.2	4.3	4.2	4.3	4.2
V_m/V_{fm}	4.6	4.4	4.3	4.1	3.9

Figure Captions

Figure 1. (A) Distribution of grid points in the radial-axial plane of cylindrical coordinate for propellant tank, and (B) Model size propellant tank adopted for numerical simulation with geometrical description.

Figure 2. Selected sequences of time evolution of fluid reorientation with liquid filled level of 30% for impulsive acceleration with frequency of 10 Hz, (A) initial profile, (B) flow profile before the initiation of geyser, (C) flow profile with geyser, and (D) flow profile after the ending of geyser.

Figure 3. Selected sequences of time evolution of fluid reorientation with liquid filled level of 50% for impulsive acceleration with frequency of 10 Hz, (A) initial profile, (B) flow profile before the initiation of geyser, (C) flow profile with geyser, and (D) flow profile after the ending of geyser.

Figure 4. Selected sequences of time evolution of fluid reorientation with liquid filled level of 65% for impulsive acceleration with frequency of 10 Hz, (A) initial profile, (B) flow profile before the initiation of geyser, (C) flow profile with geyser, and (D) flow profile after the ending of geyser.

Figure 5. Selected sequences of time evolution of fluid reorientation with liquid filled level of 70% for impulsive acceleration with frequency of 10 Hz, (A)

initial profile, (B) flow profile before the initiation of geyser, (C) flow profile with geyser, and (D) flow profile after the ending of geyser.

Figure 6. Selected sequences of time evolution of fluid reorientation with liquid filled levels of 80% for impulsive acceleration with frequency of 10 Hz, (A) initial profile, (B) flow profile before the initiation of geyser, (C) flow profile with geyser, and (D) flow profile after the ending of geyser.

Figure 7. (A) Ratio of $V_m/\bar{V}_f$ and its associated parameters in terms of liquid filled levels, (B) Ratio of $t_R/\bar{t}_f$ and its associated parameters in terms of liquid filled levels.

Figure 8. (A) Ratio of $t_m/\bar{t}_f$ and its associated parameters in terms of liquid filled levels, (B) Ratio of a_m/a_g and its associated parameters in terms of liquid filled levels.

Figure 9. (A) Ratio of $L_m/\bar{h}$ and its associated parameters in terms of liquid filled levels, (B) Ratio of V_m/V_{fm} and its associated parameters in terms of liquid filled levels.

(A)

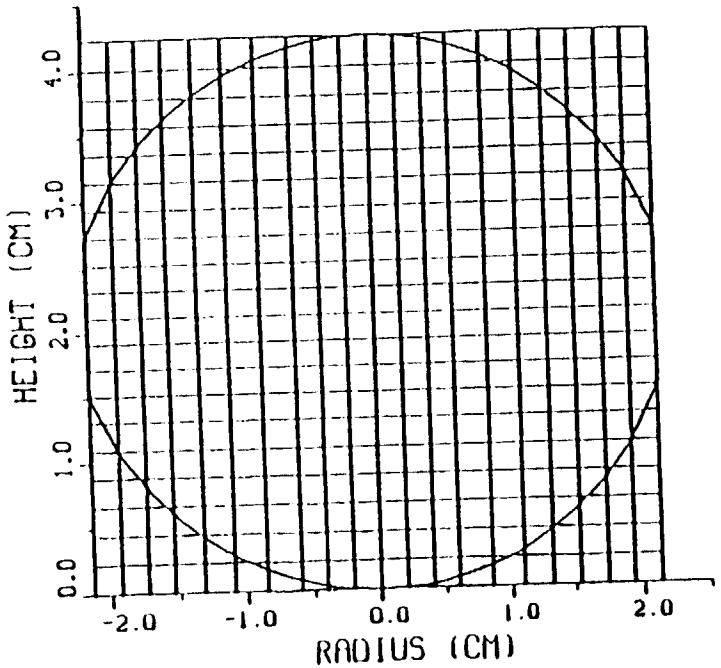

(B)

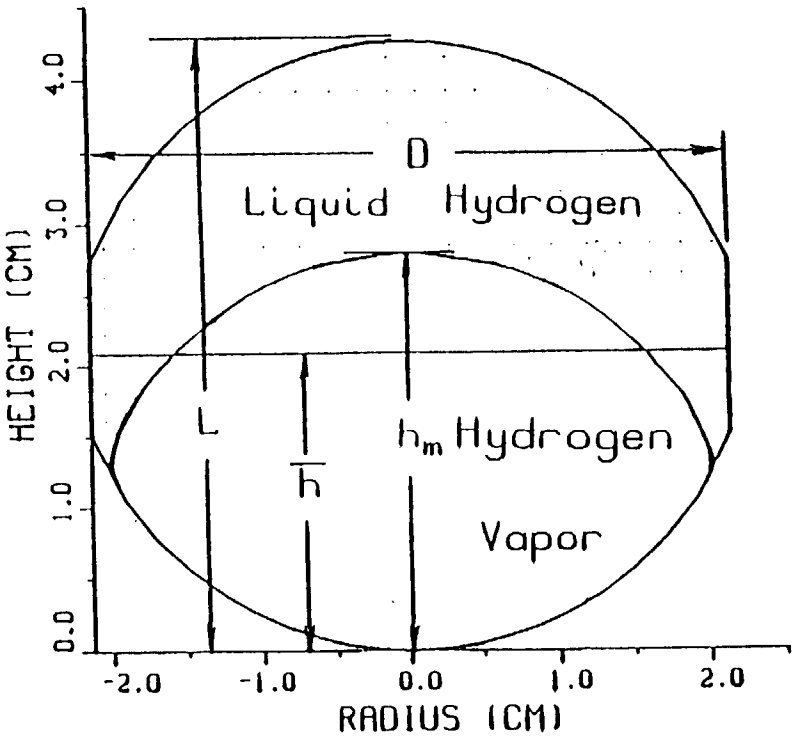

D-4.26720 CM, L-4.23672 CM

Fig 1

A. Liquid Hydrogen and Vapor
Liquid Filled=30% t= 0.00s
g=-5.50×10^{-2}g$_o$
f= 1.00×10^{1}Hz

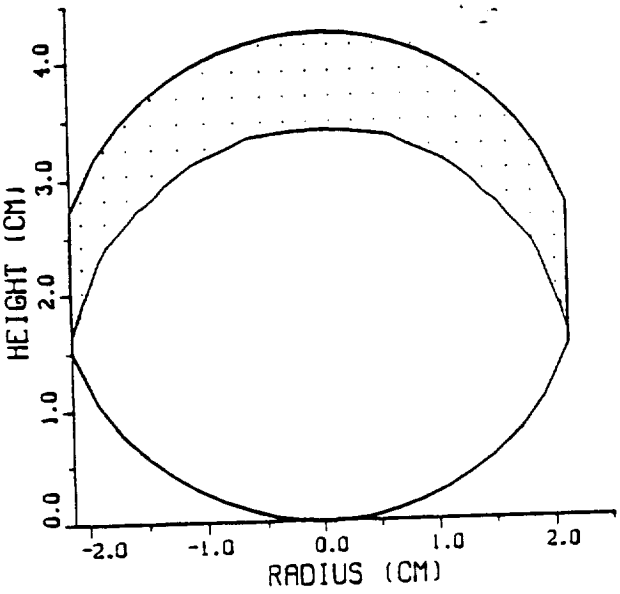

B Liquid Hydrogen and Vapor
Liquid Filled=30% t= 3.60×10^{-1}s
g=-5.50×10^{-2}g$_o$
f= 1.00×10^{1}Hz

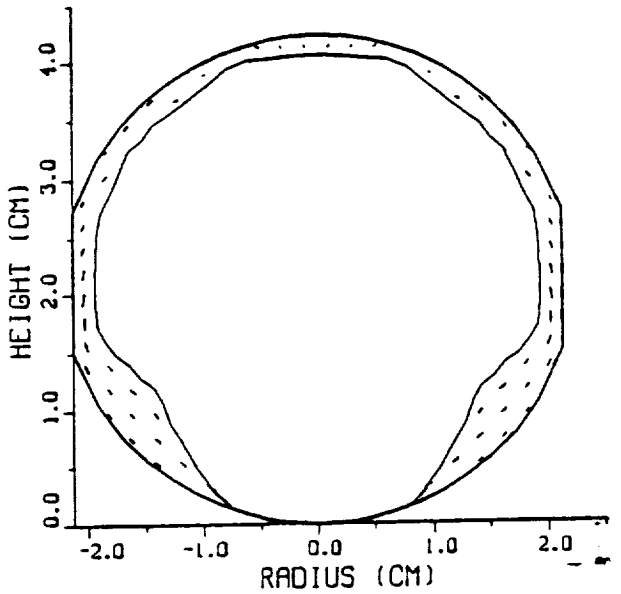

C. Liquid Hydrogen and Vapor
Liquid Filled=30% t= 5.20×10^{-1}s
g=-5.50×10^{-2}g$_o$
f= 1.00×10^{1}Hz

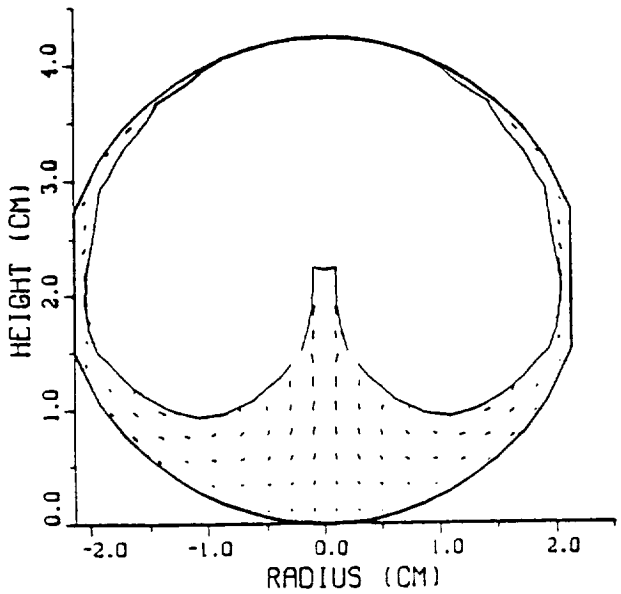

D. Liquid Hydrogen and Vapor
Liquid Filled=30% t= 8.80×10^{-1}s
g=-5.50×10^{-2}g$_o$
f= 1.00×10^{1}Hz

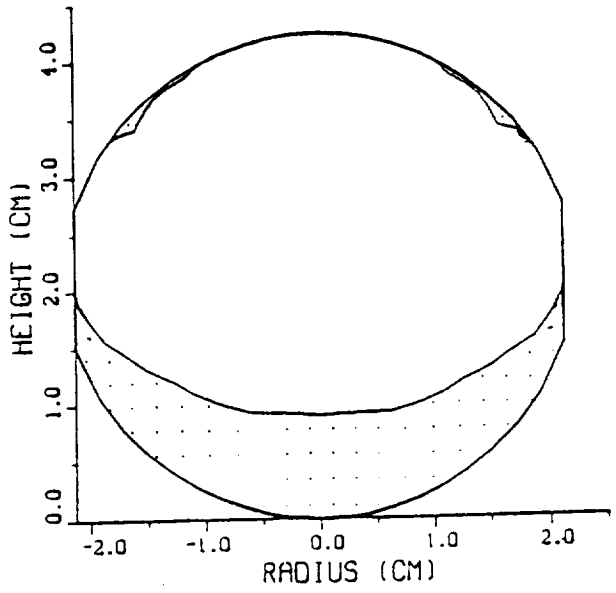

Fig 2

A. Liquid Hydrogen and Vapor
Liquid Filled=50% t= 0.00s
g=-6.52×10^{-2}g$_o$
f= 1.00×10^{1}Hz

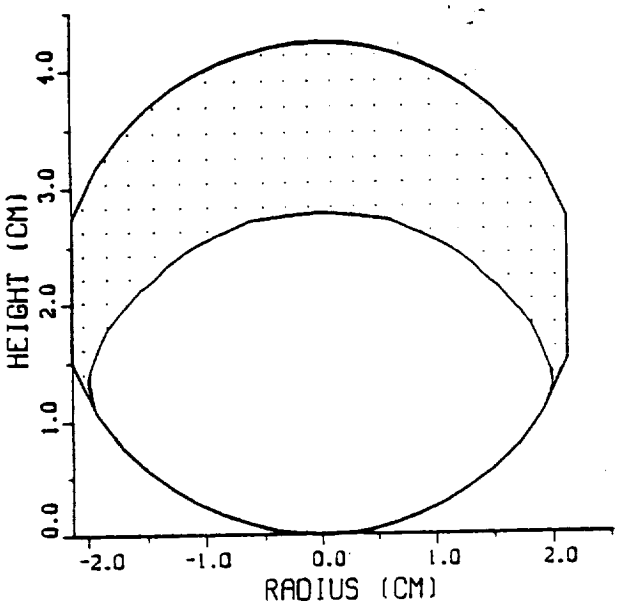

B. Liquid Hydrogen and Vapor
Liquid Filled=50% t= 2.40×10^{-1}s
g=-6.52×10^{-2}g$_o$
f= 1.00×10^{1}Hz

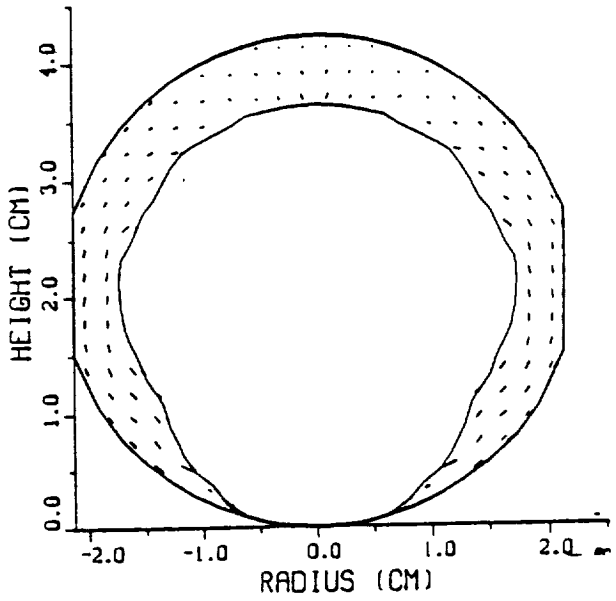

C. Liquid Hydrogen and Vapor
Liquid Filled=50% t= 3.43×10^{-1}s
g=-6.52×10^{-2}g$_o$
f= 1.00×10^{1}Hz

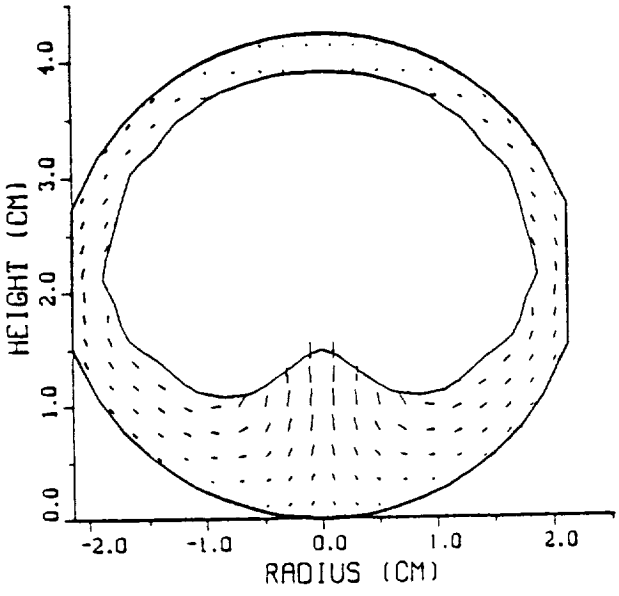

D. Liquid Hydrogen and Vapor
Liquid Filled=50% t= 5.23×10^{-1}s
g=-6.52×10^{-2}g$_o$
f= 1.00×10^{1}Hz

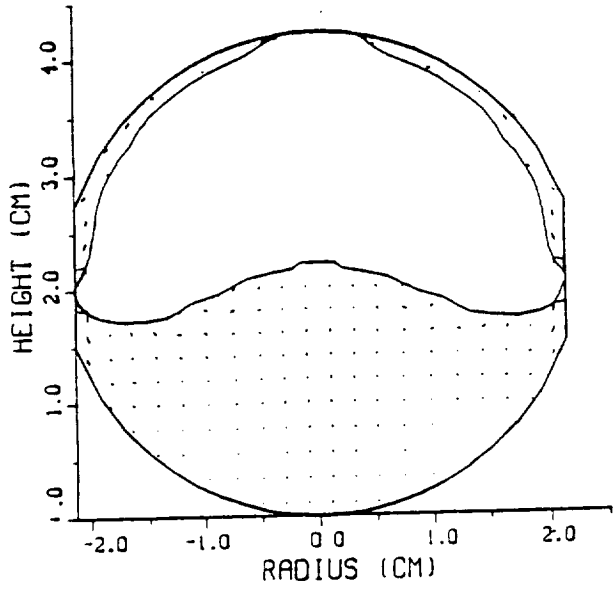

Fig 3

A. Liquid Hydrogen and Vapor
Liquid Filled-65% t= 0.00s
g=-6.60×10^{-2}g$_o$
f= 1.00×10^{1}Hz

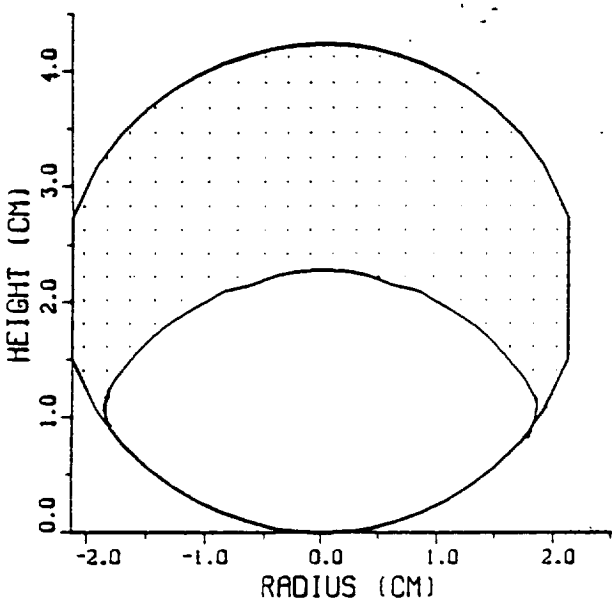

B. Liquid Hydrogen and Vapor
Liquid Filled-65% t= 2.40×10^{-1}s
g=-6.60×10^{-2}g$_o$
f= 1.00×10^{1}Hz

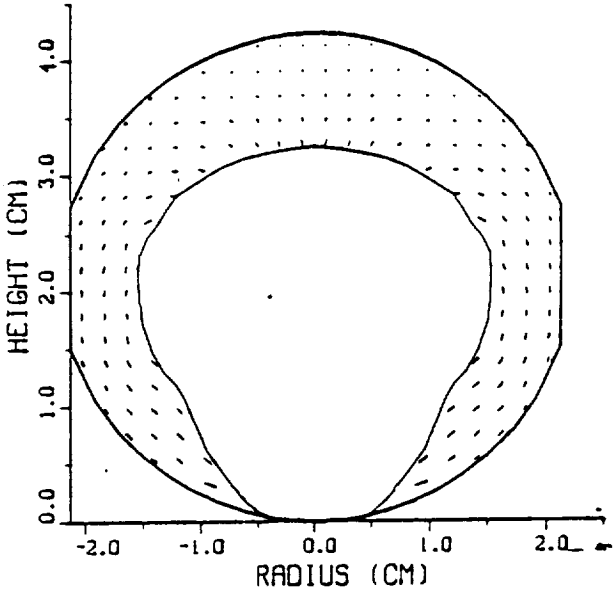

C. Liquid Hydrogen and Vapor
Liquid Filled-65% t= 3.37×10^{-1}s
g=-6.60×10^{-2}g$_o$
f= 1.00×10^{1}Hz

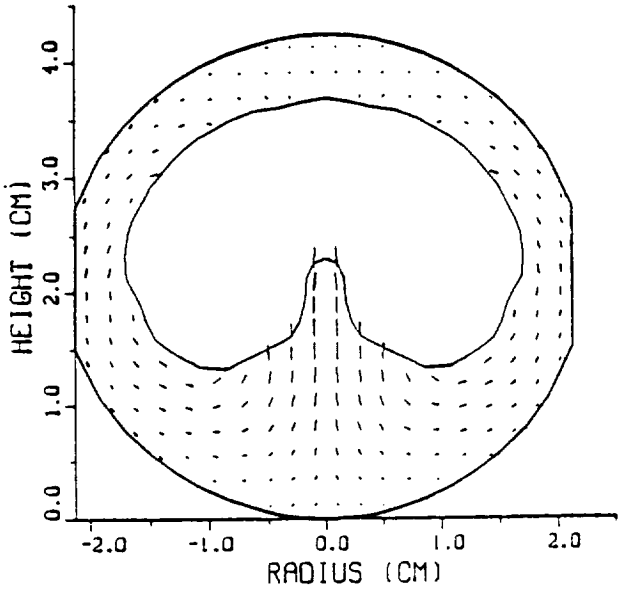

D. Liquid Hydrogen and Vapor
Liquid Filled-65% t= 7.57×10^{-1}s
g=-6.60×10^{-2}g$_o$
f= 1.00×10^{1}Hz

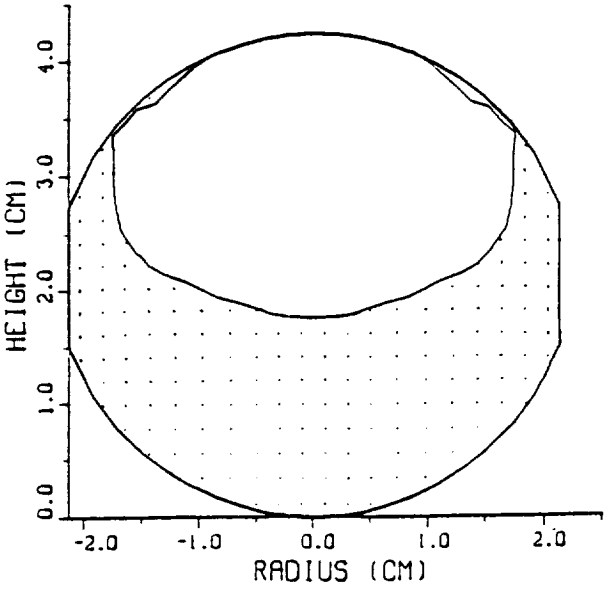

Fig 4

A. Liquid Hydrogen and Vapor
Liquid Filled-70% t= 0.00s
g=-7.00×10^{-2}g$_o$
f= 1.00×10^{1}Hz

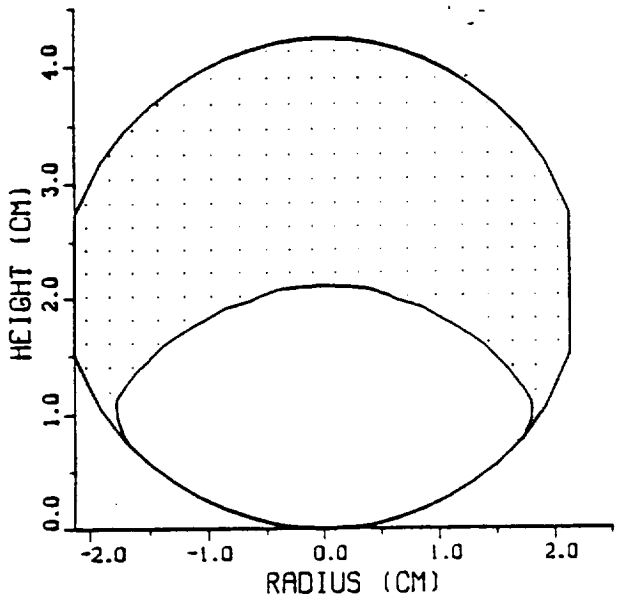

B. Liquid Hydroger and Vapor
Liquid Filled-70% t= 1.80×10^{-1}s
g=-7.00×10^{-2}g$_o$
f= 1.00×10^{1}Hz

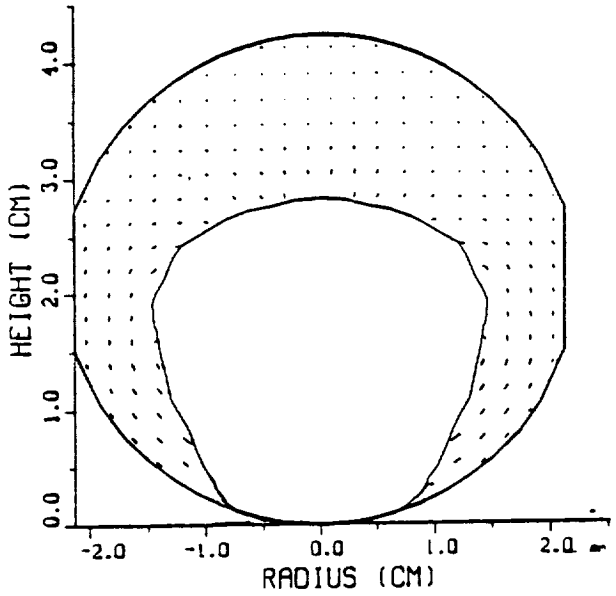

C. Liquid Hydrogen ar d Vapor
Liquid Filled-70% t= 3.33×10^{-1}s
g=-7.00×10^{-2}g$_o$
f= 1.00×10^{1}Hz

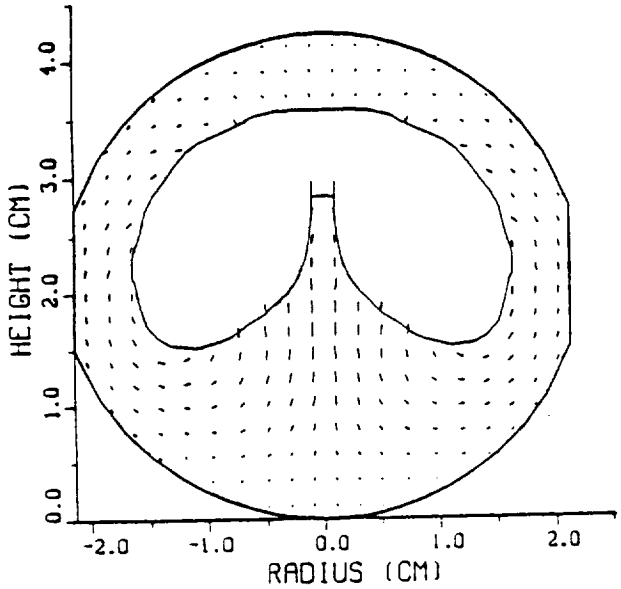

D. Liquid Hydrogen and Vapor
Liquid Filled-70% t= 8.73×10^{-1}s
g=-7.00×10^{-2}g$_o$
f= 1.00×10^{1}Hz

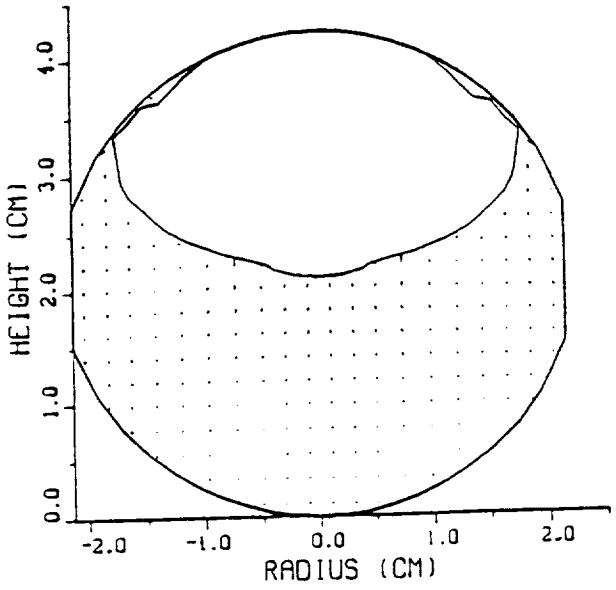

Fig 5

A. Liquid Hydrogen and Vapor
Liquid Filled-80% t= 0.00s
g=-8.20×10^{-2}g$_o$
f= 1.00×10^{1}Hz

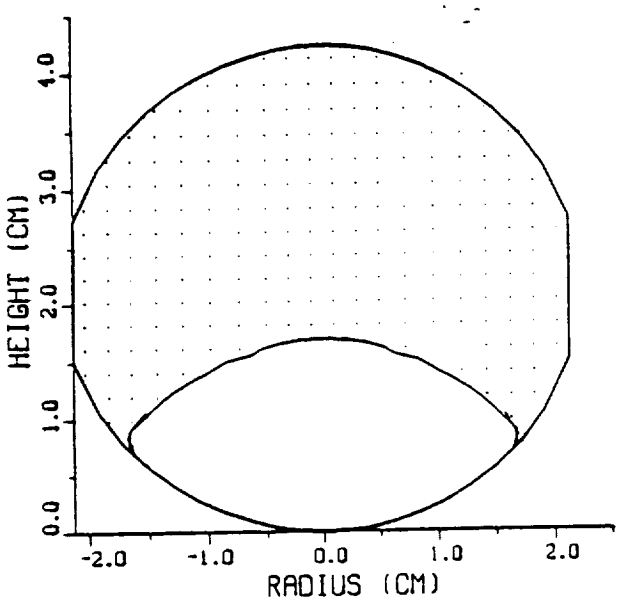

B. Liquid Hydrogen and Vapor
Liquid Filled-80% t= 1.80×10^{-1}s
g=-8.20×10^{-2}g$_o$
f= 1.00×10^{1}Hz

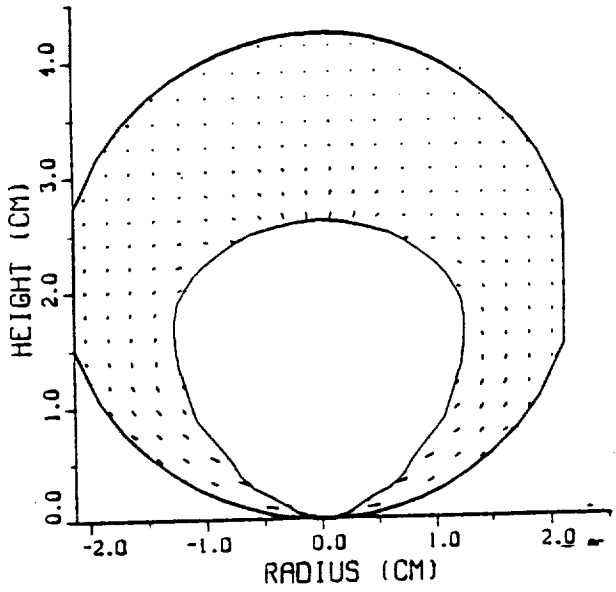

C. Liquid Hydrogen and Vapor
Liquid Filled-80% t= 3.60×10^{-1}s
g=-8.20×10^{-2}g$_o$
f= 1.00×10^{1}Hz

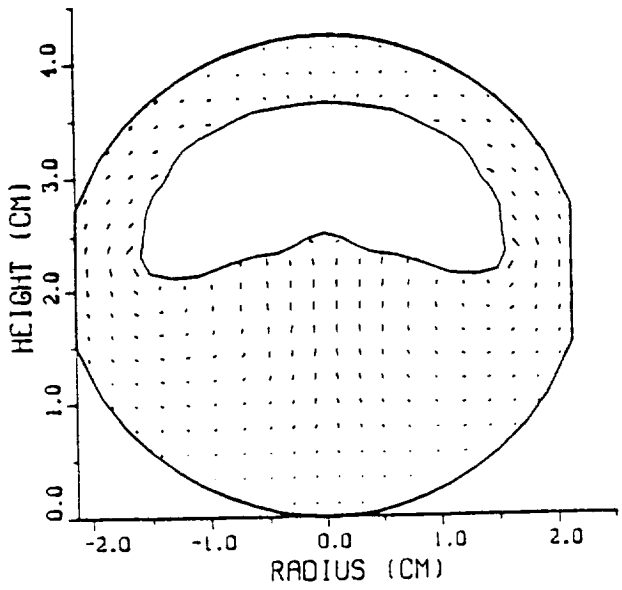

D. Liquid Hydrogen and Vapor
Liquid Filled-80% t= 7.80×10^{-1}s
g=-8.20×10^{-2}g$_o$
f= 1.00×10^{1}Hz

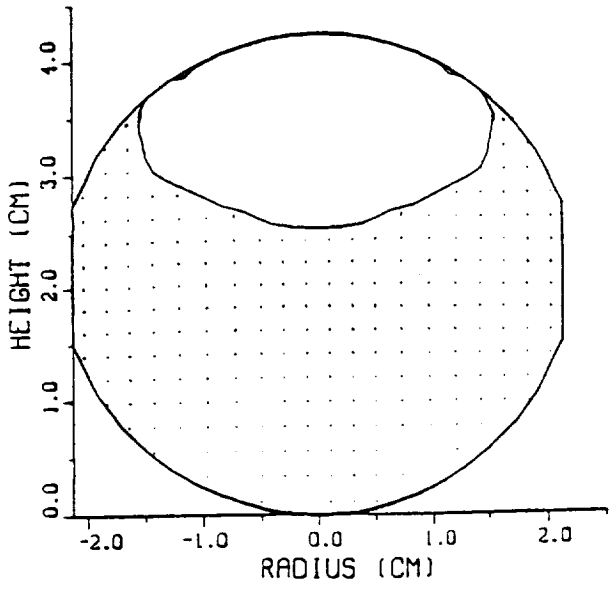

Fig 6

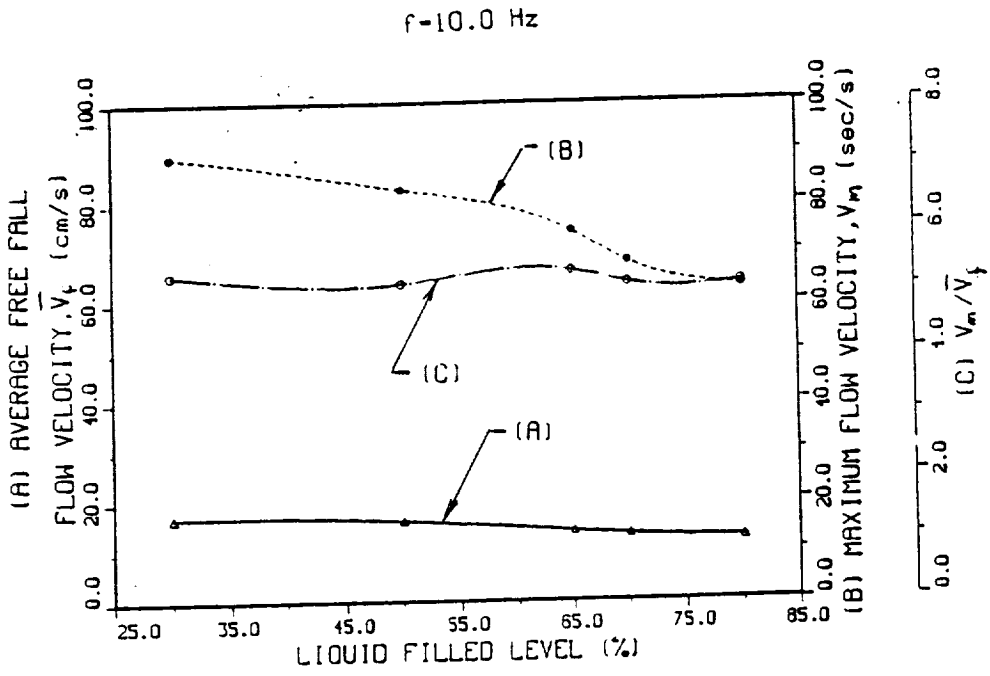
f=10.0 Hz
(A) AVERAGE FREE FALL FLOW VELOCITY, $\bar{V}_f$ (cm/s)
(B) MAXIMUM FLOW VELOCITY, V_m (sec/s)
(C) $V_m/\bar{V}_f$
(B)
(C)
(A)
LIQUID FILLED LEVEL (%)

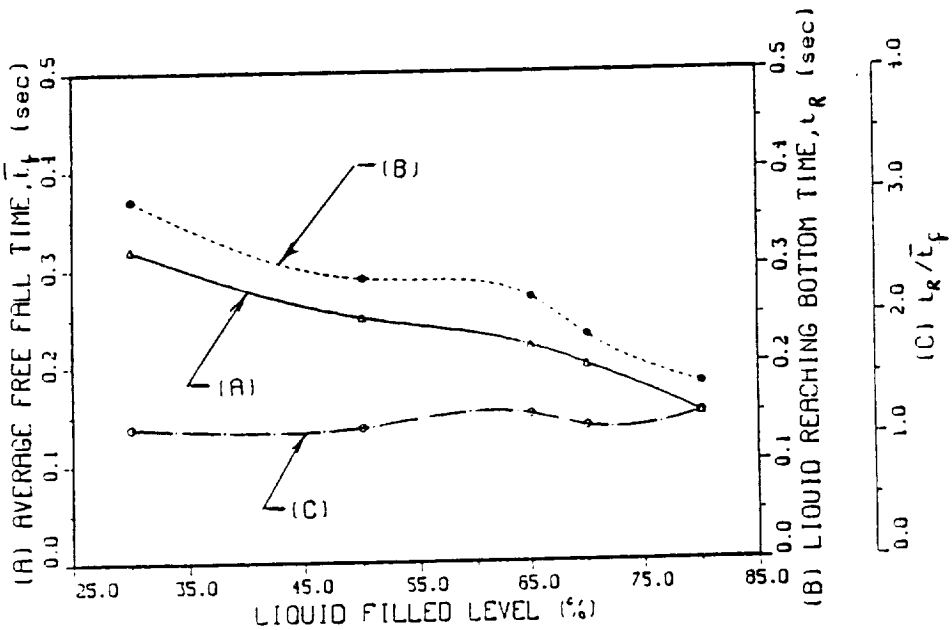
f=10.0 Hz
(A) AVERAGE FREE FALL TIME, $\bar{t}_f$ (sec)
(B) LIQUID REACHING BOTTOM TIME, t_R (sec)
(C) $t_R/\bar{t}_f$
(B)
(A)
(C)
LIQUID FILLED LEVEL (%)

Fig 7 (A,B)

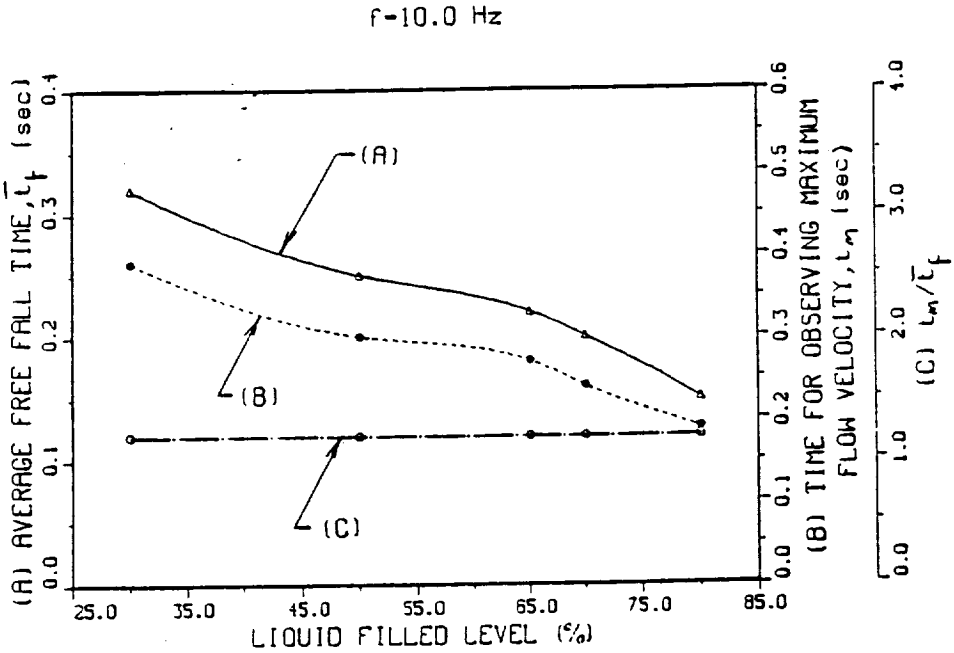
f=10.0 Hz
(A) AVERAGE FREE FALL TIME, $\bar{t}_f$ (sec)
(B) TIME FOR OBSERVING MAXIMUM FLOW VELOCITY, t_m (sec)
(C) $t_m/\bar{t}_f$
(A)
(B)
(C)
LIQUID FILLED LEVEL (%)

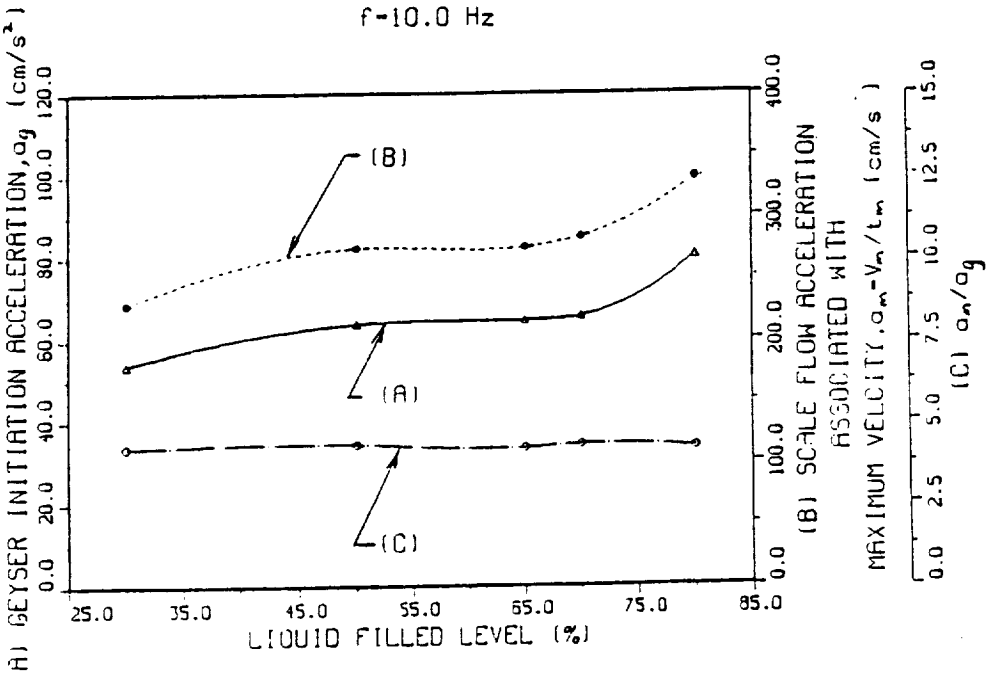
f=10.0 Hz
(A) GEYSER INITIATION ACCELERATION, a_g (cm/s²)
(B) SCALE FLOW ACCELERATION ASSOCIATED WITH MAXIMUM VELOCITY, a_m-V_m/t_m (cm/s)
(C) a_m/a_g
(B)
(A)
(C)
LIQUID FILLED LEVEL (%)

Fig 8 (A,B)

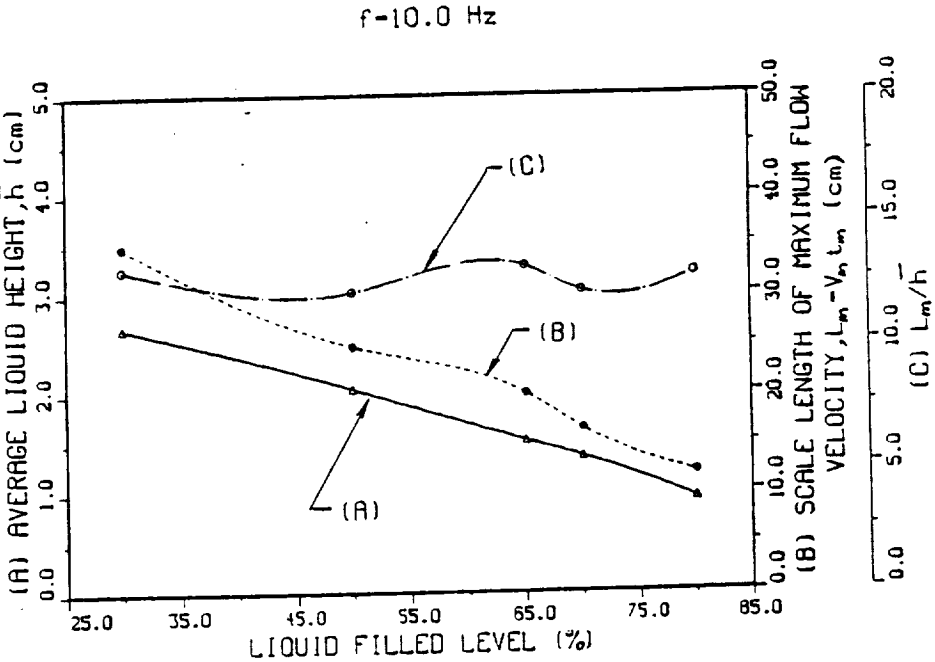
f-10.0 Hz
(A) AVERAGE LIQUID HEIGHT, $\bar{h}$ (cm)
(B) SCALE LENGTH OF MAXIMUM FLOW VELOCITY, L_m-V_m, t_m (cm)
(C) $L_m/\bar{h}$
(C)
(B)
(A)
LIQUID FILLED LEVEL (%)

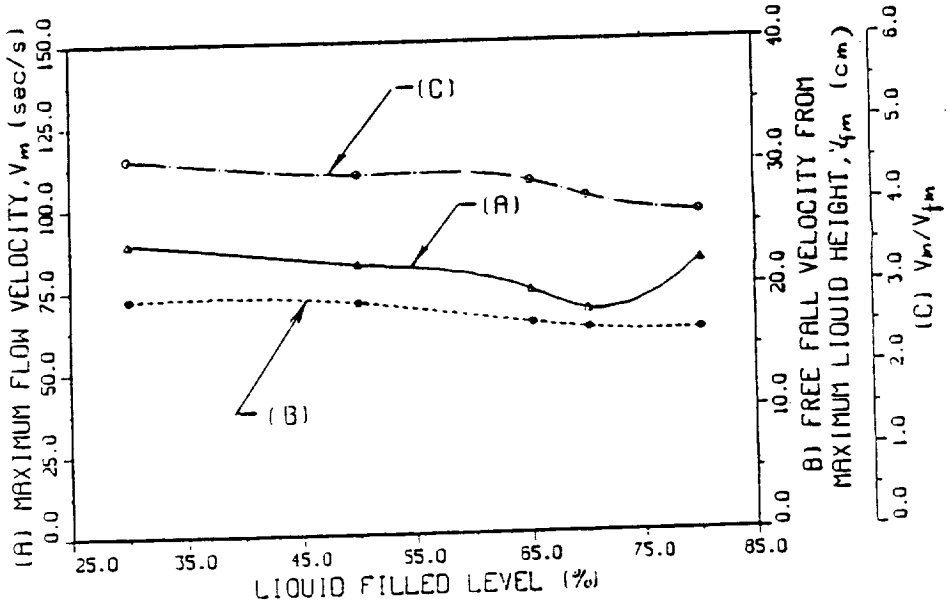
f-10.0 Hz
(A) MAXIMUM FLOW VELOCITY, V_m (sec/s)
B) FREE FALL VELOCITY FROM MAXIMUM LIQUID HEIGHT, y_{fm} (cm)
(C) V_m/V_{fm}
(C)
(A)
(B)
LIQUID FILLED LEVEL (%)

Fig 9 (A,B)

References

(1) NASA Office of Aeronautics and Space Technology, Technology for Future NASA Missions: Civil Space Technology Initiative and Pathfinder, NASA CP-3016, 1988.

(2) Hung, R. J., and Leslie F. W., Bubble Shapes in a Liquid-Filled Rotating Container Under Low Gravity, Journal Spacecraft and Rockets, 25, 70-74, 1988.

(3) Hung, R. J., Tsao, Y. D., Hong, B. B., and Leslie, F. W., Time Dependent Dynamical Behavior of Surface Tension on Rotating Fluids Under Microgravity Environment, Advances in Space Research, 8, No.12, 205-213, 1988.

(4) Hung, R. J., Tsao, Y. D., Hong, B. B., and Leslie, F. W., Axisymmetric Bubble Profiles in a Slowly Rotating Helium Dewar Under Low and Microgravity Environments, Acta Astronautica, 19, 411-426, 1989.

(5) Hung, R. J., Tsao, Y. D., Hong, B. B., and Leslie, F. W., Bubble Behaviors in a Slowly Rotating Helium Dewar in Gravity Probe-B Spacecraft Experiment, J. Spacecraft and Rockets, 26, 167-172, 1989.

(6) Hung, R. J., Tsao, Y. D., Hong, B. B., and Leslie, F. W., Dynamical Behavior of Surface Tension on Rotating Fluids in Low and Microgravity Enviroments, International Journal for Microgravity Research and Applications, 11, 81-95, 1989.

(7) Hung, R. J., Lee, C. C., and Tsao, Y. D., Fluid Behavior in Microgravity Environment, Proceed. National Sci. Council (A),

14, 21-34, 1990.

(8) Hung, R. J., Tsao, Y. D., and Leslie, F. W., Effect of G-Jitters on the Stability of Rotating Bubble Under Microgravity Environment, Acta Astronautica, 21, 309-321, 1990.

(9) Hung, R. J., Tsao, Y. D., Hong, B. B., and Leslie, F. W., Dynamics of Surface Tension in Microgravity Environment, Progress in Aeronautics and Astronautics, 127, 124-150, 1990.

(10) Hung, R. J., Lee, C. C., and Shyu, K. L., Reorientation of Rotating Fluid in Microgravity Environment With and Without Gravity Jitters, J. Spacecraft and Rockets, 27, in press, 1990.

(11) Hung, R. J., Superfluid and Normal Fluid Helium II in a Rotating Tank Under Low and Microgravity Environments, Proceed. National Sci. Council (A), 14, 289-297, 1990.

(12) Hung, R. J., Lee, C. C., and Leslie, F. W., Response of Gravity Level Fluctuations on the Gravity Probe-B Spacecraft Propellant System, J. Propulsion and Power, 6, in press, 1990.

(13) Hung, R. J., Lee, C. C., and Leslie, F. W., Gravity Jitter Response Slosh Wave Excitation on the fluid in a Rotating Dewar, Advances in Space Research, 11, in press, 1990.

(14) Hung, R. J., and Shyu, K. L., Cryogenic Hydrogen Reorientation and Geyser Initiation at Various Liquid-Filled Levels in Microgravity, Advances in Space Research, 11, in press, 1990.

(15) Hung, R. J., Lee, C. C., and Leslie, F. W., Gravity-Jitter Effected Slosh Waves on the Stability of Rotating Bubble Under Microgravity Environment, Advances in Space Research, 11, in press, 1990.